Copyright Undertaking

This thesis is protected by copyright, with all rights reserved.

By reading and using the thesis, the reader understands and agrees to the following terms:

1. The reader will abide by the rules and legal ordinances governing copyright regarding the use of the thesis.

2. The reader will use the thesis for the purpose of research or private study only and not for distribution or further reproduction or any other purpose.

3. The reader agrees to indemnify and hold the University harmless from and against any loss, damage, cost, liability or expenses arising from copyright infringement or unauthorized usage.

IMPORTANT

If you have reasons to believe that any materials in this thesis are deemed not suitable to be distributed in this form, or a copyright owner having difficulty with the material being included in our database, please contact lbsys@polyu.edu.hk providing details. The Library will look into your claim and consider taking remedial action upon receipt of the written requests.

FAULT DETECTION AND DIAGNOSIS

METHODS FOR BUILDING HVAC SYSTEMS

ZHAO YANG

Ph.D

The Hong Kong Polytechnic University

2013

The Hong Kong Polytechnic University

Department of Building Services Engineering

Fault Detection and Diagnosis Methods for Building HVAC Systems

Zhao Yang

A thesis submitted in partial fulfillment of the requirements

for the Degree of Doctor of Philosophy

May, 2013

CERTIFICATE OF ORIGINALITY

I hereby declare that this thesis is my own work and that, to the best of my knowledge and belief, it reproduces no materials previously published or written, nor material that has been accepted for the award of any other degree or diploma, except where due acknowledgement has been made in the text.

I also declare that the intellectual content of this thesis is the product of my own work, except to the extent that assistance from others in the project's design and conception or in style, presentation and linguistic expression is acknowledged.

_____(Signed)

_____Zhao Yang_____(Name of student)

Department of Building Services Engineering

The Hong Kong Polytechnic University

Hong Kong, P.R. China

May, 2013

"You need the willingness to fail all the time"

You have to generate many ideas and then you have to work very hard only to discover that they don't work. And you keep doing that over and over until you find one that does work.

- John W. Backus

ABSTRACT

Abstract of thesis entitled: Fault Detection and Diagnosis Methods for Building HVAC

Systems

Submitted by   :   Zhao Yang

For the degree of   :   Doctor of Philosophy

at The Hong Kong Polytechnic University in May, 2013

   Faults in Heating, Ventilation and Air-conditioning (HVAC) systems would lead to uncomfortable indoor environment, poor indoor air quality, occupant complains and energy waste. Fault detection and diagnosis (FDD) tools are helpful to detect and isolate faults timely. Therefore, they are essential for reliable indoor environment control, saving maintenance efforts, and eliminating the associated energy waste. There is a growing interest in developing FDD tools for HVAC systems. Over the last decades, a considerable amount of FDD methods have been developed for chillers, air handling units (AHUs) and variable air volume (VAV) terminals. However, there is still a lack of reliable, affordable and scalable solutions.

   The main objective of this PhD project is to develop enhanced and reliable FDD methods for HVAC systems in buildings. Firstly, a comprehensive literature review is made. Then, the methodologies of four FDD methods are proposed for different applications. The first two methods are improvements of conventional FDD methods. The latter two methods are new ones.

   A simplified model-based FDD method with its customization tool is proposed. It is preferable when there are limited fault-free data to train models. The basic idea is to

identify model parameters using limited training data, and then to generate benchmarks for fault detection using the calibrated models. It provides good applicability and convenience for actual applications. Based on this method, a simplified FDD strategy for centrifugal chillers is proposed. It adopts a simplified physical chiller model which can be calibrated using very limited operation or performance test data. Four schemes are developed to identify chiller model parameters based on available information and data from tests or from manufacturers. A new semi-physical sub-cooling model is adopted by the chiller model. Comparisons are made with four typical conventional FDD strategies using ASHRAE RP-1043 experimental data. The results show that this strategy has much higher detection and diagnosis ratios.

An enhanced statistical FDD method is proposed to enhance incipient fault detection and diagnosis performance of the conventional gray-box model-based methods. It is suitable when measurements are sufficient. Support vector regression (SVR) algorithm is adopted to improve accuracies of reference performance index (PI) models. It is a non-linear regression approach which is based on structural risk minimization from statistical learning theory. Exponentially weighted moving average (EWMA) control charts are introduced to detect faults in a statistical way to improve the ratios of correctly detected points. The EWMA control charts reduce the Type II error ratios through taking into account the time series information using the weighting factor. This method is applied to a centrifugal chiller FDD strategy and a system-level FDD strategy respectively. Results show that the chiller FDD performance is improved significantly, especially at low severity levels. For example, in the case of condenser fouling, the proposed strategy achieved the ratios of correctly diagnosed points of 7.7%, 45.2%, 60.7%

and 100.0% at four severity levels (SL-1 to SL-4) respectively at the confidence level of 99.73%. Using the conventional gray-box model-based method, this fault could not be correctly diagnosed at level SL-1, SL-2 and SL-3. The application on system-level fault detection is evaluated on a simulated commercial building at four severity levels and two uncertainty levels. Similar improvements are also observed.

A new pattern recognition-based FDD method is proposed using support vector data description (SVDD) algorithm. It is suitable when fault data are available. This method transforms the FDD problem as a typical one-class classification problem. The task of fault detection is to detect whether the process data are outliers of the fault-free class. The task of fault diagnosis is to find to which fault class do the process data belong. It overcomes shortcomings of available pattern recognition-based FDD methods in HVAC field. Evaluations are made using ASHRAE RP-1043 experimental data. It shows more powerful FDD capacity than other pattern recognition-based FDD methods, e.g., multi-class SVM-based FDD method and PCA-based fault detection method.

A generic diagnostic Bayesian network (DBN)-based FDD method is proposed to simulate the actual diagnostic thinking of HVAC experts. It has better performance than other FDD methods when the diagnostic information is uncertain and incomplete. It benefits to allow merging different types of knowledge and information from diverse sources. The structure of the DBN is a graphical and qualitative illustration of the intrinsic causal relationships among causal factors, faults and fault symptoms. The parameters of the DBN represent the quantitative probabilistic relationships among them. It is effective in diagnosing faults based on uncertain, incomplete and conflicting information. DBNs are developed for chiller FDD and VAV terminal FDD respectively.

A three-layer DBN is developed to detect and diagnose component faults in a 90-ton water-cooled centrifugal chiller as described in ASHRAE RP-1043. Only using measurements from building management system (BMS), the DBN has similar accuracy as rule-based chiller FDD methods when BMS measurements are complete. When BMS measurements are incomplete, the DBN still provides meaningful fault believes but rule-based chiller FDD methods fail to work. The diagnosis ratios are increased when evidences of nodes in additional information layer are used. Refrigerant overcharge and non-considerable gas can be correctly diagnosed with the help of evidences of nodes in additional information layer. A DBN is developed to detect and diagnose faults of the pressure independent VAV terminals in an office building located in Hong Kong. It is evaluated through conducting the ten typical VAV terminal faults on a dynamic simulation platform of an office building. All faults are correctly diagnosed with high confidences.

PUBLICATIONS ARISING FROM THIS THESIS

Journal Papers Published

Yang Zhao, Fu Xiao and Shengwei Wang. 2013. An intelligent chiller fault detection and diagnosis methodology using Bayesian belief network. *Energy and Buildings* 57, 278–288.

Yang Zhao, Shengwei Wang and Fu Xiao. 2013. A statistical fault detection and diagnosis method for centrifugal chillers based on exponentially-weighted moving average control charts and support vector regression. *Applied Thermal Engineering* 51: 560–572.

Yang Zhao, Shengwei Wang and Fu Xiao. 2013. Pattern recognition-based chillers fault detection method using support vector data description (SVDD). *Applied Energy* (accepted).

Yang Zhao, Shengwei Wang and Fu Xiao. 2013. A system-level incipient fault detection method for HVAC&R systems. *HVAC&R Research* (accepted).

Yang Zhao, Shengwei Wang, Fu Xiao and Zhenjun Ma. 2012. A simplified physical model-based fault detection and diagnosis strategy and its customization tool for centrifugal chillers. *HVAC&R Research* (accepted).

Journal Papers Submitted or Prepared

Fu Xiao, Yang Zhao and Shengwei Wang. A diagnostic Bayesian network for variable air volume terminals fault detection and diagnosis. submitted to *Automation in Construction*.

Yang Zhao, Shengwei Wang and Fu Xiao. A robust pattern recognition-based fault detection and diagnosis (FDD) method for chillers. submitted to *Energy and Buildings*.

Yang Zhao, Jin Wen, Fu Xiao and Shengwei Wang. Diagnostic Bayesian networks for air flow subsystems of air handling units, prepared for submission.

Conference Papers

Yang Zhao, Shengwei Wang and Fu Xiao. 2012. A novel fault detection strategy for centrifugal chiller based on support vector data description (SVDD). International Conference on Applied Energy (ICAE2012), SuZhou, China.

Yang Zhao, Shengwei Wang and Fu Xiao. 2012. A system-level incipient fault detection and diagnosis strategy for HVAC system based on EWMA control charts. International Conference on Building Energy and Environment (COBEE 2012), Colorado, USA.

ACKNOWLEDGEMETNS

TABLE OF CONTENTS

LIST OF FIGURES

LIST OF TABLES

NOMENCLATURE

Notation

A	tube surface area (m^2) /matrix
AI	Impeller exit area (m^2)
C	penalty weight/ specific heat capacity (kJkg^{-1}K^{-1})
C1- C6	Coefficients of evaporator and condenser heat transfer formulae
C7-C9	Coefficients of sub-cooling section heat transfer formula
D	distance to hypersphere center
F	air flow rate (L/s)/ high dimensional feature space
ff	Thermal resistance including tube resistance and fouling (m^{2}KkW^{-1})
h	Heat transfer coefficient (kWm^{-2}K^1)
L	width of the control limits/ sampling interval (s)
LCL	lower control limit
M	Mass flow rate (kgs^{-1})
n	amount of data in a sample group
N	Data set tested in normal condition
P	supply air pressure (Pa)
PCS	principal component subspace
PI	performance index
Q	cooling load/ cooling capacity (kW)
q	width parameter of Gaussian kernel
Q	Chiller cooling load or heat transfer rate (kW)/ Q-statistic value
R	radius

R^2	R-square
SL	Severity level
SPD	speed control signal
SPE	squared prediction error
T	temperature (°C)
TCA	condenser approach temperature (K)
TEA	evaporator approach temperature (K)
U2	Impeller tip peripheral speed (m s^{-1})
UA	overall heat transfer conductance (WK^{-1})
UCL	upper control limit
W	power (W)
W1	Chiller power losses (kW)
x	vectors of variables
Y	performance index value
Z	EWMA value

Subscripts

act	actual value in practice
cd	condenser or condensing
cd,cd	condensing section in the condenser
cd,sc	sub-cooling section in the condenser
chw	chilled water
chwr	returning chilled water

chws	supplying chilled water
cl	Cooling water
cond	condenser
cw	condensing water
design	design value
ecw	entering condenser water
ev	evaporator or evaporating
evap	evaporator
exh	extremely high
exl	extremely low
expect	expected value
fault	fault condition
frozen	frozen fault
i	Inside
in	entering
leaking	leaking fault
m	measured value
ma	mixed air
max	maximum
min	minimum
o	Outside
oa	outdoor air
out	leaving

position	position of air damper
r	Refrigerant or refrigerant side
ra	return air
ref.	reference model/performance index
reset	reset-point
sa	supply air
sc	sub-cooling
set	set-point
sh_dis	refrigerant discharge superheat
sh_suc	refrigerant suction superheat
t1, t2	temperature threshold (K)
w	water or water side
zone	zone concerned

Greek symbols

α	Lagrange multiplier/ Normalized heat transfer coefficient
α'	normalized heat transfer coefficient of a data set
β	impeller vane angle
γ	coefficient for calculating chiller power consumption
ε	error threshold/ heat exchanger efficiency
ζ, Ψ1, Ψ2	coefficients for calculating compressor hydrodynamic losses
θ	threshold
λ	opening (0-100%)/ weighting factor
μ	expectation
ξ	random error of regression/ slack variable
σ	standard deviation/ expectation

| ψ | currently available evidences |
| ϕ | nonlinear mapping |

Acronyms

AHU	air handling unit
ASHRAE	American Society of Heating, Refrigerating and Air-Conditioning Engineers
APAR	AHU performance assessment rules
BBN	Bayesian network
BMS	Building Management System
CdFoul	condenser fouling
CuSum	cumulative sum
DBN	diagnostic Bayesian network
EWMA	exponentially weighted moving average
ExOil	excess oil
HVAC	heating, refrigerating and air-conditioning
kNNDD	k-nearest neighbor data description
MLR	multiple Linear Regression
Ncg	non-condensable gas
OCSVM	one-class support vector machine
PCA	principle component analysis
RedEvW	reduced evaporator water flow rate
RedCdW	reduced condenser water flow rate
RefOver	refrigerant overcharge
RefLeak	refrigerant leakage
SVDD	support vector data description
SVR	support vector regression
SVM	support vector machine

CHAPTER 1 INTRODUCTION

1.1 Motivations

Buildings contribute to about 20%-40% worldwide energy consumption in developed countries (Pérez-Lombarda et al. 2008). Significant amount of energy is wasted in the case of design problems, operation faults, equipment and control system performance degradation and malfunction. Mills (2009) concluded that the median whole-building energy through commissioning savings were 16% in existing non-residential buildings and 13% in new construction, and more than a quarter of investigated buildings saved in excess of 30%. Similar conclusions can be found in Cibse (2000), Claridge et al. (2000), Liu et al. (2003), Katipamula and Brambley (2008), etc.

Heating, Ventilation and Air-conditioning (HVAC) systems contribute to a significant portion of energy consumption in buildings. For instance, it is estimated that HVAC systems consume about 40-60% of total electricity consumption in buildings in sub-tropical climates by an early energy audit and site survey by Lam and Chan (1995). Faults in HVAC systems would lead to uncomfortable indoor environment, poor indoor air quality, occupant complains and energy waste. Fault detection and diagnosis (FDD) are helpful to detect and isolate faults timely. They are essential for reliable indoor environment control, saving maintenance efforts, and eliminating the associated energy waste. Figure 1.1 illustrates the energy savings by monitoring-based commissioning with the help of FDD tools. This figure originally derives from Mills' report (Mills 2009). Modifications are made to show contributions of FDD tools.
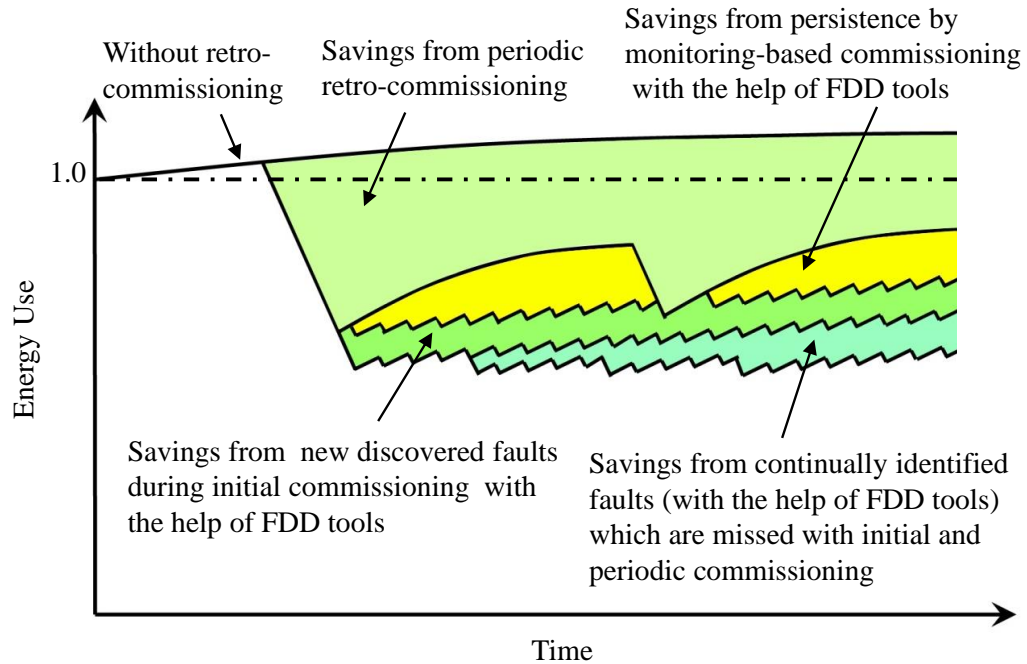
Figure 1.1 The role of FDD tools in monitoring-based commissioning

The development of FDD tools in HVAC field has been an active area of research for more than two decades. However, there is still a lack of reliable, affordable and scalable solutions (Najafi et al. 2012). FDD researchers have recognized challenges in developing FDD tools for HVAC systems:

Firstly, there are generally very few sensors equipped. Only the necessary sensors to control the components/systems are commonly installed (Qin and Wang 2005). It is data rich but information poor. The measurements are generally insufficient which makes it difficult to detect and diagnose faults. What is worse, the measurements are often not accurate due to low quality sensors and poor maintains.

Secondly, some faults may be propagated by control loops, which lead to complex relationships between faults and symptoms (Xiao 2004). For instance, supposing that supply air temperature sensor in an AHU is faulty with a positive bias in summer, the

control signal to the cooling coil will increase to maintain the supply air temperature at the set-point. This fault would be hidden if both supply air temperature and indoor air temperature are maintained at their set-points. If this fault is detected, it is hard to exclude the suspected faults using limited measurements, e.g., cooling coil fouling, heating coil valve leakage, cooling coil valve stuck, chilled water leakage and undersized cooling coil, etc.

Thirdly, extra complexities are added for the number of different types of equipment and lack of standardized control sequences (Schein 2006).

FDD is usually a complex inference process to map the symptoms to faults in fault diagnosis. In most cases, one fault may result in multiple symptoms, and meanwhile different faults may result in similar symptoms. Due to above challenges, it is still a difficult task to develop reliable, affordable and scalable FDD tools for HVAC systems.

1.2 Aim and Objectives

The aim of this PhD thesis is to develop enhanced and reliable FDD methods for HVAC systems in buildings. Conventional FDD methods will be comprehensively surveyed firstly. Then, new solutions will be proposed through addressing the following four objectives:

i. Develop a simplified model-based FDD method with its customization tool. The basic idea is to identify model parameters using limited training data, and then to generate benchmarks for fault detection using the calibrated models. It is suitable when there are limited fault-free data to train models.

ii. Develop an enhanced statistical FDD method to detect and diagnose incipient faults. The basic idea is to improve accuracy of reference models and to reduce Type II error ratios (more details refer to *Section 3.2.2*). It aims to improve performance of conventional gray-box model-based methods.

iii. Develop a new pattern recognition-based FDD method to overcome shortcomings of available pattern recognition-based FDD methods. The basic idea is to transform the FDD problem as a typical one-class classification problem. It is suitable when data are rich and fault data are available.

iv. Develop a generic FDD framework to merge different types of knowledge and information from diverse sources. The basic idea is to simulate the actual diagnostic thinking of HVAC experts. The outstanding achievements of previous publications can be integrated into the framework in an information fusion way. It is suitable to deal with incomplete or even conflicting information.

Finally, the four methods will be demonstrated and applied on chiller FDD, VAV terminal FDD and system-level FDD respectively.

The proposed methods belong to the marked categories respectively in Figure 1.2, according to the classification of FDD methods for HVAC systems (Katipamula and Brambley 2005a). The forth method (in objective iv) does not belong to any specified category since it can be used to merge methods of different categories.
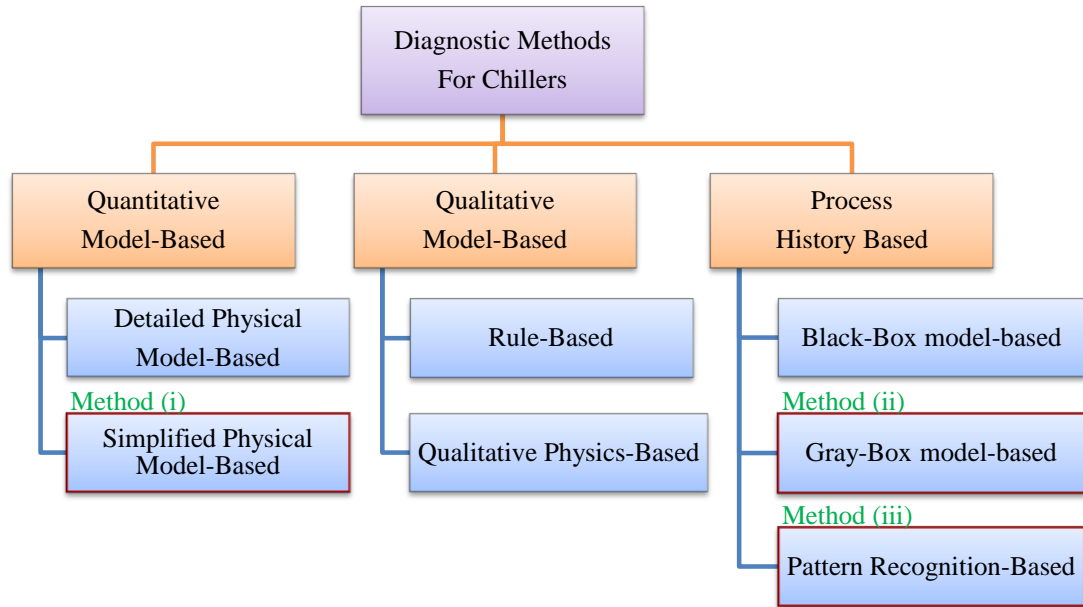
Figure 1.2 Classification of FDD methods in HVAC field

1.3 Organization of This Thesis

The organization of this thesis is shown in Figure 1.3.
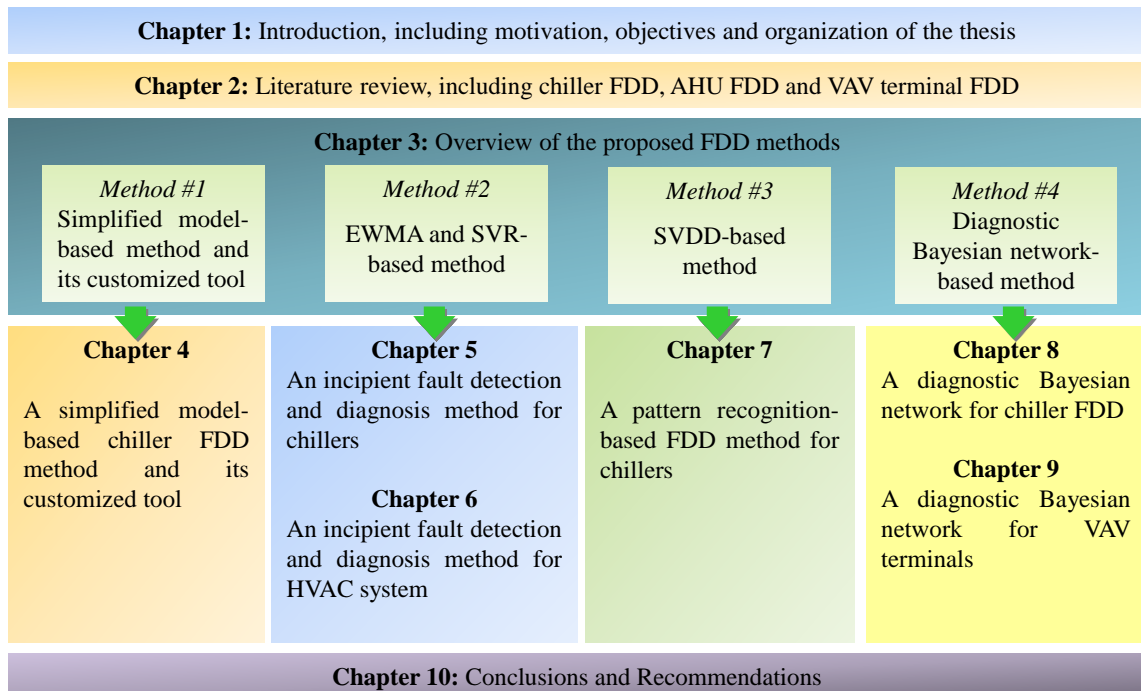
Figure 1.3 Organization of the thesis

This chapter represents the motivation and objectives of developing FDD methods for HVAC systems. The benefits of FDD methods are illustrated. The challenges of developing FDD methods are critically reviewed. Then, the objectives of this thesis are proposed. The organization of the other chapters is as follows.

Chapter 2 presents a comprehensive literature review about FDD methods for chillers, AHUs and VAV terminals.

Chapter 3 introduces the four proposed FDD methods, including a simplified model-based FDD method with its customization tool, an enhanced statistical FDD method to detect and diagnose incipient faults, a new pattern recognition-based FDD method and a generic FDD framework based on diagnostic Bayesian networks.

Chapter 4 presents the application of the simplified model-based FDD strategy with its customization tool for centrifugal chillers. It provides good applicability and convenience for actual applications. It adopts a simplified physical chiller model calibrated using very limited operation or performance test data.

Chapter 5 presents the application of the proposed incipient FDD method on centrifugal chillers. It is to propose a robust statistical FDD strategy suitable for the detection and diagnosis of chiller faults at low severity levels. Three innovations are adopted to overcome the shortcomings of the conventional gray-box model-based chiller FDD strategies.

Chapter 6 presents the application of the proposed incipient FDD strategies on system-level incipient faults in HVAC systems. It is an improvement on the system-level FDD strategy proposed by Zhou et al. (2009a). Three typical

subsystems/component are considered in this chapter, i.e. cooling tower system, chillers and heat exchanger system.

Chapter 7 presents the application of the proposed SVDD-based FDD strategy on centrifugal chillers. It considers the chiller FDD problem as a typical one-class classification problem. Fault-free data is considered as fault-free class. Each type of fault is considered as an individual fault class. The task of fault detection is to detect whether the process data are outliers of the fault-free class. The task of fault diagnosis is to find which fault class does the process data belong to.

Chapter 8 presents the application of the proposed diagnostic Bayesian network on centrifugal chiller. A three-layer diagnostic Bayesian network is developed to diagnose chiller faults.

Chapter 9 presents the application of the proposed diagnostic Bayesian network on VAV terminals. It is evaluated through conducting the ten typical VAV terminal faults on a dynamic simulation platform of an office building.

Chapter 10 summaries the work reported in this thesis, and provides recommendations for further application and research in the related area.

CHAPTER 2 LITERATURE REVIEW

This chapter presents a comprehensive literature review on FDD researches for HVAC systems. It mainly focuses on researches in the last decade, especially the last ten years.

Section 2.1 presents a literature review on chiller FDD methods, including physical model-based methods in *Section 2.1.1*, gray-box model-based methods in *Section 2.1.2*, and pattern recognition-based methods in *Section 2.1.3*.

Section 2.2 presents a literature review on AHU FDD methods. The methods concerned by most researchers are reviewed in details, i.e. rule-based methods in *Section 2.2.1*, gray-box model-based methods in *Section 2.2.2*, and pattern recognition-based method in *Section 2.2.3*.

Section 2.3 presents a literature review on VAV terminal FDD methods. There are few researches conducted on this topic in the last decades. Detailed literature reviews on the rule-based methods are presented.

2.1. Literature Review on Chiller FDD Methods

Over the last decades, there have been many publications concerning chiller FDD methods, e.g., Grimmelius el al. (1995), Stylianou (1997), Rossi and Braun (1997), Bailey (1998), McIntosh (1999), Jia and Reddy (2003), Wang and Cui (2005), Reddy (2007a; 2007b), Zhou et al. (2009a; 2009b), Han et al. (2012), etc. Detailed literature reviews on this subject can be found in the papers of Comstock et al. (2002), Reddy et al. (2001), Dexter and Pakanen (2001), Katipamula and Brambley (2005a; 2005b), Xiao et

al. (2009). ASHRAE has processed several projects to develop chiller FDD methods, such as ASHRAE Projects RP-1043 (Comstock and Braun 1999a; Comstock and Braun 1999b), RP-1139 (Reddy et al. 2001), RP-1275 (Reddy 2006) and RP-1486 (Li and Zhao 2011).
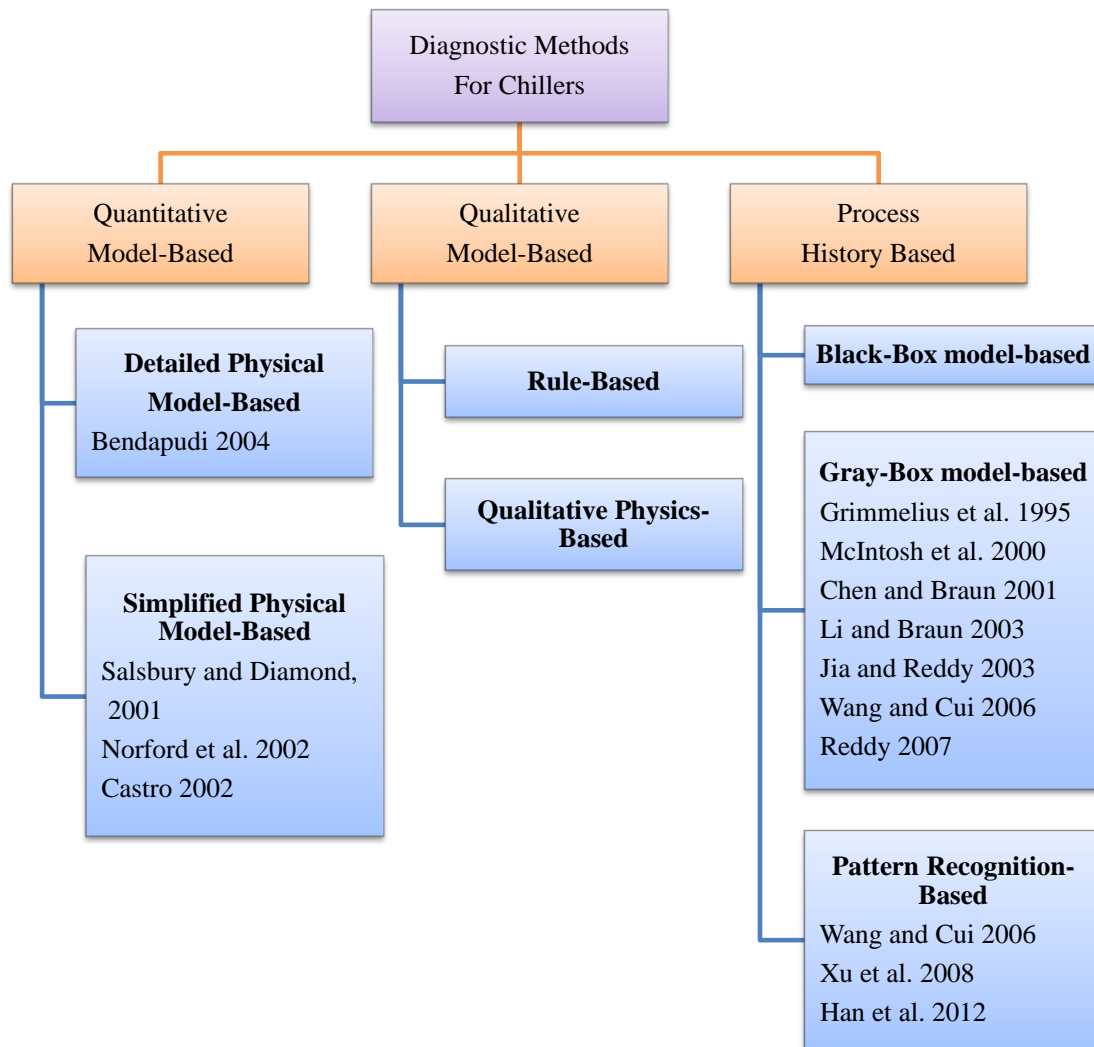
Figure 2.1. A brief classification of chiller FDD methods

The project RP-1043 made valuable efforts in generating a series of fault test data on a laboratory centrifugal chiller. A dynamic chiller model was developed for the performance simulation of fault-free and faulty chillers. RP-1139 aimed at evaluating

9

the mathematical models and developing an on-line training technique. An evaluation methodology was proposed by RP-1275 for chiller FDD methods. Four typical FDD methods were evaluated using steady-state performance data. The project RP-1486 evaluated the effectiveness of three typical FDD methods for centrifugal chillers online in laboratory and field environments.

Chiller FDD methods can be classified into three categories according to the comprehensive classification scheme by Katipamula and Brambley (2005a), as shown in Figure 2.1. A new subcategory, i.e. pattern recognition-based FDD method, is added here since more publications of this topic were found in recent years. Detailed literature reviews on the most commonly used methods are presented, i.e., physical model-based methods in *Section 2.1.1*, gray-box model-based methods in *Section 2.1.2*, and pattern recognition-based methods in *Section 2.1.3*.

2.1.1 Physical Model-Based Chiller FDD Methods

Physical model-based FDD methods include quantitative model-based methods and qualitative model-based methods. There are two kinds of physical chiller models, i.e. detailed chiller models and simplified physical chiller models. Detailed chiller models are developed on the basis of detailed information on component parameters and control loops. They can simulate some typical chiller faults (Bendapudi 2004). However, when the detailed chiller model is applied to other chillers, it will need a lot of detailed information on the chillers concerned involving serious efforts. Simplified physical chiller models are easy to be calibrated while providing major functions as detailed chiller models.

Compared with the gray-box model, simplified physical chiller models can provide more information - such as internal variables of the refrigeration process for the needs of various FDD schemes. There are some simplified physical chiller models such as the Primary HVAC Toolkit (Bourdouxhe et al. 1999), McIntosh et al.'s model (2000), Wang and Wang's model (2000). They do not include the prediction of the sub-cooling temperature, which is a necessary performance index (PI) in most of the chiller FDD methods. There are very few publications on using simplified physical chiller model for chiller FDD applications so far.

2.1.2 Gray-Box Model-Based Chiller FDD Methods

There are more publications about gray-box model-based chiller FDD methods. Typical works can be found at Grimmelius et al. (1995), McIntosh et al. (2000), Chen and Braun (2001) and Li and Braun (2003), Jia and Reddy (2003), Cui and Wang (2005) , Reddy (2007a, 2007b, 2007c).

Generally, these methods are developed as the following steps: 1) Reference PI models development. It is generally on the basis of linear regression algorithm-based models, e.g., MLR (Multiple Linear Regression) algorithm. 2) Confidence intervals (thresholds) calculation. They are usually gained through the *t*-statistic approach at a certain confidence level, e.g. 4.6% false alarm. 3) Fault detection. The residuals between benchmark PIs and current ones are calculated. A fault is detected as soon as the residuals are out of the confidence intervals. 4) Fault diagnosis. The fault is diagnosed according to the fault pattern rule table. The lessons learnt from the success of these methods can be concluded as follows. Firstly, the performance indexes (also named

11

characteristic quantities or characteristic parameters in some studies) can account for existing chiller faults efficiently. Secondly, the statistical approaches are introduced to detect faults, which can properly handle the uncertainties of both model-fitting errors and measurement errors. In the end, the expert knowledge is used to diagnose fault using rule tables.

The low severity level is defined in this thesis as the level at which chiller performance is affected slightly. The available methods failed to detect and diagnose chiller faults at low severity levels (SL). For instance, the ratios of correctly diagnosed points were 0%, 0%, 0% at SL-1 and 25%, 0%, 0% at SL-2 respectively for the refrigerant leakage, condenser fouling and excess oil in Cui and Wang (2006). The MLR and t-statistic-based method in AHSRAE RP-1275 was reported that the ratios of correctly diagnosed points were 3.7%, 0%, 0% at SL-1 and 7.4%, 0%, 0% at SL-2 the refrigerant leakage, condenser fouling and refrigerant overcharge respectively (Reddy 2007a). It means that the operators have to wait for the fault alarms until the fault archives at a serious severity level. Obviously, significant amount of energy might have been wasted. The chiller might have been damaged. Hence, removing faults at low severity levels is crucial for chiller maintenance and costs saving.

The linear regression algorithm and t-statistic-based methods have better FDD performance among all chiller FDD methods (Reddy 2006). It is valuable to analyze the reasons which might contribute to their poor FDD performances at low severity levels:

i.   The Type II errors in the *t*-statistic-based approaches. Generally, a fault is detected when the residuals of PIs are outside of the confidence intervals. However, the

12

residuals are still within the confidence interval at the low severity levels. This is the Type II error (more details can be found in *Section 3.2.2*).

ii. The accuracy of linear regression algorithm-based reference models. They have better accuracy than physical models in most of conditions. It is widely used, e.g., RP-1043 (Comstock and Braun 1999a; Comstock and Braun 1999b), Cui and Wang (2006), etc. However, chillers are typical non-linear systems. The accuracy can be improved using non-linear regression algorithms. The accuracy is important to the width of confidence interval. The lower the accuracy is, the wider the confidence interval will be, and then the FDD performance will be poor.

iii. The improper performance index for the condenser fouling. The condenser fouling has similar fault patterns with the refrigerant overcharge and non-condensable gas. To distinguish it with other faults, it is generally assumed that the deviation of sub-cooling temperature is within conference intervals or a positive value. Actually, the deviation is sometimes positive (mostly in low severity levels) and sometimes negative (mostly in serious severity levels), as shown in RP-1043 data. Such assumptions always lead to higher false diagnosis ratios.

2.1.3 Pattern Recognition-Based Chiller FDD Methods

Pattern recognition is the science of making inferences based on data. In the HVAC field, the pattern recognition-based methods, which are of the category of history-based methods, have been attracting researchers' attentions in recent years.

Principle component analysis (PCA) is the dominant algorithm among the pattern recognition algorithms in HVAC field. PCA can be used to detect fault using statistical

13

analysis, and to diagnose sensor faults using reconstruction algorithm. It has been applied to air handling unit sensor FDD (Du and Jin 2007; Du et al. 2008; Wang and Xiao 2004), variable air volume system sensor FDD (Du et al. 2007a, 2009a, 2009b), air distribution loop FDD (Xiao et. al 2006), system level FDD (Zhou et al. 2009a; Du et al. 2007b). Chen and Lan (2009) found that PCA-based fault detection method is applicable and effective to detect faults in air-source heat pump water chiller/heaters. Wang and Cui (2006) introduced PCA to detect and diagnose chiller sensor faults. Their method consisted of a model-based chiller FDD scheme and a sensor fault detection, diagnosis, and estimation (FDD&E) scheme, which handle chiller faults and sensor faults, respectively. The sensor FDD&E scheme uses a PCA-based method to capture the correlations among the major measured variables in centrifugal chillers, as it performs well even in the presence of typical chiller faults. The two parameters in PCA-based methods, i.e. the selected component count and the confidence level, are easy to be arranged. Therefore, the PCA-based methods are feasible to be applied. PCA-based methods have estimations that variables are Gaussian distributed and linear. Their FDD accuracy reduces when the ranges of variables are wider. Such estimations could not be satisfied. For instance, the experimental data in RP-1043 are highly non-Gaussian distributed, non-linear and wide-range distributed (as shown in *Chapter 7*).

Han et al. (2012) introduced support vector machine (SVM) algorithm to detect and diagnose chiller component fault. The chiller FDD problem is considered as a multi-class classification problem. The correct diagnosis ratios are generally over 90%, which are obviously higher than that of the conventional methods. Multi-class classification algorithms generally aim to classify an unknown object into one of several pre-defined

14

categories. A problem arises when the test data does not belong to any of those categories, as discussed by Khan and Madden (2010). The multi-class SVM-based chiller FDD works well when the fault data of all faults are available. If the full-set fault data are not available, the multi-class classification algorithms might be not robust (detail analysis can be found in *Chapter 7*).

Pattern recognition-based FDD methods benefit to adopt powerful algorithms which are derived from artificial intelligence field. Compared with conventional FDD methods, the pattern recognition-based FDD methods have following advantages: Firstly, the pattern recognition-based methods are flexible to be applied, which can save time and efforts significantly. It just needs to retrain the data-driven models using new data. They do not require the developers to have a deep understanding of the physics of the chillers concerned. It is not necessary to develop chiller models to generate benchmark data. Secondly, they have better FDD performance than conventional methods. They learn fault patterns from fault-free data and fault data. A well-trained pattern recognition-based model can effectively distinguish data of different classes, even when the changes of variables caused by faults are small or even tiny. Thirdly, the pattern recognition-based methods may still work well when some important variables are not available. They could learn fault patterns which might still be uniquely represented by the limited variables. Most of conditional FDD methods could not work in such situations. Finally, the pattern recognition theories and algorithms are mature, with a wealth of documented information and tools available. The tools are generally accessible from open-source software packages. Developers can focus on the applications of the algorithms rather than coding the algorithms themself. The fault-free data are usually easy to be obtained

from building management systems or on-site tests. When there are only fault-free data, the pattern recognition-based FDD methods could have better fault detection performance than conventional methods.

Pattern recognition-based FDD methods have following weaknesses: firstly, most models cannot be used to extrapolate beyond the range of the training data; secondly, a large amount of training data is needed, representing both normal and "faulty" operation; thirdly, the models are specific to the system for which they are trained and rarely can be used on other systems. Fault data are necessary if the pattern recognition-based methods are used for the purpose of fault diagnosis.

2.1.4 Discussions and Recommendations

Model-based methods are preferable when the training data are not enough. First-principle physical models consist of priori knowledge about chiller systems. It benefits to overcome the shortage of training data and to utilize more information (e.g., physical-meaningful parameters) in the models. For instance, parameters of the simplified physical chiller model of Wang and Wang (2000) can be identified using very limit of test data from tests or from manufacturers. A simplified physical model-based and customization FDD tool can be developed to provide good applicability and convenience for actual applications.

Gray-box model-based methods are suitable when there are sufficient training data. Generally, gray-box models could obtain better accuracy than physical models. Statistic approaches could be introduced to detect and diagnose incipient fault using the abundant of data. The major difference between model-based methods and gray-box model-based

16

methods is that how the benchmark models are developed. They do not need fault data for fault diagnosis since fault patterns can be obtained through first-principle analysis.

Pattern recognition-based methods are suitable to diagnose fault when fault data are available. They are new solutions for chiller FDD. The research on pattern recognition-based methods is still very limited.

2.2. Literature Review on AHU FDD Methods

AHU FDD has been attracting most of the attentions of FDD researches in HVAC field. A considerable amount of research has been carried out in the field of FDD in HVAC systems over the last decades, e.g., quantitative model-based methods (Xu et al. 2005; Seem and House 2009; Li 2009; Wang et al. 2012), rule-based methods (House et al. 2001; Schein, 2006; Schein et al. 2006; Li et al. 2012), gray-box model-based methods (Norford et al. 2000; Yoshida et al. 2001; Shaw et al. 2002; Lee et al. 2004; Fan et al. 2010; Brambley et al. 2011), data-driven methods (Wang and Xiao 2004; Xiao et al. 2006; Du et al. 2007a; Xiao et al. 2009; Najafi et al., 2012; Wall et al., 2011), as a brief classification in Figure 2.2.

The most widely researched subcategories are reviewed in details, i.e. rule-based methods in *Section 2.2.1*, gray-box model-based methods in *Section 2.2.2*, pattern recognition-based method in *Section 2.2.3*.
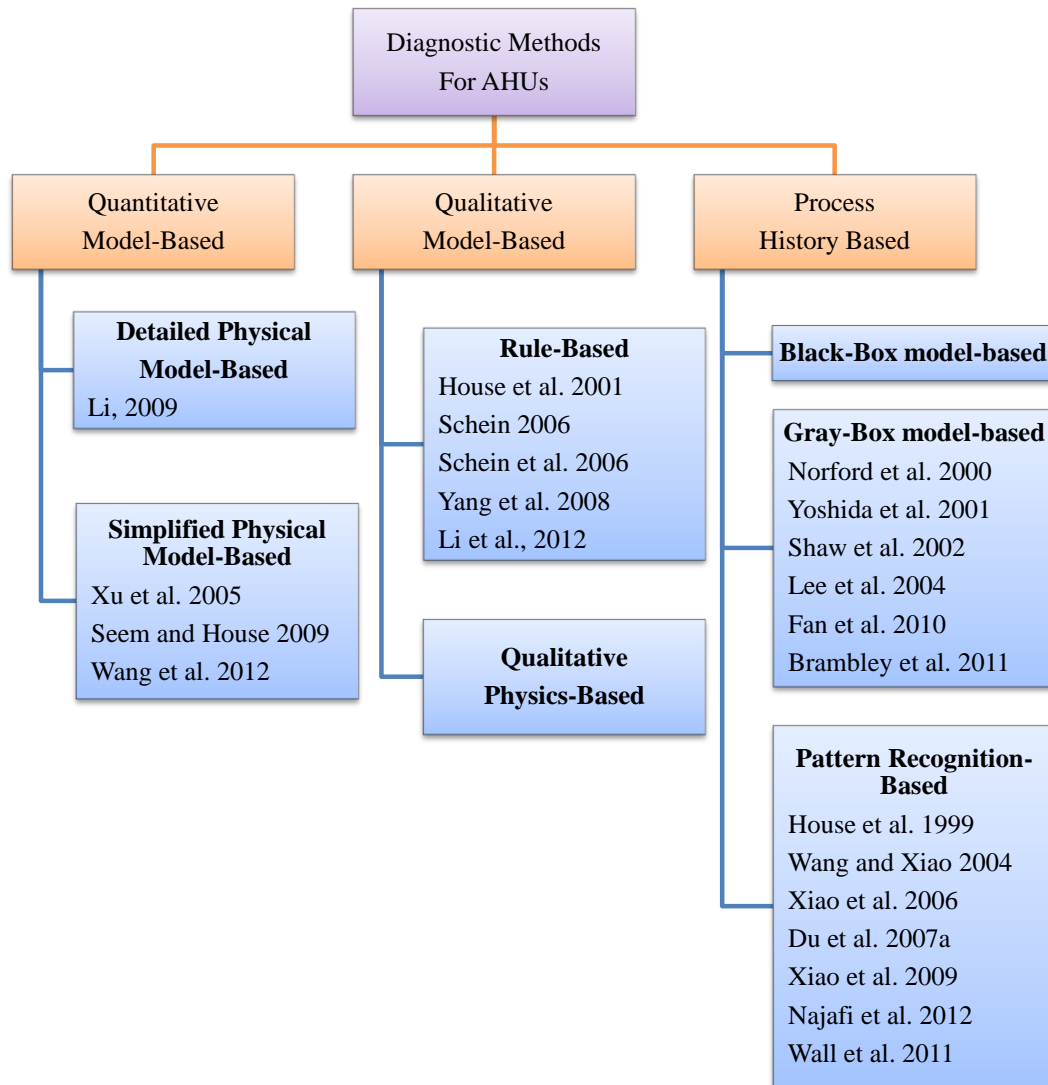
Figure 2.2 A brief classification of AHU FDD methods

2.2.1 Rule-Based AHU FDD Methods

The rules in the rule-based methods are generated from expert knowledge/experience and first-principle. The rule-based methods use *if…then…* logic or fault pattern tables to diagnose fault.

Schein et al. (2006) proposed a comprehensive set of AHU performance assessment rules (APAR) to detect AHU faults. There are 28 pieces of rules which derived from mass and energy balances. Each rule is expressed as a logical statement to indicate the presentence of a fault. Four subsets of the rules are applied to four modes because the mass and energy balances are different for each operating mode. There are also some rules which are independent of the operating mode. As discussed by Yang et al. (2008), the APAR rules can only be used to detection fault. They proposed sequential rule based algorithms for temperature sensor fault detection in AHUs which is an extended application of APAR rules. However, the method would be not robust when component faults occur. It also has to declare that some rules will not be avoided only when fault severity levels are high.

The main advantage of rule-based methods is that they are easy to apply. However, the simplicity of the methods is lost quickly as problem complexity grows or when new/additional rules are added (Katipamula and Brambley 2005a; Brambley et al. 2011; Najafi et al 2012). The rule-based methods do not consider uncertainties in AHU FDD. They require the measurements used in rule sets for diagnosing a fault are complete. They could not diagnose faults when some measurements are missing or unavailable. They only provide Boolean results, i.e. a fault exists or not. Actually, due to the uncertain and incomplete information, it is more reasonable to provide probabilities of faults than Boolean results. The fuzzy logic algorithm is a suitable solution for reasoning under uncertainty. However, as the problem complexity grows, a large number of fuzzy sets and fuzzy rules are required, which lead to the difficulty on adjusting and tuning fuzzy sets (Najafi et al 2012).

2.2.2 Gray-Box Model-Based AHU FDD Methods

Different from physical model-based AHU FDD methods, the gray-box model-based methods used regression algorithms to develop reference models. Then, the deviations between predicted values and benchmarks were used to detect fault. A main advantage is that the model is easier to be developed.

Norford et al. (2002) and Shaw et al. (2002) described models which are gray-box correlations of electrical power with exogenous variables such as airflow or motor speed, e.g., correlations of fan power with air flow rate, correlations of chilled-water pump power with cooling-coil valve position. The method showed advantages compared with first-principle model-based methods. Brambley et al. (2011) introduced similar models in their self-correcting controls for VAV system faults filter/fan/coil and VAV box sections. Electrical power responses fast to dynamics in systems which can be accurately measured. Such electrical power correlation models generally have high accuracy.

Lee et al. (2004) introduced general regression neural-network (GRNN) to develop four reference models corresponding to the supply-air temperature control system, the mixed-air temperature control system, the static-pressure control system, and the airflow difference control system. For instance, the predicted cooling coil valve control signal is a function which is regressed by supply air temperature, mixed air temperature, mixed air humidity ratio and supply air flow rate. Similarly, Yang et al. (2012) proposed a method to detect supply air temperature sensor fault in AHUs using support vector regression (SVR) algorithm. A main difference from the electrical power correlation models is that they need more measurements. These measurements are not as accurate as

20

electrical power measurements and also do not response fast to dynamics. The false FDD risk is higher since the FDD results would be totally wrong when any measurement is faulty. No comprehensive on-site tests were provided to validate their robustness in these publications.

2.2.3 Pattern Recognition-Based AHU FDD Methods

House et al. (1999) demonstrated the application of several classification algorithms on AHU FDD, i.e., k-nearest neighbor classifier, k-nearest prototype classifier, artificial neural network classifier, rule-based classifier and Bayes classifier. The Bayes classifier had the best performance at fault detection. The rule-based classifier had the best performance at fault diagnosis.

Wang and Xiao (2003; 2004) proposed PCA-based AHU sensor FDD method. Sensor faults are detected using the Q statistic (squared prediction error, SPE). They are isolated using the Q statistic and Q contribution plot supplemented by simple expert rules. Two models are employed to deal with the heat balance and pressure flow balance separately to reduce the effects of the system nonlinearity and to ensure the PCA method's validity in different control modes. The fault isolation ability of the PCA method is also improved using the multiple models. Evaluations showed that the PCA-based strategy was effective to monitor instrumentations and detect/isolate AHU sensor faults under typical operating conditions. Wang and Xiao (2006) further improved the PCA-based sensor FDD method using condition-based adaptive scheme to follow the normal shifts in the process due to changing working conditions, where the outdoor air temperature and humidity are selected to represent the outdoor operating conditions. The

scheme overcomes the shortcomings of the time-based adaptive scheme and improves the detectability of the PCA-based sensor FDD method in detecting slowly developing faults. Rules are built to determine the time when the PCA models need to be updated. PCA models generated in the adaptive process are stored in a model database. Du and Jin (2008) used PCA and Fisher discriminant analysis (FDA) to detect and diagnose multiple faults diagnosis for sensors in AHUs. The PCA-based sensor FDD methods are efficient and effective to detect and diagnose sensor faults. Due to their pure data-driven nature, additional solutions should be made to correctly isolate sensor faults when the sensors are adopted in control loop. And, PCA-based FDD methods also need solutions to avoid false diagnosis when component faults occur.

Najafi et al. (2012) proposed a static Bayesian Networks-based AHU method in machine learning way. It is based on analysing the observed behaviour of the system and comparing it with a set of behavioural patterns generated based on various faulty conditions. The FDD problem is formulated as an estimation of the posterior distribution of a Bayesian probabilistic model. Wall et al. (2011) used dynamic Bayesian network to learn the behaviour of AHU in fault and fault-free conditions. Compared with classifier-based method (House et al., 1999) and PCA-based method, the Bayesian network-based machine learning method can take into consideration more physical meanings into the structure of Bayesian network.

As discussed in *Section 2.1.3*, the pattern recognition-based FDD methods are suitable when full-set fault data are available. When only fault-free data are available, pattern recognition-based methods have good fault detection performance only.

2.2.4 Discussions and Recommendations

The main challenge in AHU FDD is the lack of sensor quantity and quality. The current sensor system is designed for local control purposes. The BMS measurements are rich but information poor. The fault detection problem has been solved properly in publications. However, there are few fault diagnosis methods. Fault diagnosis is still a problem in AHU FDD field.

Fault diagnosis can be considered to be an information fusion problem. Fault diagnosis might be more efficient and reliable if all information is utilized. A variety of information resources besides sensor measurements are helpful for fault diagnosis, e.g. maintenance records, health status of related equipment, etc. For instance, AHU is at a higher risk of filter fouling if the filter has not been properly treated for a long time. If the ΔP_{filter} is larger at a certain F_{sa}, the filter fouling fault is more suspected than the fault that F_{sa} sensor is positive biased. The features of measurements in the time dimension are also useful for diagnosis. For instance, a sensor is at higher risk of frozen fault if its value has not changed for 2 hours, especially at starting period and power off period. Conditional AHU fault diagnosis methods always use sensor measurements at current time slice only. There is a lack of an effective mathematic method to fuse different kinds of information methodologically.

The incomplete and uncertain information leads to one of the main challenges in AHU fault diagnosis. Firstly, it is data rich but information poor. There are limited sensors equipped in AHUs due to cost considerations. Only the necessary sensors to control the equipment are commonly installed. The measurements are generally insufficient which makes it difficult to diagnose the faults. Secondly, various uncertainties exist in measurements and fault patterns, etc., which cause the fault

diagnosis results unreliable. The fault-symptom relationships are uncertain. The measurements are generally low qualities due to low quality sensors and poor maintains. One fault may result in a symptom at a certain probability. One piece of evidence (observed symptom) may support the existence of several faults at different probabilities. The FDD results would be more reasonable if they are presented in the form of probabilities of fault according to the available evidences and uncertainties, rather than Boolean results (i.e., Normal or Faulty) resulted from the conventional methods.

Passive AHU FDD methods only use available measurements/information of the AHU concerned. Different from passive FDD methods, the proactive FDD methods obtain some symptoms through disturbing the normal operating of AHUs (Brambley, et al., 2011). Proactive FDD methods are good solutions to diagnose faults when information is incomplete to identify faults. Passive FDD can provide suspected fault list for decision support which can make proactive FDD to be more effective. An action of passive FDD can be saved if the fault can be diagnosed only using passive FDD tools. An AHU can be divided to two subsystems, i.e. heating/cooling coil subsystem and air flow subsystem. The heating/cooling coil subsystem maintains supply air temperature at its set-point. The air flow subsystem provides the desired amount of air to room with designed amount of fresh air. In the air flow subsystem, the speed of supply fan is controlled to maintain statistic pressure set-point. The speed of return fan is controlled by sequence control strategies which are generally a function of supply fan speed or supply air flow rate. The positions of outdoor air (OA) damper, exhaust air (EA) damper and recirculation air (RA) damper are controlled to supply a desired flow rate of fresh

air. A fault might affect other components or be distributed by control logics, which make fault diagnosis to be a complex task.

2.3. Literature Review on VAV Terminal FDD Methods

Variable air volume (VAV) air conditioning systems are widely used in offices and commercial buildings nowadays. Building professionals usually consider that VAV systems have better performance in terms of thermal comfort and energy saving than fan coil unit systems and constant air volume systems. However, VAV terminals easily suffer from various faults which cause the performance of VAV systems hardly meet the high expectations. Qin and Wang found that 20.9% of 1251 VAV terminals were ineffective in a site survey conducted in a commercial building in Hong Kong (Qin and Wang, 2005). Preventive maintenance of VAV terminals is a difficult task since a large number of VAV terminals are installed above ceilings. FDD tools for VAV terminals are essential for reliable indoor environment control, saving maintenance efforts, and eliminating the associated energy waste. There are few researches conducted on FDD of VAV terminals in the last decades. Most of methods are rule-based, as shown in Figure 2.3.
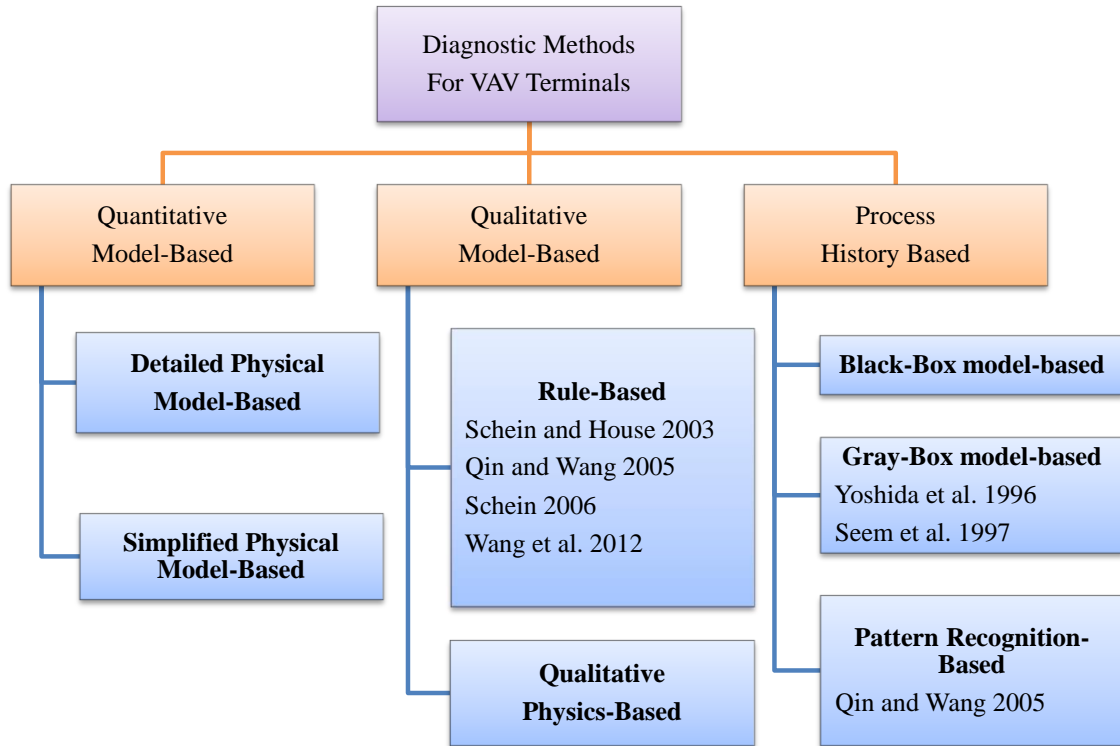
Figure 2.3 A brief classification of VAV terminal FDD methods

2.3.1 FDD Methods

Yoshida proposed an automatic regressive exogenous (RARX) model and an extended Kalman filter model to detect faults in a VAV unit and an Air Handling Unit (AHU) cooling coil system (Yoshida et al. 1996; Yoshida and Kumar 1999). Seem et al. described a set of indices to assess the performance of control loops and to detect faults in VAV terminals and AHUs. The performance indices were embedded in commercial VAV terminals controllers to quickly identify terminals that are not operating correctly (Seem et al. 1997; Seem et al. 1999). Schein proposed VAV Box Performance Assessment Control Charts (VPACC) to assess the performance of pressure independent VAV boxes with hydronic reheat coils. VPACC introduced a small number of CUSUM

charts to accumulate the error between a process output and the expected value of the output (Schein and House 2003; Schein, 2006). Most of the above-mentioned FDD methods for VAV terminals focused on fault detection and seldom considered fault diagnosis. Qin and Wang proposed a hybrid approach to diagnose ten typical faults in VAV utilizing expert rules, performance indexes and statistical process control models to address these faults (Wang and Qin 2005). Principal Component Analysis (PCA) was used to detect flow sensor biases. Wang et al. designed a rule-based classifier consisting of a set of twenty expert rules and fault isolation algorithms to diagnose fifteen faults (Wang et al. 2012). It was able to diagnose faults using sensor data and control signals which are commonly available in building management systems (BMSs).

The above FDD methods for VAV terminals can normally provide good results; however, they rarely considered the realistic situation where only uncertain and incomplete information is available for conducting FDD. Uncertainties widely exist in measurements, symptoms, fault-symptom relationships, expert knowledge, FDD results, etc. For instance, a fault may exist with certain probability when a symptom is observed. It is more reasonable to give the probabilities of faults at given symptoms in FDD results. However, most existing FDD methods report the FDD results in the Boolean format, i.e. *Yes/Present* and *No/absent*. In addition, due to the limited number of measuring instruments, incomplete records of system design and operation data, insufficient memory capacities of control stations and building automation systems, etc., the information available for conducting FDD is incomplete. These FDD methods might not work properly using incomplete information. Furthermore, some useful information, which is very helpful in FDD, was often overlooked. For instance, the prior probabilities

of the temperature sensor fault and the damper actuator failure are 25.3% and 3.8% respectively (Qin and Wang 2005). When a VAV terminal is abnormal, the possibility of the temperature sensor fault is much higher than that of the damper actuator failure. Such prior experience about faults has seldom been used in exiting FDD methods.

2.3.2 Discussions and Recommendations

FDD experts have recognized more challenges in FDD of VAV terminals are facing: Firstly, there are generally very few sensors equipped in VAV terminals. The information is extremely insufficient which makes it difficult to diagnose the faults (Qin and Wang 2005). Secondly, faults may be propagated by control loops, which lead to complex relationships between faults and symptoms. Thirdly, limitations associated with controller memory and communication capabilities further complicate the task (Schein 2006). Fourthly, the number of different types of VAV boxes and lack of standardized control sequences add extra complexities (Schein 2006). Fifthly, a large number of VAV terminals are usually installed above ceiling. There is almost no preventive maintenance (Wang et al. 2012).

It is recommended to make use of expert knowledge/experiences to overcome the information poor problems.

2.5 Summary

Comprehensive literature reviews are made about chiller FDD methods, AHU FDD methods and VAV terminal FDD methods. In the methodology point of view, each kind of method has its own suitable applications.

Physical model-based methods are preferable when the training data are not sufficient. It is possible to develop easy-to-use FDD methods with customization tools under training data poor situations. There is a lack of such tools for practical application. Gray-box model-based methods are suitable when training data are sufficient. They might fail to detect incipient faults due to the Type II errors. Pattern recognition-based methods are suitable to diagnose fault when fault data are available. It is a new research topic. There is still a long way to go before practical applications. Rule-based methods are suitable when model-based methods are not applicable. Their simplicities would be lost quickly when problem is complex. They are also lack of capacity to present uncertainties in FDD process.

The development of FDD tools in the HVAC field has been an active area of research for more than two decades. However, there is still a lack of reliable, affordable and scalable solutions. It indicates that essential innovations are more necessary rather than improving conventional methods.

CHAPTER 3 AN OVERIEW OF THE PROPOSED FDD METHODS

This chapter presents the methodologies of the four proposed FDD methods:

Section 3.1 presents a simplified model-based FDD method with its customization tool. The basic idea is to identify model parameters using limited training data, and then to generate benchmarks for fault detection using the calibrated models.

Section 3.2 presents an enhanced statistical FDD method for the detection and diagnosis of incipient faults. Support vector regression (SVR) algorithm is adopted to improve accuracies of reference PI models. Exponentially weighted moving average (EWMA) control charts are introduced to detect faults in a statistical way to improve the ratios of correctly detected points. It overcomes shortcomings of conventional gray-box model-based methods.

Section 3.3 presents a new pattern recognition-based FDD method. Support vector data description (SVDD) algorithm is introduced to transform the FDD problem as a typical one-class classification problem. The task of fault detection is to detect whether the process data are outliers of the fault-free class. The task of fault diagnosis is to find to which fault class do the process data belong. It overcomes the shortcomings of the available pattern recognition-based FDD methods in HVAC field. It also brings about some new potential applications.

Section 3.4 presents a generic diagnostic Bayesian network (DBN)-based FDD method to simulate the actual diagnostic thinking of HVAC experts. The structure of the

DBN is a graphical and qualitative illustration of the intrinsic causal relationships among causal factors, faults and fault symptoms. The parameters of the DBN represent the quantitative probabilistic relationships among them. It is effective and efficient in diagnosing faults based on uncertain, incomplete and conflicting information.

3.1 Simplified Model-Based FDD Method with Customization Tool

Simplified models are easier to be calibrated, unlike detailed physical models. Compared with gray-box models, simplified models show ability being calibrated using limit of training data due to their physical meaningful natures. Therefore, simplified model-based FDD method is preferable in training data-poor situations. For instance, this method has the capability to calibrate a chiller model using manufacturer's catalogue data only. It is meaningful in detecting and diagnosing a chiller when no fault-free data are available.

3.1.1 Customization Tools for Simplified Models

Effective customization tools should be developed to identify the unknown parameters in the simplified models. For instance, Wang and Wang (2000) proposed a simplified chiller model based on the basic principles of chillers to ensure the reliability and accuracy of the model in a wide working range. The parameters are identified using limited performance test data. Four schemes are proposed to identify chiller parameters for four different situations. Similar works can be found in the Primary HVAC Toolkit (Bourdouxhe et. al, 1999). Such models could provide good applicability and convenience for actual applications.

3.1.2 Schematic of The Simplified Model-Based FDD Method

The basic idea of the simplified model-based FDD method is to identify model parameters using limited training data, and then to generate benchmarks for fault detection using the calibrated models. The structure is shown in Figure 3.1. It includes two processes, i.e. online FDD and offline model training.
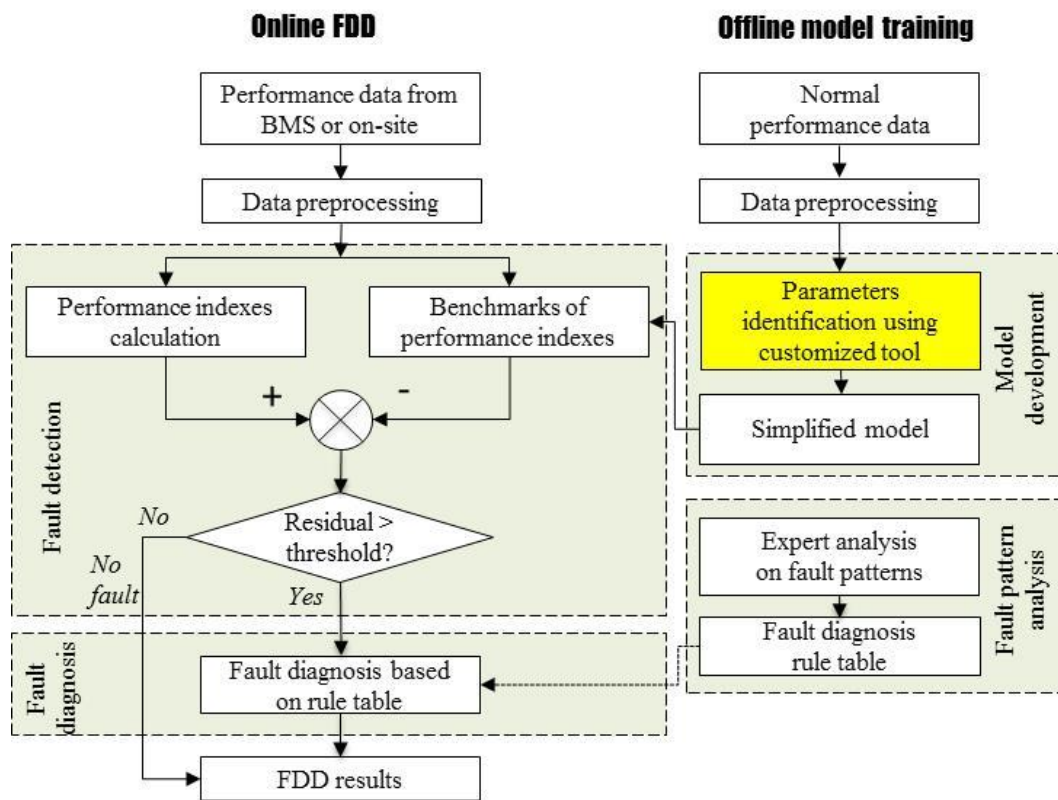
Figure 3.1 Flow chart of the simplified model-based FDD method

The offline model training process consists of three steps including: data processing, model parameter identification, and fault pattern analysis. The obvious outlying and dynamical data are removed in the step of data pre-processing if the data are obtained from BMS history databases. Then, parameters are identified using customization tool.

The fault diagnosis rule table is generated based on expert knowledge/experiences through analyzing fault patterns.

In the online FDD, the steps of data pre-processing is the same as that in the model training. The benchmarks of performance indexes are calculated using the simplified models. A fault is detected if the residuals between the current PIs and benchmark values are larger than their thresholds. Then, process of fault diagnosis will be activated employing the FDD rule table.

3.2 Incipient Fault Detection Method

As discussed in *Section 2.1.2*, the gray-box model-based methods show advantages when there are enough training data. Gray-box models were more widely used than physical models. Generally, gray-box models could obtain better accuracy than physical models. Even so, they could not detect some incipient faults effectively. There are two main reasons: firstly, the adopted gray-box algorithms are linear while HVAC systems are generally non-linear. The accuracy of reference models can be improved. Secondly, the residuals between predicted values and benchmarks are too small leading to high Type II error ratios when fault severity level is low. An incipient fault detection and diagnosis method is proposed in this chapter to overcome these two shortcomings.

3.2.1 Performance Index Model Development

Reference performance index (PI) models are developed to generate benchmark value for fault detection. There are many methods to develop PI models, e.g., quantitative physical model-based methods, qualitative model-based methods, black-

box/gray-box model-based methods, etc. Among them, the gray-box model-based methods are most widely used.

The gray-box reference PI models are developed as shown in Equation (3.1) (Cui and Wang 2006). Where, Y is PI, f is the regression function, $X_1, X_2, \ldots, X_n$ are the variables of a subsystem, and ξ is the model error, $\xi \sim (0, \sigma^2)$.

$$Y = f(X_1, X_2, \ldots, X_n) + \xi \tag{3.1}$$

The selection of inputs $(X_1, X_2, \ldots, X_n)$ is significant to the model performance. The selection should be able to determine the unique operating conditions for a certain component/subsystem. Meanwhile, the selection should not be affected by typical component/subsystem faults.

The models can be developed using algorithms like MLR, ordinary least squares (OLS), artificial neural network (ANN), auto-regressive moving average (ARMA), etc. MLR and ANN are the most adopted algorithms. As discussed in *Section 2.1.2*, MLR-based PI models are based on estimation that the HVAC systems are linear. However, most of HVAC systems are nonlinear. The disadvantages of ANN are that the number of hidden layers is difficult to choose and that the calculation may fall into a local minimum.

To improve the accuracy of PI models, a non-linear approach, namely support vector regression (SVR), is proposed to build the reference models. It is a new machine learning algorithm based on structural risk minimization from statistical learning theory. It possesses prominent advantages such as excellent properties in learning limited samples, good generalization ability, etc. It is proven that SVR has outstanding

performance according to the comprehensive comparisons of SVR with other regression approaches, as concluded in the previous publications, such as Park et al. (2010), Esen et al. (2008), Paniagua-Tineo et al. (2011) and Wang et al. (2010). More details can be found in Schölkopf et al. (1999).

3.2.2 Incipient Fault Detection Methods

In statistical test theory, there are two kinds of errors, i.e. Type I error and Type II error. Specialized to the FDD problem, a Type I error occurs when the FDD method rejects the normal data (i.e. detects normal data as faulty data), as the yellow part in Figure 3.2. A Type II error occurs when it fails to reject the fault data (i.e. fails to detect faulty data), as the green part in the figure.
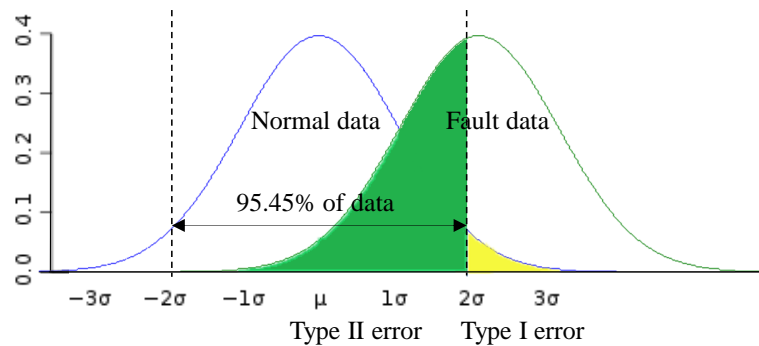
Figure 3.2. Illustration of Type I error and Type II error in the t-statistic based fault detection method

The *t*-statistic is widely used in the FDD methods in HVAC field, as described in *Section 3.3.2.1*. It is easy to be applied. The main shortcoming is that the Type II error might be too high to detect incipient fault. In this chapter, EWMA control charts are

introduced to solve such a problem, as described in *Chapter 3.1.2.2*. Comparisons between two methods will be shown in *Chapter 5* and *Chapter 6*.

3.2.2.1 *t*-Statistic-Based Fault Detection

The *t*-statistic was introduced in 1908 by Gosset (Fisher Box 1987). It is a ratio of the departure of an estimated parameter from its notional value and its standard error. It is used in hypothesis testing like Student's *t*-test, computation of certain confidence interval, etc. In the FDD methods for HVAC systems, *t*-statistics of residuals between predicted values and its benchmarks can be estimated to have asymptotically the standard normal distribution. Generally, the empirical rule can be introduced as a simple test for outliers. For instance, about 68.27%/95.45%/99.73% of the normal data lie within $\pm 1\sigma/\pm 2\sigma/\pm 3\sigma$ of the mean μ respectively, as shown in Figure 3.2. Cui and Wang (2006) introduced an online adaptive scheme to estimate and update the thresholds for detecting abnormal PIs. The adaptive scheme also introduced *t*-statistic approach.

In the *t*-statistic-based FDD methods, the confidence intervals are determined to reach a small yellow part (the Type I error) to reduce false alarm ratio, e.g. 2σ at 95.45% confidence level. However, when a fault occurs, the faulty data within the green part are also considered as normal ones (the Type II error). Particularly for the condensing fouling and refrigerant leakage at low severity levels, the deviations of the actual distributions from distributions in normal conditions are so small that most of them cannot be detected.

3.2.2.2 Exponentially Weighted Moving Average Control Chart-Based Fault Detection

In the field of statistical process control, the control charts are used to determine whether or not a process is in a state of statistical control. There are two well-known control charts for detecting small-magnitude shifts, i.e. CuSum (Cumulative Sum) and EWMA. Both are effective to detect the changes as small as one standard deviation. They are widely used in the FDD fields. For instance, Qin and Wang (2005), Wang et al. (2011) proposed FDD methods for VAV air-conditioning systems using CuSum control charts. Thomson et al. (2000) introduced EWMA control charts for the early detection of fouling of the heat recovery system. In this study, EWMA control charts are selected for the reason that the EWMA value is physically meaningful and can be used for FDD in a quantitative way.

The EWMA control chart was originally proposed by Roberts (1959) for detecting small shifts. It introduces a constant weighting factor λ ($0 < \lambda \leq 1$) to determine the importance of current group mean ($\bar{X}_i$) as defined in Equation (3.2).

$$Z_i = \lambda \bar{X}_i + (1-\lambda) Z_{i-1} \tag{3.2}$$

where, Z_i is the ith EWMA value, $Z_0 = \mu_0$. $\bar{X}_i$ is mean of ith sample group which has constant size n, $\bar{X}_i = (y_{ni} + y_{ni-1} + \ldots + y_{n(i-1)+11})/n$ is value of the ith observation. It is easy to show that Z_i is a weighted average of $\bar{X}_i, \bar{X}_{i-1}, \ldots, \bar{X}_1$:

$$Z_i = \lambda \bar{X}_i + \lambda(1-\lambda)\bar{X}_{i-1} + \lambda(1-\lambda)^2 \bar{X}_{i-2} + \ldots + \lambda(1-\lambda)^{i-1} \bar{X}_1 + (1-\lambda)^i \mu_0 \tag{3.3}$$

Weights are decreasing with the age of observations. The weight for current group is the highest one. The weights for groups at the beginning of the time series are the lowest.

It is meaningful to chiller FDD since the newest observations have more information about faults. The control limits are determined using Equation (3.4) and (3.5).

$$UCL = \mu_0 + L\sigma \sqrt{\frac{\lambda}{n(2-\lambda)}} \tag{3.4}$$

$$LCL = \mu_0 - L\sigma \sqrt{\frac{\lambda}{n(2-\lambda)}} \tag{3.5}$$

where, UCL is the upper control limit. LCL is the lower control limit. L is the width of the control limits, which determines the confidence limits (for instance, when L=3, 99.73% of the plotted points should fall within the control limits in normal conditions). The EWMA control chart takes into account the time series information using the weighting factor λ. It considers the behaviors of a set of observations rather than one (unlike t-statistic) to determine whether the process is abnormal. Therefore, it is sensitive to smaller long-term changes. Compared with t-statistic approach, the Type II error ratio is reduced. The fault detection methods using t-statistic approach only use the information of the current data. This feature makes it relatively insensitive to small shifts when a fault occurs.

3.2.3 Schematic of The Incipient Fault Detection Method

The structure of the proposed FDD method is as shown in Figure 3.3. It includes two parts, i.e. online chiller FDD and offline model training.
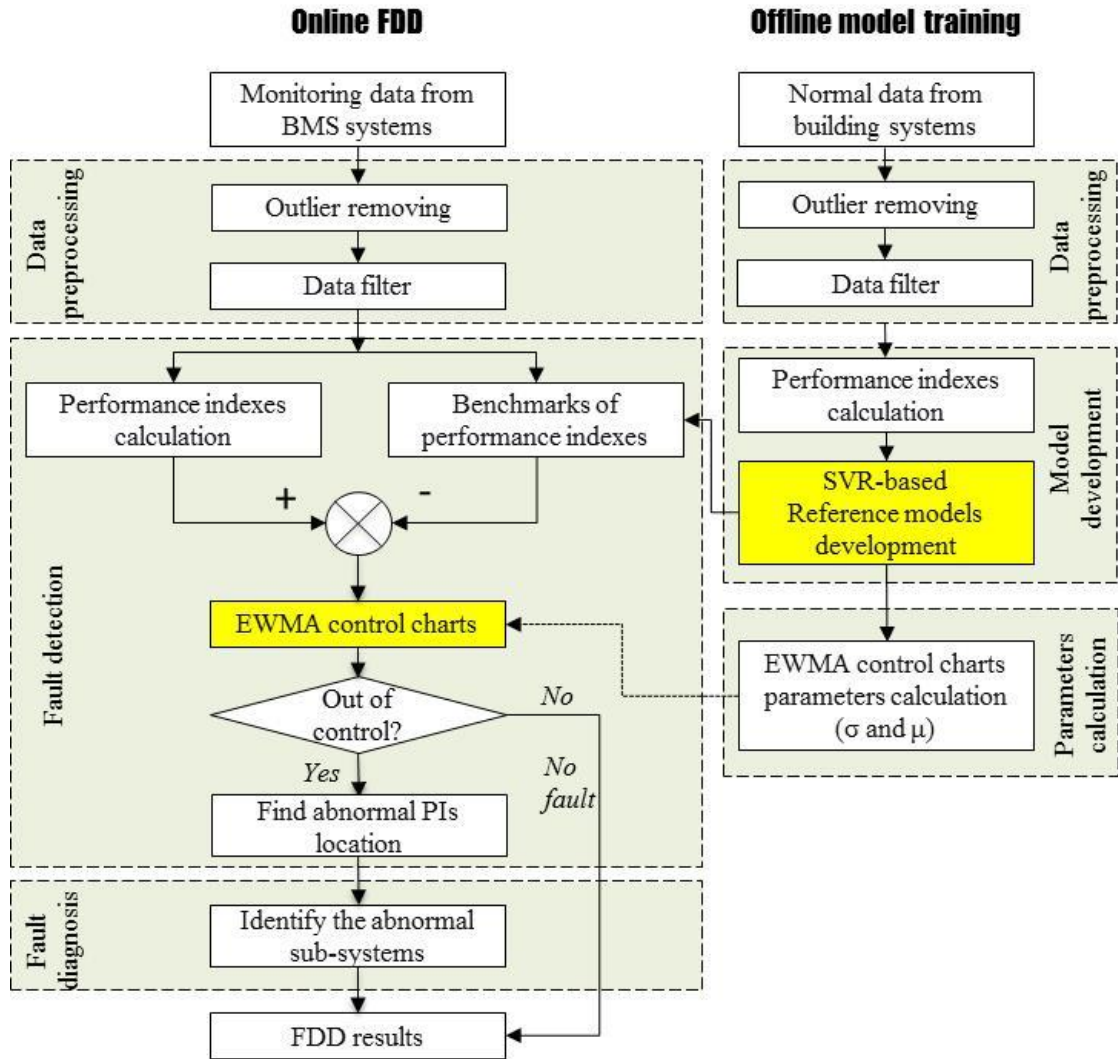
Figure 3.3. Flow chart of the incipient fault detection and diagnosis method

The offline model training consists of four steps. In the step of data pre-processing, the obvious outlying and dynamical data are filtered by the outlier detector and steady-state data filter respectively. In the step of performance indexes calculation, the four PIs are calculated using the filtered data. In the next step, SVR is adopted to develop the reference models. In the last step, the statistical characters of the reference models are

calculated, i.e. μ (the expectation) and σ (the standard deviation), which are the requirements of the EWMA model.

In the online FDD part, the steps of data pre-processing and PIs calculation are the same as that in the offline model training part. The benchmarks of performance indexes are calculated using the reference models. Then the residuals between the current PIs and benchmark values are calculated, which are inputs of the EWMA control charts. If a fault is detected, it is further diagnosed using the rule table.

3.3. Pattern Recognition-based FDD Method

Fault detection is a typical one-class classification problem. For instance, chiller measurements on the fault-free conditions are very easy and cheap to be obtained, e.g. from building management systems or on-site tests. However, the measurements on the fault conditions (e.g., chillers work with faults), would be very expensive. One-class classification algorithms show powerful capacity to solve such problem. Some one-class classification algorithms have been developed in the last decade, e.g. support vector data description (SVDD), one-class support vector machine (OCSVM), k-nearest neighbor data description (kNNDD), etc. (Tax 2012). SVDD was originally proposed by Tax and Duin in 1999 for the one-class classification problem (Tax and Duin 1999; Tax and Duin 2004), as described in *Section 3.3.1.2*. It has been successfully adopted to fault detections, e.g., microrobotic system monitoring (Cho et al. 2006), bearing performance degradation assessment (Pan et al. 2009), bath process monitoring (Ge and Gao 2011), pump failure detection (Tax and Duin 1999), analog circuit faults detection (Luo et al.

2011), semiconductor etch process motoring (Mahadevan and Shah 2009), etc. Most of studies focus on SVDD-based fault detection (process motoring).

In this Section, a SVDD-based FDD method is proposed, as described in *Section 3.3.2*. To evaluate the advantages of this method, the other two pattern recognition-based methods are also described in *Section 3.3.1*. Comparisons among these three methods are described in *Chapter 7*.

3.3.1 Pattern Recognition Algorithms in FDD Applications

3.3.1.1 Support Vector Machine

SVM is based on the structural risk minimization principle rooted in the statistical learning theory. Its basic idea is to transform the data to a higher dimensional feature space and find the optimal hyperplane in the space that maximizes the margin between the classes (Cristianini and Shawe-Taylor 2000). Given a two-classes training set $S = \{(x_1,y_1), (x_2,y_2),...,(x_n,y_n)\}$, where, x_i is input vector, and y_i is their class label, $x_i \in R^d$, $y_i=\{-1,1\}$, $i = 1,...,N$. Supposed Fault A is class -1 and Fault B is class +1, the classification of two classes using SVM is illustrated in Figure 3.4. SVM tries to the optimal hyperplane in Equation (3.6) and Equation (3.7):

$$\langle w \cdot x \rangle + b = 0 \tag{3.6}$$

$$y_i(w \cdot x + b = 0) \geq 1, i = 1,...,N \tag{3.7}$$

where, $w \in R^n(x)$ is the normal to the optimal hyperplane. b is a scalar threshold. By solving the constrained optimization problem of minimizing $\|w\|$, the optimal hyperplane can be found. With the use of Lagrange multipliers α_i, the training process

41

is to solve a convex quadratic problem. where, $0 \leq \alpha_i \leq C$, $C > 0$ is a penalty constant

(also called slack penalty). The solution is a unique globally optimized result, which has

the properties as Equation (3.8). where, x_i can be called support vector when the

corresponding $\alpha_i > 0$.

$$w = \sum_{i}^{N} \alpha_i y_i x_i \tag{3.8}$$

When the training process of SVM is completed, the decision function can be

defined as Equation (3.9).

$$f(x) = \text{sign}(\sum_{i=1}^{N} \alpha_i y_i (x \cdot x_i) + b) \tag{3.9}$$

For a linear non-separable case, kernel function $k(x_i, x)$ can be introduced to

perform a non-linear mapping of the input vector x from the input space into a higher

dimensional Hilbert space, as Equation (3.10).

$$f(x) = \text{sign}(\sum_{i=1}^{N} \alpha_i y_i k(x \cdot x_i) + b) \tag{3.10}$$
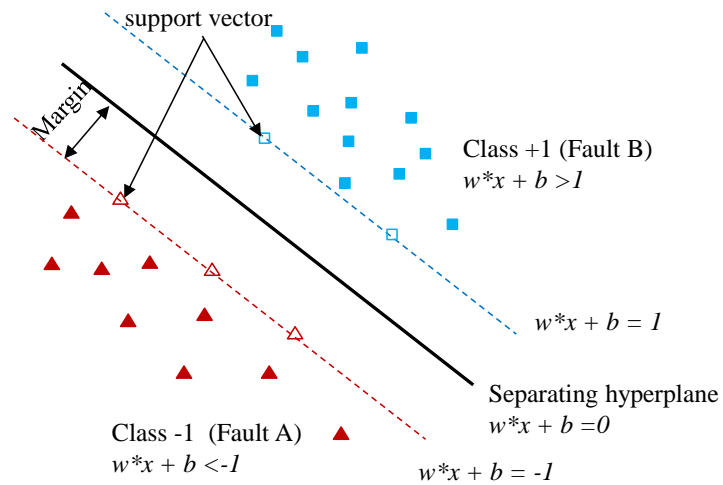
Figure 3.4. Illustration of two-class classification SVM for fault detection and diagnosis

42

In this study, Gaussian kernel function is selected because it has the best chiller FDD performance. The two parameters in SVM, i.e. C and γ (width parameter of Gaussian kernel), should be optimized to obtain better classification performance. There are generally more than two classes of chiller faults. The one-against-one (1-vs-1) algorithm, which constructs one two-class SVM between each pair of classes, is introduced in this study to solve this problem. It is proved to have slightly better performance than the one-against-all algorithm by Han et al (2012). A complete description about SVM can be found in Cristianini and Shawe-Taylor (2000).

3.3.1.2 Support Vector Data Description

Tax and Duin proposed the SVDD algorithm in 1999 (Tax and Duin 1999). Given a target object set $x_i \in R^d$, $i = 1,...,N$, the basic idea of SVDD is to find a minimum-volume hypersphere in high dimensional space with center a_F and radius D to enclose most of the objects, as Equation (3.11).

$$\text{Minimize } O_p(D, a_F, \xi) = D^2 + C \sum_{i=1}^{N} \xi_i$$

$$\text{Subject to } \|\phi(x_i - a_F)\|^2 \leq D^2 + \xi_i, \xi_i \geq 0 \; \forall i = 1, ..., N$$

$$(3.11)$$

where, C controls the trade-off between the volume of the hypersphere and the errors. ξ_i are slack variables which allows a probability that some of the training samples can be wrongly classified. ϕ is a nonlinear mapping which maps the input objects into a high dimensional feature space F. The dual problem of Equation (3.11) is as Equation (3.12). Where, $K(x_i, x_j)$ is the kernel function.

$$\text{Maximize } O_d(\alpha) = 1 - \sum_{i=1}^{N} \sum_{j=1}^{N} \alpha_i \alpha_j K(x_i, x_j)$$

$$\text{Subject to } \sum_{i=1}^{N} \alpha_i \; 0 \le \alpha_i \le C \;\; i = 1, \dots, N \;\; C \in [1/N, 1] \tag{3.12}$$

where, α is Lagrange multiplier. In this study, Gaussian kernel, $K(x_i, x_j) = \phi(x_i) \cdot \phi(x_j) = exp(-\|x_i - x_j\|^2/2\sigma^2)$, is selected. It is because Gaussian kernel has only one free parameter to be tuned and is shown to yield tighter boundaries than other kernel choices. According to the Kuhn-Tucker conditions, the objects can be classified into three categories: 1) the objects with $\alpha_i = 0$ are inside of the hypershphere; 2) the objects whose $0 < \alpha_i < C$ are on the hypershphere boundary; and 3) the objects whose $\alpha_i = C$ fall outside the hypershphere and have nonzero ξ_i. The objects with $\alpha_i > 0$ are the support vectors. Objects lying on the hypershphere boundary ($0 < \alpha_i < C$) are called unbounded support vectors. Objects lying outside the hypershphere ($\alpha_i = C$) are called bounded support vectors. The center can be expressed as Equation (3.13). And its radius D can be determined by utilizing the distance between a_F and any support vector x on the ball boundary (unbounded support vectors), as Equation (3.14). Finally, for the test object x, the output can be obtained by comparing its distance to the center a_F with radius D in F. The SVDD decision function is as Equation (3.15). where, $c = (1 - D^2) + \sum_{i=1}^{N_s} \alpha_i \alpha_j K(x_i, x_j)$ is a constant.
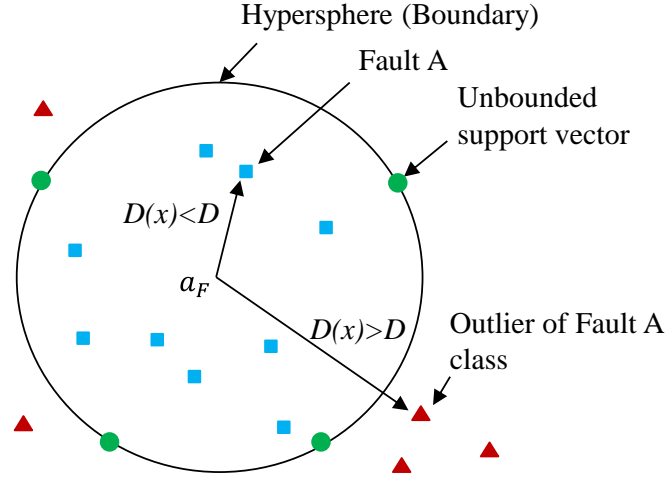
Figure 3.5. Illustration of SVDD sketch map in two dimensions for FDD

$$a_F = \sum_{i=1}^{N_s} \alpha_i \varphi(x_i) \tag{3.13}$$

$$D = (1 - 2\sum_{x_i \in SVs} \alpha_i K(x_i, x_k) + \sum_{x_i \in SVs} \sum_{x_j \in SVs} \alpha_i \alpha_j K(x_i, x_k))^{\frac{1}{2}} \tag{3.14}$$

$$D(x) = \|\varphi(x_i - a_F)\|^2 - D^2 = c - 2\sum_{i=1}^{N_s} \alpha_i K(x, x_i) \tag{3.15}$$

For the purpose of chiller fault detection in this study, a fault is detected when the real-time monitoring data x is rejected by fault-free class. For the purpose of chiller fault diagnosis, a fault is identified if the real-time monitoring data x is accepted by a fault class, as illustrated in Figure 3.5 in two dimensions. Fault A is the target class. If process data are within the hypersphere, this fault is detected and diagnosed. If not, this fault does not exist.

In this study, there are two parameters which are needed to be tuned, i.e. C and γ. C controls the tradeoff between the volume of the hypersphere and the classification error of the model. By changing the value of the width parameter $\gamma = 1/2\sigma^2$ in the Gaussian

kernel, the description transforms from a solid hypersphere to a Parzen density estimator (Ge et al. 2011). The smaller σ is, the tighter the decision boundary is.

3.3.1.3 Principle Component Analysis

PCA is the most widely used unsupervised multivariate statistical-analysis technique for dimension and feature extraction. It transforms a group of correlated variables into a new group of variables which are uncorrelated or orthogonal to each other. PCA separates the high dimensional space into a lower dimensional subspace capturing the systematic variations of the process and a subspace containing random noise. According to PCA, the measurement vector x of the process variables can be decomposed into two parts, as Equation (3.16). Where $\hat{x}$ is the modeled part which represents the projection on the principal component subspace (PCS), as Equation (3.17). $\tilde{x}$ is the un-modeled part on the residual subspace (RS), as Equation (3.18).

$$x = \hat{x} + \tilde{x} \tag{3.16}$$

$$\hat{x} = LL^T x = Ax \tag{3.17}$$

$$\tilde{x} = (1 - A)x = \tilde{A}x \tag{3.18}$$

With the respect to fault detection application of PCA, the Q-statistic can be used as an index of faulty conditions, which is also known as the squared prediction error (SPE). The Q-statistic measures the total sum of variation in the residual vector. Therefore, faults can be detected by using the Q-statistic, as Equation (3.19). Where, Q_θ is the threshold for the Q-statistic and can be statistically determined according to measurements of the training matrix.

$$Q\text{-statistic} = \text{SPE} = \|\tilde{x}\|^2 = x^T(1 - A)x \le Q_\theta \qquad (3.19)$$

When there is no fault, the correlations among the measurements of variables remain unchanged, the Q-statistic will be less than Q_θ. When a fault occurs, the correlations will be destroyed and value of Q-statistic will be higher. As soon as it exceeds Q_θ, a fault is detected. More details about PCA-based chiller fault detection can be found in Wang and Cui (2006), Cui and Wang (2006) and Xu et al. (2008).

3.3.2 Schematic of The SVDD-based FDD Method

In this study, SVDD algorithm is introduced to model the fault-free class and each fault class respectively. A fault is detected when the monitoring data are rejected by the SVDD-based fault-free class. A fault can be confirmed if the monitoring data are accepted by a SVDD-based fault class. An unknown fault is alarmed if the process data are rejected by fault-free class and all fault classes. Applications of the proposed SVDD-based FDD method includes two processes, i.e. offline models training and online FDD.

3.3.2.1 Offline training of SVDD models

In the process of offline models training, SVDD models are trained for fault-free class and each fault classes respectively, as illustrated in Figure 3.6.

Firstly, the process data are collected and pre-processed. Fault-free data and fault data are collected from historical database or on-site tests. The obvious outlying and dynamic data are filtered by an outlier detector and a steady-state data filter respectively. Then, the variables are properly selected. This step can be tried many times to get the best variable selection. The data of selected variables, including fault-free data and fault

data, are normalized to improve FDD performance. Finally, the pre-processed data are divided into two parts randomly, i.e. training data and test data.

Secondly, SVDD models are trained. The confidence level is assigned before model training, e.g. 95%. It means that the Type I error is 5% using the training data of its own class. The two parameters, i.e. C and γ, are optimized through cross-validation.
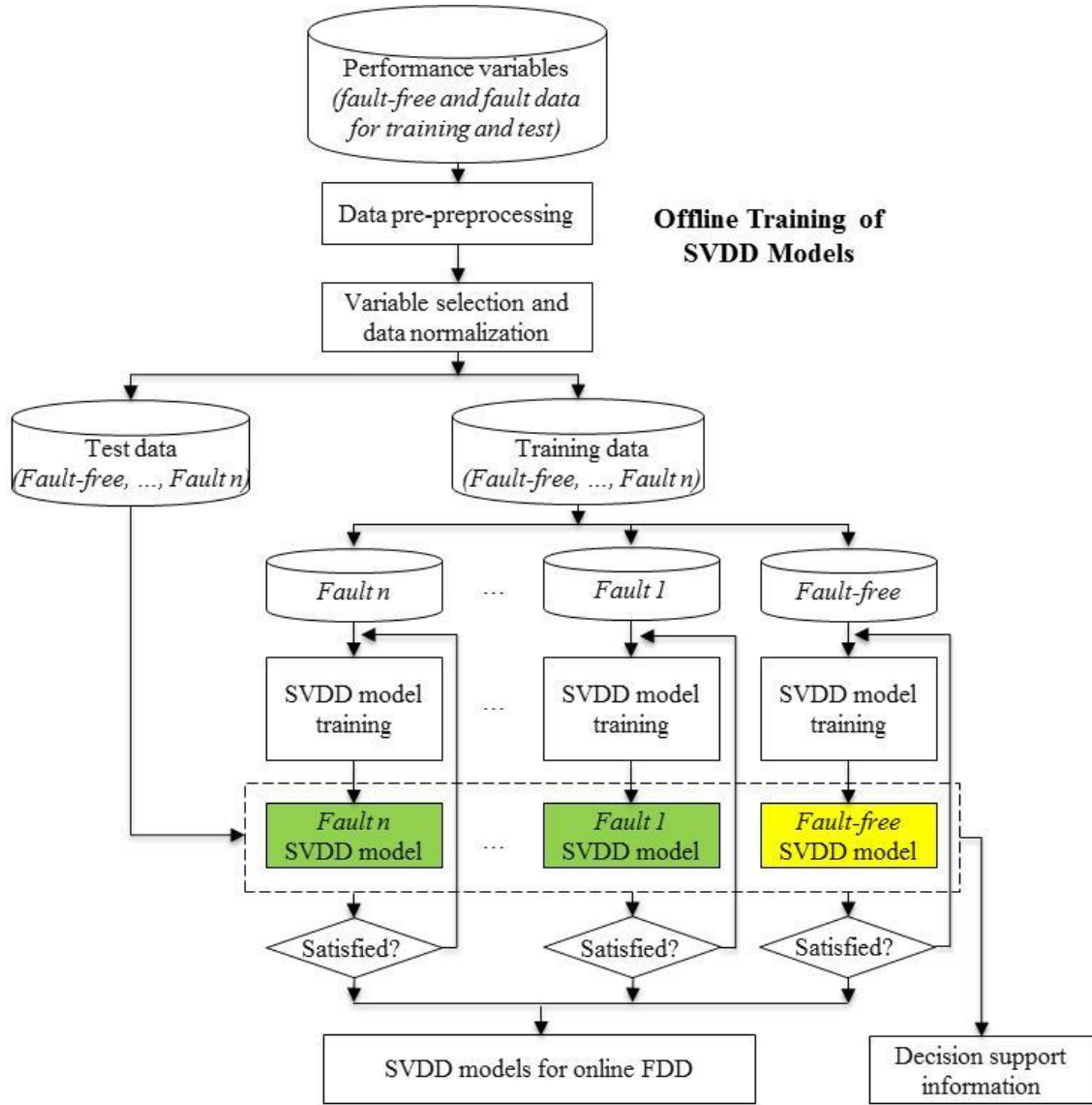
Figure 3.6 Flow chart of the offline SVDD models training

Thirdly, the models are validated using test data. False diagnosis occurs when a SVDD model falsely identifies data of its own class to be outliers (Type I error), or falsely identifies fault data to be inliers (Type II error). For each model, the Type I error should be lower than 5% when it is validated using test data of its own class. If not, the model is retrained through adjusting the two parameters until it satisfies the requirement. A good model should reject data of other classes efficiently. The Type II error should be as small as possible. However, it might be high when some data of two classes are undistinguishable. All models are validated using test data of other classes. The Type II error ratios are acceptable when they are lower than a threshold, e.g. 60%. If Type II error ratio is higher than the threshold, the SVDD model is retrained through adjusting the two parameters. In such condition, the Type I error ratio can be increased, e.g. 10%.

3.3.2 SVDD-based online FDD method

In the process of online FDD, the SVDD models are used to detect and diagnose fault, as illustrated in Figure 3.7.

Firstly, the real-time data are pre-processed the same as the offline model training process, i.e. data pre-processing, variable selection and data normalization. Secondly, the fault-free SVDD model is used to detect fault. The chiller is healthy if the data belong to the fault-free class. A fault is detected if the data are outliers of fault-free class. Then, the data are diagnosed using all fault SVDD models. A fault is identified if the data belongs to any fault classes. If not, an unknown fault is reported. At last, the FDD results are inputted to the decision support module. The decision support function calculates the ratios that the data belong to fault-free class and each fault class within a

moving window. If the fault-free ratio is larger than a threshold (e.g. 90%), the chiller is fault-free. If not, it is abnormal. The one with the largest fault ratio is the most suspected fault. A fault is reported if its ratio is larger than a threshold (e.g. 75%).
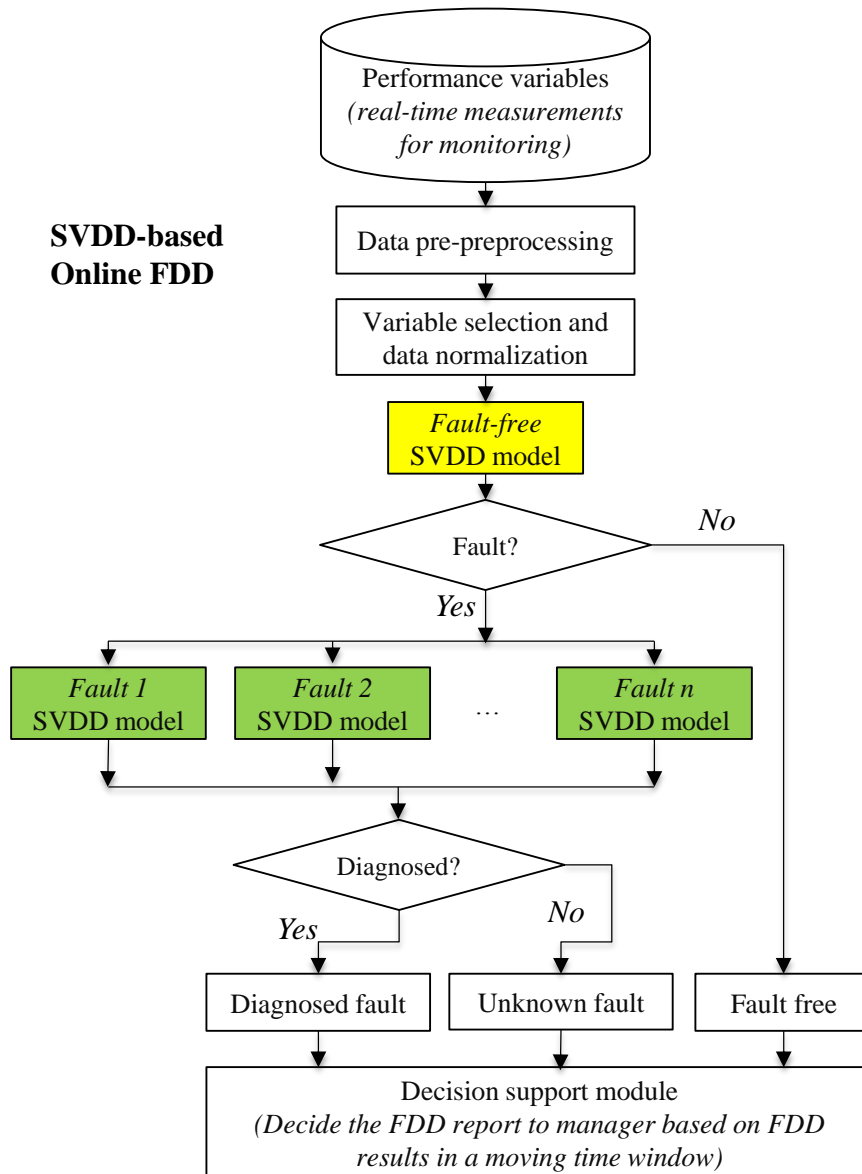
Figure 3.7 Flow chart of online SVDD-based FDD application

3.4 Diagnostic Bayesian Network-based FDD Method

Bayesian belief network (BBN), or Bayesian network, is a probabilistic graphical model that represents relationships of probabilistic dependence within a group of variables via a directed acyclic graph. Since its introduction by Pearl in early 1980s (Pearl 1985; Pearl 1986), it has been successfully applied in the domain of knowledge discovery and probabilistic inference. In the medical field, BBN was adopted to develop commercial computer-assisted diagnostic decision support systems, e.g., MUNIN (Andreassen et al. 1987), ALARM (Beinlich et al. 1989), Sleep Consultant (Nino-Murcia and Shwe 1991), and QMR-DT (Shwe et al. 1991). In the industrial field, the BBN-based diagnostic systems have attracted a lot of interest. Applications can be found in nuclear power systems (Kang and Golay 1999), aircraft engines (Sahin et al. 2007), sensor fault detection and identification (Mehranbod et al. 2005), semiconductor manufacturing systems (Yang and Lee 2012), etc. BBN is a powerful tool to represent and to reason about complex systems with uncertain, incomplete and conflicting information. It has shown superior performance compared with neural networks, support vector machines, decision trees, etc. BBN is becoming an increasingly important area of research and application in the field of artificial intelligence (Xu 2012). There are few applications of BBN in the HVAC field. Najafi et al. (2012) adopted BBN to detect and diagnose AHU faults. Wall et al. (2011) adopted dynamic BBN to tackle faults in AHU, too. Both works used BBN as a machine learning algorithm to learn the fault patterns and required a full set of fault data for the learning. In most conditions, it might be difficult or expensive to obtain a full set of fault data. Different from their works, the proposed method adopts BBN to diagnose faults mainly based on expert knowledge.

3.4.1 Bayesian Network Theory

3.4.1.1 Bayesian theorem and inference

Bayesian theorem is used for calculating conditional probabilities. Supposing A and B are two random events. The probability of B is larger than zero, i.e., $P(B)>0$. Given the event B, the conditional probability of the event A, denoted by $P(A/B)$, is

$$P\left(A|B\right)=\frac{P(AB)}{P(B)}=\frac{P(A)P(B\,|\,A)}{P(B)} \tag{3.20}$$

where $P(AB)$ is the joint probability, $P\left(AB\right)=P\left(B\right)P\left(A|B\right)=P(A)P(B\,|\,A)$.

Assume that $B_1, B_2, ..., B_n$ are a set of random variables and satisfy: (i) $P\left(B_i\right)>0, i=1,2,\ldots,n$; (ii) $\sum_{i=1}^{n} B_i = S$, S is the certain event; (iii) they are mutually exclusive (Xu 2012). For any given event A, the marginal probability of A is

$$P\left(A\right)=\sum_{i=1}^{n}P(B_i)P(A\,|\,B_i) \tag{3.21}$$

Bayesian theorem relates the conditional and marginal probabilities of stochastic events A and B_i using Equation (3.21).

$$P\left(B_i|A\right)=\frac{P(AB_i)}{P(A)}=\frac{P(B_i)P(A\,|\,B_i)}{\sum_{i=1}^{n}P(B_i)P(A\,|\,B_i)} \tag{3.22}$$

The items on the right hand side of Equation (3.22) are prior probabilities which are known in advance. The item on the left hand side is the posterior probability. Bayesian theorem provides the way to calculate the posterior probability from the prior

52

probabilities. This is the basic idea of the Bayesian inference. When using the Bayesian inference for fault diagnosis, B_i represents a fault and A represents a fault symptom. The prior probability of the fault B_i ($P(B_i)$) and the conditional probability of the symptom A given B_i ($P(A|B_i)$) can be obtained from maintenance record, historical data, survey or be assigned by experts. Then, the posterior probability $P(B_i|A)$ can be calculated using Equation (3.22). If this posterior probability is high, the fault B_i can be confirmed at the given symptom A.

Generally, the actual situation is rather complex. There could be a large number of related events (e.g., faults and symptoms in the Bayesian-based fault diagnosis), which will expand the required prior probabilities exponentially and cause the computation load unaffordable. The BBN theory provides an effective method to handle such difficulties.

3.4.1.2 Topology of BBN

A BBN is defined by two components, i.e., structure and parameters. The structure of a BBN is a graphical and qualitative illustration of the relations among the modeled variables. Generally, a node represents a variable. A variable has several possible states (e.g., *true* and *false*). Each state is an event. When an event occurs, it is an evidence (or observed state). A simple example is shown in Figure 3.8, which is illustrated using a directed acyclic graph. In Figure 3.8, the nodes (X_1, X_2... X_5) represent random variables and arcs represent direct probabilistic dependences among them. Each arc starts from a parent node and ends at a child node (e.g., X_2 is the parent node of X_4 in Figure 3.8). The node without any input arc is the root node (e.g., X_1 and X_2 in Figure 3.8). A BBN

53

represents the quantitative probabilistic relationships among the nodes using parameters/probabilities. Each root node has prior probabilities for each state (e.g., $P(X_1=true)=0.7$, $P(X_1=false)=0.3$). Each child node has a conditional probability table based on parental values.
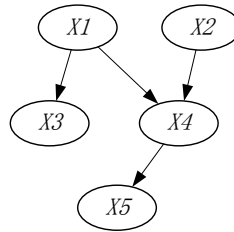
Figure 3.8. A simple Bayesian network

The structure and parameters of a diagnostic BBN can be obtained in two ways: deducing from expert knowledge and using machine learning from historical data. These two methods can be used individually or jointly.

3.4.1.3 Independence assumption of BBN

The independence assumption is introduced to overcome the difficulties in Bayesian inference as mentioned in *Section 2.1*. If event *A* and event *B* are independent of each other, Equation (3.23) is satisfied.

$$P(AB) = P(A)P(B) \tag{3.23}$$

There are generally three cases under the assumption (Xu, 2012). (i) All of the root nodes are independent of each other. For example, for the two root nodes X_1 and X_2 in Figure 3.8, it satisfies $P(X_1X_2)=P(X_1)P(X_2)$. (ii) If two nodes have common immediate parent nodes and there is no direct arc between these two nodes, they are conditionally

independent of each other given the states of their immediate parent nodes. For instance, X_1 is parent of X_3 and X_4. Given X_1, X_3 and X_4 are conditionally independent of each other, i.e. $P(X_3/X_1X_4)=P(X_3/X_1)$. (iii) For any non-root node, it is conditionally independent of its non-immediate parent nodes given the states of all of its immediate parent nodes. For instance, when the immediate parent node X_4 is given, X_5 is independent of X_1, X_2, X_3, $P(X_5/X_1X_2X_3X_4)=P(X_5/X_4)$. The independence assumption is of particular importance to the Bayesian inference.

For the simple BBN shown in Figure 3.8, the joint probability distribution of all nodes can be calculated by Equation (3.24).

$$
\begin{aligned}
P\left(X_1X_2X_3X_4X_5\right) &= \prod_{i=1}^{5}P\left(X_i|X_1,\ldots,X_{i-1}\right) \\
&=P\left(X_1\right)P\left(X_2|X_1\right)P\left(X_3|X_1X_2\right)P\left(X_4|X_1X_2X_3\right)P\left(X_5|X_1X_2X_3X_4\right)
\end{aligned}
\tag{3.24}
$$

Based on the independence assumption, the joint probability distribution can be simplified using Equation (3.25).

$$
P\left(X_1X_2X_3X_4X_5\right)=\prod_{i=1}^{5}P\left(X_i|Pa_i\right)=P\left(X_1\right)P(X_2)P\left(X_3|X_1\right)P\left(X_4|X_1X_2\right)P(X_5\mid X_4)
$$

$$
\tag{3.25}
$$

where, Pa_i are all the immediate parent nodes of the node X_i. Assuming that all nodes are Boolean, which have only two states, the number of the BBN parameters (the prior probabilities of root nodes and the conditional probabilities of non-root nodes) required in this case is reduced from 31 to 10 by introducing the independence assumption.

The independence assumption brings two benefits. Firstly, it simplifies the inference procedure. Secondly, it significantly reduces the number of parameters required. Besides, the joint probability distribution can be solely determined only if the two kinds of prior probabilities on the right hand side of Equation (3.25) are given, i.e. the prior probabilities of all root nodes and the conditional probabilities of all non-root nodes given all possible combinations of their immediate parent nodes. However, the number of parameters required in the conditional probability table might be still too large to be assigned by chiller experts.

3.4.1.4 Noisy-MAX node

The conditional probability table of a child node should consider all of the possible combinations of states of its parent nodes. The number of parameters needed in the conditional probability table exponentially grows with the number of its parents. In case of a child node with two Boolean states has n parents which are also Boolean, 2^{n+1} parameters are to be specified. For instance, in the BBN in Figure 3.8, if X_4 is a fault symptom and X_1, X_2 are two chiller faults, chiller experts can easily assign the conditional probabilities of X_4 given X_1, X_2 separately. However, it is difficult for them to assign $P(X_4 = true \mid X_1=true, X_2=true)$.

Noisy-MAX is a solution to reduce the number of parameters needed to specify conditional probability distributions. It is based on the assumption that parent nodes act independently in producing the effect on a child node. If a node is considered as a Noisy-MAX node, the number of parameters is reduced from exponential to linear in the number of parents. Assume all nodes in a BBN are Boolean, only $2*(n+1)$ parameters

56

are needed, rather than 2^{n+1}. More details about Noisy-MAX can be found in (Zagorecki and Druzdzel 2006).

3.4.1.5 BBN-based inference

The inference using a BBN is to calculate the posterior probability $P(X_q/X_e)$, where X_q is the node of interest (e.g. the fault concerned) and X_e is the node or a set of nodes in which a state has been observed. The probabilities of observed states are set to 100%. With the joint probability distribution, it is possible to calculate any types of posterior probabilities in principle. For instance, the probability of X_4 is *true* in the BBN shown in Figure 3.8 can be calculated by Equation (3.26).

$$P(X_4 = true) = \sum_{X_1 X_2 X_3 X_5} P(X_1, X_2, X_3, X_4 = true, X_5) \qquad (3.26)$$

If X_4 is a node representing a certain fault, and X_5 is a symptom caused by X_4 directly, the probability of X_4 given X_5 can be calculated by Equation (3.27).

$$P(X_4 = true \mid X_5 = true) = \frac{P(X_4 = true, X_5 = true)}{P(X_5 = true)}$$
$$= \frac{\sum_{X_1 X_2 X_3} P(X_1, X_2, X_3, X_4 = true, X_5 = true)}{\sum_{X_1 X_2 X_3 X_4} P(X_1, X_2, X_3, X_4, X_5 = true)} \qquad (3.27)$$

There are many algorithms for performing the inference, which can be classified into two categories: exact algorithms and approximate algorithms. The exact algorithms calculate the exact probabilities of nodes. It is suitable for simple networks. When it comes to complex network, the calculation is an N-P hard problem (Pearl 1988). The approximate algorithms calculate the approximate probabilities of nodes using statistical

methods. In the chiller FDD application, the BBN is generally not very complex. The exact algorithms are applicable.

3.4.2 Schematic of The Diagnostic Bayesian Networks

3.4.2.1 Structure of a DBN

All nodes in a DBN can be classified into three groups: fault nodes, BMS evidence nodes, and additional information nodes. Fault nodes represent the faults concerned. BMS evidence nodes represent symptoms which can be identified from data recorded in BMSs. Additional information nodes are introduced to represent the evidences which can be obtained by on-site investigation and maintenance records.

The structure of a DBN qualitatively illustrates the relationships among faults, BMS symptoms and additional information. It is worth noticing that the structure of a DBN for a problem is not unique. It is an expression of diagnostic thinking of experts. Different expert might have different diagnostic thinking. To develop an efficient DBN, the developer should have enough experience/knowledge about HVAC systems, and fully utilize the available diagnostic information. There are already a significant amount of publications about FDD methods for HVAC systems. The outstanding achievements can be integrated into a DBN in an information fusion way. For instance, the APAR (AHU performance assessment rules) proposed by NIST can be used in a DBN for AHU (Schein 2006). The *if…then…* logics in APAR rules can be represented as the relationships between BMS evidence nodes and fault nodes.

3.4.2.2 Parameters of the DBN

The parameters of a DBN represent the quantitative dependences in probabilities among faults, BMS evidence nodes and additional information nodes. There are two kinds of parameters, i.e., prior probabilities of root nodes and conditional probabilities between nodes. Root nodes are generally BMS evidence nodes and additional information nodes. The prior probabilities of root nodes can be obtained by survey or estimated by experts. A conditional probability table represents all possible combinations of states of a child node and states of its parent nodes. The conditional probabilities can be obtained by two means. If the full-set fault data are available, the conditional probabilities can be obtained by statistical calculation or using machine learning algorithms. If the full-set of fault data are not available, the conditional probabilities can be estimated by experts. It is easy to obtain conventional probabilities when a node has only one parent node. However, it is generally difficult to obtain conditional probabilities when a node has more than one parent nodes. Such node is suggested to be Noisy-MAX nodes.

3.4.2.3 DBN-Based FDD

The DBN-based FDD is to calculate the posterior probabilities of fault nodes on the basis of observed evidences. The inputs of the DBN are the observation of BMS evidence nodes and additional information nodes which are obtained from operation and maintenance records, in-situ investigation and the fault detection process. The observed states of nodes are set to be 100%. The outputs are the posterior probabilities of fault nodes, which are also named believes. Diagnostic rules are needed to isolate a fault

depending on the component concerned. Taking chiller FDD for instance, a fault will be reported if one of the following two rules is satisfied:

Rule 1: The one with the largest fault probability and such largest fault probability is larger than a certain threshold ε_1 (e.g. $\varepsilon_1 = 80\%$); or

Rule 2: The difference between the largest fault probability and the second one is larger than a certain threshold ε_1 (e.g. $\varepsilon_2 = 30\%$).

3.5 Summary

Four FDD methods are proposed in this chapter for different applications.

The proposed simplified model-based FDD method is suitable when there are limited fault-free data to train models. The method has advantages compared with gray-box model-based FDD method and SVDD-based FDD method. However, a customization tool is needed to identify unknown model parameters.

The proposed incipient fault detection and diagnosis method is suitable when measurements are sufficient. The use of EWMA control charts reduces the Type II errors through taking into account the time series information using the weighting factor. Therefore, the EWMA-based methods can achieve much higher diagnosis ratios compared with the *t*-statistic-based methods. SVR could be more efficient than MLR approach since it is a non-linear regression approach based on structural risk minimization from statistical learning theory.

The proposed SVDD-based FDD method is suitable when fault data are available. When fault data and fault-free data are available, it is expected that this method has

better fault detection and fault diagnosis performance compared with gray-box model-based FDD methods and Bayesian network-based FDD methods. It might also work when some important sensors are unequipped. In theory, this method has advantages compared with PCA-based fault detection method and SVM-based FDD method.

The proposed Bayesian network-based FDD method might have better performance compared with other FDD methods when the diagnostic information is uncertain and incomplete. It has the benefit in merging different types of knowledge and information from diverse sources. It also has a strong ability in dealing with incomplete or even conflicting information. It can be used to simulate the diagnostic thinking and diagnosis process of HVAC experts.

CHAPTER 4 A SIMPLIFIED MODEL-BASED CHILLER FDD STRATEGY AND ITS CUSTOMIZATION TOOL

This chapter presents a simplified FDD strategy for centrifugal chillers, which provides good applicability and convenience for practical applications. It adopts a simplified physical chiller model calibrated using very limited operation or performance test data and a customization tool. Four schemes are developed to identify chiller model parameters based on available information and data from tests or from manufacturers. A new semi-physical sub-cooling model is adopted by the chiller model. The overall heat transfer coefficient of condenser is assumed consisting of two parts, including one presenting the condensing section and the other presenting sub-cooling section. By analyzing the changing trends of two proposed performance indexes (i.e. the normalized heat transfer performance and the fictitious sub-cooling temperature), the patterns in fault conditions can be obtained.

4.1 Outline of The FDD Strategy

The structure of the proposed FDD strategy is shown in Figure 4.1. It consists of two major groups of tasks, i.e. offline model training and online FDD.
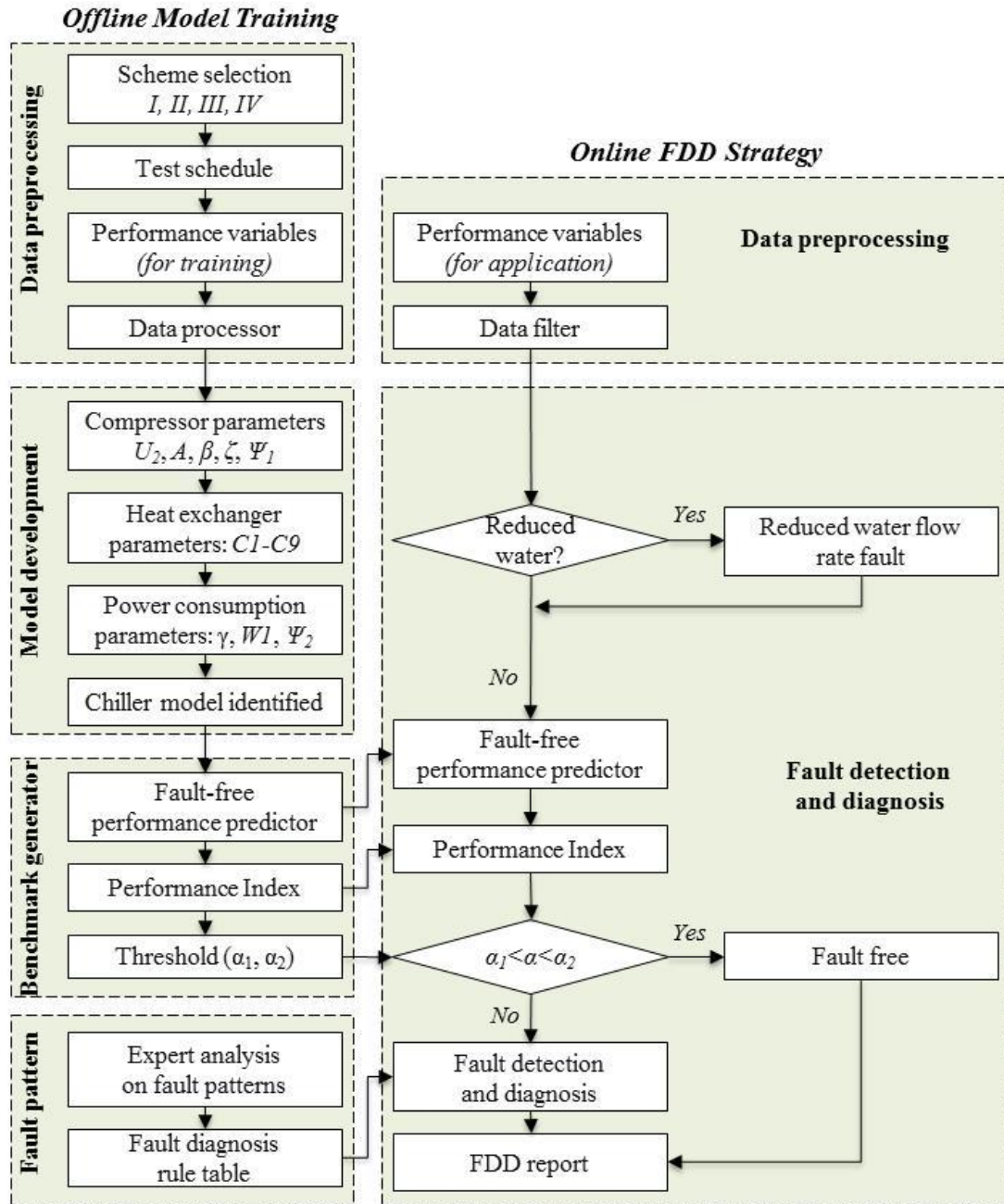
Figure 4.1 Flow chart of the FDD strategy and associated customization tool

The offline model training task consists of four steps including: data processing, model parameter identification, benchmark generation and fault pattern identification. The available information and measurements might be various for different chillers. To

simplify the model development in practice, a customization tool is introduced to identify chiller parameters effectively in different situations. The situations are determined by the availability of the geometric parameters of chiller compressor (U, A, β), as well as the evaporating temperature and condensing temperature (T_{ev} and T_{cd}) in the chiller performance catalogue or field measurement data, as shown in Table 4.1. For each situation, an identification scheme is developed to estimate the unknown parameters respectively. Multiple input data files (Data-1, Data-2 and Data-3) are required for each scheme. Data-1 contains full load condition performance data. Data-2 contains both full and part load condition performance data. Data-3 contains the chiller performance data of those working points at which the evaporator and condenser temperatures (T_{cd}, T_{ev}) are given. The step of data processing is to obtain Data-1, Data-2 and Data-3 (for Scheme *I* and *III*) as inputs of the customization tool. It includes scheme selection, performance test and data processing. A suitable scheme is selected according to available information and measurements. Then, experimental tests are designed and conducted to generate chiller performance data in both full and partial load conditions. Before the data are used, a data filter is used to rule out those data with significant dynamics or outliers (Rossi, 1995). At the step of model parameter identification, the customization tool is used for the chiller model parameter identification. At the step of benchmark generation, the chiller model is used to generate the fault-free performance data. Using the chiller model, the two proposed PIs can be calculated, which are used at the later step as benchmarks. One of the performance indexes - α (the normalized heat transfer performance in condensing section) is used for fault detection. The threshold is decided according to a given false alarm rate in fault-free condition using *t*-statistic

approach. At the step of fault pattern identification, four typical important faults are considered, i.e. condenser fouling, non-condensable gas, refrigerant overcharge and discharge. The impacts of the faults on the system performance depend on the system design and the type of heat exchangers. Expansion valves and control strategies also have important impacts. Based on expert knowledge, the fault patterns of different kinds of faults can be obtained as qualitative FDD rules.

The online FDD consists of two major steps, including data processing and FDD. The step of data processing aims to get steady-state data of selected performance variables. At the FDD step, firstly, faults of condenser and evaporator reduced water flow rate are detected using the flow measurements directly. Secondly, the fault-free performance is generated using the calibrated chiller model. Then, benchmarks of the performance indexes are calculated. If α is outside its threshold region, process of fault diagnosis, employing a FDD rule table, will be activated.

4.2 Description of The Physical Chiller Model

4.2.1 Chiller Model

The chiller model used in this study is developed on the basis of the simplified physical chiller model of Wang and Wang (2000). It is based on the basic principles of chillers to ensure the reliability and accuracy of the model in a wide working range. The parameters are identified using limited performance test data. The equations for compressor model and power consumption refer to Wang and Wang (2000). The evaporator is simulated using the classical heat exchanger efficiency method assuming constant temperature at the refrigerant side. The overall heat transfer coefficient, UA_{ev},

is represented empirically considering the effects of water flow rate and heat flux by Equations (4.1)-(4.3). The first term on the right-hand side of Equation (4.3) represents the effect of water flow rate on the water side. It can be obtained by assuming a small wall-fluid temperature difference and turbulent flow pattern with constant water thermo-physical properties in the evaporator. The second term represents the effects of heat transfer rate (Q_{ev}) on the boiling process of refrigerant in evaporator. It is derived from the correlation of heat flux as a function of wall superheat (Stephan and Abdelsalam 1980) and pool boiling (Garey 1992). Where, *C1, C2, C3* are constants, which can be identified by the pre-processor using chiller performance data.

$$\varepsilon_{ev} = 1 - \exp(-\frac{UA_{ev}}{c_{p,w}M_{w,ev}}) \tag{4.1}$$

$$Q_{ev} = c_{p,w}M_{w,ch}\varepsilon_{ev}(T_{ch,in} - T_{ev}) \tag{4.2}$$

$$UA_{ev} = [C_1 M_{w,ch}^{-0.8} + C_2 Q_{ev}^{-0.745} + C_3]^{-1} \tag{4.3}$$

In the condenser, it can be divided into two parts, i.e., condensing section and sub-cooling section. The condensing section is represented by Equations (4.4)-(4.9). The subscript '*cd,cd*' is the condensing section in the condenser. The first term on the right-hand side of Equation (4.6) is obtained using the same assumptions in the evaporator model. The second term on the right-hand side represents the effects of the condenser heat transfer rate (Q_{cd}) on the condensing process of the refrigerant in the condenser. Film condensation is assumed neglecting the effect of vapour superheat on condensation heat transfer. Since the sub-cooling section does not have an obvious effect on condenser load, Equation (4.5) was used directly to estimate the load of the condensing section. Where, *C4-C6* are constant coefficients.

$$\varepsilon_{cd,cd} = 1 - \exp(-\frac{UA_{cd,cd}}{c_{p,w}M_{w,cl}}) \tag{4.4}$$

$$Q_{cd,cd} = c_{p,w}M_{w,cl}\varepsilon_{cd,cd}(T_{cd} - T_{cl,in}) \tag{4.5}$$

$$UA_{cd,cd} = [C_4 M_{w,ch}^{-0.8} + C_5 Q_{cd,cd}^{1/3} + C_6]^{-1} \tag{4.6}$$

A new empirical sub-cooling model is developed in this study by taking into account the effects of water flow rate and refrigerant flow rate as in Equation (4.3). The subscript '*cd,sc*' is the sub-cooling section in the condenser. The exponents -0.8 and -0.99 in $M_{w,ch}^{-0.8}$ and $Q_{ev}^{-0.99}$ of Equation (4.7) were calibrated by using the test data in fault-free condition from RP-1043 (Comstock and Braun 1999). Equation (4.8) and Equation (4.9) are developed for chillers in which the bottoms of condensers are used for sub-cooling and the cooling water enters into the sub-cooling section firstly, as the chiller used in RP-1043. Equation (4.8) is the computation model of the heat exchanger efficiency of sub-cooling section, which is defined as Equation (4.9). It is assumed to be applicable to pass arrangements commonly used in sub-cooling section.

$$UA_{cd,sc} = [C_7 M_{w,ch}^{-0.8} + C_8 Q_{cd}^{-0.99} + C_9]^{-1} \tag{4.7}$$

$$\varepsilon_{cd,sc} = 1 - \exp(-\frac{UA_{cd,sc}}{c_{p,r}M_r}) \tag{4.8}$$

$$\varepsilon_{cd,sc} = \frac{T_{cd} - T_{r,sc,out}}{T_{cd} - T_{cl,in}} = \frac{T_{sc}}{T_{cd} - T_{cl,in}} \tag{4.9}$$

Since the sub-cooling model is developed based on rules of heat transfer theory, it would be suitable to apply to chillers with shell-and-tube condenser and keep a similar accuracy as the condenser and evaporator models used previously.

4.2.2 Customization Tool For Parameter Identification

A customization tool is developed to identify the parameters of the chiller model. The required input data for the pre-processor, i.e. evaporator and condenser water flow rates, evaporator outlet and inlet water temperatures and condenser inlet water temperature, are generally available in practice, as shown in Figure 4.2. Four schemes are proposed to identify chiller parameters for four different situations as shown in Table 4.1.

Table 4.1 Four schemes for chiller parameters estimation based on available information.

Scheme	Available parameters	Required Dataset
I	U, A, β and T_{cd}, T_{ev}	Data-1, Data-2, Data-3
II	U, A, β	Data-1, Data-2
III	T_{cd}, T_{ev}	Data-1, Data-2, Data-3
IV	/	Data-1, Data-2
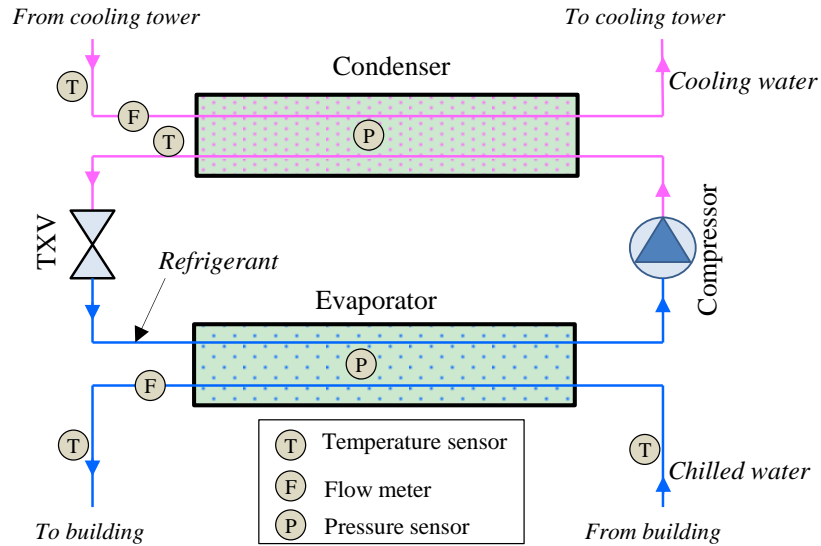
Figure 4.2. Sensors needed for model training and FDD

The flow charts of the identification schemes are reported in a previous work (Wang and Wang 2000). The parameters of the chiller model can be estimated with a small amount of chiller performance test data or using catalogue data in full load. This is an obvious advantage comparing with the gray-box model, the empirical chiller model and the FDD strategies based on progress history data.

In this study, T_{cd} and T_{ev} are available for model training. Scheme *III* is selected accordingly to perform the chiller parameter identification. The input variables of the model are shown in Figure 4.2. The output variables include condensing temperature, evaporating temperature, refrigerant flow rate, internal compression power, power consumption, compressor pre-rotation vane angle, etc.

4.3 The Chiller FDD Strategy

There are two faults which are easy to be diagnosed, i.e. reduced condenser water flow rate and reduced evaporator water flow rate which can be detected and diagnosed by flow measurements directly. The other four faults are difficult to be handled, which make chiller FDD more complex and hard for applications. Such faults include condenser fouling, non-condensable gas, refrigerant overcharge and refrigerant leakage. Therefore, in this study, special attention is paid to find an easy-to-use solution for them. The overall heat transfer conductance of condensing section $UA_{cd,cd}$ and sub-cooling section $UA_{cd,sc}$ are found to be the essential physical reason for the deviations of condensing and sub-cooling temperatures in fault conditions. Based on them, two important performance indexes are proposed, i.e. α (normalized heat transfer performance) and T'_{sc} (fictitious sub-cooling temperature). A FDD rule table is proposed as illustrated in Table 4.2. This rule table works for typical centrifugal chillers with tube-and-shell heat exchangers, as shown later in *Section 4.3.3*.

Table 4.2 The fault pattern rule table for fault detection and diagnosis

	Fault type	Mcd	Mev	T'_{sub}	α
1	Reduced condenser water flow rate	-	▼	*	*
2	Reduced evaporator water flow rate	▼	-	*	*
3	Condenser fouling	-	-	▼	▼
4	Refrigerant leakage	-	-	▼	▲
5	Refrigerant overcharge	-	-	▲	▼
6	Non-condensable gas	-	-	▲	▼

Note: The ▲ and ▼ indicate the changes of characteristic features compared to its fault-free state. The - indicates no obvious change. The * indicates faults are detected and diagnosed in the beginning and no condensation in following FDD steps.

4.3.1 Normalized Heat Transfer performance

$UA_{cd,cd}$ is reduced in the case of any of the faults: condenser fouling, refrigerant overcharge and non-condensable gas. It is increased in the case of refrigerant leakage as analysed in more details in Section 4.3.3 (*Description and analysis of the FDD rule table*). A normalized heat transfer performance, α, is defined as Equation (4.10) to indicate the relative level of heat transfer coefficient. $[\alpha_1, \alpha_2]$ is the confidence interval for the fault free conditions with a particular confidence level. Generally, confidence level of 95.4% is acceptable for chiller FDD (Reddy 2006). The confidence interval is calculated based on the fault free samples using *t*-statistic approach (Manly, 2005). If the actual value of α is outside of the confidence interval, a fault is detected.

$$\alpha = \frac{UA_{cd,cd}}{UA_{cd,cd,ref.}} \quad \begin{cases} \text{Health: } \alpha \in [\alpha_1, \alpha_2] \\ \text{Fault: } \alpha \notin [\alpha_1, \alpha_2] \end{cases} \tag{4.10}$$

where, $UA_{cd,cd,ref.}$ is the reference value of $UA_{cd,cd}$, which is generated using its benchmark chiller model. According to the value of α, the test data can be classified into three categories including: 1): fault free ($\alpha \in [\alpha_1, \alpha_2]$), 2): refrigerant leakage ($\alpha > \alpha_2$), 3): refrigerant overcharge, condenser fouling or non-condensable gas ($\alpha < \alpha_1$). A fault can be confirmed when its diagnosed ratio is larger than a threshold (e.g. 15%).

4.3.2 Fictitious Sub-cooling Temperature

Sub-cooling temperature is a good candidate to distinguish the above three faults which have the same pattern ($\alpha < \alpha_1$). In the case of refrigerant overcharge or non-condensable gas, T_{sc} will be larger than $T_{sc,ref.}$ (the reference value of T_{sc}). However, it cannot be used to diagnose condenser fouling since T_{sc} is sometimes larger than $T_{sc,ref.}$ and sometimes smaller or equal to $T_{sc,ref.}$. Therefore, it is not a good approach if employing T_{sc} directly. In this study, T'_{sc} (the fictitious sub-cooling temperature) is adopted to overcome the problem.

According to Equation (4.9), in case of fault, ΔT_{sc} is affected by two factors (i.e. $\Delta \varepsilon_{cd,sc}$ and ΔT_{cd}) as shown in Equation (4.1).

$$T_{sc} = (\varepsilon_{cd,sc,ref.} + \Delta \varepsilon_{cd,sc}) \cdot (T_{cd,ref.} + \Delta T_{cd} - T_{cl,in}) \qquad (4.11)$$

Assuming that $\Delta \varepsilon_{sc}$ is zero, the fictitious sub-cooling temperature is obtained as defined in Equation (4.12).

$$T'_{sc} = \varepsilon_{cd,sc,ref.} \cdot (T_{cd,ref.} + \Delta T_{cd} - T_{cd,water,in}) = \varepsilon_{cd,sc,ref.} \cdot (T_{cd} - T_{cl,in}) \qquad (4.12)$$

$\Delta \varepsilon_{cd,sc}$ is negative ($T'_{sc} < T_{sc}$) in the case of condenser fouling. $\Delta \varepsilon_{cd,sc}$ is positive ($T'_{sc} > T_{sc}$) in the case of refrigerant overcharge or non-condensable gas. Therefore, T'_{sc} can be used to distinguish condenser fouling with refrigerant overcharge or non-condensable gas when a fault is detected to be outside $[\alpha_1, \alpha_2]$.

4.3.3 Description and Analysis of the FDD Rule Table

Based on the above analysis, a fault diagnosis rule is proposed as shown in Table 4.2. The refrigerant overcharge fault and non-condensable gas have similar patterns and cannot be uniquely identified when chillers are working. The non-condensable gas is the

easiest fault to be detected since the condenser pressure is obviously higher than the saturated pressure at the power off condition.

If rule table (i.e. Table 4.2) can work in typical centrifugal chillers with tube-and-shell heat exchangers, the proposed FDD strategy could be applied in these chillers without fault data. This rule table is therefore analysed theoretically and a qualitative analysis is made on a 90 ton centrifugal chiller in ASHRAE RP-1043 as an example.

The physical reason for the deviations of condensing and sub-cooling temperatures in fault conditions can be analysed in theory using Equations (4.13) and (4.14).

$$\frac{1}{UA_{cd,cd}} = \frac{1}{h_{r,cd,cd}A_{o,cd,cd}} + \frac{1}{h_w A_{i,cd,cd}} + \frac{ff_{cd,cd}}{A_{i,cd,cd}} \qquad (4.13)$$

$$\frac{1}{UA_{cd,sc}} = \frac{1}{h_{r,cd,sc}A_{o,cd,sc}} + \frac{1}{h_w A_{i,cd,sc}} + \frac{ff_{cd,sc}}{A_{i,cd,sc}} \qquad (4.14)$$

Where, h_r is the heat transfer coefficient at refrigerant side. h_w is the heat transfer coefficient at water side. A_o is the outside tube surface area. A_i is the inside tube surface area. ff represents the thermal resistance including tube resistance and fouling.

Condenser fouling

In the case of condenser fouling, $ff_{cd,cd}$ and $ff_{cd,sc}$ are larger than normal ones. It leads to smaller $UA_{cd,cd}$ and $UA_{cd,sc}$ definitely. Condensing temperature will be higher to build a larger temperature difference to reject the same account of heat. According to Equation (4.8) and (4.9), there are two factors affecting the sub-cooling temperature. One is $UA_{cd,sc}$, which has a lower value in case of fouling. The second factor is the condensing temperature. In the case of fouling, the condensing temperature will be higher which leads to larger difference between water inlet and refrigerant temperatures.

The eventual trend of the sub-cooling temperature change depends on which factor is dominant. It is also the reason why T'_{sc} is used instead of T_{sc} in the rule table.

Refrigerant charge overcharge and refrigerant leakage

The refrigerant charge level has a significant effect on the performance of chiller. The sensitivity of the sytem performance to charge level depends on the design of the system and the type of heat exchangers as well as their refrigerant storage capacities (Grace 2005). Conclusion can be made on the basis of many literatures that the degree of super heat, sub-cooling temperature and condensing temperature are the most sensitive indexes. Different expansion valves and control strategies also have different effects on the level of charge faults (Reddy 2007b). When overcharge or leakage occurs, refrigerant level in evaporter or condenser will change sygnificantly, disregarding system design and control strategies (Zhao 2011).

When the refrigerant overcharge occurs, there is more tube surface area below the liquid level since the refrigerant level in condenser is higher. There is more tube surface area in sub-cooling section. The $A_{cd,sc}$ is larger. It leads to a larger $UA_{cd,sc}$ according to Equation (4.14). Hence, the heat transfer capacity of sub-cooling section increases and more heat ($Q_{cd,sc}$) is transferred from refrgerant to water. Under the same operating condition, the M_r is almost unchanged in case of refrigerant overcharge or refrigerant leakage (Cui and Wang 2006). Therefore, T_{sc} will be higher according to Equation (4.15).

$$T_{sc} = \frac{Q_{cd,sc}}{c_{p,r}M_r} \tag{4.15}$$

At the same time, there is less $A_{cd,cd}$ left for condensing section. $UA_{cd,cd}$ is smaller according to Equation (4.13). It leads to a smaller $\varepsilon_{cd,cd}$ according to Equation (4.4). T_{cd} increases to maintain a same $Q_{cd,cd}$ according to Equatioin (4.5). In the case of refrigerant leakage, the refrigerant level is lower. There is an opposite trend. T_{sc} will be lower, and T_{cd} will be higher.

Non-condensable gas

Chiller system performance is very sensitive to the fault of non-condensable gas. Even 1% non-condensable gas by weight can cause some chillers completely unusable. Non-condensable gas tends to accumulate in the condenser. Generally, the condensing temperature is calcluated on the base of the saturated pressure. When it occurs, the calculated condensing temperature is higher than actural value dramatically. Meanwhile, the heat transfer resistance $h_{r,cd}$ in condensing sectioin is increased and worsens the heat transfer capacity. As a result, the temperature difference between inlet cooling water and condensing temperatures is larger. Consequently, an obvious higher sub-cooling temperature occurs.

Reduced water flow rate in condenser and evaporator

Reduced water flow rates in condenser and evaporator can be detected and diagnosed using flow measurements directly. According to Euqations (4.3) and (4.6), the reduced water flow rates reduce water-side heat transfer coefficients and lead to lower UA_{cd} or UA_{ev}. However, the effects of variable water flow rates are included in the models of the chiller evaporator, condenser and subcooling, and therefore, the FDD outputs will not be affected when the reduced water flow rate occurs.

4.4 Evaluation Using Experimental Data

In this section, the proposed customization tool and FDD strategy are evaluated using experiment data on a real chiller.

4.4.1 RP1043 Experimental Data Description

The experimental data from ASHRAE Research Project 1043 (RP-1043) are introduced here to validate the proposed strategy. These data were generated on a 90-ton centrifugal water-cooled chiller, which was equipped with a shell-and-tube evaporator and condenser and controlled by a thermostatic expansion valve (TXV). For each type of faults, four severity levels (measured in percentage) were tested. Different strategies were employed to generate these fault data as illustrated in Table 4.3. For instance, the condenser fouling fault was introduced though plugging 12%, 20%, 30% and 45% of tubes in the condenser for SL-1, SL-2, SL-3 and SL-4, respectively.

Table 4.3 Severity levels (SL) conduction in the ASHRAE Project 1043

Fault Type	SL-1	SL-2	SL-3	SL-4	Faults Generation Strategy
Reduced condenser water flow	- 10%	- 20%	- 30%	- 40%	Reducing water flow by percentage
Reduced evaporator water flow	- 10%	- 20%	- 30%	- 40%	Reducing water flow by percentage
Condenser fouling	- 12%	- 20%	- 30%	- 45%	Plugging tubes by percentage
Refrigerant overcharge	10%	20%	30%	40%	Overcharging refrigerant by weight

Refrigerant leakage	-	-	-	-	Discharging refrigerant by
	10%	20%	30%	40%	weight
Non-condensable gas	1.0	1.7	2.4	5.7	Adding nitrogen by volume
	%	%	%	%	

Seven typical chiller faults are concerned in this thesis which account for a significant frequency of the service calls according to Comstock and Braun' survey (2002). The faults include: condenser fouling (*CdFoul*), refrigerant overcharge (*RefOver*), refrigerant leakage (*RefLeak*), non-condensable gas (*Ncg*), reduced evaporator water flow rate (*RedEvW*), reduced condenser water flow rate (*RedCdW*) and excess oil (*ExOil*). For each fault, four severity levels (SLs) were considered, i.e. SL-1, SL-2, SL-3 and SL-4, from lower severity level to higher level. Each fault at every SL was tested under 27 operating conditions. Each operating condition lasted about 30 minutes to archive a steady-state. Each test lasted about 864 minutes in total. There are three data sets for each test, i.e. 'Complete data set', 'Reduced data set', 'Steady States'. The only difference between two data sets is their sampling rate, i.e. ten seconds and two minutes respectively. 'Complete data set' has 5191 series of data. The sampling interval was 10 seconds. 'Reduced data set' has 433 series of data. The sampling interval was 2 minutes. 'Steady States' has 27 series of data. It selected a series of steady-state data for each operating condition. More details can be found in Comstock and Braun (1999).

In this study, four sets of data tested in fault-free conditions, i.e. 'Normal', 'Normal1', 'FWC20' and 'FWE20', were used for chiller model parameter

identification. 'Normal' and 'Normal1' are the sets of data tested in the fault free conditions. 'FWC20' is the data tested through reducing the condenser water flow rate by 20%. 'FWE20' is the data tested through reducing the evaporator water flow rate by 20%.

The data sets, i.e. 'Normal1', 'Normal2', 'Normal_CF' and 'Normal_R1', were employed to determine the confidence interval in fault free conditions. 'Normal_CF' and 'Normal_R1' are another two sets of data tested in the fault free conditions. The data sets of four severity levels for each fault type were used to evaluate the performance of the FDD strategy proposed.

4.4.2 Chiller Model Evaluation

According to the available information and parameters in the RP-1043 report, Scheme *III* was used to identify chiller model parameters. All these data were re-partitioned into three parts including Data-1, Data-2 and Data-3 as follows: (1) Data-1 is composed of the full load condition performance data. (2) Data-2 is composed of the chiller performance data in both full and part load conditions. (3) Data-3 is composed of the chiller performance data in which the evaporating and condensing temperatures (T_{ev}, T_{cd}) are available. All these three sets of data were used as the inputs of the pre-processor defined. The outputs include compressor parameters (U_2, AI, β, ζ, Ψ_1), heat exchanger parameters ($C1$-$C9$) and power consumption parameters (γ, $W1$, Ψ_2).
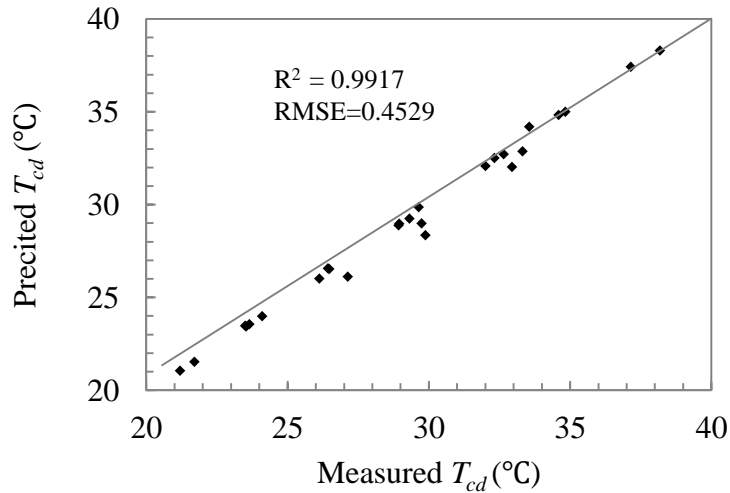
Figure 4.3 Comparison between measured and predicted condensing temperatures
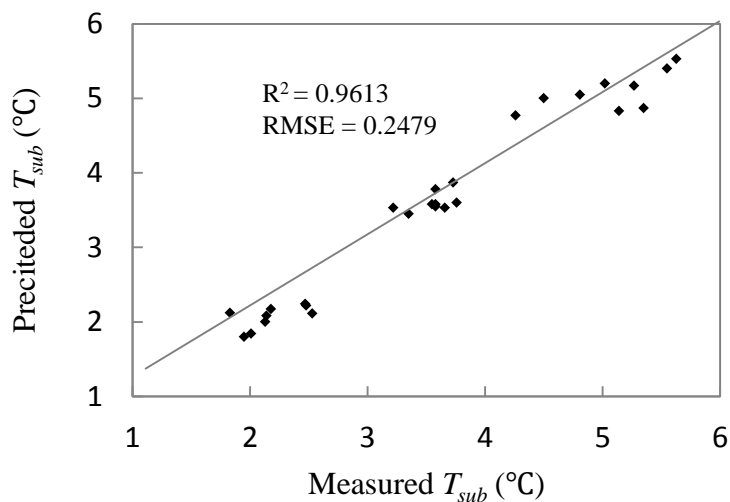
Figure 4.4 Comparison between measured and predicted sub-cooling temperatures

Once the model parameters were identified, 'Normal2', which was tested in the fault free condition, was then used for model evaluation. The model evaluation results are illustrated in Figure 4.3 and Figure 4.4 in terms of the condensing and sub-cooling temperature, respectively. R^2 is a measure of the goodness of the fitting. The higher the R^2 is, the better the fitting result is. As shown in both figures, the R^2 of the condensing temperature is 0.9917 and the R^2 of the sub-cooling temperature is 0.9613. It

demonstrates that the model has good performance in prediction and can be used and is acceptable for FDD purpose.

4.4.3 Evaluation of $UA_{cd,cd}$ Variations in Fault Conditions

The four types of faults described previously with four severity levels were used to evaluate the $UA_{cd,cd}$ variations in fault conditions. The normalized heat transfer performance for a severity level of the fault, named α', is used to describe the effects of faults in various operating conditions. It is calculated by the least square method. Using α', the predicted condensing temperatures can be calculated. The results are summarized in in Table 4.4.

Table 4.4 Normalized heat transfer performance (α') and their goodness-of-fit (R^2) at each severity level for different types of faults

	Cdfoul		RefOver		RefLeak		Ncg	
	α'	R^2	α'	R^2	α'	R^2	α'	R^2
SL 1	0.9	0.993	0.85	0.993	1.0	0.987	0.6	0.976
SL 2	0.9	0.991	0.83	0.994	1.1	0.989	0.4	0.972
SL 3	0.8	0.988	0.62	0.976	1.3	0.989	0.4	0.956
SL 4	0.7	0.991	0.5	0.991	1.5	0.993	0.4	0.927

From Table 4.4, it can be found that the R^2 was above 0.95 for most cases, which indicates the good fitting results. In the case of the condenser fouling, the average R^2 was 0.9907. The value of α' decreased with the increased severity level, i.e. 0.93, 0.90, 0.83 and 0.74 for SL-1, SL-2, SL-3 and SL-4, respectively. This demonstrated that the heat transfer coefficient is reduced when the condenser suffered from the condenser fouling. In the case of the refrigerant overcharge, the average R^2 was 0.9885 and the

80

values of α' were 0.85, 0.83, 0.62 and 0.50 for SL-1 to SL-4, respectively. In the case of the refrigerant leakage, the average R^2 was 0.9894 and the values of α' were 1.01, 1.08, 1.34 and 1.53 for SL-1 to SL-4, respectively. This indicated that the liquid refrigerant level in the condenser is directly affected by the amount of the refrigerant, resulting in a lower (in case of overcharge) or higher (in case of leakage) heat transfer coefficient in the condenser. In the case of the non-condensable gas, although the R^2 were relatively low as compared with the other cases, the lowest R^2 was still higher than 0.90, which is acceptable the FDD strategy in this study as illustrated at Figure 9. The values of α' were 0.59, 0.44, 0.42 and 0.38 respectively. It indicates that performance is degraded significantly even at the slight severity level of non-condensable gas

The above results are consistent with the assumptions described in *Section 4.3.3*. Namely, the value of α' decreases when the operation of chillers suffer from condenser fouling, refrigerant overcharge or non-condensable gas, while it increases when the refrigerant leakage happens. Therefore, the normalized heat transfer performance α is a suitable performance index to describe the effects of faults on the condenser.

4.4.4 Evaluation of the FDD Strategy

As presented earlier, in this study, there are four data sets, i.e. 'Normal1', 'Normal2', 'Normal_CF' and 'Normal_R1', were used to obtain the confidence interval $[\alpha_1, \alpha_2]$. Both model errors and measurement uncertainties are taken into consideration using the confidence interval. A fault is detected when the residual between measured value and its benchmark is out of confidence interval. The larger the model errors and measurement uncertainties are, the wider the confidence interval will be. In this study,

the confidence interval is obtained using *t*-statistic at a confidence level of 95.4% (false alarm ratio was 4.6% in the fault free condition).

Each severity level of each fault consists of 27 observation points, for which the α (the normalized heat transfer performance) and T'_{sc} (the fictitious sub-cooling temperature) were calculated respectively and graphically shown in Figures (4.5)-(4.9). It can be found that the confidence interval [α_1, α_2] divided the 2-demensional space into three categories, i.e. 1) refrigerant leakage, 2) fault-free and, 3) refrigerant overcharge, condenser fouling and non-condensable gas. The T'_{sc} curve further divided the category (3) into two sub-categories, i.e. a) condenser fouling and b) refrigerant overcharge and non-condensable gas. The FDD results are summarized in Table 4.5. As illustrated in Figure 4.5, in the fault free conditions, four observation points among 108 series of data (4/108) were falsely diagnosed as the condenser fouling, while the rest one was falsely diagnosed as the refrigerant leakage.
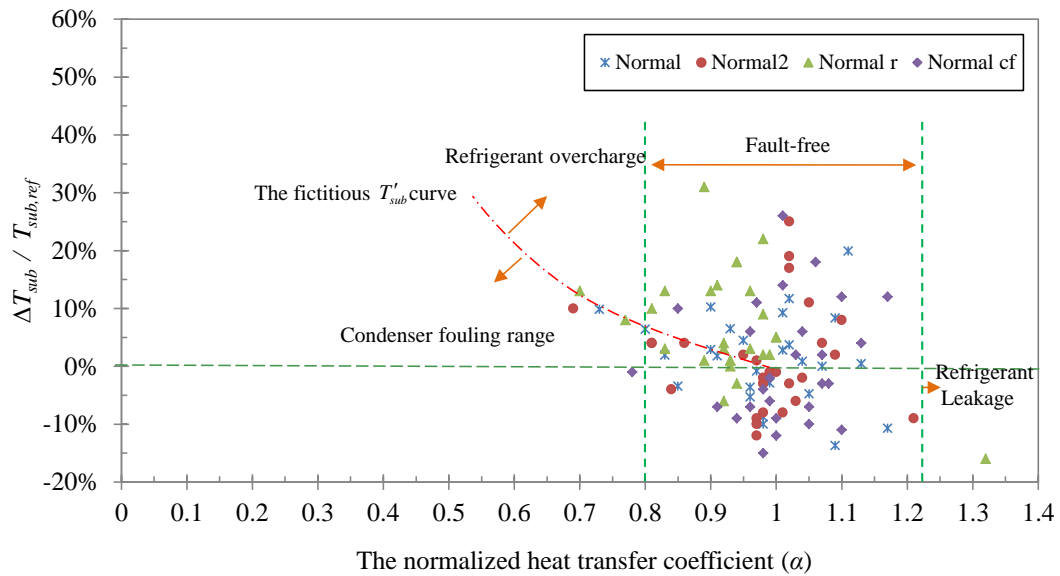
Figure 4.5 Graphic illustration of fault detection and diagnosis results for fault-free condition

In the case of condenser fouling, the successfully diagnosed ratios are 1/27, 1/27, 6/27 and 20/27 for SL-1 to SL-4 respectively, as illustrated in Figure 4.6. It is hard to detect and diagnose this kind of fault at slight severity levels, which is the same as conclusion from RP-1275.
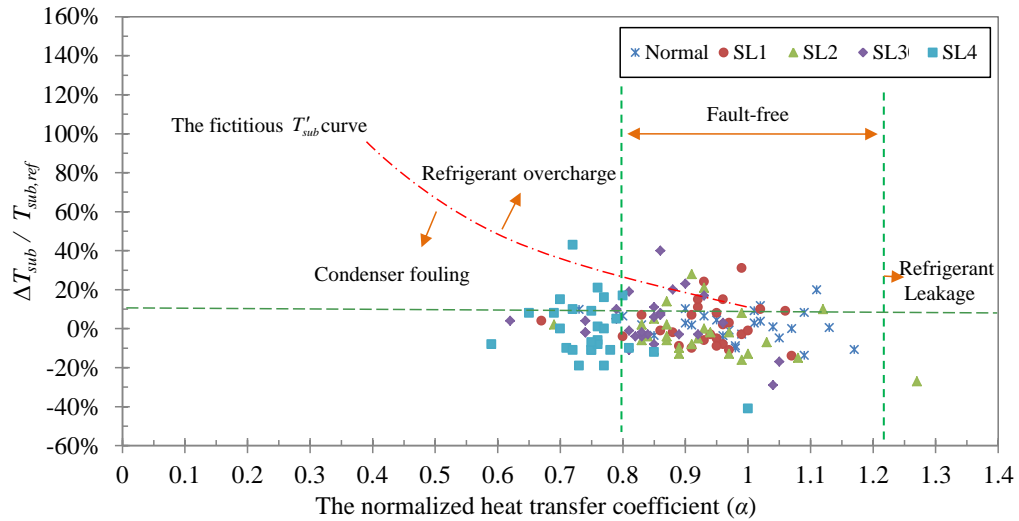
Figure 4.6 Graphic illustration of fault detection and diagnosis results for condenser fouling at four severity levels

In the case of refrigerant leakage, the successfully diagnosed ratios are 4/27, 5/27, 22/27 and 24/27, while the falsely diagnosed ratios are 4/27, 3/27, 0/27 and 0/27, for SL-1, SL-2, SL-3 and SL-4 respectively, as illustrated in Figure 4.7. At the SL-1, the falsely diagnosed ratio is the same to the correctly ones. However, 2/27 was falsely diagnosed under the condenser fouling and the remained 2/27 under the refrigerant overcharge. The correctly diagnosed ratio (4/27) is obvious larger than any others, which can be used as criteria for FDD. Similarly results were observed at the SL-2. At the SL-3 and SL-4, the fault was diagnosed successfully.
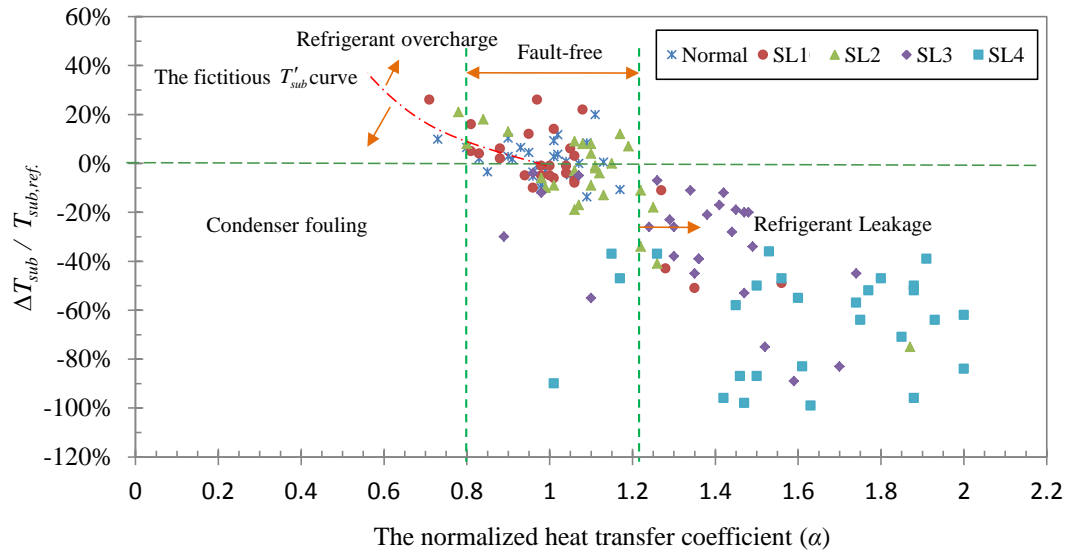
Figure 4.7 Graphic illustration of fault detection and diagnosis results for refrigerant

leakage at four severity levels
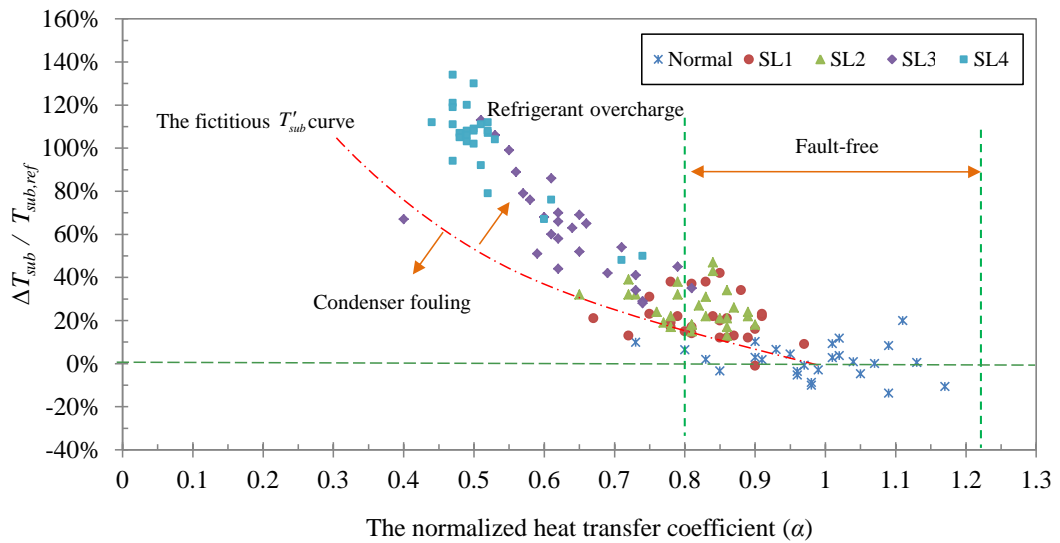
Figure 4.8 Graphic illustration of fault detection and diagnosis results for refrigerant

overcharge at four severity levels

In the case of the refrigerant overcharge, the successfully diagnosed ratios are 12/27, 18/27, 26/27 and 27/27, while the falsely diagnosed ratios are 2/27, 0/27, 1/27 and 0/27, for SL-1, SL-2, SL-3 and SL-4 respectively, as illustrated in Figure 4.8.The fault can be easily diagnosed at each severity level.

In the case of the non-condensable gas, the faults were 100% correctly diagnosed for each severity level, as illustrated in Figure 4.9. It has the same pattern as the refrigerant overcharge. However, it should be the easiest fault to be detected since the condenser pressure is obviously higher than the saturated pressure during the power off condition when there is non-condesable gas in the system.
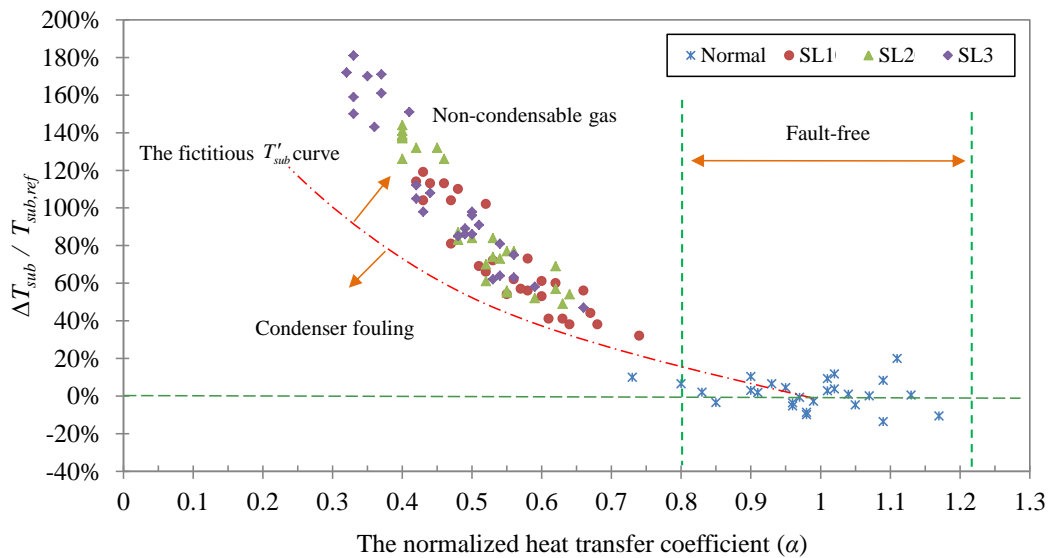
Figure 4.9 Graphic illustration of fault detection and diagnosis results for non-condensable gas at four severity levels

It should be noted that some fault data might fall into the confidence interval. Particularly at lower severity levels, most of the data are within the confidence interval.

This is the typical II error in statistical test theory which fails to reject fault data (more details refer to Section 3.2.2). The typical II error cannot be avoided theoretically. In this study, the fault diagnosis ratio is introduced to enhance the robustness of FDD results. A fault is confirmed when its diagnosis ratio is larger than a threshold, i.e. 15% in this study.

It is worthwhile to point out that the virtual $T^{'}_{sc}$ lines in Figure (4.4)-(4.8) are used for easy understanding only. Under different operating conditions, the observation points with the same α might have different fictitious sub-cooling temperatures. The fictitious temperature was not used when $\alpha > \alpha_2$. This is because there is only refrigerant leakage in this area. It is worthwhile to point out that most small and mid-size chiller systems do not have flow meters because they are costly and require annual calibration. In this case, the water flow rate can be estimated through simulation or field tests. In the literatures, there are some strategies that have already been available for simulating the water flow rates, such as Sun (2010) and Zhao (2011).

Table 4.5 Successful detection and diagnosis numbers of the proposed FDD strategy using RP-1043 data – Sample number: 27 for each severity level (SL). Confidence level: 95.4%.

Fault type	Normal				Condenser fouling				Refrigerant leakage				Refrigerant overcharge				Non-condensable gas			
Severity level (SL)	N2	N1	NCF	NR1	1	2	3	4	1	2	3	4	1	2	3	4	1	2	3	4
Fault detected	1	1	1	2	1	2	6	23	5	6	22	24	8	10	25	27	27	27	27	27
Condenser fouling	1	1	1	1	**1**	**1**	**6**	**20**	0	0	0	0	2	0	1	0	0	0	0	0
Refrigerant leakage	0	0	0	1	0	1	0	0	**4**	**5**	**22**	**24**	0	0	0	0	0	0	0	0
Refrigerant overcharge	0	0	0	0	0	0	0	3	1	1	0	0	**6**	**10**	**25**	**27**	27	27	27	27
Non-condensable gas	0	0	0	0	0	0	0	0	0	0	0	0	6	10	25	27	**27**	**27**	**27**	**27**

Table 4.6 Successful detection and diagnosis numbers of the proposed FDD strategy using RP-1043 data – Sample number: 27 for each severity level (SL). Confidence level: 90.7%.

Fault type	Normal				Condenser fouling				Refrigerant leakage				Refrigerant overcharge				Non-condensable gas			
Severity level (SL)	N2	N1	NCF	NR1	1	2	3	4	1	2	3	4	1	2	3	4	1	2	3	4
Fault detected	3	4	1	2	3	5	13	25	8	8	22	24	14	18	27	27	27	27	27	27
Condenser fouling	3	3	1	1	**3**	**4**	**12**	**21**	2	1	0	0	2	0	1	0	0	0	0	0
Refrigerant leakage	0	1	0	1	0	1	0	0	**4**	**5**	**22**	**24**	0	0	0	0	0	0	0	0
Refrigerant overcharge	0	0	0	0	0	0	1	4	2	2	0	0	**12**	**18**	**26**	**27**	27	27	27	27
Non-condensable gas	0	0	0	0	0	0	0	0	0	0	0	0	12	18	26	27	**27**	**27**	**27**	**27**

4.4.5 Comparison with Four Typical FDD Strategies

The training data sets and confidence level of the evaluation are the same as ASHRAE Project 1275 (RP-1275). A comparison was made between the proposed strategy and other four strategies studied in RP-1275. One main objective of RP-1275 was to evaluate the four typical chiller FDD strategies (#1, #2, #3 and #4) against steady-state chiller performance data (both fault-free data and fault data) gathered from RP-1043 with the intention of identifying the "best" one for subsequent field evaluation (Reddy, 2006). FDD#1 is the model-free fault detection strategy with a diagnosis table. FDD#2 is the MLR (Multiple Linear Regression) gray-box model based strategy with a diagnosis table. FDD#3 is the PCA (Principal Component Analysis) model based strategy with a diagnosis table. FDD#4 is the linear discrimination and classification strategy. The outputs from the RP-1275 report indicated that the FDD capabilities from the best to poorest of the four strategies are FDD#1 > FDD#2 > FDD#4 > FDD#3.

Table 4.7 Comparison between the successful detection and diagnosis numbers using the proposed strategy and the four typical FDD strategies – Sample number: 27 for each severity level (SL)

FDD Strategy	CdFoul				RefLeak				RefOver				Ncg			
Severity level	1	2	3	4	1	2	3	4	1	2	3	4	1	2	3	4
FDD#1	5	8	13	24	4	5	21	27	14	20	26	27	27	27	27	27
FDD#2	0	0	0	1	1	2	10	21	0	0	20	25	27	27	27	27
FDD#3	1	0	2	14	2	1	1	1	0	0	0	0	0	0	0	2
FDD#4	7	12	22	27	2	3	21	27	0	0	13	25	0	0	4	27
Proposed strategy	**1**	**1**	**6**	**20**	**4**	**5**	**22**	**24**	**6**	**10**	**25**	**27**	**27**	**27**	**27**	**27**

FDD#1: Model-free fault detection with diagnosis table strategy, FDD#2: MLR gray-box model with diagnosis table strategy, FDD#3: PCA model with diagnosis table strategy, FDD#4 Linear discrimination and classification strategy.

Table 4.7 summaries the successful fault detection and diagnosis numbers of different strategies. It can be observed that the proposed strategy has the best performance when the operation of the system suffers from the refrigerant leakage and non-condensable gas. It is the second best choice in the case of the refrigerant overcharge. Although the performance is at an intermediate level in the case of the condenser fouling, it is still better than MLR and PCA based strategies. Therefore, it can be concluded that the proposed strategy to be superior in fault detection and diagnosis ratio. However, the proposed strategy does not require the fault data for training, which is the obvious advantage in practice, as compared to the other strategies.

4.5 Summary

A novel chiller FDD strategy was developed in this study, which is convenient for practical applications without requiring any fault data for model training. The four typical faults, which are difficult to handle, (i.e. condenser fouling, refrigerant overcharge, refrigerant leakage and non-condensable gas) are detected and diagnosed based on two new performance indexes, i.e. α (the normalized heat transfer performance) and T'_{sc} (the fictitious sub-cooling temperature). The ASHRAE RP-1043 data were used to validate the proposed strategy and make qualitative comparisons with the four typical FDD strategies studied in the ASHRAE RP-1275.

The test results showed that the proposed strategy is capable of detecting and diagnosing the non-condensable gas (successfully ratios were 100% at each severity level) and refrigerant overcharge (22%, 37%, 93% and 100% for SL-1, SL-2, SL-3 and SL-4). Although the performances were not perfect for the refrigerant leakage (15%, 19%, 81% and 89% for SL-1 to SL-4) and condenser fouling (4%, 4%, 22% and 74% for SL-1 to SL-4), it was still better than most of the referred strategies. More important, the proposed strategy does not require any fault data for model training, which is essentially important for practical applications.

A customization tool was developed based on a simplified physical chiller model in order to identify the unknown chiller parameters. The customization tool and FDD strategy can be used in typical centrifugal water-cooled chillers equipped with the shell-and-tube evaporator and condenser and controlled by thermostatic expansion valves.

CHAPTER 5 AN INCIPIENT FAULT DETECTION AND

DIAGNOSIS STRATEGY FOR CHILLERS

This chapter presents the application of the proposed incipient FDD strategy on centrifugal chillers. Three innovations are adopted to overcome the shortcomings of the commonly used strategy based on MLR and t-statistic. Firstly, SVR is adopted to develop the reference PI models. A new PI, namely the heat transfer efficiency of the sub-cooling section (ε_{sc}), is proposed to improve the FDD performance. Secondly, EWMA control charts are introduced to detect faults in a statistical way to improve the ratios of correctly detected points. Thirdly, when faults are detected, diagnosis is conducted, which is based on a proposed FDD rule table. Six typical chiller component faults are considered in this chapter. This strategy is validated using the real-time experimental data from the ASHRAE RP-1043.

5.1 Overview of The Chiller FDD Strategy

5.1.1 Performance Indexes and FDD Rule Table

A new performance index, namely the heat transfer efficiency of sub-cooling section (ε_{sc}), which has the same definition as heat exchanger efficiency commonly used for heat exchangers, is proposed in this study as Equation (5.1). The heat transfer efficiency is defined as the ratio of the heat transfer in the actual heat exchanger to the heat transfer in the ideal heat exchanger. It is calculated using data from the commonly available sensors.

$$\varepsilon_{sc} = \frac{T_{sub}}{T_{cd} \text{-} T_{ecw}} \tag{5.1}$$

Four performance indexes are introduced in this study as illustrated in Table 5.1. They are physically meaningful and sensitive to one or several faults. They indicate the health state of chillers. It is noted that the selections of PIs might be different for different types of chillers. Virtual sensors can also be used as PIs (Li and Braun 2007). The performance indexes can be calculated directly from measurements which are generally available in the building management systems (BMSs).

Table 5.1 Definitions of performance indexes

	Performance indexes	Formulations
1	Evaporator water temperature difference	$\Delta T_{chw} = T_{chwr} - T_{chws}$
2	Condenser water temperature difference	$\Delta T_{cw} = T_{lcw} - T_{ecw}$
3	Heat exchanger efficiency of the Sub-cooling section	$\varepsilon_{sc} = \dfrac{T_{sub}}{T_{cd} - T_{ecw}}$
4	Logarithm mean temperature difference of condenser	$LMTD_{cd} = \dfrac{T_{lcw} - T_{ecw}}{\ln(\dfrac{T_{ecw} - T_{cd}}{T_{lcw} - T_{cd}})}$

Six typical faults are condered in this study, which account for a major portion of the service calls according to the survey conducted by Comstock and Braun (2002), including: reduced evaporator water flow rate, reduced condenser water flow rate, condenser fouling, refrigerant leakage, refrigerant overcharge, non-condensable gas.

The fault patterns are illustrated in Table 5.2. Where, the sign ▲ and ▼ indicate the changes of performance index compared to its benchmark of normal state. The sign - indicates no obvious change. The sign * indicates that the faults are detected and diagnosed in the beginning which are not considered in following steps. The correlations in Table 5.2 are based on the impacts of the faults on the performance indexes, which are interpreted as follows:

Table 5.2 Fault detection and diagnosis rule table

	Fault type	ΔT_{chw}	ΔT_{cw}	ε_{sc}	$LMTD_{cd}$
1	Reduced evaporator water flow rate	▲	-	*	*
2	Reduced condenser water flow rate	-	▲	*	*
3	Condenser fouling	-	-	▼	▲
4	Refrigerant leakage	-	-	▼	▼
5	Refrigerant overcharge	-	-	▲	▲
6	Non-condensable gas	-	-	▲	▲

i. *Reduced evaporator water flow rate*. The evaporator water temperature difference ΔT_{chw} is significantly increased to keep the same amount of cooling load when the evaporator water flow rate is reduced ($\Delta T_{chw} = \dfrac{Q_{evap}}{c_w M_{evap,w}}$). In this study, a constant threshold is set for the residuals of ΔT_{chw}.

ii. *Reduced condenser water flow rate.* Similar to the previous fault, the condenser water temperature difference ΔT_{cw} is increased ($\Delta T_{cw} = \dfrac{Q_{cond}}{c_w M_{cond,w}}$). In this study, a constant threshold is set for the residuals of ΔT_{cw}.

iii. *Condenser fouling.* When this fault exists, the overall heat transfer conductance of condensing section (UA_{cd}) and sub-cooling section (UA_{sc}) will be reduced. Thus, this results in larger $LMTD_{cd}$ and smaller ε_{sc}.

iv. *Refrigerant leakage.* The decreased liquid refrigerant level in the condenser results in less heat transfer surface area for sub-cooling. Therefore the ε_{sc} is reduced. Meanwhile, the corresponding surface area is used for condensing section. The UA_{cd} is increased, which leads to a smaller $LMTD_{cd}$. For more analysis about this fault refer to Tassou (Tassou and Grace 2005).

v. *Refrigerant overcharge.* It is opposite to the leakage fault patterns. Both ε_{sc} and $LMTD_{cd}$ are larger than normal values.

vi. *Non-condensable gas.* The non-condensable gas is gathered at the condenser and leads to a higher condensing pressure. The condensing temperature increases substantially because it is usually calculated based on the measured condensing pressure. Therefore, both calculated $LMTD_{cd}$ and ε_{sc} increase dramatically. It has the same fault patterns as the refrigerant overcharge. However, it is the easiest fault to be diagnosed (Chen and Braun 2001). Non-condensable gas tends to accumulate in the condenser. Techinicians can detect this fault when the chiller is turned off. The condenser pressure reading is higher than the actual saturation pressure when non-condensable gas exists in the chiller system (Comstock and Braun 1999a). The

94

actual saturation pressure can be derived based on the measured saturation temperature.

5.1.2 Reference Models of Performance Indexes

The reference models are developed to calculate the benchmarks of performance indexes in normal condition. Assuming the water flow rates are constant in condenser and evaporator, the chiller performance is primarily a function of three variables, i.e. Q_{ev} (evaporator cooling load), T_{ecw} (entering condenser water temperature) and T_{chws} (leaving evaporator water temperature (Comstock and Braun 2002). A simple chiller reference model is presented as shown in Equation (5.2). Where, $Y = [\Delta T_{chw}, \Delta T_{cw}, \varepsilon_{sc}, LMTD_{cd}]$, $\xi \sim (0, \sigma^2)$.

$$Y = f(Q_{evap}, T_{ecw}, T_{chws}) + \xi \tag{5.2}$$

To develop such models, the polynomial gray-box Multiple Linear Regression (MLR) approach has been widely used by Cui and Wang (2006), Li and Braun (2003), Reddy (2007a) and so on. However, the chiller is a typical non-linear system. The limitation of MLR is that it is a linear approach. To improve the accuracy, a non-linear approach namely the Support Vector Regression (SVR) is adopted to build the reference models. It is a new machine learning algorithm based on structural risk minimization from statistical learning theory. It possesses prominent advantages such as excellent properties in learning limited samples, good generalization ability, etc.

5.1.2 Configuration of the EWMA Control Charts

In this study, the sample group size n of EWMA control charts is set to be 1 to obtain more groups at each operating condition, considering that the amount of the experimental data at each operating condition is small (about 5 data in average). If n is set to be a larger value, e.g. 5, there will be only 1 group at each operating condition in average. Also, when the moving window moves from one operating condition to another, the physical meaning is also not clear to calculate the average value $\overline{X}_i$ of the sample group which contains samples of different operating conditions. In practice, the amount of operating data at an operating condition is generally large enough. It is advised to use a larger sample group size n because it is better to use group mean to reduce noises in measurements. When the weighting factor λ is smaller, the chart is more sensitive to smaller long-term deviations caused by the gradually generated faults, e.g. condenser fouling and refrigerant leakage. In this study, the λ is optimized using fault data of condenser fouling and refrigerant leakage at SL 1. The best performance is obtained when λ is 0.15. The L is assigned to be 2 (confidence level is 95.45%) and 3 (confidence level is 99.73%) respectively in the case studies. The 95.45% confidence level is acceptable for actual application as discussed in previous studies (Reddy 2006). The training data used in the offline FDD process are residuals between predicted PIs and actual values. σ is the standard deviation of the residuals. μ_0 is the expectation of the residuals.

5.2 Evaluation of the FDD Strategy

5.2.1 Experimental Data and Data Pre-processing

The 'Reduced data set' from RP-1043 is introduced here. It included transient data between the different steady-state operating conditions. The steady-state data filter developed by Rossi (Rossi 1995) is used to remove the obvious dynamic data. It regresses samples of a variable using the OLS (Ordinary Least Squares) strategy with a fixed moving time window length, and then obtains the slope of the regression line, which can also indicate the change rate of the variable. Actually, only not more than 10% data are in steady-state if all performance variables are selected as state characteristics. It is too few for fault detection and diagnosis. Therefore, there is a compromise between the amount of remaining data and the steady-state level of remaining data. In this study, the chilled water supply temperature (T_{chws}), the chilled water return temperature (T_{chwr}) and the entering condenser water temperature (T_{ecw}) are used by the filter for steady-state detection. They are actually the inputs of reference models. About 30%-40% data were remained eventually. It is worth noting that the sub-cooling temperature (T_{sc}) in the remained data might be not steady all the time. They are only closed to steady states sometimes. It is because T_{sc} hardly archives steady state. If T_{sc} is also required to be steady in the data pre-processing process, there would be only about 10% data remained eventually. The amount is too small for the purpose of FDD. Although T_{sc} is not absolutely steady most of the time, the deviations of T_{sc} caused by the remained dynamics are still obviously smaller than the deviations caused by faults. The dynamics will reduce fault detection ratios of the PI ε_{sc}.

97

5.2.2 Development of The Reference Models

The normal data set 'normal2' from the RP-1043 are used to train the reference models. Comparisons between the predicted values (using SVR models) and the current values of performance indexes are shown in Figure 5.1. The R-squares (R^2) show desirable goodness-of-fits of the SVR models. The R^2 is 0.8355 for ε_{sc}. It was poor for the reason that the sub-cooling temperatures are not steady at most of the time. The threshold for this PI will be larger which might lead it to be not sensitive to faults. However, it is still acceptable for chiller FDD application.
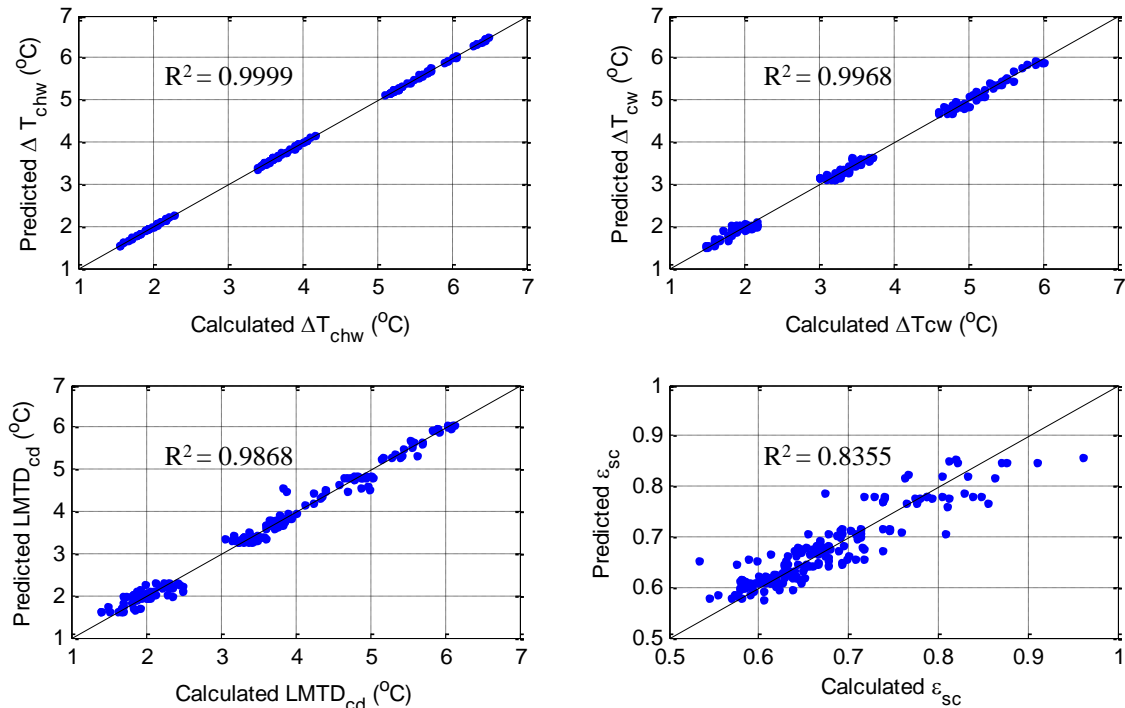
Figure 5.1 Comparisons between predicted and calculated values of performance indexes using ASHRAE RP-1043 data

Table 5.3 Fitness SVR-based and MLR-based performance index models applied to

ASHRAE RP-1043 data

		ΔT_{chw}	ΔT_{cw}	ε_{sc}	$LMTD_{cd}$
MLR	R^2	0.9999	0.9950	0.8181	0.9782
	σ_{MLR}	0.0141	0.0961	0.0341	0.1945
SVR	R^2	0.9999	0.9968	0.8355	0.9868
	σ_{SVR}	0.0139	0.0776	0.0325	0.1517
$\sigma_{SVR}/\sigma_{MLR}$		98.6%	80.7%	95.4%	78.0%

The accuracy of SVR models and MLR models are illustrated in Table 5.3. The performances of SVR models are better in all PIs. The R-squares were improved. The standard deviations are smaller obviously. The ratio of standard deviations, $\sigma_{SVR}/\sigma_{MLR,}$ of the two important PIs (i.e. ε_{sc} and $LMTD_{cd}$) were 95.4% and 78.0% respectively. Therefore, the confidence intervals are narrowed down by the same ratio.

5.2.3 Comparison of Fault Detection and Diagnosis Between Four Strategies

In order to validate the advantages of SVR and EWMA on chiller FDD, comparisons are made between four strategies, which were different combinations of regression approaches (MLR or SVR) and fault detection approaches (*t*-statistic or EWMA), i.e., Strategy #1, MLR + *t*-statistic; Strategy #2, MLR + EWMA; Strategy #3, SVR + *t*-statistic; Strategy #4, SVR + EWMA. Among them, Strategy #1 is the commonly used chiller FDD strategy. It is the same as the MLR-FDD strategy used in ASHRAE RP-1275, while the difference is that the proposed rule table is used. Strategy #4 is the proposed strategy in this chapter, which will be analyzed in detail. The confidence level

was 99.73% (3σ). The ratio of correctly diagnosed points is the amount of correctly diagnosed points divided by the total amount of test points. The ratio of false diagnosed points is the amount of false diagnosed points divided by the total amount of test points.

Normal condition

Table 5.4 Diagnosis ratios of four different strategies at confidence level of 99.73% in normal condition

FDD Strategy	Normal		Normal1		Normal2	
	Correct	False	Correct	False	Correct	False
Strategy #1	96.2%	0.0%	92.3%	0.0%	98.9%	0.0%
Strategy #2	86.2%	0.0%	79.8%	0.0%	92.1%	0.0%
Strategy #3	93.7%	0.0%	90.5%	0.0%	98.3%	0.0%
Strategy #4	86.2%	0.0%	76.2%	0.0%	98.9%	0.0%

Three normal experimental data sets from the ASHRAE RP-1043 are introduced to evaluate the four strategies in normal conditions, i.e. 'normal', 'normal1' and 'normal2'. The results are illustrated in Table 5.4. It can be found that all of the false alarm ratios are 0.0% and all of the four strategies are robust in the normal conditions.
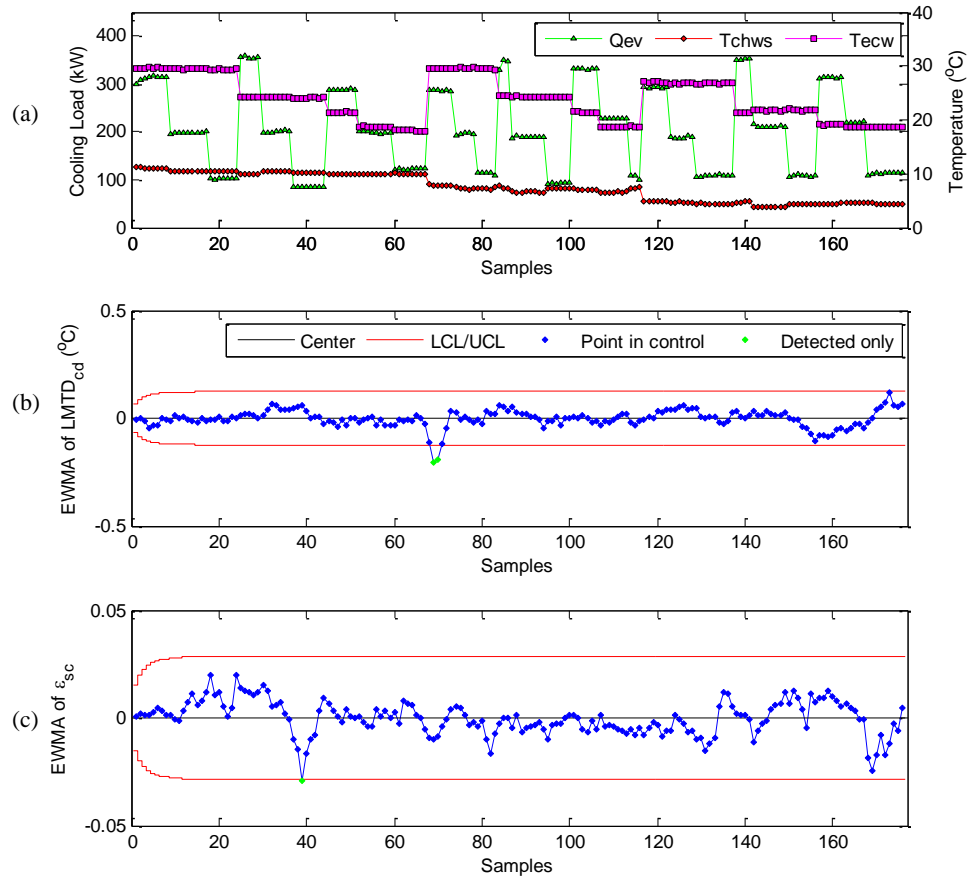
Figure 5.2. Operating conditions and control charts using normal data set 'normal2'.

(a) Operating condition, (b) EWMA control chart of $LMTD_{cd}$, (c) EWMA control chart

of ε

It is also noticed that the ratios of health points (both PIs were within the confidence intervals) of the t-statistic-based strategies (Strategy # 1 and #3) are about 8% higher than that of the EWMA-based ones (Strategy #2 and #4) in average. It is because that the EWMA control chart is more sensitive to the small shifts of the deviations. The MLR-based strategies (Strategy #1 and #2) are slightly better than the SVR based ones (Strategy #3 and #4). It is because that the MLR-based strategies have wider confidence intervals. However, it does not mean that the strategies using EWMA and SVR are not robust. It is a compromise between the correct diagnosis ratio when a fault occurs and

the false alarm ratio in normal condition. Generally, if the sensitivities to shifts of deviations are higher and the confidence intervals are narrower, the strategy will be able to detect more faulty points. But it will be hard to keep low false alarm ratios in normal conditions. The strategy using EWMA and SVR (Strategy #4) has higher diagnosis ratios of faulty points and 0.0% false alarm ratios. Therefore, it is the best one.

Figure 5.2 illustrates the FDD results when using Strategy #4 for the normal data set 'normal2'. The control charts of $LMTD_{cd}$ and ε_{sc} are not violated at the same time and therefore the false alarm ratio was 0.0%.

Condenser fouling

Using the EWMA-based strategies (Strategy #2 and #4), the highest ratios of correctly diagnosed points are 7.7%, 45.2%, 68.4% and 100.0% at SL-1, SL-2, SL-3 and SL-4 respectively at both confidence levels, as shown in Table 5.5. Using the t-statistic-based strategies (Strategy # 1 and #3), the highest ratios of correctly diagnosed points are 0.7%, 1.3%, 2.6% and 54.7% at SL-1, SL-2, SL-3 and SL-4 respectively at both confidence levels. The *t*-statistic-based strategies cannot correctly diagnose this fault until SL-4. Comparing the strategies using EWMA (Strategy #2 and #4), the SVR approach improves 5% correctly diagnosed points at SL-1 and SL-2.

The FDD results when using Strategy #4 are as shown in Figure 5.3. The points are labeled by four classes, i.e., the correctly diagnosed, the wrongly diagnosed, the detected only and the normal point. The 'detected only' means that a point only violated one control chart and it could not be diagnosed. The ratios of correctly diagnosed points are 7.7%, 45.2%, 60.7% and 100% for SL-1, SL-2, SL-3 and SL-4 respectively. The corresponding false diagnosis ratios are 3.3%, 8.3%, 3.8% and 0.0% respectively.

Table 5.5 Diagnosis ratios of four different strategies at confidence level of 99.73%

FDD Strategy	Severity Level 1		Severity Level 2		Severity Level 3		Severity Level 4	
	Correct	False	Correct	False	Correct	False	Correct	False
Condenser fouling								
Strategy #1	0.7%	0.0%	0.0%	1.9%	0.7%	0.7%	53.3%	0.0%
Strategy #2	1.9%	0.7%	40.0%	3.2%	68.4%	0.0%	100.0%	0.0%
Strategy #3	0.0%	0.0%	1.3%	4.5%	2.6%	4.5%	54.7%	0.0%
Strategy #4	7.7%	3.2%	45.2%	8.3%	60.7%	3.8%	100.0%	0.0%
Refrigerant leakage								
Strategy #1	5.2%	0.0%	13.5%	0.0%	41.9%	0.0%	90.4%	0.0%
Strategy #2	21.4%	3.9%	34.8%	5.7%	87.2%	1.7%	100.0%	0.0%
Strategy #3	10.4%	0.0%	17.0%	0.0%	46.9%	0.0%	96.6%	0.0%
Strategy #4	20.1%	2.6%	36.2%	7.1%	88.3%	1.1%	100.0%	0.0%
Refrigerant overcharge								
Strategy #1	6.6%	0.0%	12.7%	0.0%	76.1%	0.0%	89.4%	0.0%
Strategy #2	89.5%	0.0%	98.7%	0.0%	100.0%	0.0%	100.0%	0.0%
Strategy #3	4.0%	0.0%	15.2%	0.6%	78.6%	0.0%	90.2%	0.0%
Strategy #4	90.1%	0.0%	100.0%	0.0%	100.0%	0.0%	100.0%	0.0%
Non-condensable gas								
Strategy #1	37.2%	0.0%	61.3%	0.0%	77.7%	0.0%	93.4%	0.0%
Strategy #2	97.4%	0.0%	99.3%	0.0%	99.3%	0.0%	100.0%	0.0%
Strategy #3	36.5%	0.0%	64.2%	0.0%	79.7%	0.0%	100.0%	0.0%
Strategy #4	98.7%	0.0%	99.3%	0.0%	100.0%	0.0%	100.0%	0.0%

In the case of SL-1, the 3.3% false diagnosis might be caused by two possible reasons. One possible reason is the dynamics of the sub-cooling temperature in both training and testing data sets. Another possible reason is the way how this fault is

conducted in the experiment. It might not be proper to simulate the effects of condenser fouling on sub-cooling section at SL-1 by plugging 12% tubes in the condenser. However, the false diagnosis ratio is not more than 50% of the ratio of correctly diagnosed points. This threshold can be used as the criteria to report faults in practice.

Refrigerant leakage

Using the EWMA-based strategies (Strategy #2 and #4), the ratios of correctly diagnosed points are more than two times of that of the *t*-statistic-based strategies (Strategy # 1 and #3) at SL-1, SL-2 and SL-3, as shown in Table 5.5. Even at SL-1, 20.1% points are correctly diagnosed by the EWMA-based strategies. When used in the *t*-statistic-based strategies (Strategy #1 and #3), the SVR approach improves the correct diagnosis ratio for about 5% at four severity levels. It improves about 2% of the correct diagnosis ratios when used in the EWMA-based strategies (Strategy #2 and #4).

The FDD results when using Strategy #4 are as shown in Figure 5.4. The ratios of correctly diagnosed points are 20.1%, 36.2%, 88.3% and 100.0% at SL-1, SL-2, SL-3 and SL-4 respectively. The corresponding false diagnosis ratios are 2.6%, 7.1%, 1.1% and 0.0% respectively. It is also noticed that 49.4% and 7.8% of points exceed the UCL of the $LMTD_{cd}$ control charts at SL-1 and SL-2 in spite of exceeding the LCL (in Figure 5.4b). However, these points are not wrongly diagnosed for the reason that the ε_{sc} is in control at that time.
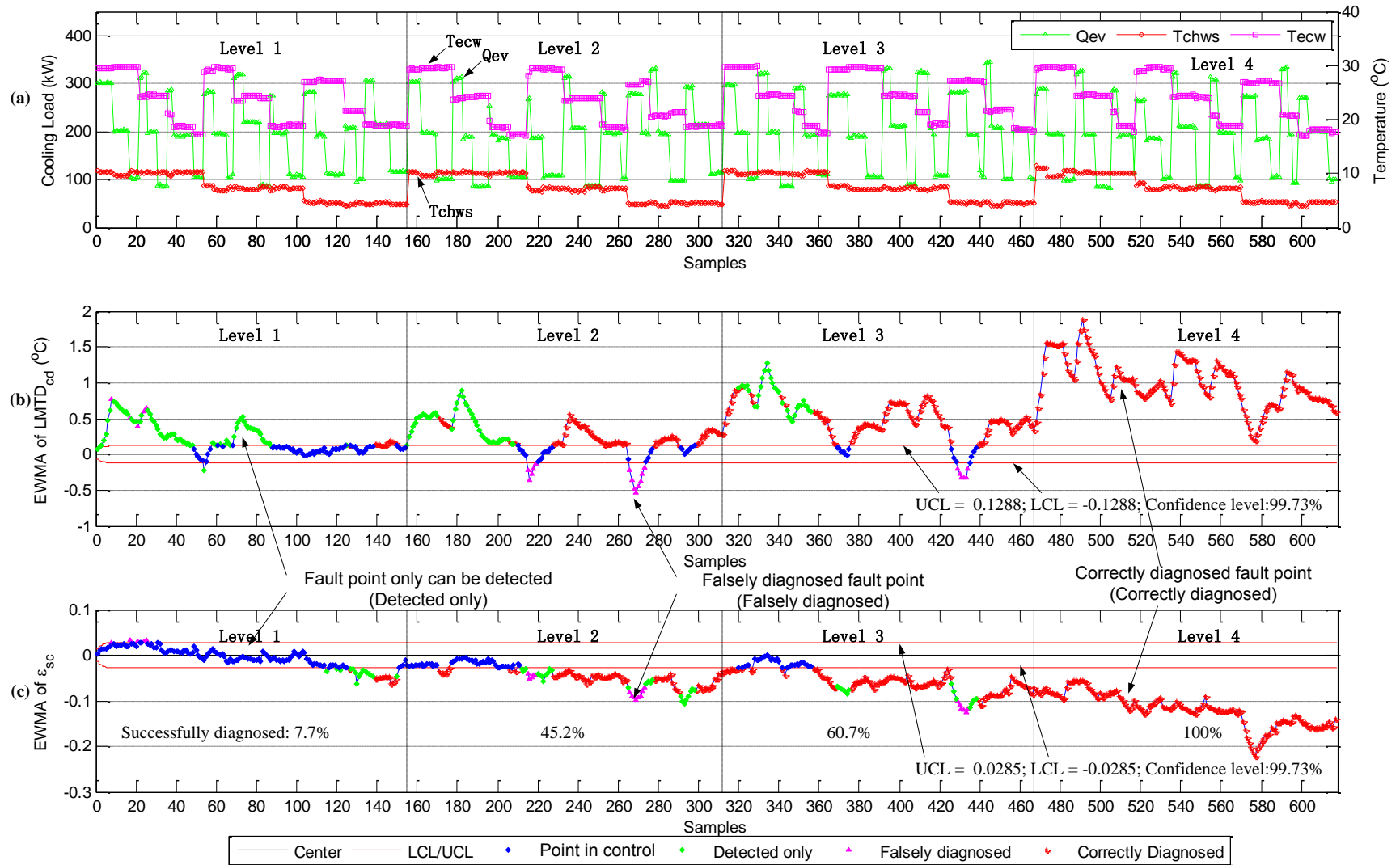
Figure 5.3 Operating conditions and control charts in the case of condenser fouling at four severity levels.

(a) Operating condition, (b) EWMA control chart of *LMTD*$_{cd}$, (c) EWMA control chart of ε_{sc}.
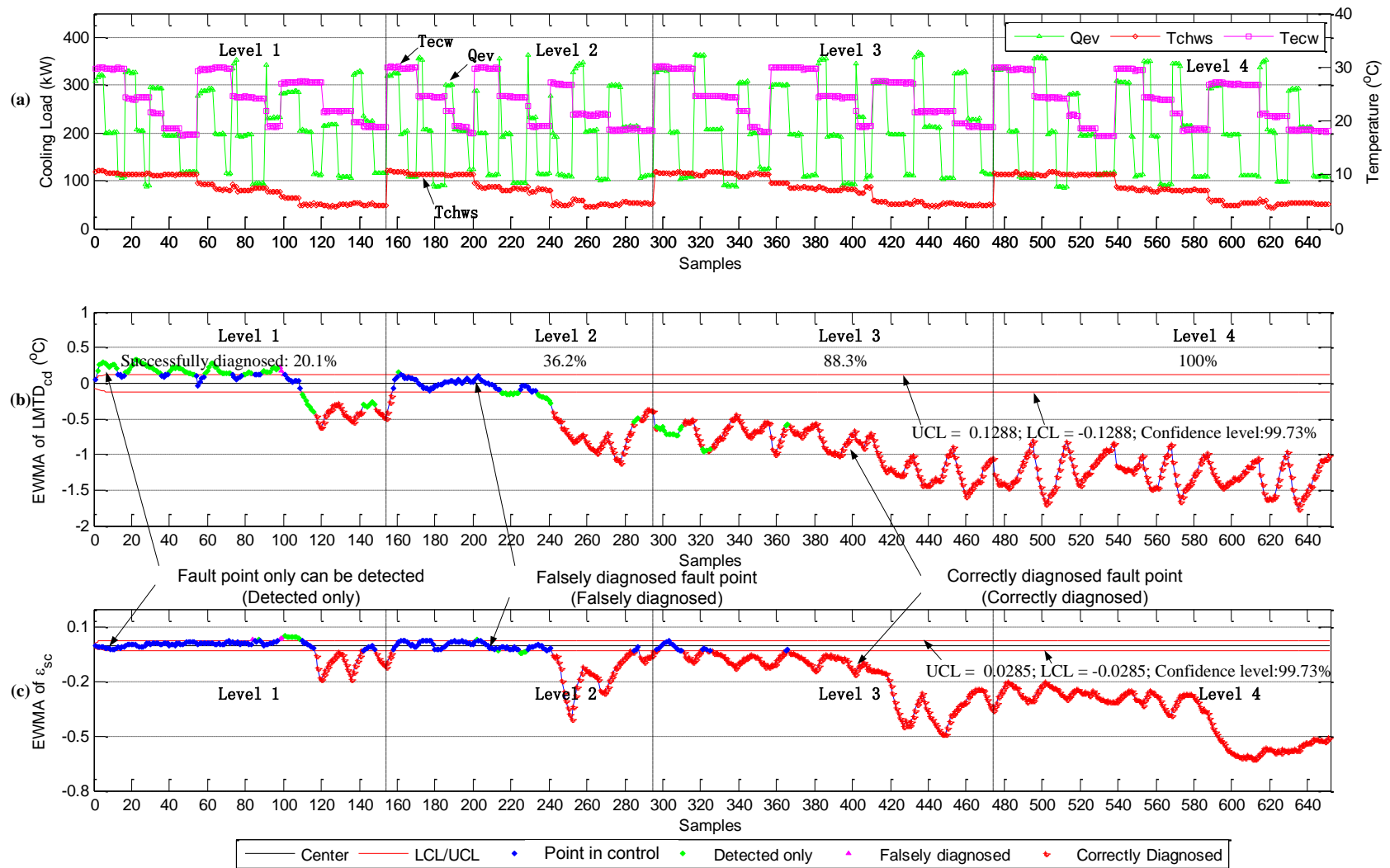
Figure 5.4 Operating conditions and control charts in the case of refrigerant leakage at four severity levels.

(a) Operating condition, (b) EWMA control chart of *LMTD_cd*, (c) EWMA control chart of ε_{sc}.
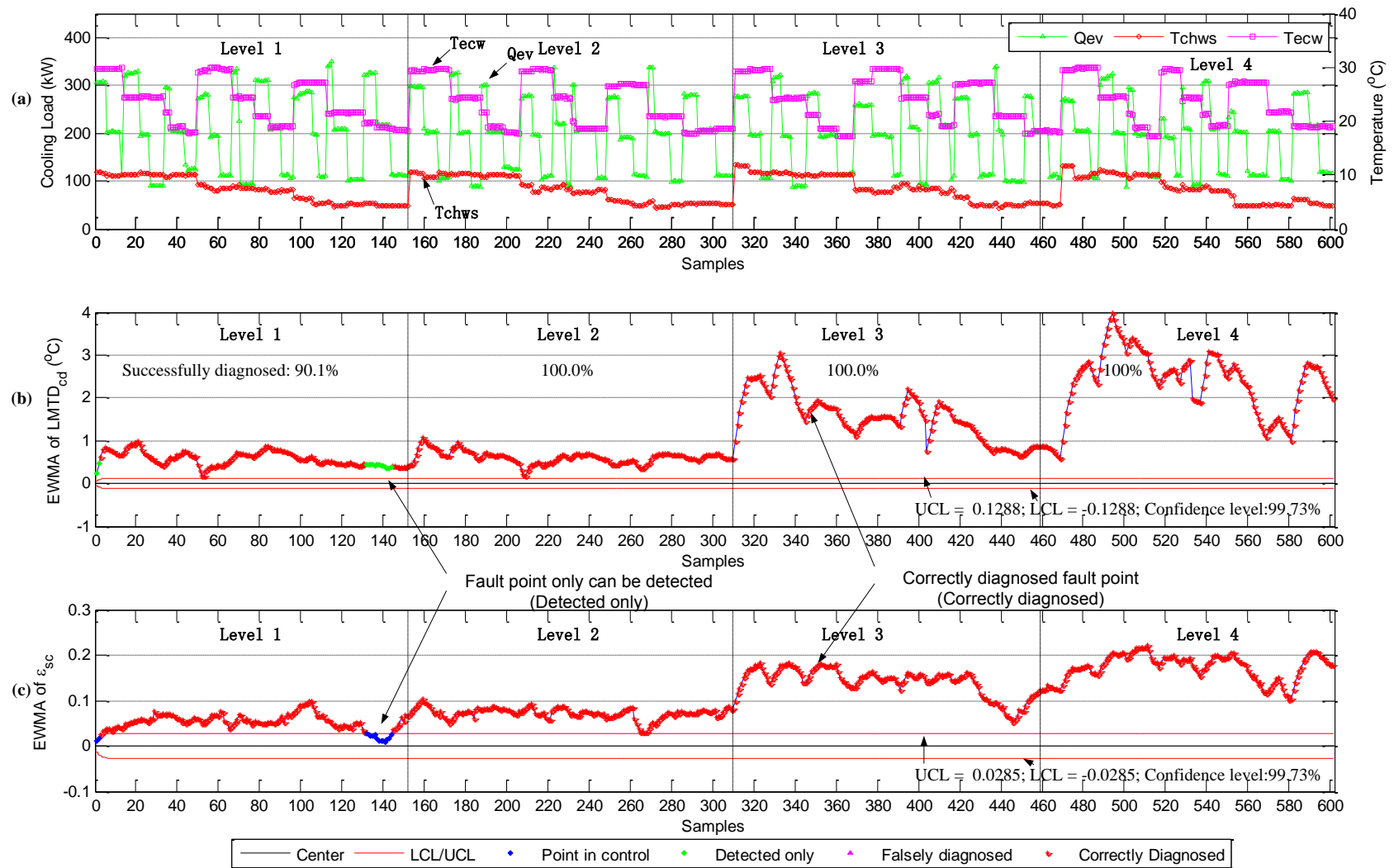
Figure 5.5 Operating conditions and control charts in the case of refrigerant overcharge at four severity levels.

(a) Operating condition, (b) EWMA control chart of $LMTD_{cd}$, (c) EWMA control chart of ε_{sc}.

107
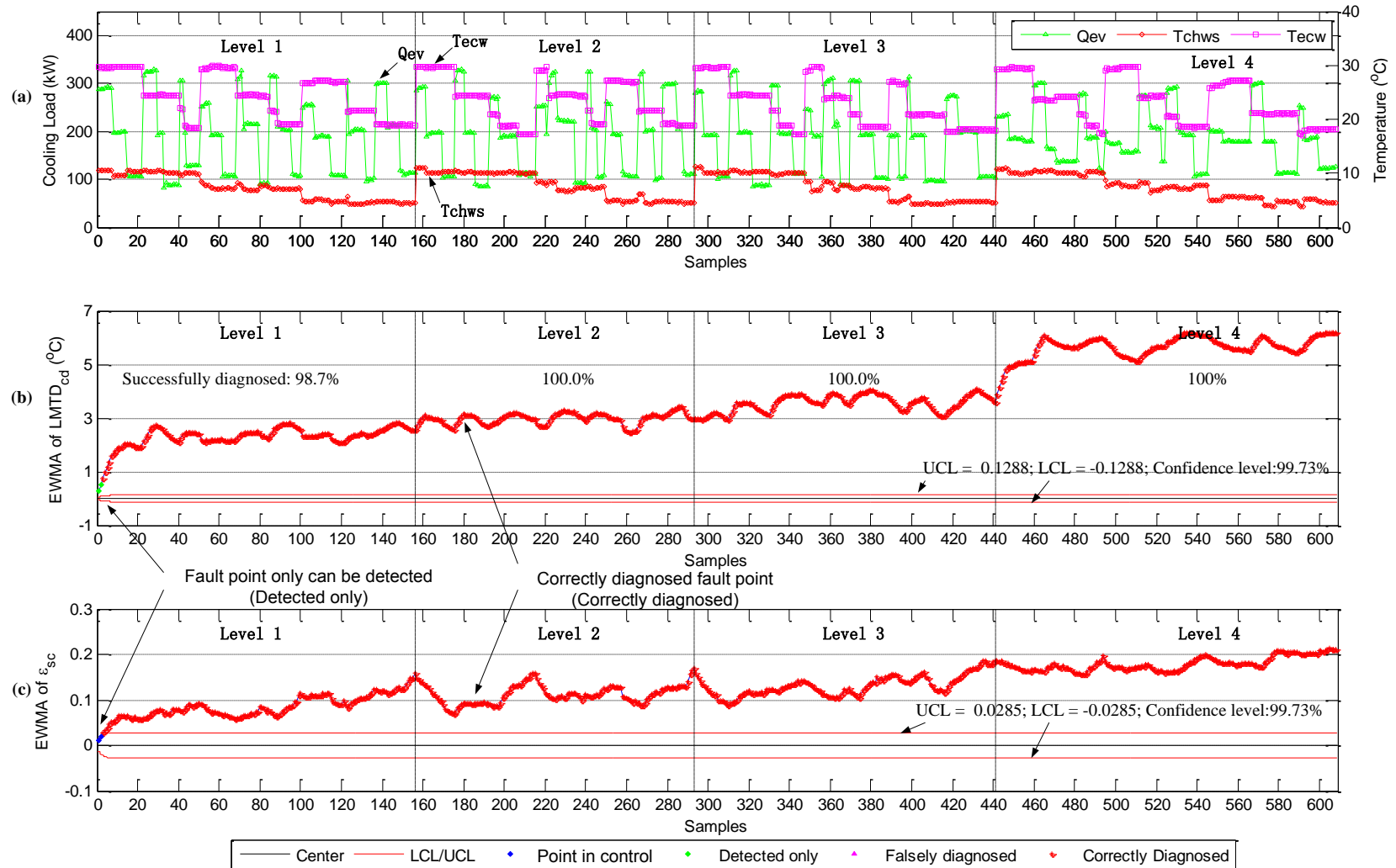
Figure 5.6 Operating conditions and control charts in the case of Non-condensable gas at four severity levels.

(a) Operating condition, (b) EWMA control chart of *LMTD~cd~*, (c) EWMA control chart of *ε~sc~*.

Refrigerant overcharge

Using the EWMA-based strategies (Strategy #2 and #4), the highest ratios of correctly diagnosed points are 90.1%, 100.0%, 100.0% and 100.0% at SL-1, SL-2, SL-3 and SL-4 respectively, as shown in Table 5.5. However, the best results for the t-statistic-based strategies (Strategy # 1 and #3) are 6.6%, 15.2%, 78.6% and 90.2% at SL-1, SL-2, SL-3 and SL-4 respectively. The SVR approach has limited improvements at the correctly diagnosed points for the two strategies.

The FDD results by Strategy #4 are as shown in Figure 5.5, the ratios of corrected points are 90.1%, 100.0%, 100.0% and 100.0% at SL-1, SL-2, SL-3 and SL-4 respectively. The falsely diagnosed ratios aer 0.0% at all of the four severity levels. Even at SL-1, the average deviations of $LMTD_{cd}$ and ε_{sc} are 4.5 and 1.9 times of the corresponding thresholds (UCL).

Non-condensable gas

Using the EWMA-based strategies (Strategy #2 and #4), the ratios of correctly diagnosed points are more than 97.0% at four severity levels. However, the best results for the *t*-statistic-based strategies (Strategy # 1 and #3) are 37.2%, 64.2%, 79.7% and 100.0% at SL-1, SL-2, SL-3 and SL-4 respectively, as shown in Table 5.5. The SVR approach also has limited improvements at the correctly diagnosed points for the EWMA-based strategies, i.e. about 2% improvement when used in the t-statistic-based strategies in average.

The results when using Strategy #4 are as shown in Figure 5.6, the ratios of correctly diagnosed points are 98.7%, 100.0%, 100.0% and 100.0% at SL-1, SL-2, SL-3 and SL-4

respectively. The falsely diagnosed ratios are 0.0% at all of the four severity levels. At SL-1, the average deviations of $LMTD_{cd}$ and ε_{sc} are 17.9 and 3.0 times of the corresponding thresholds (UCL). Conclusion can be made that the proposed strategy can detect and diagnose the non-condensable gas without any problem.

Reduced water flow rate faults

The reduced condenser water flow rate and reduced evaporator water flow rate are the two faults which are most easily handled. In most studies, both faults can be 100.0% detected and diagnosed. It is no necessary to detect the small shifts in the water flow rates, e.g., the water flow rate reduced by 1%, 3%, or even 5%. The proposed strategy can handle these two faults easily. The EWMA values of ΔT_{cw} and ΔT_{chw} were several times of the confidence intervals in the cases of reduced condenser water flow rate and reduced evaporator water flow rate. In average, it was 5.5 times when evaporator water flow rate was reduced by 10%. It was 5.2 times in the case when condenser water flow rate was reduced by 10%. In this study, the constant thresholds for ΔT_{cw} and ΔT_{chw} were set to be 2.0K as confidence intervals. Both faults were more than 95% correctly diagnosed at all of the four severity levels.

5.2.4 Discussions

The false diagnosis ratios of the t-statistic-based strategies (Strategy # 1 and #3) are high at low severity levels. It is caused by two factors, i.e. 1) the dynamics in the test data which are not removed completely, and 2) the uncertainties of both model-fitting errors and measurement errors. Using the EWMA control charts, it is good in weakening the dynamics and errors through the weighting factor. The small shifts of deviations

caused by faults can be correctly detected using the time series information of historical data in a statistical way. Therefore, the EWMA-based strategies (Strategy # 2 and #4) are more effective than the t-statistic-based ones at low severity levels. The SVR approach improves 5.6% and 22.2% of the accuracy of the two PIs (i.e. ε_{sc} and $LMTD_{cd}$) respectively in the normal data set. It is found that the ratios of correctly diagnosed points are improved for about 5% at low severity levels for condenser fouling and refrigerant leakage.

The performance indexes are sensitive to the operating conditions. Generally, the lower the T_{chws} is, the higher the deviation of $LMTD_{cd}$ would be. In contrast, the lower the T_{chws} is, the lower the deviation of ε_{sc} would be. Q_{ev} and T_{ecw} affected the deviations of performance indexes too. For instance, in the case of the condenser fouling, the curves of $LMTD_{cd}$ are similar at the same operating condition (when T_{chws} is about 10°C) of different severity levels. The deviation increased as the severity level is higher, as shown in Figure 5.2-5.6. It is worthy of note that the EWMA values in Figure 5.3-5.6 are calculated without breaks between different severity levels in order to represent the trends of PIs from SL-1 to SL-4.

5.3 Comparison between The proposed FDD Strategy and A Commonly Used FDD Strategy

In *Section 5.2*, the four strategies under study (including the proposed strategy) are compared in the condition that they use the same performance indexes and rule table proposed in this study. It is great interest to compare the proposed strategy with the existing strategies commonly used by researchers.

In the ASHRAE RP-1275, a commonly used strategy was evaluated and recommended. The strategy adopts MLR for reference model development, t-statistic for fault detection, as well as the rule table specified in Table 5.6 for diagnosis, namely Typical MLR-t for short in this paper. In Table 5.6, the sign 0 indicates no obvious change. The real-time data generated in the RP-1043 were also used here. Since such strategies are usually validated at the confidence level of 95.45% in the related publications, comparisons are made at both confidence levels of 95.45% (2σ) and 99.73% (3σ) respectively. Only four faults are considered here, excluding two faults (i.e. reduced evaporator and condenser water flow rate) which are easy to be handled.

Table 5.6 Fault diagnosis rule table recommended in the RP-1275 (only four faults included)

Fault type	T_{sc}	TCA	$UA_{cond.}$
refrigerant leakage	▼	▼	▲
refrigerant overcharge	▲	▲	▼
condenser fouling	0	▲	▼
non-condensable gas	▲	▲	▼

5.3.1 Normal Condition

Three normal experimental data sets from the ASHRAE RP-1043 are used in the comparison study in normal condition, i.e. 'normal', 'normal1' and 'normal2', as shown in Figure 5.7. For both strategies, the performances at the confidence level of 99.73% are better than that at 95.45%. False alarm ratios when using the Typical MLR-t strategy are about 4.0% and 2.4% at the confidence levels of 95.45% and 99.73% respectively, while there are 3.6% and 0.0% only when using the proposed strategy. The proposed

strategy is noticeably better than the Typical MLR-t strategy. It is worth noticing that the Typical MLR-t strategy achieved higher ratios within both confidence intervals.
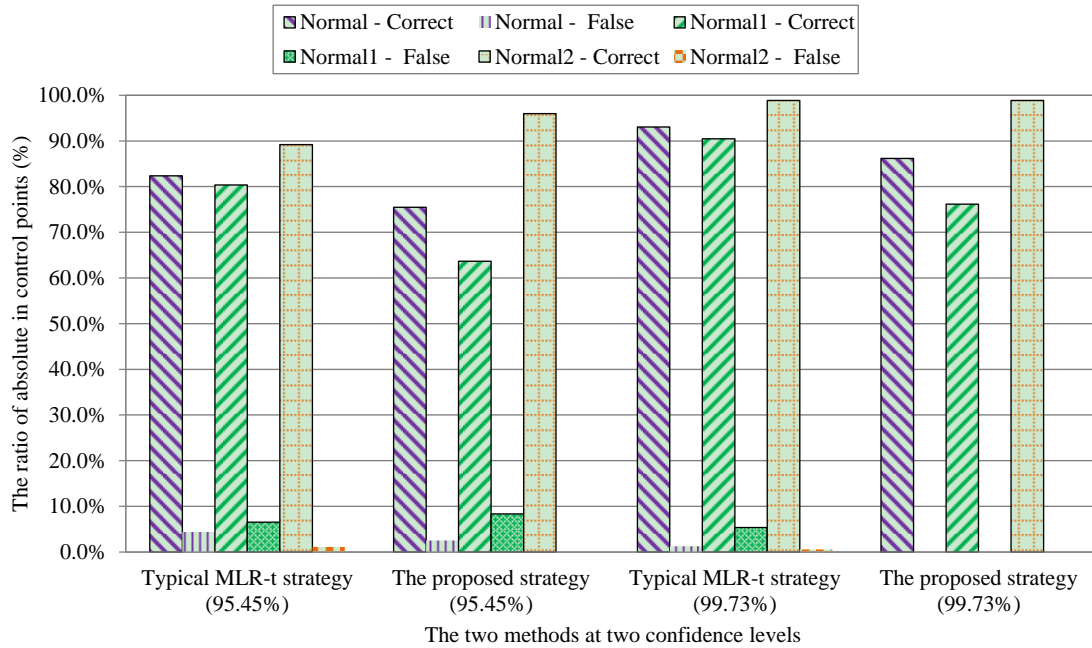
Figure 5.7 Correct diagnosis and false diagnosis ratios using proposed strategy and Typical MLR-t strategy under the normal conditions

5.3.2 Condenser Fouling

Using the Typical MLR-t strategy, the highest ratios of correctly diagnosed points are 0.7%, 5.1%, 14.8%, 53.3% at SL-1, SL-2, SL-3 and SL-4 respectively at both confidence levels, as shown in Figure 5.8. The corresponding false diagnosis ratios are 6.5%, 8.9%, 16.1% and 18.7%. It does not effectively diagnose this fault because the ratios of correctly diagnosed points are even lower than the false diagnosis ratios at SL-1, SL-2 and SL-3. This is mainly caused by the performance index T_{sc}, which is assumed not being affected by this fault. As shown in same figure, it is obvious that the proposed strategy is more effective than the Typical MLR-t strategy. At the confidence level of

99.73%, the ratios of correctly diagnosed points are 7.7%, 45.2%, 60.7%, 100.0% at SL-1, SL-2, SL-3 and SL-4 respectively.
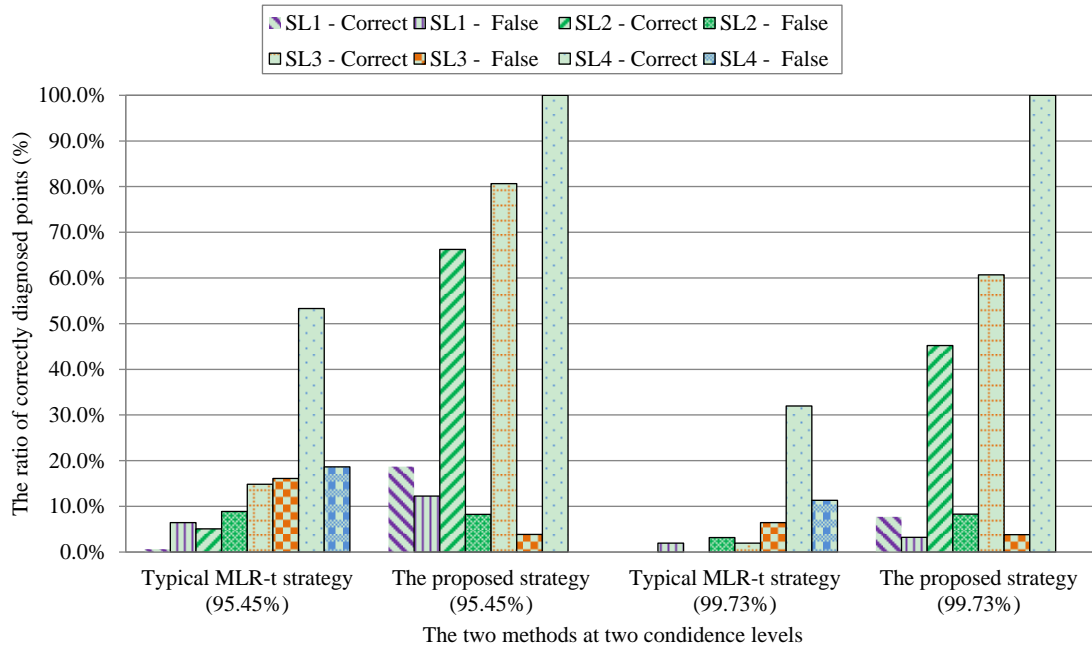
Figure 5.8 Correct diagnosis and false diagnosis ratios using proposed strategy and Typical MLR-t strategy in the case of condenser fouling

5.3.3 Refrigerant Leakage

Using the Typical MLR-t strategy, the highest ratios of correctly diagnosed points are 14.3%, 21.3%, 81.0% and 99.4% at SL-1, SL-2, SL-3 and SL-4 at both confidence levels, as shown in Figure 5.9. They are almost half of the ratios of the proposed strategy. At the confidence level of 99.73%, the ratio of correctly diagnosed points is only 6.5% at SL-1 using the Typical MLR-t strategy. This ratio is so low that it could not be distinguished with the false diagnosis ratios in the case of condenser fouling (3.2% and 6.5% at SL-1 and SL-2 respectively). Using the proposed strategy at confidence level of 99.73%, the ratios of correctly diagnosed points are 20.1% and 36.2% at SL-1

114

and SL-2 respectively. They are about three and two times of the results of the Typical

MLR-t strategy (6.5% and 17.0%) respectively.
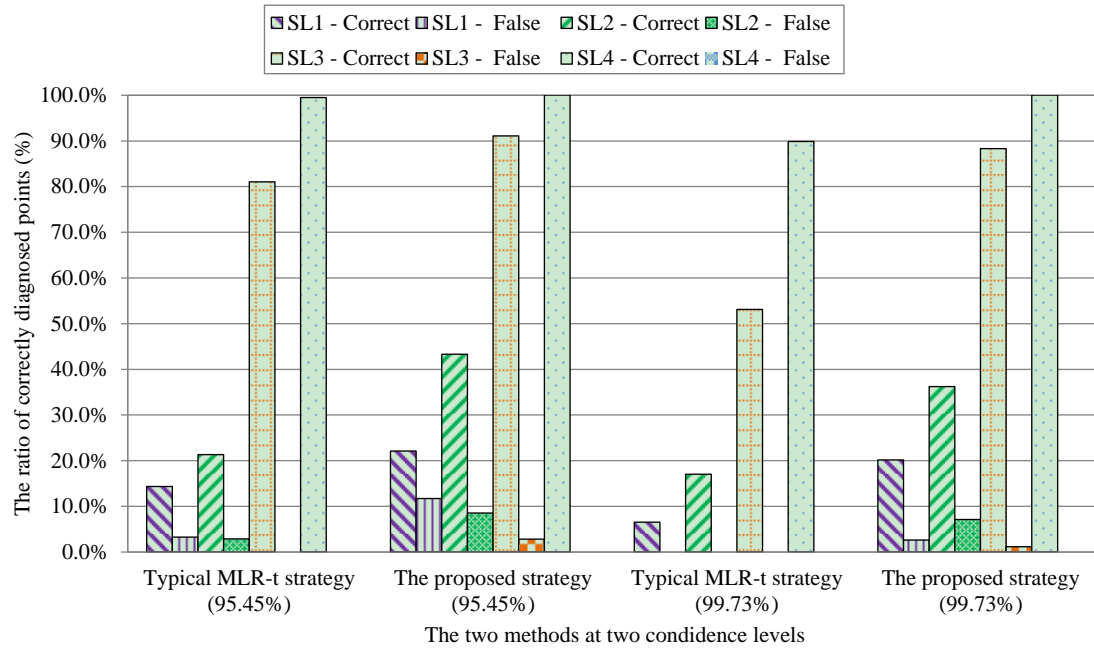
Figure 5.9 Correct diagnosis and false diagnosis ratios using proposed strategy and

Typical MLR-t strategy in the case of refrigerant leakage

5.3.4 Refrigerant Overcharge

Using the Typical MLR-t strategy, the ratios of correctly diagnosed points at SL-1

and SL-2 are 42.1% and 47.5% at confidence level of 95.45%, and they were 7.2% and

8.9% at confidence level of 99.73%, as shown in Figure 5.10. For the proposed strategy

at both confidence levels, the lowest ratios of correctly diagnosed points are 89.5%,

98.7%, 100.0%, 100.0% at SL-1, SL-2, SL-3 and SL-4 respectively. The wrongly

diagnosed ratios are 2.6%, 3.9% at SL-1 using the Typical MLR-t strategy at both

confidence levels. They are 0.0% at four severity levels at both confidence levels using

the proposed strategy. The improvements of FDD performances are obvious.
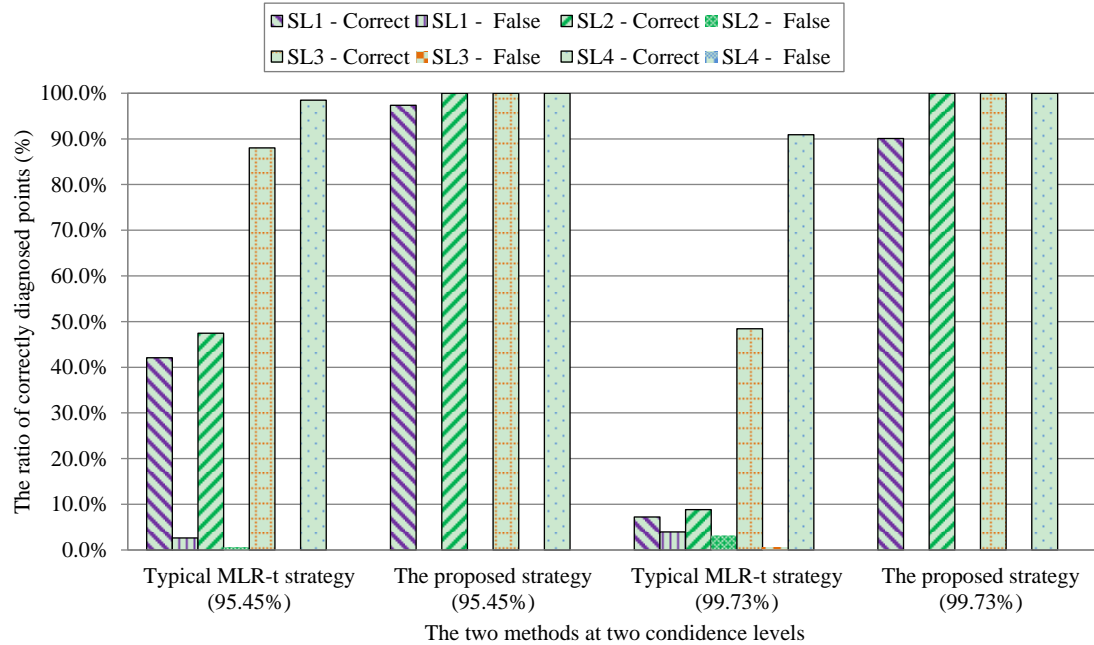
Figure 5.10. Correct diagnosis and false diagnosis ratios using proposed strategy and

Typical MLR-t strategy in the case of refrigerant overcharge

5.3.5 Non-condensable Gas

Using the Typical MLR-t strategy, the ratios of correctly diagnosed points are 100.0% at four severity levels for both confidence levels, as shown in Figure 5.11. Using the proposed strategy, the ratios of correctly diagnosed points are 99.4% and 98.7% at SL-1 at two confidence levels respectively, and they were 100.0% at SL-2, SL-3 and SL-4. Both strategies could correctly diagnose the non-condensable gas without any problem.
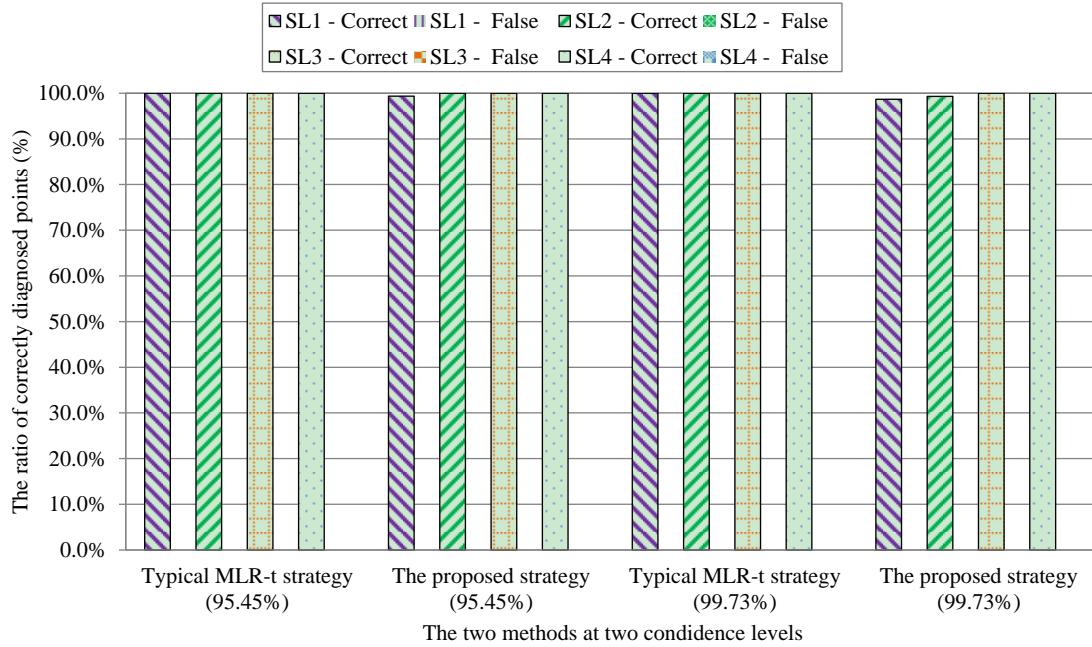
Figure 5.11 Correct diagnosis and false diagnosis ratios using proposed strategy and

Typical MLR-t strategy in the case of non-condensable gas

5.4 Summary

A new statistical fault detection and diagnosis strategy is proposed in this chapter, which adopts three main innovations including a new performance index (ε_{sc}), the EWMA control charts and the SVR based reference models. Two comprehensive comparison studies are conducted using the experimental data from the ASHRAE RP-1043.

It is found that the proposed strategy improved the FDD performances significantly, especially at low severity levels. For example, in the case of condenser fouling, the proposed strategy achieves the ratios of correctly diagnosed points of 7.7%, 45.2%, 60.7% and 100.0% at four severity levels (SL-1 to SL-4) respectively at the confidence level of 99.73%. Using the other strategies including a commonly used strategy, this fault could

not be correctly diagnosed at level SL-1, SL-2 and SL-3. Significant improvements can also be found in the cases of other two typical faults (refrigerant leakage and refrigerant overcharge). Other three faults (i.e. non-condensable gas, reduced evaporator water flow rate and reduced condenser water flow rate) can be easily diagnosed similarly as other strategies.

The EWMA control charts contribute the most to the improvement on FDD performance. It reduces the Type II errors through taking into account the time series information using the weighting factor. Therefore, the EWMA-based strategies achieves much higher correct diagnosis ratios compared with the t-statistic-based strategies. The heat transfer efficiency of the sub-cooling section (ε_{sc}) is an effective performance index to represent the effects of faults on the thermal performance of sub-cooling section. It is especially useful in improving the FDD performance for condenser fouling. As a new machine learning algorithm based on structural risk minimization from statistical learning theory, SVR could be more efficient than MLR approach using the actual site data of higher uncertainty level.

CHAPTER 6 AN INCIPIENT FAULT DETECTION AND DIAGNOSIS STRATEGY FOR HVAC SYSTEMS

This chapter presents a system-level incipient fault detection and diagnosis strategy for HVAC systems. It is an improvement of the system-level FDD strategy proposed by Zhou et al. (2009). Evaluations are made on a simulation platform for a super-rise commercial building in Hong Kong. Three typical subsystems are considered in this chapter, i.e. cooling tower system, chillers and heat exchanger system, at four severity levels and two uncertainty levels. Comparisons are made between SVR-based models and MLR-based models, as well as the proposed strategy and MLR-t-statistic-based strategy.

6.1 Outline of the System Level FDD Strategy

Component-level FDD strategies focus on detecting and identifying reasons of faults in a targeted component of HVAC systems. In contrast, the system-level FDD strategies are developed to identify the components which contribute to the performance degradation of HVAC systems. Compared with the component-level FDD, the system-level FDD mainly focus on the energy consumptions (Zhou et al. 2009). Up to now, there are very few practical applications of component-level FDD strategies. System-level FDD strategies seem to be easier to be applied for energy saving purposes at current stage.

A model-based system-level FDD strategy was proposed by Zhou et al. (2009). It was enhanced by considering sensor FDD (Wang, S.W. et al. 2010). MLR was used to

develop reference performance index (PI) models to generate benchmarks. PIs can be direct measurements, such as power and temperature or the direct products of measurements. They usually have physical meanings. A typical example of PI for chillers is the coefficient of performance (COP). An online adaptive scheme was developed to estimate and update the thresholds for detecting abnormal PIs. The uncertainties coming from both model-fitting errors and measurement errors were analysed. The FDD performance was good on faults at higher severity levels. However, it was poor on the incipient faults which were at lower severity levels. It reveals two shortcomings of conventional FDD strategies. Firstly, in the conventional strategies, a fault is detected when the residuals of PIs are outside of their predefined confidence intervals, which are generated using t-statistic approach, adaptive threshold approach, etc. These approaches only use the information of current data. This feature makes these strategies relatively insensitive to small shifts of residuals when an incipient fault occurs. However, when a strategy is applied to the incipient faults, most of the residuals might be still within the confidence interval, which are considered to be normal. This is the so called Type II error in statistical test theory. Secondly, HVAC systems show obvious nonlinear character. The MLR algorithm, which is widely adopted in HVAC FDD, is still a linear regression algorithm. The accuracy of reference models might be improved if nonlinear regression approaches are introduced. However, the Type II error contributes the most to the poor FDD performance on incipient faults.

The FDD strategy in this chapter aims to improve fault detection performance concerning system-level incipient faults. Firstly, SVR is adopted to develop reference PI

models in order to achieve higher accuracy. Secondly, the EWMA control charts are implemented to detect the shifts of PI residuals.

6.2 Case Study: Application on A HVAC System

6.2.1 Descriptions of the HVAC System

The HVAC system concerned in this study is in a new super-rise commercial building in Hong Kong. In the system, the speeds of cooling tower fans are controlled to maintain an optimized outlet water temperature. For the cooling tower system, the inputs are total heat rejection, inlet water temperature and inlet air web-bulb temperature. For the chillers, the inputs are the chilled water supply temperature, the chilled water return temperature and the entering condenser water temperature. The pumps before heat exchangers are controlled to maintain the outlet water temperature after heat exchangers. The pumps after heat exchangers are controlled to maintain the remote differential pressure. For the heat exchanger system, the inputs are water flow rate after heat exchangers, inlet water temperatures and outlet water temperatures of heat exchangers.

The building is divided into five zones to avoid the chilled water pipelines and terminal units from suffering extremely high pressure. The floors below the sixth floor are Zone 1. This study concerns the cooling water subsystem, chillers and chilled water system serving Zone 1. There are eleven cooling towers, six chillers, two heat exchangers, six constant-speed condenser pumps, six constant-speed primary pumps, two secondary variable-speed pumps after/before heat exchangers. The same simulated system used in a previous study (Zhou et al. 2009) is used for the evaluation tests in this

study. It is a dynamic HVAC simulation platform which was developed by Ma (2008) using TRNSYS, as shown in Figure 6.1. More details can be found in Ma (2008).
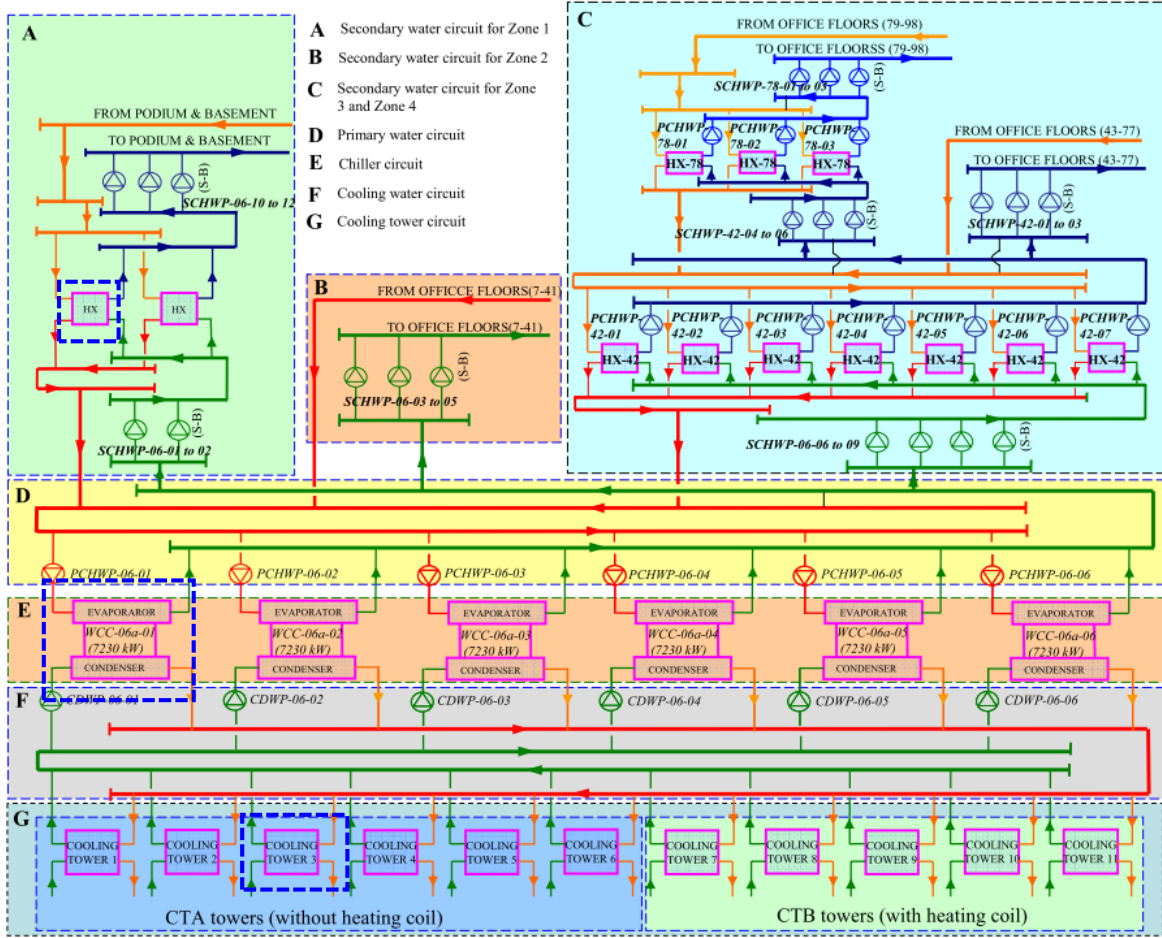
Figure 6.1 Illustration of the simulation platform and the selected subsystems for evaluations

6.2.2 Data Description

Both fault-free data and fault data are generated using the simulation platform. Five typical days, which are in the third week of July, are selected to validate the proposed strategy. In the first three days, fault-free data are generated for reference PI models

development. In the other two days, different kinds of faults are conducted at four severity levels (SLs) on the subsystems which are marked out in Figure 6.1. Fault-free data are also generated in the other two days to evaluate the reference PI models.

Uncertainties in variables. Uncertainties in variables are significant to fault detection performance. In this study, the uncertainties (sensor noises) are assumed to be normal distribution (Jaynes 2003). Normally distributed noises are randomly generated and added to the variables. The uncertainty levels in actual measurements depend on the quality of sensors and their maintenances. They are rather different in different buildings. In this study, two uncertainty levels are considered. At uncertainty level 1 (UL-1), the standard deviations are 0.2℃ on all temperature sensors, and 3% on all water flow meters and power meters. At uncertainty level 2 (UL-2), the standard deviations are doubled.

Fault data description. The fault data are obtained through introducing faults on the simulation platform. Three typical subsystems are considered in this study, i.e. cooling tower system, chillers and heat exchanger system.

The typical faults in cooling tower systems are fan motor degradation and heat transfer degradation. These two faults result in extra fan power consumption. In this study, both faults are simulated by reducing the number of transfer units (NTU). Fan motor degradation will increase tower fan power to maintain a certain NTU. Therefore, reducing NTU can simulate the effects of fan motor degradation fault on PI. The typical faults in chillers are compressor motor degradation, condenser fouling and evaporator fouling. When such faults occur, both COP and power consumptions will deviate from their healthy values. The degradations are simulated by increasing electromechanical

123

power loss. The typical faults in the heat exchanger systems are tube fouling and blockage. Both faults are simulated by reducing the UA of heat exchangers.

6.2.3 Reference PI Models

The PIs represent the health statuses of the subsystems. For a subsystem, there would be many PIs. In this study, only a typical PI is selected for each subsystem to evaluate the proposed strategy. Table 6.1 presents the typical faults concerned on the selected subsystems. It shows the way to model the faults as well as the formulations of typical PIs. M_{w_bfHX} is the flow rate of chilled water which is measured before the heat exchanger concerned.

Table 6.1 Typical faults of HVAC subsystems and corresponding performance indexes (PIs)

Subsystem	Typical Faults	Fault modeling	PI formulation
Cooling tower system	Motor degradation; heat transfer degradation	NTU ratio reduction (5%, 10%, 15%, 20%)	W_{ct}, measured value
Chiller system	Compressor motor degradation; condenser; evaporator fouling	Increase electromechanical power loss (5%, 10%, 15%, 20%)	COP, calculated value
Heat exchanger system	Tube fouling; blockage	Decrease in the heat transfer coefficient (5%, 10%, 15%, 20%)	M_{w_bfHX}, measured value

Compared with physical models, such kind of gray-box models have two main advantages. One advantage is that the models are easy to be developed. The other advantage is that the models might have higher accuracy. SVR offers prominent advantages such as excellent learning capability using limited samples and good

generalization ability. The main disadvantage of gray-box models is that they only work well within the range of operating conditions of the training data. Therefore, the gray-box models should be trained using data of wide range operating conditions.

6.3 Results and Discussions

6.3.1 Evaluation of the PI models

The fault-free data of the first three days are used to train reference PI models. The fault-free data of the other two days are used to validate the models. The comparisons are made between SVR-based models and MLR-based models using data without the normally distributed noises. In this study, it is found that both strategies have rather different regression performances (e.g. R^2 and RMSE) when different noises are added which are generated at the same way. For instance, two sets of noises are randomly generated using the same noise function. Then, two sets of training data are generated by the simulation platform through adding two sets of noises to variables. SVR-based models and MLR-based models are trained using the two training data sets respectively. Their regression performances are different at each training data set. It is because the noises are different each time although they are of the same distribution, e.g. mean and standard deviation. Therefore, the comparisons between SVR-based models and MLR models are made using the data without noises.

The evaluation results are as shown in Table 6.2 and Figures 6.2-6.4. R^2 is a measure of the goodness of the fitting. The higher the R^2 is, the better the fitting result is. From Table 6.2, it can be observed that the performance of W_{ct} model is improved obviously. Its R^2 increases from 0.8413 (MLR-based model) to 0.9809 (SVR-based model). The R^2

of M_{w_bfHX} model increases from 0.9954 (MLR-based model) to 0.9969 (SVR-based model). The R^2 of *COP* model reduces from 0.9985 (MLR-based model) to 0.9984 (SVR-based model). It shows that SVR-based models have better performance overall.

Table 6.2 Performance of SVR-based PI models and MLR-based PI models

PI	SVR-based		MLR-based	
	R^2	*RMSE*	R^2	*RMSE*
W_{ct}	0.9809	1.2488	0.8413	3.6020
COP	0.9984	0.0073	0.9985	0.0069
M_{w_bfHX}	0.9969	0.4018	0.9954	0.4837
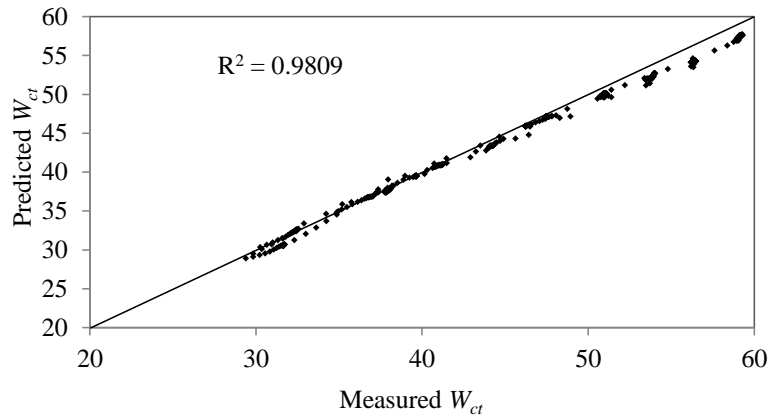
Figure 6.2 Comparison between measured and predicted W_{ct}
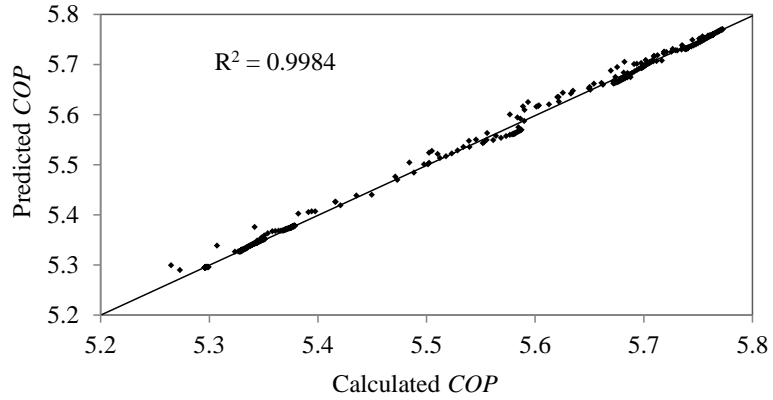
Figure 6.3 Comparison between calculated and predicted *COP*
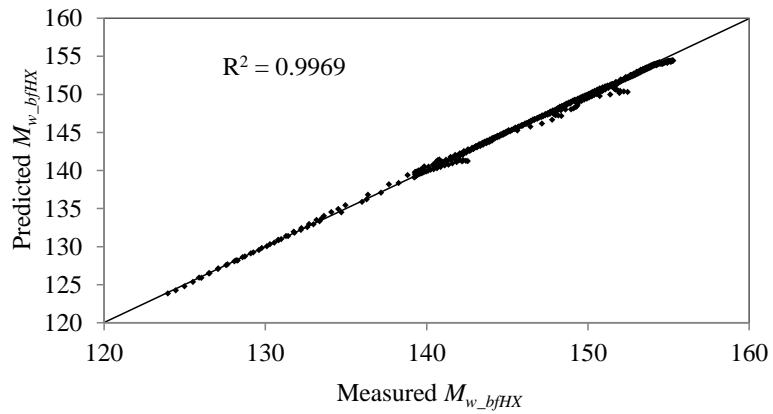
Figure 6.4 Comparison between measured and predicted M_{w_bfHX}

6.3.2 Evaluation of The Fault Detection Performance

Comparisons are made between SVR-EWMA-based strategy and MLR-*t*-statistic-based strategy at two uncertainty levels, as illustrated in Table 6.3. For each subsystem fault at uncertainty level 2, the fault detection results of 100 samples are as shown in Figures 6.5-6.7. In this study, fault detection ratio is the percentage that a fault is detected, as shown in Table 6.3.
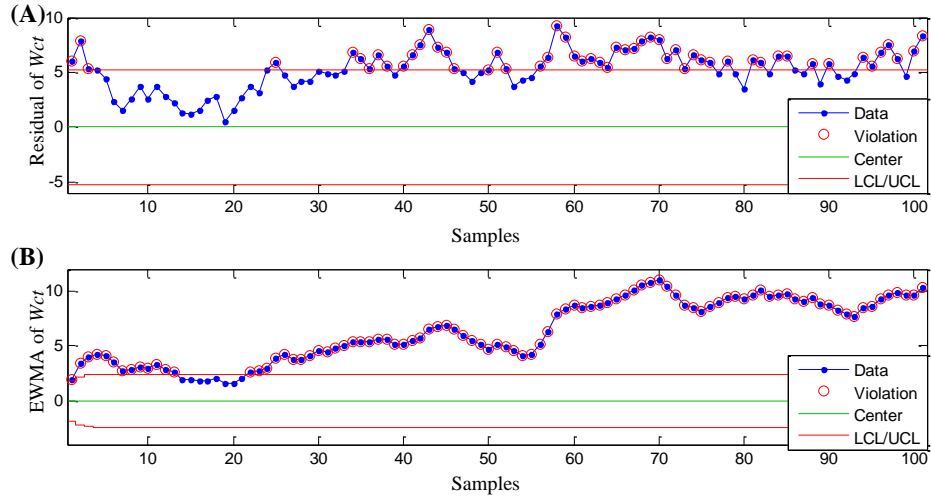
Figure 6.5 Fault detection performance on cooling tower fault (NTU is 5% reduced) at uncertainty Level 2-(A): MLR-*t*-statistic-based; (B): SVR-EWMA-based

Table 6.3 Fault detection ratios on three subsystems using two strategies

Subsystem	Strategy	Uncertain level (UL)	Severity Level (SL)			
			SL-1	SL-2	SL-3	SL-4
	NTU ratio		*0.95*	*0.9*	*0.85*	*0.80*
Cooling tower	SVR-EWMA	UL-1	91%	91%	98%	100%
		UL-2	90%	92%	98%	100%
	MLR-*t*-statistic	UL-1	69%	86%	92%	100%
		UL-2	56%	79%	88%	96%
	Power loss ratio		*1.05*	*1.1*	*1.15*	*1.20*
Chiller	SVR-EWMA	UL-1	89%	100%	100%	100%
		UL-2	77%	100%	100%	100%
	MLR-*t*-statistic	UL-1	47%	98%	100%	100%
		UL-2	38%	87%	99%	100%
	UA ratio		*0.95*	*0.9*	*0.85*	*0.80*
Heat exchanger	SVR-EWMA	UL-1	55%	93%	99%	99%
		UL-2	36%	77%	87%	96%
	MLR-*t*-statistic	UL-1	8%	51%	90%	100%
		UL-2	5%	19%	41%	80%
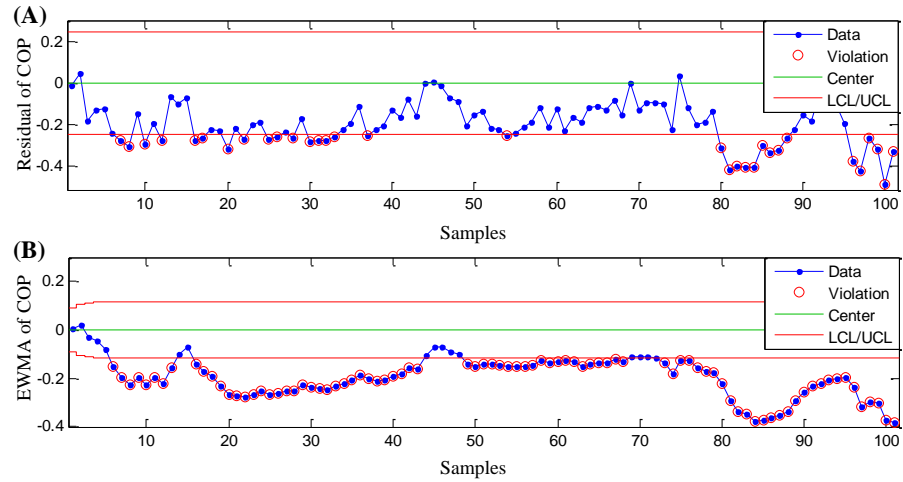
Figure 6.6 Fault detection performance on chiller fault (power loss is 5% increased) at uncertainty Level 2 - (A): MLR-*t*-statistic-based strategy, (B): SVR-EWMA-based strategy
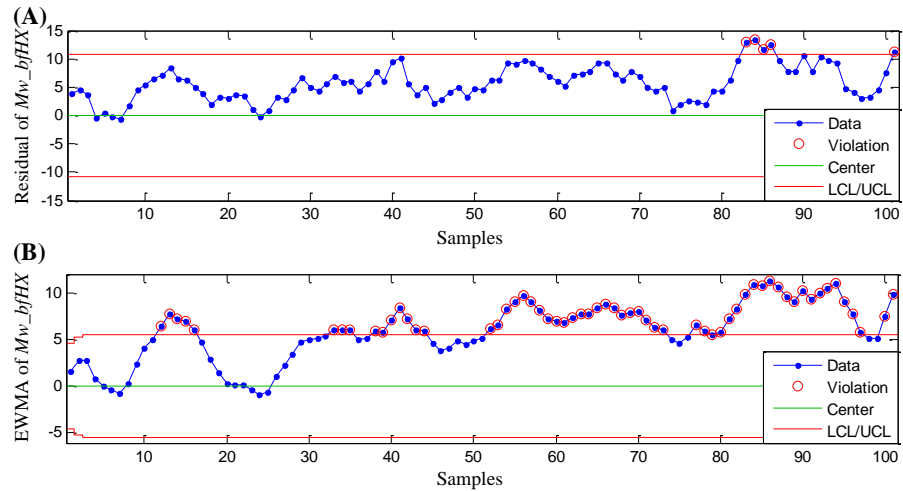
Figure 6.7 Fault detection performance on heat exchanger fault (UA is 5% reduced) at uncertainty Level 2 - (A): MLR-*t*-statistic-based strategy, (B): SVR-EWMA-based strategy

It can be found that the SVR-EWMA-based strategy improves the fault detection performance significantly compared with the MLR-*t*-statistic-base strategy. The control

chart is more sensitive to smaller long-term deviations when the weighting factor λ is smaller. However, it increases with Type I error ratio in fault free condition. Most of the incipient faults in HVAC field are gradually generated faults. λ can be optimized to keep Type I error ratio within acceptable level in fault free condition, e.g., around 5%. In this study, the fault detection performance in fault free condition is the best when λ is within [0.3, 0.4]. The parameters of EWMA control charts are as follows: L is 2.5758 to obtain 99.0% confidence level. λ is 0.35 to balance the fault detection performance and robustness under fault-free condition. The sample group size n is 1.

The fault-free data of the last two days are used to validate the proposed strategy. The Type I error ratios are normally around 5% at two uncertainty levels on three sub-systems. It is found that the EWMA-based strategy is sensitive to the noise introduced. The Type I error ratios would be rather different when introducing different noises randomly generated using the same standard deviation. If the noises are not added to the test data, most of the Type I errors are 0.0%. Therefore, the outlier detector and steady-state filter should be properly designed to pre-process the simulated data with noises added.

In the case that the NTU of cooling tower is reduced by 5%, the fault detection ratios are improved from 69% to 91% at uncertainty level 1 (UL-1) and from 56% to 90% at uncertainty level 2 (UL-2) using the SVR-EWMA-based strategy, as shown in Table 6.3. Figure 6.5(A) shows that a significant amount of fault data is within the confidence interval using t-statistic. Figure 6.5(B) shows that the EWMA values of W_{ct} are obviously outside of the confidence interval most of the time. The Type II error ratio is reduced significantly using the EWMA control chart. It is because that EWMA control

130

chart takes into account the time series information to reduce the Type II error. It is sensitive to the deviation of the distribution of process. The fault detection ratios are also improved when the NTU reduces 10%, 15% and 20%, as shown in Table 6.3.

In the case when the electromechanical power loss of chiller is increased by 5%, the fault detection ratios are improved from 47% to 89% at uncertainty level 1 and from 38% to 77% at uncertainty level 2 using the SVR-EWMA-based strategy, as shown in Figure 6.6. Figure 6.6(A) shows the fault detection performance of MLR-t-statistic-based strategy. The distribution of residuals is obviously changed. However, most of residuals are still within the confidence interval which causes a higher Type II error ratio. Figure 6.6(B) shows the fault detection performance of the SVR-EWMA-based strategy. Most of EWMA values of *COP* are outside of the confidence interval. The fault detection ratios are improved slightly using the SVR-EWMA-based strategy when the power loss is increased by 10% and 15%, as shown in Table 6.3. Both strategies can detect 100% of the fault when the power loss is increased by 20%.

In the case when the UA of heat exchanger is reduced by 5%, MLR-t-statistic-based strategy detects 8% and 5% of fault data at uncertainty level 1 and uncertainty level 2 respectively. Meanwhile, SVR-EWMA-based strategy detects 55% and 36% of the fault data at uncertainty level 1 and uncertainty level 2 respectively. Figure 6.7 shows the fault detection performance of both strategies. The SVR-EWMA-based strategy detects some fault data which are considered to be fault-free by MLR-t-statistic-based strategy. When the UA of heat exchanger is reduced by10%, the fault detection ratios of MLR-t-statistic-based strategy are still low, i.e. 51% at Level 1 and 19% at Level 2. The ratios are 93% and 77% using SVR-EWMA-based strategy.

6.4 Summary

A system-level incipient fault detection strategy is proposed in this chapter. It involves two main innovations, i.e. the SVR-based PI models and the EWMA control charts, to improve the fault detection performance on incipient faults.

Evaluations are made on a simulated commercial building at four severity levels and two uncertainty levels. The proposed strategy improves the fault detection performance significantly especially when incipient faults are concerned. At SL-1 and UL-2, the fault detection ratios are 56% and 90% (cooling tower fault), 38% and 77% (chiller fault), 5% and 36% (heat exchanger fault) using the MLR-t-statistic-based strategy and the proposed strategy respectively. The EWMA control chart strategy contributes the most to the improvements. It takes the time series information into account to reduce the Type II error. The SVR-based PI models are slightly better than MLR-based PI models. The SVR-EWMA-based strategy achieves much higher fault detection ratio compared with MLR-t-statistic-based strategy. To reduce the risk of false alarm, a subsystem is reported to be faulty if the fault detection ratio is higher than a threshold, e.g. 30%.

In this study, only one PI is introduced for each subsystem. Actually, more PIs can be introduced to improve the fault detection performance or to diagnose faults. It can also be used to develop reference PI models considering a subsystem to be one component. The proposed strategy is validated using simulation data in this study.

CHAPTER 7 A PATTERN RECOGNITION-BASED FDD STRATEGY FOR CHILLERS

This chapter represents an application of the proposed pattern recognition-based FDD strategy on centrifugal chiller. Different from conventional chiller FDD strategies, it considers the FDD problem as a typical one-class classification problem. Fault-free data are considered as a fault-free class. Each type of fault is considered as an individual fault class. The task of fault detection is to detect whether the process data are outliers of the fault-free class. The task of fault diagnosis is to find out which fault class does the process data belong to. SVDD algorithm is introduced for the one-class classification. The basic idea of SVDD-based strategy is to find a minimum-volume hypersphere in a high dimensional feature space to enclose most of the data of an individual class. The proposed strategy is validated using ASHRAE RP-1043 experimental data.

7.1 Outline of The SVDD-based Chiller FDD strategy

As presented in *Section 3.3.2*, the applications of the proposed SVDD-based FDD method includes two processes, i.e. offline models training and online FDD. In the process of offline models training, SVDD models are trained for fault-free class and each fault classes respectively, as illustrated in Figure 3.6. In the process of online FDD, the SVDD models are used to detect and diagnose fault, as illustrated in Figure 3.7. More details refer to *Section 3.3.2*.

7.2 Evaluation of The SVDD-based Chiller FDD Strategy

7.2.1 Experimental Data and Data Pre-processing

The 'Complete data set' from RP-1043 is selected here since pattern recognition-based strategies need more data for training. A steady-state detector is introduced to remove dynamic data, which was developed for vapor compression system (Kim et al. 2008). Five variables are selected as steady-state indexes in this study, i.e. sub-cooling temperature, superheat temperature, evaporating temperature, evaporator approach temperature and condenser approach temperature. There are about 1500 data remained after data pre-processing (about 30% of 5191) for each dataset. 400 series of data are randomly selected for evaluations of online FDD. The rest ones are training data.

There are 64 variables recorded on the RP-1043 chiller. The variable selection affects significantly the accuracies of pattern recognition-based FDD strategies. The selecting criterions are as follows: 1) They should be able to determine the unique operating conditions; 2) They can be properly information redundancy to enhance the robustness of FDD; 3) The number of variables should be not very large to maintain its sensitivities to faults at slight severity levels, and to reduce computational complexity. Or, feature extraction approaches can be introduced to reduce dimensionality. In this study, 16 variables are selected as shown in Table 7.1. At the end of data pre-processing, the training data are normalized to improve the performances of SVM models and SVDD models (Han et al. 2012).

The normality of each variable is assessed using the Shapiro-wilk test. The p-value for each variable is calculated to quantify the strength of the evidence against the null

hypothesis in favor of the alternative. A p-value<0.05 means that the null hypothesis is rejected and the data is highly unlikely to be Gaussian distributed. A shown in Table 7.2, it can be found that all variables are obviously non-Gaussian distributions. The normality tests of T_{cd} (condensing temperature) and T_{sc} (sub-cooling temperature) are illustrated at Figure 7.1 and Figure 7.2 respectively as examples. The red points represent the actual distribution of T_{cd} (Figure 7.1) and T_{sc} (Figure 7.2). The blue lines represent the Gaussian distribution.

Table 7.1 Variables selected for validations of SVDD-based method and SVM-based method

No.	Measurement	No.	Measurement
1	Chilled-water supply temperature	9	Entering condenser water temperature
2	Entering evaporator water temperature	10	Chiller electrical power input
3	Leaving condenser water temperature	11	Evaporating temperature
4	Evaporator approach temperature	12	Condensing temperature
5	Condenser approach temperature	13	Refrigerant suction temperature
6	Sub-cooling temperature	14	Refrigerant suction superheat temperature
7	Refrigerant discharge temperature	15	Refrigerant discharge superheat temperature
8	Temperature of oil in sump	16	Pressure of oil feed

Table 7.2 Shapiro-wilk test for each variable selected for fault detection (p-value<0.05 means it is highly unlikely to be Gaussian distributed)

No.	p-value	Distribution	No.	p-value	Distribution

1	4.75E-05	non-Gaussian		9	8.53E-05	non-Gaussian
2	2.44E-11	non-Gaussian		10	3.61E-06	non-Gaussian
3	5.49E-10	non-Gaussian		11	8.59E-09	non-Gaussian
4	2.86E-05	non-Gaussian		12	1.99E-08	non-Gaussian
5	2.91E-09	non-Gaussian		13	1.17E-05	non-Gaussian
6	5.19E-05	non-Gaussian		14	2.94E-09	non-Gaussian
7	4.00E-06	non-Gaussian		15	0.01552	non-Gaussian
8	7.43E-07	non-Gaussian		16	0.01354	non-Gaussian
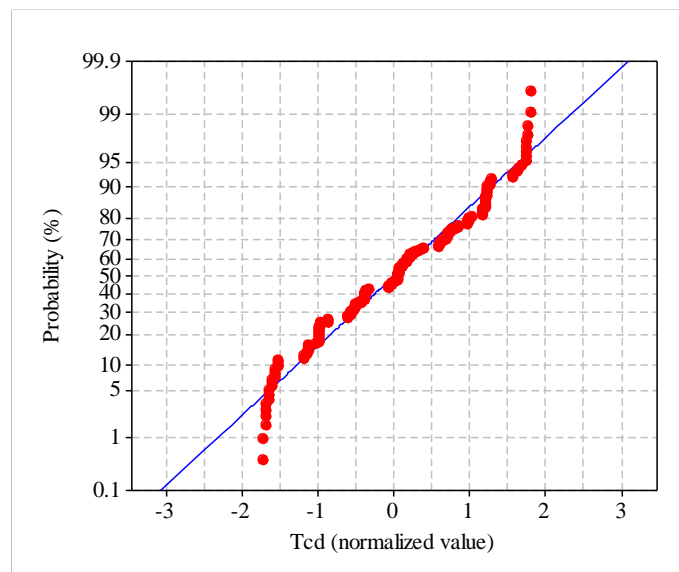
Figure 7.1 Normality test of T_{cd} (non-Gaussian distribution)
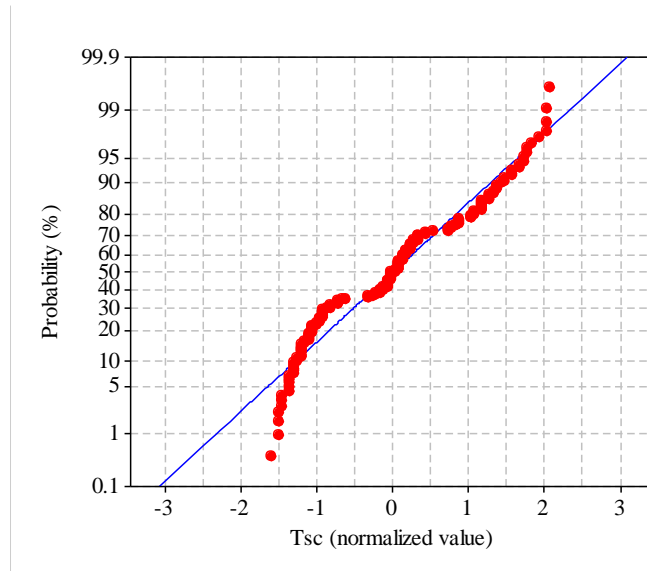
Figure7.2 Normality test of T_{sc} (non-Gaussian distribution)

7.2.2 Performance Test of The Proposed SVDD-based FDD Strategy

7.2.2.1 Optimization of parameters

Libsvm is a library for support vector machines. The SVDD tool in Libsvm is used to validate the SVDD-based FDD strategy. In the SVDD tool, a parameter *nu* is introduced which is equivalent to *C*. Gaussian radial basis function (RBF) kernel is selected. There are two parameters, i.e. *nu* and *γ*, should be properly optimized.

The cross-validation procedure can prevent the over fitting problem when optimizing the parameters. In *v*-fold cross-validation, the training data set is divided into *v* equally-sized subsets firstly. Sequentially, one subset is tested using the classifier trained on the remaining *v*-1 subsets. In this way, each instance of the whole training set is predicted once so the cross-validation accuracy is the percentage of data which are correctly classified. This study uses a grid-search on *nu* and *γ* using 5-fold cross-validation. Various pairs of *nu* and *γ* are tried and the one of the best cross-validation accuracy is picked up. Therefore, the accuracies of the SVDD models on training data

137

set are different from their cross-validation accuracies. In this study, the cross-validation accuracies on training data set are controlled around 95%. Further discussion can be found in *Section 7.2.1*.

7.2.2.2 Fault detection results

The task of fault detection is to detect outliers which do not belong to the fault-free class. The fault-free SVDD model is trained using the pre-processed fault-free training data which is named 'normal2' in RP-1043. The false alarm ratio is 0.4% using training data and 0.5% using test data. The fault-free SVDD model is validated using test data of the seven typical faults at four severity levels. The results are shown in Table 7.2, where R is data set.

Table 7.3 Fault detection ratios (outlier ratios) of fault data using fault-free SVDD model

Severity Level	R_{CdFoul}	$R_{RefOver}$	$R_{RefLeak}$	R_{Ncg}	R_{RedEvW}	R_{RedCdW}	R_{ExOil}
SL-1	100%	95%	74%	100%	52%	85%	98%
SL-2	100%	99%	81%	100%	44%	89%	99%
SL-3	100%	100%	97%	100%	76%	100%	100%
SL-4	100%	100%	100%	100%	93%	100%	100%

The higher the severity level is, the higher detection ratio will be. The fault-free SVDD model can successfully detect all faults. The best performances are obtained at R_{CdFoul}, R_{Ncg} and R_{ExOil}. Almost 100% of them are detected at each severity level. The worst performance is obtained at R_{RedEvW}, i.e. 52%, 44%, 76% and 93% at Sl-1, Sl-2, SL-3 and SL-4 respectively. The ratios are still high enough to alarm a fault.

7.2.2.3 Diagnosis results when involving all classes in training

The task of fault diagnosis is to identify to which fault class the data belong. Seven fault SVDD models were trained using training data of all the seven faults at SL-1. Then, each model was validated using test data of every class (at SL-1). Table 7.3 shows the inlier ratio of each fault data set, identified by a SVDD model. For instance, the *CdFoul* SVDD model (M_{CdFoul}) identifies 4% of fault-free data (R_{Normal}) to be condenser fouling. Where, M is the fault SVDD model. R_{Normal} is 'normal2' data set. $R_{training}$ is the fault data set for training.

Table 7.4 Fault diagnosis ratios (inlier ratios) using SVDD-based strategy at SL-1

SVDD model	$R_{training}$	R_{Normal}	R_{CdFoul}	$R_{RefOver}$	$R_{RefLeak}$	R_{Ncg}	R_{RedEvW}	R_{RedCdW}	R_{ExOil}
M_{CdFoul}	4%	0%	96%	0%	0%	0%	0%	0%	0%
$M_{RefOver}$	4%	11%	0%	95%	36%	0%	4%	3%	18%
$M_{RefLeak}$	2%	16%	0%	30%	96%	0%	11%	3%	13%
M_{Ncg}	2%	0%	0%	0%	0%	96%	0%	0%	0%
M_{RedEvW}	2%	42%	0%	2%	5%	0%	95%	25%	0%
M_{RedCdW}	5%	42%	0%	4%	6%	0%	54%	93%	0%
M_{ExOil}	3%	0%	0%	1%	4%	0%	0%	0%	95%

All fault SVDD models correctly identified fault data of their own class with high ratios, i.e. 96% (R_{CdFoul}), 95% ($R_{RefOver}$), 96% ($R_{RefLeak}$), 96% (R_{Ncg}), 95% (R_{RedEvW}), 93% (R_{RedCdW}) and 95% (R_{ExOil}). The best performances were obtained using M_{CdFoul} and M_{Ncg}, which are 0% on the other fault classes. Most of false ratios are lower than 30%. The worst results are 54% (M_{RedCdW} on R_{RedEvW}), 42% (M_{RedCdW} and M_{RedEvW} on R_{Normal}), 36% ($M_{RefLeak}$ on $R_{RefOver}$). However, the faults can still be diagnosed correctly. It is an information fusion task to determine the diagnosis result. Taking R_{RedEvW} for instance, it is correctly alarmed with 52% detection ratio using M_{Normal}. Although the false diagnosis ratio is 54% by M_{RedCdW}, the correct diagnosis ratio is obviously higher by M_{RedEvW}, i.e. 95%. *RedEvW* is still correctly reported.

Another case is made using test fault data at SL-2, as shown in Table 7.4. The performance is better. Taking the same R_{RedEvW} for instance, the false diagnosis ratio using M_{RedCdW} dropped from 54% to 42%.

It should be mentioned that most of the model-based/rule-based chiller FDD strategies did not work well at SL-1 and SL-2. For instance, using the ASHRAE RP-1043 experimental data, the correct diagnosis ratios were 0%, 0%, 0% at SL-1 and 25%, 0%, 0% at SL-2 respectively for the *RefLeak*, *CdFoul* and *ExOil* in Cui and Wang (2005). The MLR and t-statistic-based strategy in AHSRAE RP-1275 was reported that the ratios of correctly diagnosed points were 3.7%, 0%, 0% at SL1 and 7.4%, 0%, 0% at SL2 the *RefLeak*, *CdFoul* and *ExOil* respectively (Reddy 2006).

Table 7.5 Fault diagnosis ratios (inlier ratios) using SVDD-based strategy at SL-2

SVDD model	$R_{training}$	R_{Normal}	R_{CdFoul}	$R_{RefOver}$	$R_{RefLeak}$	R_{Ncg}	R_{RedEvW}	R_{RedCdW}	R_{ExOil}
M_{CdFoul}	2%	0%	96%	0%	0%	0%	0%	0%	0%
$M_{RefOver}$	6%	2%	0%	93%	8%	0%	0%	2%	2%
$M_{RefLeak}$	4%	13%	0%	14%	97%	0%	5%	3%	18%
M_{Ncg}	4%	0%	0%	0%	0%	94%	0%	0%	0%
M_{RedEvW}	2%	50%	0%	2%	30%	0%	96%	12%	0%
M_{RedCdW}	2%	47%	0%	8%	7%	0%	42%	96%	0%
M_{ExOil}	3%	0%	0%	1%	5%	0%	0%	0%	94%

7.2.2.4 Diagnosis results when not involving all classes in training

The fault diagnosis ratios in this test are the same as that in the tests when involving all classes in training. It is because that SVDD models are robust naturally when using data of classes which are not involved in training since the purpose of one-class classification algorithm is to reject all data of other classes. As shown in Table 7.3 and Table 7.4, each SVDD model accepts more than 90% of their own class data. Meanwhile, they effectively reject data which do not belong to their own classes. At SL-1, R_{CdFoul} and R_{Ncg} are rejected with 100% ratio by SVDD models of other classes. Similar conclusions can be found at SL-2. The top 3 false diagnosis ratios are 54% (R_{RedCdW} using M_{RedCdW}) and 42% (R_{Normal} using M_{RedCdW} and M_{RedEvW}). However, three faults are still correctly reported since they are identified, by their own SVDD models, with higher ratios.

7.2.3 Comparisons With SVM-based FDD Strategy

7.2.3.1 SVM tool and parameters optimization

There are many types of SVMs. In this study, C-SVC is selected from Libsvm (Chang and Lin 2011). Gaussian radial basis function (RBF) kernel is selected. The two parameters in each C-SVC model, i.e. C and γ, are also optimized using 5-folder cross-validation through grid-search.

7.2.3.2 Fault diagnosis performance by SVM-based FDD strategy

A SVM model was trained using the same training data. Then, the SVM model was validated using same test data. The fault diagnosis results are shown in Table 7.5. Take R_{CdFoul} for instance, 94% of the data are classified to *CdFoul* and the rest 6% are classified to *Normal*. The correct diagnosis ratios are classes are 94% (*CdFoul*), 95% (*RefOver*), 94% (*RefLeak*), 94% (*Ncg*), 96% (*RedEvW*), 95% (*RedCdW*), 95% (*ExOil*) and 100% (*Normal*) respectively. They are similar to the results using SVDD models.

Table 7.6 Fault diagnosis ratios using SVM-based FDD strategy at SL-1

Fault data	CdFoul	RefOver	RefLeak	Ncg	RedEvW	RedCdW	ExOil	Normal
R_{CdFoul}	94%	0%	0%	0%	0%	0%	0%	6%
$R_{RefOver}$	0%	95%	0%	0%	0%	0%	0%	5%
$R_{RefLeak}$	0%	0%	94%	0%	0%	0%	0%	6%
R_{Ncg}	0%	0%	0%	94%	0%	0%	0%	7%
R_{RedEvW}	0%	0%	0%	0%	96%	0%	0%	4%

R_{RedCdW}	0%	0%	0%	0%	0%	95%	0%	5%
R_{ExOil}	0%	0%	0%	0%	0%	0%	95%	5%
R_{Normal}	0%	0%	0%	0%	0%	0%	0%	100%

Similarly, a SVM model was trained and validated at SL-2. The fault diagnosis results are shown in Table 7.6. The performance is similar to that at SL-1. The diagnosis ratios improve slightly from 95%, 95% to 96%, 100% for *RefOver*, and *RedCdW* respectively. The other diagnosis ratios drop slightly from 94%, 94%, 96%, 95% and 100% to 93%, 91%, 94%, 94% and 99% for *RefLeak*, *Ncg*, *RedEvW*, *ExOil* and *Normal* respectively. All faults are correctly detected and diagnosed.

Table 7.7 Fault diagnosis ratios using SVM- based FDD strategy at SL-2

Fault data	*CdFoul*	*RefOver*	*RefLeak*	*Ncg*	*RedEvW*	*RedCdW*	*ExOil*	*Normal*
R_{CdFoul}	94%	0%	0%	0%	0%	6%	0%	0%
$R_{RefOver}$	0%	96%	0%	0%	0%	4%	0%	0%
$R_{RefLeak}$	0%	0%	93%	0%	0%	6%	0%	2%
R_{Ncg}	0%	0%	0%	91%	0%	9%	0%	0%
R_{RedEvW}	0%	0%	0%	0%	94%	5%	0%	2%
R_{RedCdW}	0%	0%	0%	0%	0%	100%	0%	0%
R_{ExOil}	0%	0%	0%	0%	0%	7%	94%	0%
R_{Normal}	0%	0%	0%	0%	0%	1%	0%	99%

Using SVM-based strategy, a series of data is only classified to one class. It is rather different using SVDD-based strategy, in which a series of data could be classified to more one class.

7.2.3.3 Diagnosis results when not involving all classes in training

Same training data sets and test data sets as in the tests of session 4.2.3 are used here. In fact, when training each SVM model, data of one fault class were not involved. The SVM model was then validated using all the test data at SL-1. The evaluation results are shown in Table 7.7.

Table 7.8 Fault diagnosis ratios of new classes using SVM-based strategy at SL-1

Fault data	CdFoul	RefOver	RefLeak	Ncg	RedEvW	RedCdW	ExOil	Normal
R_{CdFoul}	-	0%	0%	38%	1%	20%	42%	0%
$R_{RefOver}$	0%	-	86%	0%	0%	5%	2%	7%
$R_{RefLeak}$	0%	13%	-	0%	10%	5%	11%	62%
R_{Ncg}	4%	33%	0%	-	0%	63%	0%	0%
R_{RedEvW}	0%	0%	1%	0%	-	14%	0%	85%
R_{RedCdW}	0%	8%	3%	0%	27%	-	0%	62%
R_{ExOil}	1%	5%	94%	0%	0%	0%	-	1%

The fault diagnosis results are totally wrong. R_{CdFoul} is identified to be *Ncg* (38%) and *ExOil* (42%). $R_{RefOver}$ is identified to be *RefLeak* (86%). $R_{RefLeak}$ is identified to be Normal (62%). R_{Ncg} is identified to be *RedCdW* (63%). R_{RedEvW} is identified to be *Normal* (85%). R_{RedCdW} is identified to be *Normal* (62%). R_{ExOil} is identified to be *RefLeak* (94%).

The SVM-based model has good FDD performance when it is used to classify data whose classes are included in training datasets. However, when it is used to classify data whose classes are not included in training, the results are totally wrong. There are more than twenty chiller faults including the typical seven faults. It is almost impossible to obtain fault data of all faults. Therefore, SVM-based chiller FDD strategy will likely not be robust when not all faults are included in training data.

7.2.4 Comparisons With PCA-based Fault Detection Strategy

Both PCA model and SVDD model are trained using the same fault-free training data. The PCA model retained the first three largest eigenvalues because they can explain 96.7% of the total variance of the training data. The false ratio is 3.9% when using the fault-free training data and 0.0% when using the fault-free test data. Then, both modes were validated using test data of each fault at four severity levels, as shown in Table 7.8.

Table 7.9 Comparisons between SVDD-based and PCA-based fault detection strategy

Fault Type	SL-1	SL- 2	SL-3	SL-4

	PCA	SVDD	PCA	SVDD	PCA	SVDD	PCA	SVDD
CdFoul	100%	100%	100%	100%	100%	100%	100%	100%
RefOver	64%	95%	63%	99%	95%	100%	99%	100%
RefLeak	36%	74%	27%	81%	88%	97%	96%	100%
Ncg	100%	100%	100%	100%	100%	100%	100%	100%
RedEvW	14%	52%	6%	44%	3%	76%	14%	93%
RedCdW	28%	85%	28%	89%	100%	100%	100%	100%
ExOil	94%	98%	94%	99%	100%	100%	100%	100%

The SVDD-based strategy shows more powerful fault detection capacity, particularly at lower severity levels (i.e. SL-1 and SL-2) where it improves the fault detection ratios significantly. For instance, fault detection ratios increase from 64%, 36%, 14%, 28% to 95%, 74%, 52%, 85% for *RefOver*, *RefLeak*, *RedEvW* and *RedCdW* respectively at SL-1. Similarly, the ratios increase from 63%, 27%, 6%, 28% to 99%, 81%, 44%, 89% for the same faults at SL-2. The most significant improvements are observed on *RedEvW*. Fault detection ratios are improved from 14%, 6%, 3%, 14% to 52%, 44%, 76%, 93% at SL-1, SL-2, SL-3 and SL-4 respectively. Similar comparison was also reported in the authors' previous work [7] with similar observations. However, the amount of data used in this study is ten times larger than that used in the previous study.

7.3 Optimization of Parameters and Application Issues

7.3.1 Optimization of Parameters

The two parameters, i.e. *nu* and *γ*, have significant effects on the FDD performance of SVDD models. Grid-search can be used to optimize *nu* and *γ* based on *v*-fold cross-validation. As discussed by Hsu et al. (2003), trying exponentially growing sequences of *nu* and *γ* is a practical strategy to identify good parameters. A complete grid-search may be time-consuming. A coarse grid is suggested first. After identifying a "better" region on the grid, a finer grid search on that region can be conducted. The cross-validation procedure is suggested to calculate the classification ratio at each *nu* and *γ*. It helps to prevent the over fitting problem and to obtain good generalization performance.

nu controls the tradeoff between the volume of the hypersphere and the classification error of the model. The smaller *nu* is, the larger radius of the hypersphere will be. *γ* controls the shape of the hypersphere. The smaller *γ* is, the less tighter the decision boundary will be. A case was made on fault-free data set. It introduced grid-search on *nu* [2^{-10}, 2^{-1}] and *γ* [2^{-10}, 2^{10}] using 5-fold cross-validation, as shown in Figure 7.3.
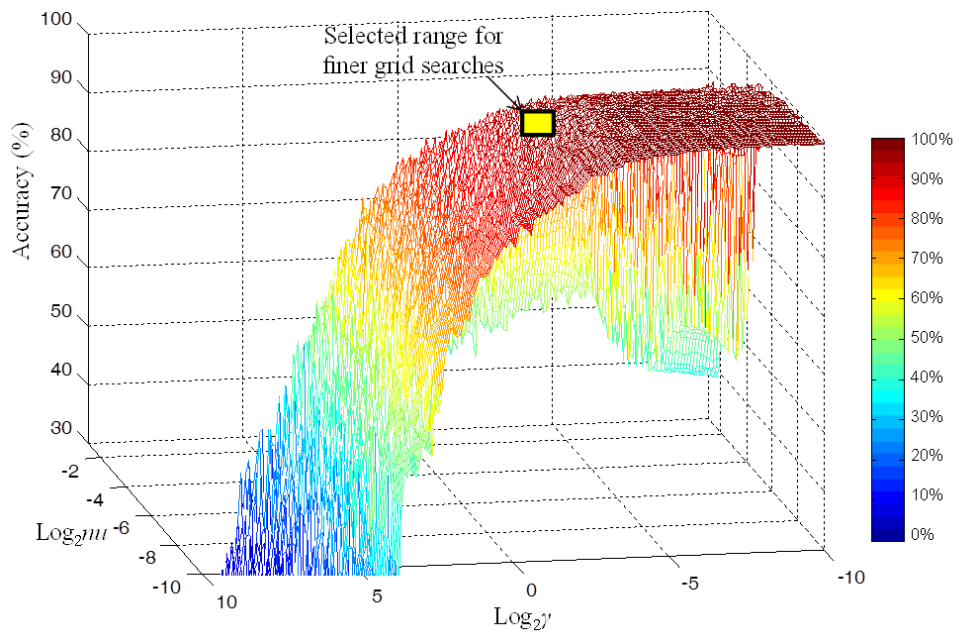
Figure 7.3 Grid-search on *nu* [2^{-10}, 2^{-1}] and *γ* [2^{-10}, 2^{10}] using 5-fold cross-validation

Actually, parameters optimization is a common problem when applying support vector machine in many fields, and some solutions have been proposed for specific applications. On the basis of mature solutions, the criteria to determine the "better" region for chiller FDD in this study include: the cross-validation accuracy is higher than 90%; and the *nu* and *γ* are the higher the better. When using the RP-1043 experimental data, cross-validation accuracy is larger than 90% within a wide range of [*nu, γ*]. The finer grid searches are made in the regions of *nu* [2^{-5}, $2^{-4.5}$] and *γ* [2^{-3}, 2^{-2}] to train every SVDD models.

It is recommended to validate the fault-free SVDD model using fault data. If there are only fault-free data available, the fault data could be obtained through conducting the fault of *RedCdW* which would be easy to be conducted. High Type II error ratios indicate that the parameters are not good enough and adjustment is necessary.

7.3.2 Robustness of the SVDD-based FDD Strategy

It was pointed out that pattern recognition-based FDD strategies generally have following weaknesses (Katipamula and Brambley 2005a; 2005b). Firstly, most models cannot work well beyond the range of the training data. Secondly, a large amount of training data is needed, including normal data and fault data. Thirdly, the models, which are trained for a specific system, can rarely be used on other systems.

The SVDD-based strategy inherits the main weaknesses of pattern recognition-based FDD strategies. The following are the possible solutions to enhance its performance. The first weakness can be overcome through introducing an operating condition filter.

FDD will not be processed, if the filter detect that the process operating conditions are far from the operating conditions for model training. The second weakness cannot be avoided if fault data are not available. Generally, there are sufficient fault-free data from building management systems. In such condition, SVDD-based strategy can still be used for fault detection. For the third weakness, further evaluations are needed to check whether SVDD models trained on a chiller are adoptable to chillers of the same mode. However, as discussed in the *Introduction*, if training data are enough, SVDD models would be easier to be applied to new systems compared with conventional FDD strategies.

In this study, the training data are evenly distributed in 27 operating conditions. It is possible in practical applications that, data are abundant in some ranges of operating conditions but few in other ranges of operating conditions. The minorities would be regarded to be outlier during SVDD model training process which will cause false detection or false diagnosis. This is another common problem of pattern recognition-based FDD strategies. Solutions can refer to (Li 2011; Tian et al. 2011). In this study, only 27 discrete operating conditions are considered. Further evaluations are necessary using data of more operating conditions.

7. 3.3 Potential Applications of the SVDD-based FDD Strategy

The SVDD-based strategy is a pure data-driven strategy. It has several potential applications as follows. If fault data of all typical faults are available (Case-1), which is the best situation, SVDD models can be trained to detect and diagnose these faults. If there is no fault data available (Case-2), fault-free SVDD model can be developed to

detect faults. The fault-free data are easy to be obtained from historical database of building management systems. If a fault has been confirmed (Case-3), the data of the fault can be obtained. Using the fault data, a fault SVDD model can be trained. When the same fault occurs in the next time, it can be diagnosed effectively using the model. If some faults (e.g. *CdFoul* and *RefLeak*) are strongly concerned by owners or manufacturers (Case-4), the fault data can be obtained by on-site tests or factory tests. For instance, the *CdFoul* data can be obtained through blocking some fin area if the chillers are air-cooled. Then, SVDD models can be developed for the concerned faults.

In this study, only chiller component faults are studied. However, FDD results would be unreliable if any sensor is faulty (Li and Zhao 2011). There are few publications about chiller sensor FDD using PCA algorithm (Wang and Cui 2005, 2006; Xu et al. 2008). One-class classification algorithms can also be used for sensor FDD. One basic idea is to do a simple feature selection which involves identifying the optimum subset of the variables in the dataset that gives the best separation or classification accuracy between the normal data and the fault data. Mahadevan and Shah provide a solution using SVM Recursive Feature Elimination algorithm, which is similar to that of PCA contribution to residuals plots (Mahadevan and Shah 2009).

7.4 Summary

This chapter presents a SVDD-based chiller FDD strategy which transforms the chiller FDD problem into a typical one-class classification problem. The test results show that the fault-free SVDD model could identify 99.5% of fault-free data correctly and detect all faults involved. The fault SVDD models can correctly identify more than

90% data of their own classes to be inliers and also effectively reject data of other classes.

Compared with the existing FDD strategies which use multi-class classification algorithms, the SVDD-based strategy is robust when the process data do not belong to any class involved in training. In such case, the SVM-based strategy could not report any correct FDD result. For instance, 94% data of *ExOil* is diagnosed to be *RefLeak* when the fault data of *ExOil* are not involved in training. Using the SVDD-based strategy, this fault is detected correctly but not diagnosed. The false FDD report is avoided.

Compared with the PCA-based strategy, the SVDD-based strategy has no Gaussian assumption and is effective for nonlinear process modeling. That results in more powerful capacity in describing process data. The fault detection ratios are improved significantly. For instance, using the PCA-based strategy, fault detection ratios are 64%, 36%, 14% and 28% for *RefOver*, *RefLeak*, *RedEvW* and *RedCdW* respectively at SL-1. Using the SVDD-based strategy, the ratios increase to 95%, 74%, 52% and 85% respectively.

Compared with model-based and rule-based FDD strategies, SVDD-based strategy has much higher FDD ratios, particularly at low fault severity levels, where those FDD strategies usually do not work well. For instance, using the MLR and t-statistic-based strategy, the ratios of correctly diagnosed points were 3.7%, 0%, 0% at SL-1 and 7.4%, 0%, 0% at SL-2 for *RefLeak*, *CdFoul* and *ExOil* respectively. Using SVDD-based strategy, such ratios are all increased to over 90% at both severity levels.

It is flexible for practical fault diagnosis applications. If the fault data can be obtained by on-site tests or manufactory tests, the proposed SVDD-based strategy can be used for both fault detection and diagnosis. It can be used for fault detection if only fault-free data are available.

CHAPTER 8 A DIAGNOSTIC BAYESIAN NETWORK

FOR CHILLER FDD

A generic intelligent FDD strategy is proposed in this chapter to simulate the actual diagnostic thinking of chiller experts. A three-layer diagnostic Bayesian network is developed to diagnose chiller faults based on the Bayesian belief network theory. The structure of the DBN is a graphical and qualitative illustration of the intrinsic causal relationships among causal factors in Layer 1, faults in Layer 2 and fault symptoms in Layer 3. The parameters of the DBN represent the quantitative probabilistic relationships among the three layers. To diagnose chiller faults, posterior probabilities of the faults under observed evidences are calculated based on the probability analysis and the graph theory. Compared with other FDD strategies, the proposed strategy can make use of more useful information of the chiller concerned and expert knowledge. It is effective and efficient in diagnosing faults based on uncertain, incomplete and conflicting information. Evaluation of the strategy was made on a 90-ton water-cooled centrifugal chiller reported in ASHRAE RP-1043.

8.1 A Generic Strategy for The DBN-Based Chiller FDD

In this section, a generic framework of DBN is developed for intelligent chiller FDD, as shown in Figure 8.1. In this framework, all useful information about target chiller and expert knowledge are merged into the DBN to simulate what FDD experts do in practice. Therefore, information collection and expert knowledge expression are prerequisite. For FDD applications, the task is to correctly identify a fault according to one or multiple

symptoms observed. It can be easily understood that faults and fault symptoms should be included in the DBN as different layers. Fault diagnosis in previous chiller FDD strategies is mainly based on fault symptoms which are abnormal sensor measurements or deduced performance indices. It resulted that a lot of meaningful information has been overlooked, such as the maintenance records. Therefore, the first layer is developed in the DBN to utilize other qualitative information. The details of the three layered DBN and its application for FDD as well as its advantages are introduced as follows.
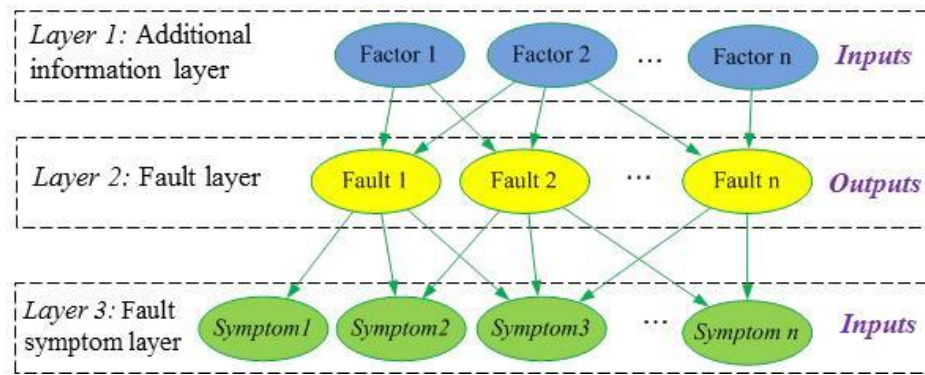
Figure 8.1 Flow chart of the intelligent fault detection and diagnosis strategy

8.1.1 Structure of The Proposed DBN

Different from DBNs for AHU FDD and VAV terminal FDD, the proposed DBN for chiller FDD has a clear structure which consists of three layers, including additional information layer (Layer 1), fault layer (Layer 2) and fault symptom layer (Layer 3). The nodes at each layer depend on available information and selected fault detection strategies. Layer 1 includes factors which are directly related to the probabilities of occurrence of faults, e.g., repairing service, abnormal operation records, the healthy

154

states of the related equipment, routine maintenances. Information included in Layer 1 helps to diagnose the faults in Layer 2 more accurately. For instance, refrigerant overcharge (one typical fault in Layer 2) is impossible to occur if it had been eliminated during refrigerant charging service (information in Layer 1). The risk of condenser fouling (one typical fault Layer 2) is lower if the condensing water has been properly treated recently (information in Layer 1). Layer 1 usually composes qualitative information which is available through checking service records/history or conducting on-site investigation. The fault layer composes the faults in chiller concerned. The fault symptom layer contains the sensor measurements and performance indices which are sensitive to corresponding faults.

8.1.2 Parameters of The Proposed DBN

In the proposed DBN, prior probabilities of root nodes are needed. Besides, conditional probabilities are needed to represent direct probabilistic dependences among nodes in the three layers. Generally, the nodes in Layer 3 have complex relationships with the nodes in Layer 2. To simplify the development of the DBN, the nodes in Layer 3 can be considered as Noisy-MAX nodes. Nodes in Layer 2 can be considered as general nodes (non-Noisy-MAX). For a general child node, the parameters are specified in a conditional probability table. For a Noisy-MAX node, the parameters include the conditional probabilities and *LEAK* probabilities.

The conditional probabilities can be obtained in two ways. (i) If the full-set fault data are available, the conditional probabilities can be obtained by statistically calculation or using machine learning algorithms (Pearl, 1985). In the chiller FDD

155

application, it is usually difficult to obtain the full-set fault data. The equipment manufacturers and building owners are reluctant to perform such experiments as manually introducing faults to their equipment and systems. Therefore this strategy is ruled out here. (ii) If the full-set of fault data are not available, the conditional probabilities can be estimated by chiller experts. Chiller FDD experts normally have an in-depth knowledge about chiller concerned and know the possibility of a fault given symptoms observed. What they need to do is to quantify those conditional probabilities. This sounds to be subjective; however experts' knowledge ensures those conditional probabilities reliable. Previous research on chiller FDD also provides valuable experiences in setting the parameters. The same conditional probabilities between fault layer nodes and fault symptom layer nodes are usually applicable for chillers of the same type. However, it is worthwhile to note that the conditional probabilities among root nodes and fault layer nodes are different even for the same type of chiller which depends on the operation and maintenance of the chiller concerned. To handle this diversity, the states of root nodes may be defined using levels, such as good, medium and poor. Different conditional probabilities can be assigned to each state. The states should be clear enough for chiller professionals to select according to the maintenance records, in-site inspection and various documentations.

Prior probabilities of faults are the normalized frequencies of faults. It is obvious that a fault with higher prior probability is more suspected to occur than one with lower prior probability. The prior probabilities of faults are useful for FDD, especially when information is incomplete. For instance, the prior probability of condenser fouling is 2.9 times of refrigerant overcharge in the survey of ASHRAE RP-1043. Both faults lead to a

156

higher condensing temperature. When only one piece of evidence is available, i.e. the condensing temperature is higher, the condenser fouling should be more suspected than refrigerant overcharge. However, in the proposed DBN, the probabilities of faults are actually posterior probabilities calculated on the basis of prior probabilities of root nodes and conditional probabilities between nodes of three layers. When no evidences are considered, it represents a condition that the chiller concerned is used and maintained at average level. In such a condition, the probabilities of faults should equal to the prior probabilities of faults.

The prior probabilities of root nodes can be obtained by the following strategies: set by chiller experts based on their knowledge and experiences, calculated as posterior probabilities in case the prior probabilities of fault nodes are available, and the hybrid strategy of these two strategies. Therefore, when develop the DBN, prior probabilities of root nodes and conditional probabilities usually need fine-tune to ensure that the posterior probabilities of them calculated from the prior probabilities and conditional probabilities are consistent with the prior probabilities of faults obtained from survey or estimated by chiller experts.

8.1.3 Fault Detection

In this framework, the fault detection process can examine whether the system is normal and specify the states of nodes in the fault symptom layer. A number of chiller fault detection strategies have been developed over the last decades. In principle, the framework doesn't rule out any fault detection strategy, which is one of the main purposes of developing this framework. It is also possible to adopt more than one fault

detection strategy in the framework. When designing the DBN, the fault detection strategy adopted will influence both the structure and parameters of the DBN. In *Section 4* of this paper, a detailed example is given to show how to determine the nodes at each layer.

8.1.4 Fault Diagnosis

The DBN-based inference is to calculate the posterior probabilities of unobserved nodes on the basis of evidences of observed nodes. While using the DBN for chiller fault diagnosis, the inputs of the DBN are the evidences, i.e. the states of nodes in Layer 1 and Layer 3, obtained from operation and maintenance records, in-situ investigation and the fault detection process. The observed states of nodes are set to be 100%. The outputs are the posterior probabilities of nodes at the fault layer. Basically, two rules can be used to isolate a fault as follows:

Rule 1: The one with the largest fault probability and its fault probability is larger than a certain threshold ε_1 (e.g. $\varepsilon_1 = 80\%$); or

Rule 2: The difference between the largest fault probability and the second one is larger than a certain threshold ε_1 (e.g. $\varepsilon_2 = 30\%$).

All faults concerned are filtered by the rules. The thresholds ε_1 and ε_2 are constant values. Their initial values can be determined by experts. They can be optimized during the FDD process. They are suggested to be 80% and 30% respectively in the beginning.

8.1.5 Advantages of the Strategy

The proposed framework based on DBN has following advantages:

i.   It is robust against uncertainties in various information and data used in the chiller FDD. The use of probabilities to quantify the occurrence possibilities of faults enables the DBN-based strategy to be tolerant of uncertainties which widely exist in casual relationships (between casual factors and faults, faults and fault symptoms), expert knowledge, measurements, symptoms, FDD results, etc. Fault inference is based on probability analysis and graph theory. FDD results are probabilities of concerned faults and they are more reasonable than Boolean results (i.e., Normal or Faulty) which adopted in most of previous FDD strategies.

ii. It provides an effective approach to merge different types of knowledge and information from a diversity of sources in one network, including physical laws, experts' knowledge/experiences, operation and maintenance records, historical and real-time measurements, observed symptoms, etc. It utilizes all kinds of useful knowledge and information as fully as possible to infer fault just like the actual diagnostic thinking of chiller experts.

iii. It has a strong ability to deal with incomplete or even conflicting information. The reasoning results provide the most reasonable explanation for observed evidences of nodes in additional information layer and fault symptom layer. Of course, the more evidences are used, the more reliable the results are.

In addition, from a methodological point of view, the framework can also embrace all outstanding achievements of the previous FDD research works, and makes a further

step by intelligently merge various knowledge and information. The framework also provides a possible solution to detect and diagnose multiple simultaneous faults in chiller, which is a prominent problem in chiller FDD (Li and Braun 2007).

8.2. Evaluation of the DBN-Based Chiller FDD

In this section, a DBN is developed according to the framework introduced above for the 90-ton water-cooled centrifugal chiller used in ASHRAE RP-1043. The chiller system consisted of a shell-and-tube evaporator, a shell-and-tube condenser, a pilot-driven expansion valve, a centrifugal compressor and other fittings. Both the evaporator and condenser were flooded-type 2-pass shell-and-tube heat exchangers and used water as the secondary-coolant. The water flowed in the tubes and the refrigerant flowed outside. The refrigerant was R134a. The compressor was driven by a constant speed motor. The controller adjusted the compressor's inlet guide vanes to maintain a specified water outlet temperature at the evaporator. More detailed information about the chiller system can be found in Comstock and Braun (2002).

The development of DBN structure and the way to obtain its parameters are described step by step in detail. Evaluations were made in different ways.

8.2.1 Structure of the DBN

The structure of the DBN is shown in Figure 8.2. The nodes in the fault layer are determined firstly. It consists of six nodes representing six typical faults, which account for a major portion of the service calls according to the survey conducted by Comstock and Braun (2002), i.e., *Ncg*, *RefOver*, *RefLeak*, *Cdfoul*, *RedCdW*, *RedEvW*. Each node

has two states, i.e. *Present* and *Absent*, indicating presence and absence of the corresponding fault given observed evidences, respectively.
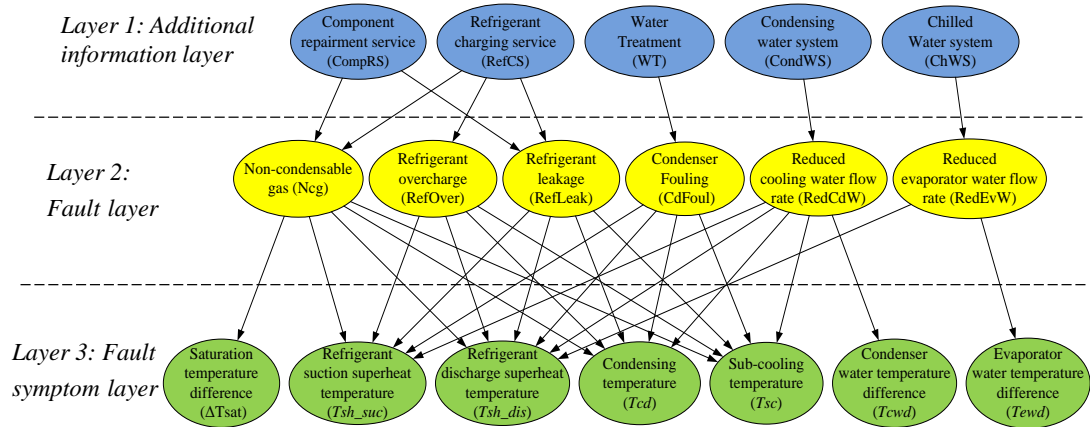
Figure 8.2 Structure of the Bayesian diagnostic network for the chiller in ASHRAE RP-1043

The nodes in the additional information layer are determined secondly. It is desirable to include all possible causal factors. In this study, five major casual factors are selected, as shown in Table 8.1. The states of each node are defined in the fourth column, and the major considerations of including each factor are given in the third column. It should be declared that information about those casual factors is not available in ASHRAE RP-1043 report. Among them, CompRS, RefCS and WT represent the services on the chiller which can usually be easily obtained from facility management records. CondWS and ChWS represent the healthy states of the condensing water pump system and chilled water pump system respectively. These two systems work together with the chiller, and their healthy states surely affect the operation of the chiller.

Table 8.1 The nodes and their states in the additional information layer

Node	State	Prior probability	Event	Major considerations
CompRS	*Yes*	0.15	Component repairing service	Many refrigerant is leaked or non-condensable gas is charged during the service, e.g., repairing or replacing evaporator, condenser, compressor, valve, etc.
	No	0.85		
RefCS	*Yes*	0.1	Refrigerant charging service	Refrigerant is overcharged or leaked, and non-condensable gas is charged.
	No	0.90		
WT	*Yes*	0.80	Water treatment service	The water treatment has not been done;
	No	0.20		The service quality is poor.
CondWS	*Sick*	0.05	The health status of the condensing water pump system	The performance degradation of condensing water pumps; The valve position was changed; False pump sequence control.
	Healthy	0.95		
ChWS	*Sick*	0.05	The health status of the chilled water pump system	The performance degradation of condensing water pumps; The valve position was changed; False pump sequence control.

The nodes in the fault symptom layer are determined at last, which are usually performance indices (PIs). The selection of fault symptoms or PIs depends on available sensor measurements and the FDD strategies adopted. The fault patterns in the selected FDD strategies are described using arcs and parameters (the conditional probability table). Different FDD strategies could be integrated. In this study, the FDD strategy based on multiple linear regression (MLR) was adopted which have been widely used in previous research on chiller FDD. More details about the MLR-based strategy are given in S*ection 4.3*. For the purpose of generalization, seven PIs from sensor measurements which are easy to be obtained are selected, i.e., saturation temperature difference ($\varDelta T_{sat}$), refrigerant suction superheat temperature (T_{sh_suc}), refrigerant discharge superheat temperature (T_{sh_dis}), condensing temperature (T_{cd}), sub-cooling temperature (T_{sc}),

condenser water temperature difference (ΔT_{cw}), and evaporator water temperature difference (ΔT_{chw}). ΔT_{sat} is the temperature difference between the tested saturation temperature and the calculated value using the condenser pressure when the chiller is power off. Each node, except for ΔT_{sat}, has three states, i.e. *Higher*, *Lower* and *Normal*. The ΔT_{sat} has two states, i.e. *Present* and *Absent*.

8.2.2 Parameters of The DBN

Firstly, the conditional probability tables among nodes in the additional information layer and nodes in the fault layer are set based on the knowledge and experiences of authors. The sick severity levels of CondWS and ChWS are considered to 30% reduced water flow rate of condenser and evaporator. Each node has two states, i.e., *Yes/No*, or *Sick/Healthy*. It is worthwhile to note that the nodes in the additional information layer are generally necessary but not sufficient for detecting and diagnosing the faults in the fault layer. For instance, when RefCS and ComRS are *NO*, *RefLeak* is also possible to occur due to other factors, e.g. sealing problems of chiller system. Those factors are not represented using individual nodes in Layer 1 in the DBN. In this case, the effects of unconcerned factors on faults are represented using the conditional probabilities between states *No/Healthy* of nodes in Layer 1 and states of faults in Layer 2. When casual factors of a fault are absent (states *No/Healthy*), there would be still a probability of fault. It means that the value of *P*(*fault = present | casual factor = absent*) plus *P*(*fault = present | unconcerned factors*) was used instead of *P*(*fault = present | unconcerned factors*). The conditional probabilities are set as shown in Table 8.2-8.6.

Table 8.2 Conditional probability table of RefCS, CompRS and *Ncg*, *RefLeak*

	RefCS	YES		NO	
Fault	CompRS	YES	NO	YES	NO
Ncg	Present	0.13	0.1	0.06	0.02
	Absent	0.87	0.9	0.94	0.98
RefLeak	Present	0.25	0.23	0.2	0.15
	Absent	0.75	0.77	0.8	0.85

Table 8.3 Conditional probability table of RefCS and *RefOver*

Fault	RefCS	Yes	NO
RefOver	Present	0.3	0
	Absent	0.7	1

Table 8.4 Conditional probability table of WT and *CdFoul*

Fault	WT	YES	NO
CdFoul	Present	0.05	0.25
	Absent	0.95	0.75

Table 8.5 Conditional probability table of CondWS and *RedCdW*

Fault	CondWS	Healthy	Sick
RedCdW	Present	0.05	0.95
	Absent	0.95	0.05

Table 8.6 Conditional probability table of ChWS and *RedEvW*

Fault	ChWS	Healthy	Sick
RedEvW	Present	0	0.95
	Absent	1	0.05

Secondly, the conditional probabilities among the nodes in the fault layer and the nodes in the symptom layer are statistically calculated using 2/3 experimental data of each fault at severity level 3 from ASHRAE RP-1043, as the bold quantities in Table 8.7. The rest 1/3 are used for evaluation of FDD results as presented in *Section 4.5*. Many fault nodes connect to T_{sh_dis}, T_{sh_suc}, T_{cd}, T_{sc} nodes in Layer 3. It is almost impossible to obtain conditional probabilities of all combinations. Therefore, the nodes in the symptom layer are set to Noisy-MAX nodes. The conditional probabilities in Table 8.7 are used as parameters for those Noisy-MAX nodes. An example of T_{cd} is provided here as Table 8.8. The *LEAK* probabilities represent the influences of fault nodes that are not explicitly included in the Niosy-MAX, i.e. all parent nodes were *Absent*. In this study, the *LEAK* is considered to be *normal*.

Thirdly, the prior probabilities of root nodes are calculated as posterior probabilities using prior probabilities of faults from ASHRAE survey. In the ASHRAE RP-1043, the frequencies of faults were surveyed from 170 service records detailing the various kinds of faults that occur in centrifugal chillers. From the results, the normalized probabilities of typical faults are shown in Figure 8.3. The normalized probabilities are used as prior probabilities of faults directly, as shown in Table 8.9. RefOver was ignored in the survey and the prior probability is estimated to be 3.0% in this study.

Table 8.7 Parameters for the Noisy-MAX node T_{cd}

Parent	CdFoul	RefOver	Ncg	RefLeak	RedCdW	LEAK
State	Present	Present	Present	Present	Present	
Higher	0.75	0.97	1	0	0.74	0
Lower	0.06	0	0	0.92	0.16	0
Normal	0.19	0.03	0	0.08	0.1	1
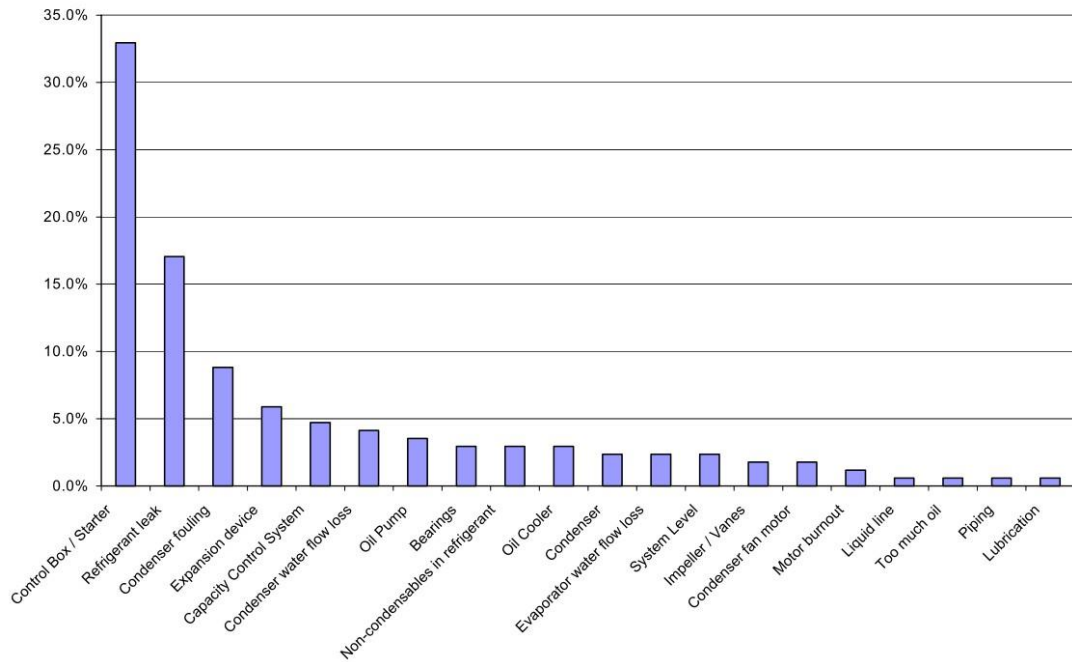
Figure 8.3 Detailed survey results sorted by frequency from ASHRAE RP-1043 report

for Centrifugal chiller

Table 8.8 The conditional probabilities among nodes in the fault layer and nodes in the

symptom layer using ASHRAE RP-1043 data at severity level 3.

Fault	Symptom	T_{sh_suc}	T_{sh_dis}	T_{cd}	T_{sc}	ΔT_{cw}	ΔT_{chw}
	Higher	0.04	0.59	1.00	1.00	0.10	0.18
Ncg	Lower	0.56	0.09	0.00	0.00	0.10	0.00
	Normal	0.40	0.31	0.00	0.00	0.80	0.82
	Higher	0.36	0.55	0.97	1.00	0.77	0.12
RefOver	Lower	0.10	0.05	0.00	0.00	0.00	0.01
	Normal	0.54	0.40	0.03	0.00	0.23	0.87
	Higher	0.11	0.02	0.00	0.00	0.18	0.09
RefLeak	Lower	0.35	0.50	0.92	0.91	0.03	0.02
	Normal	0.54	0.47	0.08	0.09	0.79	0.89
	Higher	0.11	0.32	0.75	0.25	0.35	0.11
CdFoul	Lower	0.39	0.14	0.06	0.15	0.01	0.01
	Normal	0.50	0.54	0.19	0.60	0.65	0.88
	Higher	0.01	0.63	0.74	0.75	0.92	0.01
RedCdW	Lower	0.92	0.17	0.16	0.16	0.05	0.03
	Normal	0.08	0.21	0.10	0.09	0.03	0.96
	Higher	0.07	0.66	0.03	0.03	0.08	1.00
RedEvW	Lower	0.54	0.09	0.44	0.46	0.46	0.00
	Normal	0.39	0.25	0.54	0.50	0.46	0.00

Table 8.9 The prior probabilities of six typical faults from RP-1043 survey

Fault Type	NC	RO	RL	CF	FWC	FEW	Total
Surveyed Value	2.9%	3.0%*	17.0%	8.7%	3.8%	2.5%	37.9%

The prior probability of RO is an estimated value which is absent in the survey of RP-1043.

Up to now, all the necessary specifications for the intelligent DBN-based chiller FDD tool are introduced. The performance of the tool is examined below using the rest 1/3 data at fault severity level 3 in ASHRAE RP-1043 chiller.

8.2.3 Fault Detection

Abundant experiment data of the chiller operating under both normal and faulty conditions were produced in the ASHRAE RP-1043. The experimental data includes transient data between the different steady-state operating conditions. The steady-state data filter developed by Rossi (1995) is used to remove the obvious dynamic data. About 30%-50% data are remained eventually. The MLR-based fault detection strategy is adopted in the intelligent DBN-based chiller FDD tool. The MLR reference models use the cooling load (Q_{ev}), chilled water supply temperature (T_{chws}), and the entering condenser water temperature (T_{ecw}) as inputs as shown in Equation (8.1).

$$Y = f\left(Qev,Tecw,Tchws\right)+\xi \tag{8.1}$$

where, $Y = [T_{sh\_dis}, T_{sh\_suc}, T_{cd}, T_{sc}, \Delta T_{cw}, \Delta T_{chw}]$, $\xi \sim (0,\sigma^2)$. The t-statistic approach is used to determine whether a monitored variable was abnormal. In this study, confidence level of 95.45% (2σ) is selected. The confidence intervals are doubled (4σ) for ΔT_{cw} and

168

ΔT_{chw} because they are unstable in some tests. Compared with the reference values, the monitored PIs are classified to three categories, i.e. *higher*, *lower* and *normal*. A fault is detected when the residuals between PIs and its benchmark values (they were calculated using MLR reference models) are out of their confidence intervals.

8.2.4 Fault Diagnosis

8.2.4.1 Fault diagnosis using only evidences from the fault symptom layer

Table 8.10 Fault probabilities when only evidences from the symptom layer are used

Fault	Fault diagnosis result					
	Ncg	*RefOver*	*RefLeak*	*CdFoul*	*RedCdW*	*RedEvW*
Ncg	68%	20%	23%	24%	5%	0%
RefOver	40%	42%	12%	20%	0%	0%
RefLeak	0%	0%	100%	1%	0%	0%
CdFoul	0%	0%	0%	100%	0%	0%
RedCdW	8%	4%	16%	13%	98%	0%
RedEvW	0%	0%	3%	35%	0%	98%

This case aims to evaluate the intelligent DBN-based FDD strategy using only nodes (except for ΔT_{sat}) at the fault symptom layer as most of previous FDD researchers did. It is assumed that each node in the fault symptom layer is observed respectively. The evidence provided by a node is that the state of the node with largest probabilities in Table 8.9 is observed. For instance, for Ncg fault, the probabilities of T_{sh_dis} are 0.59, 0.09, 0.31 for *higher*, *lower* and *normal* respectively. It is similar to the way used by

previous researcher in developing expert rules. Given such an evidence, the observed state (T_{sh_dis} is *higher*) is set to be 95% considering uncertainties in the DBN. The posterior probabilities of faults are shown in Table 8.10.

The fault probabilities are 100% in the cases of RefLeak and CdFoul, and 98% in the case of RedCdW and RedEvW. All of these four faults are correctly diagnosed. In the case of *RefOver*, *Ncg* (40%) and *RefOver* (42%) are the top two suspected faults. They could not be distinguished without ΔT_{sat}. The result is the same as conclusions obtained in previous research (Li and Braun, 2007; Chen and Braun, 2001). If additional evidence is introduced, i.e. ΔT_{sat} is *normal*, the fault probability of *RefOver* increased to 65% and that of *Ncg* reduced to 1%. In the case of Ncg, it is interesting to see that the fault probability of *Ncg* is 68% and it could be distinguished with RefOver correctly. It is because that *Ncg* and *RefOver* have the same symptoms except for T_{sh_suc}. The T_{sh_suc} is *lower* in the case of Ncg and is *normal* in the case of RefOver. The conditional probabilities between fault nodes (Ncg and RefOver) and the state (T_{sh_suc} is *normal*) are 0.40 and 0.54 respectively. The difference is too small to isolate *RefOver* from *Ncg*. The conditional probabilities between fault nodes (*Ncg* and *RefOver*) and the state (T_{sh_suc} is *lower*) are 0.56 and 0.10 respectively. When *Ncg* occurrs, it could be isolated from *RefOver* since T_{sh_suc} is *lower*.

Only using nodes (except for ΔT_{sat}) in the fault symptom layer, the FDD performance of the proposed strategy is similar to previous rule-based strategies in diagnosing the five faults except for *Ncg*. In the case of *Ncg*, it has better performance.

8.2.4.2 Fault diagnosis using incomplete and uncertain information

Five cases are studied to evaluate the proposed intelligent FDD strategy using incomplete and uncertain information. In practical applications, especially for manual FDD, not all the symptoms in Layer 1 and Layer 3 are available and reliable due to various uncertainties, shortage of measuring instrument, incomplete records, sensor faults, etc. In the five cases, it is assumed only several rather than all nodes in Layer 1 and Layer 3 are observed. The five cases are listed in Table 8.11.

Table 8.11 Five fault diagnosis case using incomplete and uncertain evidences

Case	Step	Evidence	Fault diagnosis result (%)					
			Ncg	*RefOver*	*RefLeak*	*CdFoul*	*RedCdW*	*RedEvW*
Case-1	1	T_{cd} is *lower*	0%	0%	93%	5%	6%	3%
	2	T_{sc} is *lower*	0%	0%	99%	2%	0%	3%
Case-2	1	ΔT_{chw} is *higher*	3%	3%	17%	9%	5%	84%
	2	T_{sh_dis} is *higher*	5%	4%	17%	11%	7%	97%
Case-3	1	T_{cd} is *higher*	22%	19%	18%	45%	24%	3%
	2	WT is *No*	13%	11%	17%	73%	15%	3%
Case-4	1	T_{cd} is *higher*	22%	19%	18%	45%	24%	3%
	2	RefCS is *Yes*	24%	68%	23%	18%	10%	3%
	3	ΔT_{sat} is *higher*	94%	33%	23%	10%	5%	3%
Case-5	1	T_{cd} is *higher*	22%	19%	18%	45%	24%	3%
	2	T_{sc} is *higher*	33%	29%	19%	23%	29%	3%
	3	RefCS is *No*	38%	0%	16%	31%	42%	3%
	4	CondWS is *Healthy*	61%	0%	16%	44%	0%	3%
	5	WT is *Yes*	74%	0%	16%	30%	0%	3%
	6	ΔT_{sat} is *normal*	5%	0%	16%	95%	0%	3%

In the diagnosis process, evidences are examined one by one according to the steps specified in Table 8.11 which is also more like the diagnostic thinking of chiller FDD experts. The DBN generates fault probabilities under given incomplete evidences in Table 8.11.

Case 1 assumes only the nodes of T_{cd} and T_{sc} are observed. At step 1 (evidence: T_{cd} is *lower*), the fault probability of *RefLeak* (93%) is apparently larger than others'. It is because that this symptom only occurred in *RefLeak*. When the other evidence (T_{sc} is *lower*) is added at step 2, the fault probability increases to 99%. The fault of *RefLeak* surely occurs.

Case 2 assumes only the nodes of T_{wev} and T_{sh_dis} are observed. At step 1 (evidence: T_{wev} is *higher*), the fault probability of *RedEvW* is 84%. At step 2 (added evidence: T_{sh_dis} is *higher*), the probability increases to 97%. The fault of *RedEvW* is successfully diagnosed with high confidence.

Case 3 assumes only the node of T_{cd} and WT (in service records) are observed. At step 1 (evidence: T_{cd} is *higher*), the fault probability of *CdFoul* is 45%, which is two times of the values of the other three faults (*RefOver, Ncg, RedCdW*). It is because that the prior probability of CdFoul is higher. Therefore, it is the most suspected fault when only T_{cd} is available. At step 2 (added evidence: WT is *No*), the fault possibility of *CdFoul* increases to 73%. The CdFoul can be diagnosed with a high confidence in this case.

Case 4 assumes the nodes of T_{cd}, RefCS and ΔT_{sat} are observed. At step 1 (evidence: T_{cd} is *higher*), the fault probability of *Ncg* is 22%, which is about half of that of CdFoul

(45%). At step 2 (added evidence: RefCS is *Yes*), RefOver (68%) is the most suspected fault. The fault probability of Ncg (24%) is slightly increased under the new evidence. RefOver is more likely to occur than Ncg under both evidences. At step 3 (added evidence: ΔT_{sat} is *higher*), the fault probability of *Ncg* increases from 24% to 95% and that of *RefOver* decreases from 68% to 33%. It is because the new evidence is a unique index for *Ncg*.

Case 5 assumes existing of complex and even conflicting evidences. The step 1 is the same as that in Case 4, which results in *CdFoul* (45%), *RedCdW* (24%) and *Ncg* (22%) as the top three suspected faults. At step 2 (added evidence: T_{sc} is *higher*), the fault probability of *CdFoul* reduces to 23% and that of *Ncg* (33%) is the highest one. At step 3 (added evidence: RefCS is *No*), the fault probability of RefOver reduces to 0%, while *RedCdW* (42%) is the most suspected fault. At step 4 (added evidence: CondWS is *Healthy*), the *RedCdW* reduces to 0%. *Ncg* (61%) and *CdFoul* (43%) are the two most suspected faults. At step 5 (added evidence: WT is *Yes*), the fault probability of *CdFoul* reduces to 30% and that of *Ncg* increases to 74%. Under previous evidences, the posterior probability of the state (ΔT_{sat} is *normal)* is 27%, which is a comparatively small probability. However, if it is assumed at step 6, it is interesting to see that the fault probability of Ncg reduces to 5%, while that of CdFoul increases from 30% to 83%. Such a result is the most plausible explanation according to the six evidences. The results of *RefOver* (0%) and *RedCdW* (0%) are strongly supported by RCS and CondWS. They are eliminated from the suspected fault list. The *RefLeak* is also eliminated because it violates the two evidences at step 1 and step 2. The *RedEvW* is impossible to occur since no evidence supports it. At last, the *CdFoul* is the only suspected fault.

Although the evidence (WT is *Yes*) is conflicting, CdFoul is still possible to occur under this evidence, since the conditional probability is not zero, i.e. *P*(*CdFoul* is *Present* | CondWS is *Yes*) = 5% as shown in Table 8.4.

The results show that the proposed strategy can diagnose fault efficiently from incomplete information. It is significantly meaningful for the chiller FDD in the situations that limited information is available. Previous research on the chiller FDD seldom considered this point.

8.2.4.3 Fault diagnosis using ASHRAE RP-1043 data

This case aims to evaluate online FDD capacity of the proposed strategy. In each test, only one piece of evidence of in Layer 1 is added to evaluate the influences of Layer 1 nodes on FDD performance. The FDD result should be less accurate when one piece of evidence from Layer 1 does not support the occurrence of a target fault (it seldom occurs in reality), and be more accurate on the contrast (it happens in most of time). All nodes in Layer 3 are observed according to the fault detection results. The test data are the left 1/3 steady state data (from *section 4.4*) of severity level 3 from ASHRAE RP-1043 experimental data. The FDD results are summarized in Table 8.12. The thresholds of ε_1 and ε_2 are set to be 80% and 30% respectively. The successful diagnosis ratios are calculated for test data of each fault.

In the test of *Ncg*, the successful diagnosis ratio is 37% without evidence from Layer 1. It increases to 43% (CompRS is *Yes*), 61% (RefCS is *No*), and 99% ($\varDelta T_{sat}$ is *Present*). When the evidences in Layer 1 do not support Ncg, the diagnosis ratio ($\varDelta T_{sat}$ is *Absent*) of Ncg is 0% and that of RefOver is 26%. It is because the Ncg would never occur under

such evidence. The diagnosis ratio (RefCS is *Yes*) of Ncg is 0% and that of *RefOver* is

53%. It is because *RefOver* is more likely to exist in such situation.

Table 8.12 Evaluation results using the rest ASHRAE RP-1043 experimental data

| Fault | Node | State | Fault diagnosis result | | | | | | |
			Ncg	*RefOver*	*RefLeak*	*CdFoul*	*RedCdW*	*RedEvW*	Unknown
Ncg	-	-	37%	9%	0%	0%	0%	0%	53%
	CompRS	Yes	43%	9%	0%	0%	0%	0%	48%
	CompRS	No	37%	9%	0%	0%	0%	0%	53%
	RefCS	Yes	0%	53%	0%	0%	0%	0%	47%
	RefCS	No	61%	0%	0%	0%	0%	0%	39%
	ΔT_{sat}	Present	99%	0%	0%	0%	0%	0%	1%
	ΔT_{sat}	Absent	0%	26%	0%	0%	0%	0%	68%
RefOver	-	-	1%	13%	0%	7%	47%	0%	32%
	CompRS	Yes	3%	3%	0%	7%	40%	0%	48%
	CompRS	No	1%	13%	0%	7%	47%	0%	32%
	RefCS	Yes	0%	77%	0%	0%	6%	0%	17%
	RefCS	No	1%	0%	0%	25%	47%	0%	26%
RefLeak	-	-	0%	0%	94%	2%	0%	0%	4%
	CompRS	Yes	0%	0%	94%	0%	0%	0%	6%
	CompRS	No	0%	0%	94%	2%	0%	0%	4%
	RefCS	Yes	0%	0%	94%	0%	0%	0%	6%
	RefCS	No	0%	0%	94%	2%	0%	0%	4%
CdFoul	-	-	0%	1%	1%	62%	1%	0%	30%
	WT	Yes	1%	1%	7%	55%	1%	0%	35%
	WT	No	0%	0%	6%	85%	0%	0%	9%
RedCdW	-	-	1%	4%	6%	6%	79%	0%	4%
	CondWS	Sick	0%	0%	2%	1%	96%	0%	1%
	CondWS	Health	16%	10%	12%	20%	0%	0%	43%
RedEvW	-	-	0%	0%	26%	2%	0%	68%	4%
	ChWS	Sick	0%	0%	16%	1%	0%	82%	1%
	ChWS	Health	0%	0%	29%	43%	0%	0%	28%

In the test of *RefOver*, the successful diagnosis ratio is 77%. It is because that RefOver only occurres when RefCS is *Yes*. The diagnosis ratio of RefOver is 0% and that of *RedCdW* is 47% under the evidences of CompRS (*Yes* and *No*), RefCS (*No*), or no evidence from Layer 1. Actually, the suspected *RedCdW* could be removed using further evidence (e.g. CondWS is *health*).

In the test of RefLeak, the successful diagnosis ratio is 94% all the time using various evidences or no evidence from Layer 1. It is because the evidences from Layer 3 strongly support RefLeak. In the test of *CdFoul*, the successful diagnosis ratio increases from 62% (no evidence from layer 1) to 85% (WT is *No*), and is decreased to 55% (WT is *Yes*). In the test of *RedCdW*, the successful diagnosis ratio increases from 79% (no evidence from layer 1) to 96% (*CondWS* is *Sick*), and decreases to 20% (*CondWS* is *Health*). In the case of *RedEvW*, the successful diagnosis ratio increases from 68% (no evidence from layer 1) to 82% (*CondWS* is *Sick*), and decreass to 43% (*CondWS* is *Health*).

8.3 Summary

A novel framework for intelligent chiller FDD is proposed in this chapter using Bayesian Diagnosis Network. A three-layer DBN is found to be sufficient for chiller FDD. From a methodological point of view, the framework can take advantage of all useful information of the chiller concerned and chiller experts' knowledge. The framework can also integrate the outstanding achievements of previous FDD research into the development of the structure and parameters of the DBN. The DBN can properly account for uncertainties in the chiller FDD based on the probability analysis

and graph theory. It allows merging different types of knowledge and information (i.e. quantitative and qualitative) from diverse sources. It also has a strong ability in dealing with incomplete or even conflicting information. The DBN simulates the diagnostic thinking and diagnosis process of chiller expert. It can be used for online automatic FDD and manual FDD. The more information is embraced in the development of DBN, the more intelligent it would be. Similarly, the more evidences added to DBN in the FDD process, the more accurate the results would be.

A case study of implementing the framework for detecting and diagnosing faults of the chiller studied in ASHRAE RP-1043 is conducted. The DBN has similar accuracy as rule-based chiller FDD strategies using ideal evidences in symptom node layer. It is powerful to diagnose faults using incomplete and even conflicting information. Evaluation of its online FDD performance is made using experimental data from ASHRAE RP-1043. Except refrigerant overcharge and non-considerable gas, the rest four faults are correctly diagnosed only using evidences from fault symptom nodes. The diagnosis ratios are increased when evidences of nodes in additional information layer are used. Refrigerant overcharge and non-considerable gas can be correctly diagnosed with the help of evidences of nodes in additional information layer. It is worth noticing that the difficulty in development of DBN is to obtain parameters. Further efforts are needed to reduce the difficulty.

CHAPTER 9 A DIAGNOSTIC BAYESIAN NETWORK

FOR VAV TERMINAL FDD

This chapter presents a diagnostic Bayesian network (DBN) for fault detection and diagnosis (FDD) of variable air volume (VAV) terminals. The structure of the DBN illustrates qualitatively the casual relationships between faults and symptoms. The parameters of the DBN describe quantitatively the probabilistic dependences between faults and evidence. The inputs of the DBN are the evidences which can be obtained from measurements in building management systems (BMSs) and manual tests. The outputs are the probabilities of faults concerned. Two rules are adopted to isolate the faults on the basis of the fault probabilities to improve the robustness of the strategy. Compared with conventional rule-based FDD strategies, the proposed strategy can provide better performance concerning uncertain and incomplete information. The faults are reported with probabilities rather than in the Boolean format. Evaluations are made on a dynamic simulator of a VAV air-conditioning system serving an office space using TRNSYS.

9.1 VAV Terminal Description and Typical VAV Terminal Faults

9.1.1 Description of VAV Terminal

The pressure-independent controller is widely used in large complex VAV air-conditioning systems due to its better control stability and faster response to load changes. The controller consists of two control loops, i.e. the temperature control loop and the flow control loop, as shown in Figure 9.1. The temperature control loop resets

the flow rate set-point based on the deviation of the measured zone temperature from its set-point. The flow control loop adjusts the VAV damper to maintain the measured air flow rate at its set-point. The influence of the fluctuation in the supply air pressure is eliminated because the flow control loop response quickly to it before the space temperature control is affected.
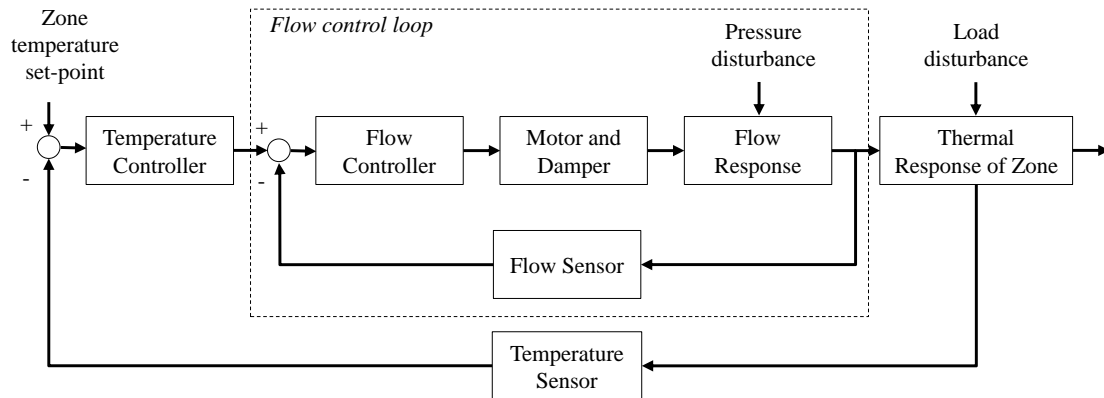
Figure 9.1 Control loops of pressure-independent VAV terminals (Qin and Wang 2005)

9.1.2 Typical VAV Terminal Faults

Qin and Wang conducted a comprehensive investigation of the 1251 pressure-independent VAV terminals in a 39-storey commercial building in Hong Kong (Qin and Wang, 2005; Wang and Qin, 2005). They found that 20.9% (i.e., 261/1251) of the VAV terminals are suspected to be faulty. Through detailed checking, 12 typical faults in VAV terminals were identified. The consequences of the faults include poor indoor environment quality, waste of energy, unreachable design value and physical damages. The ten root faults identified in their study, as shown in Table 9.1, are considered in this study.

Table 9.1 Ten typical faults and their default prior probabilities

No.	Fault node	States	Rules for defining state	Prior probability
F1	Zone temperature sensor reading frozen	*Positive frozen*	T_{zone} *is frozen, and* $T_{zone} - T_{set} > \varepsilon_{t1}$	6%
		Negative frozen	T_{zone} *is frozen, and* $T_{zone} - T_{set} < -\varepsilon_{t1}$	6%
		Frozen at set-point	T_{zone} *is frozen, and* $|T_{zone} - T_{set}| \leq \varepsilon_{t1}$	2%
		Fault-free	T_{zone} *is not frozen*	86%
F2	Flow sensor reading frozen	*Frozen*	F_{air} *is frozen*	12%
		Fault-free	F_{air} *is not frozen*	88%
F3	Damper stuck	*Positive stuck*	$F_{air} - F_{air,set} > \varepsilon_F$	4%
		Negative stuck	$F_{air} - F_{air,set} < -\varepsilon_F$	4%
		Fault-free	$|F_{air} - F_{air,set}| \leq \varepsilon_F$	92%
F4	Flow sensor biased	*Biased*	$|F_{air} - F_{air,acv}| > \varepsilon_\lambda$	16%
		Fault-free	$|F_{air} - F_{air,acv}| \leq \varepsilon_\lambda$	84%
F5	Improper supply air pressure	*Positive*	$P_{supply} - P_{supply,set} > \varepsilon_{Psupply}$	2%
		Negative	$P_{supply} - P_{supply,set} < -\varepsilon_{Psupply}$	4%
		Fault-free	$|P_{supply} - P_{supply,set}| \leq \varepsilon_{Psupply}$	94%
F6	Improper supply air temperature	*Positive*	$T_{supply} - T_{supply,set} > \varepsilon_{Tsupply}$	4%
		Negative	$T_{supply} - T_{supply,set} < -\varepsilon_{Tsupply}$	2%
		Fault-free	$|T_{supply} - T_{supply,set}| \leq \varepsilon_{Tsupply}$	94%

F7	VAV terminal undersize	*Undersize*	$Q < 0.8*Q_{max,acv}$	4%
		Fault-free	$Q \geq 0.8*Q_{max,\,acv}$	96%
F8	Extreme cooling load	*Positive*	$Q > 1.2*Q_{max,\,acv}$	3%
		Negative	$Q < 0.1*Q_{max,\,acv}$	2%
		Fault-free	$0.1*Q_{max} \leq Q \leq 1.2*Q_{max,\,acv}$	95%
F9	Zone temperature sensor biased	*Positive*	$T_{zone} - T_{zone,acv} > \varepsilon_{Tset}$	8%
		Negative	$T_{zone} - T_{zone,acv} < -\varepsilon_{Tset}$	8%
		Fault-free	$|T_{zone} - T_{zone,acv}| \leq \varepsilon_{Tset}$	84%
F10	Improper zone temperature set-point	*Positive*	$T_{zone} - T_{zone,acv} > \varepsilon_{Tset}$	6%
		Negative	$T_{zone} - T_{zone,acv} < -\varepsilon_{Tset}$	6%
		Fault-free	$|T_{zone} - T_{zone,acv}| \leq \varepsilon_{Tset}$	88%

9.2 Diagnostic Bayesian Network (DBN) for VAV Terminal FDD

A DBN is developed for diagnosing the ten root faults in the VAV terminals. The development of the structure and parameters of this DBN is explained in the following parts. The application of the DBN for FDD of VAV terminals and its advantages are also discussed in the later parts.

9.2.1 Basic Ideas and Structure

The structure of the DBN is a graphical illustration of experts' diagnostic thinking, which can illustrate qualitatively the relationships among faults and symptoms. There are usually two approaches for developing the structure of a DBN, i.e. manually developed by experts and machine learning using full data sets (including both normal and fault data). The second approach is impractical because the full data sets of VAV

terminals are hardly available in practice. Therefore, the first approach is adopted in this study.

Figure 9.2 Diagnostic Bayesian network for fault detection and diagnosis of VAV terminals

In developing the DBN for FDD of VAV terminals, the diagnostic thinking process of FDD experts are reflected and simulated. FDD experts usually diagnose faults based on the observed fault symptoms. Therefore, the DBN should consist of two types of nodes at least, i.e. the fault nodes and the fault symptom nodes. Considering that some fault symptoms can be collected from BMS automatically and others may need manual inputs, the symptom nodes are further divided into two groups, i.e. the BMS evidence nodes and the additional information nodes, as shown in Figure 9.2. Fault nodes

represent the ten root faults shown in Table 9.1. BMS evidence nodes represent symptoms which can be obtained from BMS database, as summarized in Table 9.2. Additional information nodes represent the evidences which can be obtained by site investigation, manual test and maintenance records.

Table 9.2 Twelve BMS evidence nodes

No.	BMS evidence node	State	Rules for defining state
E1	T_{zone} - T_{set}	*Extremely positive*	T_{zone} - $T_{set} > \varepsilon_{t2}$
		Fairly positive	$\varepsilon_{t2} \geq T_{zone}$ - $T_{set} > \varepsilon_{t1}$
		Within threshold	$|T_{zone}$ - $T_{set}| \leq \varepsilon_{t1}$
		Fairly negative	$-\varepsilon_{t2} \leq T_{zone}$ - $T_{set} < -\varepsilon_{t1}$
		Extremely negative	T_{zone} - $T_{set} < -\varepsilon_{t2}$
E2	F_{supply} - F_{set}	*Positive*	F_{air} - $F_{set} > \varepsilon_F$
		Within threshold	$|F_{air}$ - $F_{set}| \leq \varepsilon_F$
		Negative	F_{air} - $F_{set} < -\varepsilon_F$
E3	Air flow rate set-point	*Maximum value*	$|F_{set}$ - $F_{max}| \leq \varepsilon_F$
		Within threshold	$|F_{set}$ - $F_{max}| > \varepsilon_F$, and $|F_{set}$ - $F_{min}| > \varepsilon_F$
		Minimum value	$|F_{set}$ - $F_{min}| \leq \varepsilon_F$
E4	Air flow rate in ON period	*Frozen*	F_{air} reading is unchanged for 3 hours, and $|T_{zone}$ - $T_{set}| \leq \varepsilon_{t1}$, and $|F_{air}$ - $F_{set}| \leq \varepsilon_{t1}$,
		Not frozen	If *Frozen* is not detected
E5	Air flow rate in OFF period	*Frozen*	F_{air} is unchanged during power off period
		Not frozen	If *Frozen* is not detected
E6	Air flow rate set-point reversal number	*Too many reversal*	Larger than 4 within 1.5 hours
		Within threshold	Smaller than 4 within 1.5 hours
E7	The relationship between air flow rate and damper position	*Positive*	$|F_{air}$ - $F_{max}| \leq \varepsilon_F$, λ_{max}- $\lambda > 20\%$
		Negative	$|F_{air}$ - $F_{min}| \leq \varepsilon_F$, λ- $\lambda_{min} > 20\%$
		Within threshold	If above states are not detected
E8	P_{supply} - $P_{supply,set}$	*Positive*	P_{supply} - $P_{supply,set} > \varepsilon_{Psupply}$
		Negative	P_{supply} - $P_{supply,set} < -\varepsilon_{Psupply}$
		Within threshold	$|P_{supply}$ - $P_{supply,set}| \leq \varepsilon_{Psupply}$
E9	T_{supply} - $T_{supply,set}$	*Positive*	T_{supply} - $T_{supply,set} > \varepsilon_{Tsupply}$
		Negative	T_{supply} - $T_{supply,set} < -\varepsilon_{Tsupply}$

		Within threshold	$|T_{supply} - T_{supply,set}| \leq \varepsilon_{Tsupply}$
E10	T_{set} - $T_{set,design}$	Positive	T_{set} - $T_{set,design} > \varepsilon_{Tset}$
		Negative	T_{set} - $T_{set,design} < - \varepsilon_{Tset}$
		Within threshold	$|T_{set}$ - $T_{set,design}| \leq \varepsilon_{Tset}$
E11	Zone temperature reading in OFF period	Frozen	T_{zone} is unchanged for 0.5 hours in OFF period
		Not frozen	If *Frozen* is not detected
E12	Zone temperature reading in ON period	Positive frozen	T_{zone} - $T_{zone, set} > \varepsilon_{t1}$, and T_{zone} reading is unchanged for *3* hours
		Negative frozen	T_{zone} - $T_{zone, set} < -\varepsilon_{t1}$, and T_{zone} reading is unchanged for *3* hours
		Frozen at set-point	$|T_{zone}$ - $T_{zone, set}| \leq \varepsilon_{t1}$, and T_{zone} reading is unchanged for *3* hours,
		Not frozen	If above states are not detected

After determining the nodes, the state of each node should be defined. A fault node may have several states, as shown in the third column of Table 9.1. It helps to lower the difficulty in estimating the conditional probabilities of the fault evidence given the fault. Besides, it can provide the more detailed information of the fault, which helps to bring the system back to normal. The rules in the fourth column of Table 9.1 define the corresponding states. Taking *F1* (zone temperature sensor frozen) for instance, it has four states, i.e. *Positive frozen*, *Negative frozen*, *Frozen at set-point and Fault-free,* which means the measured zone temperature is higher than, lower than or equal to the zone temperature set-point, as well as fault-free, respectively.

Twelve BMS evidence nodes are used as shown in Table 9.2. Similarly to Table 9.1, states of each node and the corresponding rules to determine the states of the nodes are also given in Table 9.2. Most of the rules are straightforward and can be understood easily. For instance, *E12* represents the behavior of the zone temperature sensor (T_{zone}) when the VAV system is in operation (ON period). It has four states, i.e. *Positive frozen*,

Negative frozen, *Frozen at set-point* and *Not frozen*. The state of T_{zone} frozen is confirmed if the measurement does not change in 3 hours. The *Positive frozen* state is observed if T_{zone} is larger than the sum of T_{set} and ε_{t1}. *E6* represents the behavior of the flow rate set-point within a moving window. The flow set-point reversal is counted when F_{set} - F_{air} exceeds the threshold (ε_F) and the reversal number is added by one once F_{set} - F_{air} exceeds the threshold at the opposite direction. Within a moving window, the reversal number will be larger than a threshold when the flow sensor reading is frozen. Qin and Wang (2005) advised the threshold of the reversal number to be 4 in the moving window of 1.5 hours.

Nine additional information nodes are given in Table 9.3. The last column explains how to get the additional information. The additional information nodes are useful only if faults cannot be distinguished using BMS evidence nodes. For example, there are more than one fault are suspected according to the DBN inference from the BMS evidence nodes. However, the posterior probabilities of those faults are very close to each other which cannot help to isolate the actual fault. In such situation, the additional information nodes are needed. The posterior probabilities (believes) of the states of the additional information nodes will be inferred from the suspected fault nodes. A manual test list selected from the last column of Table 9.3 will be recommended to check those states with high posterior probabilities.

Table 9.3 Nine additional information nodes

No.	Additional information node	State	Rules for defining state	Action
M1	Site measured supply air flow rate - BMS measured supply air flow rate?	*Yes*	$\|F_{supply,m}-F_{supply}\|> \varepsilon_F$	Manual test
		No	$\|F_{supply,m}-F_{supply}\|\leq \varepsilon_F$	
M2	Is damper stuck?	*Yes*		Manual test
		No		
M3	Does measured supply air temperature equal its set-point?	*Yes*	$\|T_{supply,m} - T_{supply,set}\|\leq \varepsilon_{t1}$	Manual test
		No	$\|T_{supply,m} - T_{supply,set}\|> \varepsilon_{t1}$	
M4	Is temperature in similar zones (T'_{zone}) higher or lower than its set-point?	*Higher*	$T'_{zone} - T_{zone,set}> \varepsilon_{t1}$	Manual test/analyze BMS data
		Lower	$T'_{zone} - T_{zone,set}< \varepsilon_{t1}$	
		No	$\|T'_{zone} - T_{zone,set}\|\leq \varepsilon_{t1}$	
M5	Was VAV terminal undersize fault detected and reported before?	*Yes*		Facility management records
		No		
M6	Is weather extremely hot or extremely cold?	*Extremely hot*	$T_{oa} > T_{exh}$	Site investigation
		Extremely cold	$T_{oa} < T_{exl}$	
		Absent	$T_{exl} \leq T_{oa} \leq T_{exh}$	
M7	Is occupant number extremely large? Is window open?	*Too many*	5 times of design occupant number	Site investigation
		Open		
		Absent		
M8	No fault detected, but occupants complain zone temperature is hot/cold.	*Too hot*		Facility management record
		Too cold		
		No complain		
M9	Does, manually measured zone temperature ($T_{zone,m}$) equal zone temperature set-point?	*Yes*	$\|T_{zone,m} - T_{zone,set}\|\leq \varepsilon_{t1}$	Manual test
		No	$\|T_{zone,} - T_{zone,set}\|> \varepsilon_{t1}$	

After manually input the states needed, the posterior probabilities of the faults suspected will be calculated again and the actual fault will be successfully diagnosed.

Examples on how to utilize additional information nodes are given in the later part. The additional information can help to enhance the reliability of the DBN-based FDD strategy considering incompleteness of necessary information. However, considering the convenience in obtaining necessary information, the BMS evidence nodes will be used firstly and the additional information is not always needed. Meanwhile, a manual test list can be recommended by the DBN to check those necessary additional information nodes which can substantially reduce the manual work load.

The DBN for FDD of VAV terminals is shown in Figure 9.2 which illustrates the three types of nodes and how they connect with each other. Taking the fault node *F1*, i.e. zone temperature sensor reading frozen, for example, if this fault occurs, the BMS evidence nodes *E1*, *E2*, *E3*, *E4*, *E11* and *E12* will be influenced. Therefore, *F1* connects to these BMS evidence nodes directly using arcs. It should be noted that developing DBN is usually a complex and time-consuming task. After all, simulating the thinking process of FDD experts is not easy. The knowledge and experience of the developer of DBN is critically important. However, the DBN developed in this study is not customized for a special VAV terminal, but for a large number of similar VAV terminals widely used in many VAV systems. The effort is worthwhile.

9.2.2 Parameters of the VAV Terminal DBN

Parameters of a DBN represent the quantitative dependences among faults and symptoms using probabilities. A conditional probability table is used to define the probabilities of all states of a child node given the states of its parent nodes. In this study, nodes with only one parent node are considered to be general nodes. Nodes with more

than one parent nodes are assumed to be Noisy-MAX nodes. For the Noisy-MAX nodes, the conditional probabilities and *LEAK* probabilities are needed. In the DBN for VAV terminal FDD, *LEAK* probabilities represent the probabilities of each state of child node when all parent nodes are at fault-free states. Therefore, there are three kinds of parameters in the DBN for FDD of VAV terminals, i.e. prior probabilities of root nodes, conditional probability tables of general nodes as well as conditional probabilities and *LEAK* probabilities of noisy-MAX nodes. In the DBN shown in Figure 9.2, the root nodes include all fault nodes except for *F7*, *F8* and *F10* and the additional information nodes *M5*, *M6*, and *M7* (parent nodes of *F7* and *F8*).

It is reasonable to assume that the probability of a frequently occurred fault is higher than that of a rarely occurred fault when a VAV terminal is abnormal. For instance, when the zone temperature is higher than its set-point, *F1* (zone temperature sensor reading frozen) is more possible to occur than F8 (extremely High/Low cooling load), since the former's prior probability is obviously larger than that of the later as proven in Qin and Wang's survey results. Such kind of prior knowledge is utilized by giving prior probabilities to faults in the DBN-based FDD. Field survey is the best way to obtain the prior probabilities of faults. However, there were few survey results available. Yoshida conducted a survey to collect information on a range of faults in air handling units using the reference system diagram. Survey was made from design engineers, fabricating engineers and maintenance engineers. There were two VAV terminal related faults among the ten most typical faults in air handling units, i.e. too much or less air volume at top 5 and false opening signal to a VAV unit controller at top 7. Wang and Qin made a survey on the VAV air conditioning system in a 39-storey commercial building in

188

Hong Kong. They found 261 abnormal ones in a total of 1251 VAV terminals. The temperature sensor error contributed 25.3% of all faults, which was the largest one. The second one was the direct digital controller error (17.6%). 11.5% of VAV boxes were not accessible due to unknown reason. In this study, the prior probabilities of faults in the last column of Table 9.1 were estimated by authors based on available survey results and knowledge and experience of the authors. The assignment of prior probabilities seems subjective to some extent. A detailed analysis of the sensitivity of the FDD results to the probabilities assigned is given in the later part.

The conditional probabilities between the fault nodes and the BMS evidence nodes or the additional information nodes are estimated by the authors. Taking the general nodes *E11* and *E12* for example, the assignment of conditional probabilities is explained as follows. Table 9.4 illustrates the conditional probability table between *F1* and *E11*. When T_{zone} reading is frozen, a higher value, i.e. 0.98, is given to the conditional probability of *E11* at the state of *Frozen*, considering the close cause-effect relationship between *F1* and *E11*. It leaves 0.02 for various uncertainties, such as induced electrical noise, sensor wiring fault, etc. When the T_{zone} sensor is normal, there is still a little chance that its reading is frozen during the power OFF period. In view of this, a small value, i.e. 0.1, is given to this probability. Similarly，the conditional probability table between *F1* and *E12* is defined by Table 9.5.

Table 9.4 Conditional probability table between F1 and E11

| E11 | F1: T_{zone} reading frozen | | | |
	Higher	*Lower*	*Tset*	*Absent*
Frozen	0.98	0.98	0.98	0.1
Not frozen	0.02	0.02	0.02	0.9

Table 9.5 Conditional probability table between F1 and E12

| E12 | F1: T_{zone} reading frozen | | | |
	Positive frozen	Negative frozen	Frozen at set-point	Fault-free
Positive frozen	0.98	0	0	0.01
Negative frozen	0	0.98	0	0.01
Frozen at set-point	0	0	0.98	0.03
Not frozen	0.02	0.02	0.02	0.95

E2 is assumed to be a noisy-MAX node. Due to the space limitation, Table 9.6 only shows the conditional probabilities of *E2* given *F2* and *F5* as well as its LEAK probabilities. The assignment of the conditional probabilities is similar to Table 9.4 and 9.5. For a noisy-MAX node, the state *Fault-free* of each fault should be in Boolean format, i.e. *Yes* (0) and *No* (1). *LEAK* represents the probabilities when both *F4* and *F5* are *Fault-free*. If *E2* is a general node, it should consider all of the possible combinations of states of its parent nodes in the conditional probability table, e.g. *P(E2=Positive/F4=Fmax, F4= Biased).* It is reasonable to assume that at one moment there is only one fault occurring; therefore *E2* can be assumed to be a noisy-MAX node. It shows that the assumption saves efforts significantly without sacrificing the FDD reliability.

Table 9.6 Conditional probabilities of Noisy-MAX node E2 given F4 and F5 and its LEAK probabilities

| E2 F_{supply} - F_{set} | F4: Flow sensor bias fault | | F5: Supply air pressure fault | | | LEAK |
	Biased	Fault-free	Positive	Negative	Fault-free	
Positive	0.01	0	0.8	0	0	0.01
Negative	0.01	0	0	0.8	0	0.01
Within the threshold	0.98	1	0.2	0.2	1	0.98

9.2.3 DBN-Based Fault Detection and Diagnosis

The flow chart of the proposed DBN-based VAV terminal FDD strategy is illustrated in Figure 9.3.
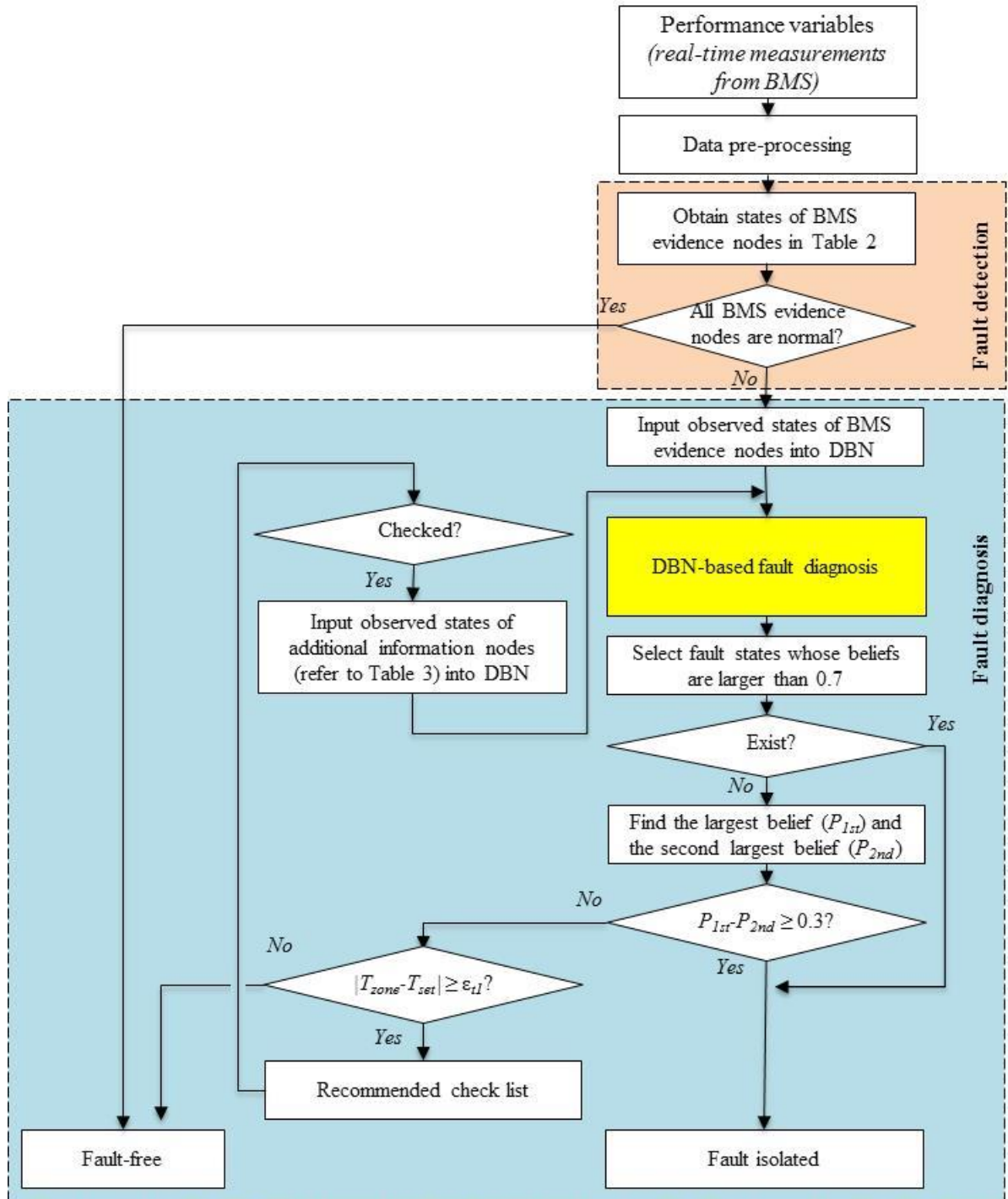
Figure 9.3 Flow chart of the DBN-based VAV terminal FDD strategy

The evidences from the BMS measurements are used firstly since they can usually be obtained conveniently from BMS. The real-time measurements are collected and stored in BMS. Then, the data are pre-processed to remove obvious outliers. The rules in Table 9.2 are used to determine the states of all BMS evidences nodes. If all of them are normal (i.e. w*ithin the threshold* or *Not frozen* as shown in Table 9.2), the VAV terminal is considered to be fault-free. If not all of the states are normal, fault is alarmed and fault diagnosis is conducted. All of the observed states of the BMS evidence nodes are inputted into the DBN. The probabilities of the observed states of nodes are set to be 1.0. The DBN calculates the believes (posterior probabilities) of each fault under inputted evidences. Usually, the larger the fault belief is, the higher the possibility of the corresponding fault is. To improve the robustness of the diagnosis, the following two rules are used to determine the FDD results in this study:

Rule A: if the largest fault belief is larger than 0.7, then the fault with the largest belief is reported; or,

Rule B: if the largest fault belief is 0.3 larger than the second largest one, then the fault with the largest probability is reported.

If the DBN inference results cannot meet either of the two rules, the zone temperature (T_{zone}) needs to be checked to see if it is maintained at its set-point (T_{set}). The VAV serving that zone is considered to be fault-free if T_{zone} is maintained at T_{set}. Otherwise, a recommended check list is generated according to the posterior probabilities of the additional information nodes. The states of the additional information nodes obtained by the manual tests are then inputted to the DBN as new evidences to infer the belief of the

suspected faults again and the actual fault can be successfully diagnosed. The recommended check list minimizes the manual tests needed and is a good guide for repairing works.

9.3 Evaluations of the DBN-Based VAV Terminal FDD Strategy

9.3.1 Descriptions of The Simulation Platform

A dynamic simulator of an office building VAV air-conditioning system built on the TRNSYS platform was used to evaluate the proposed DBN-based FDD strategy for VAV terminals. The prototype of the simulated VAV system comes from the typical floor of a forty-six commercial building located in Hong Kong (Wang, 1999). In the simulator, half of a floor is considered. It consists about 1166 m^2 floor office area which is divided into eight zones. It was served by a central AHU, 40 VAV terminals, and over a hundred air diffusers. The VAV terminals are pressure-independent type.

The PID control was used by the local DDC controllers. The pitch angel of the VAV supply (axial) fan is moderated to control the supply air statistic pressure. The return (axial) fan controls the exfiltration flow rate by maintaining the difference between the total supply and return air flow rates within threshold through moderating the pitch angle of return fan. Wang developed a simulation model to dynamically simulate the VAV air-conditioning system of the half of a floor using TRNSYS as platform (Wang, 1999), as shown in Figure 9.3. It includes simplified building model, duct model, fan model, cooling coil model, sensor and actuator models, DDC controller. A fluid flow rate and pressure calculation model was introduced to simulate the pressure-flow

balance. The model parameters were determined using manufacturer catalogues, and/or empirical correlations given in handbooks, and on-site performance data.

In the simulated system, a 'realistic' controller model was developed to simulate the DDC controllers representing the follow functions: DDC functions, discrete-time operation of digital controllers and supervisory control strategies. The time scheduling of a sampling cycle is considered to be four steps, i.e. process variable sampling, control outputs computation, control signal output, and waiting time for the next sampling cycle. The ISA algorithm was used in the PID control function in DDC loops. The actuator considered the hysteresis in the linkage between actuators and valves or dampers. The dynamics sensor model was used to simulate the temperature, pressure and flow using the time constant strategy.

The daily operation of the simulated air-conditioning system is from 7:45 to 20:00. The supply air temperature set-point is 13℃. The statistic pressure is 750 Pa. The chilled water temperature to cooling coil is 8℃. The zone temperature set point is 24°C. The weather data of a typical day in summer is selected as simulation conditions. In this study, the generally available measurements/parameters are selected to detect and diagnose faults, including: zone temperature sensor measurement, air flow meter measurement, air flow rate set-point, zone temperature set-point, maximum air flow rate and minimum air flow rate. Fault data were obtained through introducing the ten faults concerned into the simulated system.

9.3.2 Evaluations of The DBN-Based VAV Terminal FDD Strategy

9.3.2.1 Detecting and diagnosing the ten typical faults in VAV terminals

In this section, the performance of the DBN-based FDD strategy is evaluated using simulation tests. In each test, one of the ten typical faults is introduced to the simulator. In the simulator, the measurements are sampled at the interval of 5 minutes. The BBN inference is computationally efficient; therefore the DBN-based FDD is conducted on each sample. Table 9.7 gives the values of parameters needed in Table 9.1-9.3 for determining the states. Some parameters are obtained from design values, such as $\underline{F_{Max}}$, $\underline{F_{Min}}$, $\underline{P_{supply,set}}$, $\underline{T_{supply,set}}$, $\underline{T_{set}}$ and $T_{set,design}$. Some parameters are estimated according to the domain knowledge and experiences, such as ε_{Tset}, ε_{t2}, ε_{λ}, $\varepsilon_{Psupply}$ and $\varepsilon_{Tsupply}$. Some parameters are obtained using the *t*-statistic analysis with confidence level of 95.45%, such as $\underline{\varepsilon_F}$ and $\underline{\varepsilon_{t1}}$.

Table 9.7 Parameters used in the DBN-based FDD strategy

Parameter	Value	Parameter	Value
$\underline{F_{Max}}$	727 L/s	$\underline{\varepsilon_{t1}}$	0.18 K
$\underline{F_{Min}}$	170 L/s	ε_{t2}	2 K
$\underline{P_{supply,set}}$	700 Pa	$\underline{\varepsilon_F}$	34 L/s
$\underline{T_{supply,set}}$	13 °C	$\varepsilon_{Psupply}$	200 Pa
$\underline{T_{set}}$	24 °C	$\varepsilon_{Tsupply}$	4 K
ε_{Tset}	3 K	m	4

F1: Zone temperature sensor reading frozen

This fault is simulated by fixing the output of the dynamic sensor model in Zone 6 at 23°C, 24°C and 25°C respectively from 11:30 to 20:00. The VAV terminal is totally out

of control. The flow set-points obtained in the cascade control loop are fixed at the

minimum (frozen at 23℃), maximum (frozen at 25℃) and a small range at partial

position (frozen at set-point, 24℃) respectively. The FDD result of the zone temperature

sensor frozen at 25°C is shown in Figure 9.4.
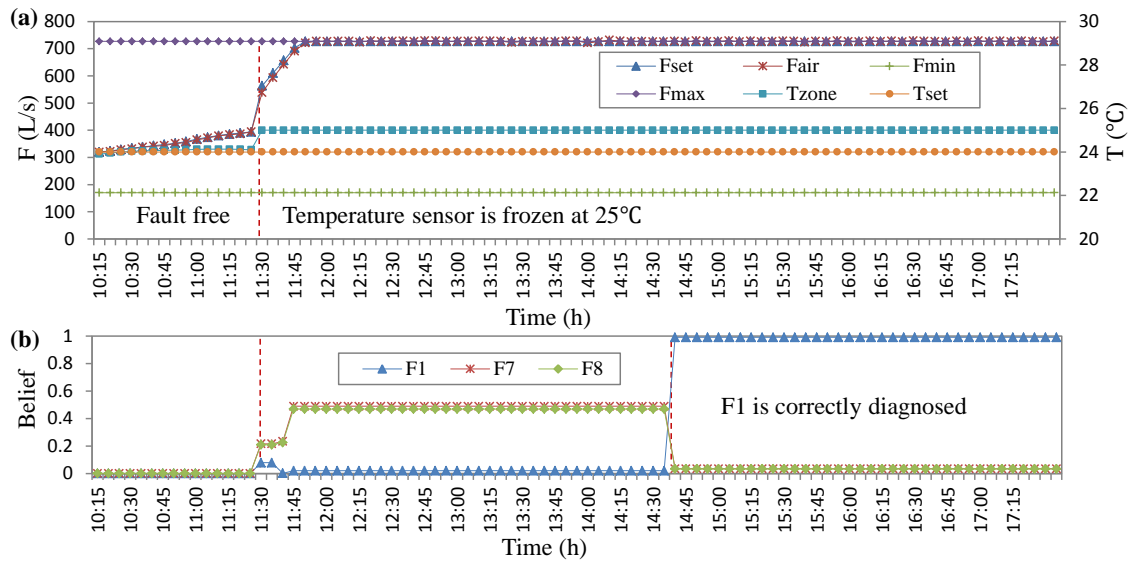
Figure 9.4 Temperature sensor reading is frozen at 25℃ from 11:30 in zone 6.

(a) Behaviour of the VAV terminal ; (b) FDD results.

The behavior of the VAV terminal when the zone temperature reading is frozen at 25℃

is as shown in Figure 9.4(a). The top 3 suspected faults inferred by the DBN are shown

in Figure 9.4(b). The fault is successfully detected by E12 three hours later and then

diagnosed with a belief of 1.00 (at 14:35). Probabilities of the other two most suspected

faults are obviously lower, i.e. 0.11 for F2 and 0.06for F4. When zone temperature

reading frozen at 22℃, the FDD results are similar.

When the zone temperature reading is frozen at the set-point, i.e.24℃, the fault

symptoms are similar to those of the flow sensor reading frozen fault (F2). It could not

be distinguished until the *Positive frozen* state of E12 is observed 3 hours later, or E11 was observed 0.5 hour after the system is shut down.

F2: VAV flow sensor reading frozen

This fault is simulated by fixing the flow sensor reading of the VAV terminal in Zone 6 at 402 L/s (corresponding to 52% opening position) from 11:30 to 20:00. The behavior of the VAV terminal is shown in Figure 9.5(a). The VAV terminal control loop oscillates when this fault exists. The zone temperature oscillates around the set-point within a small range. The FDD results (top 3 suspected faults) are shown in Figure 9.5(b). This fault is correctly diagnosed at belief of 0.75 from 14:45.
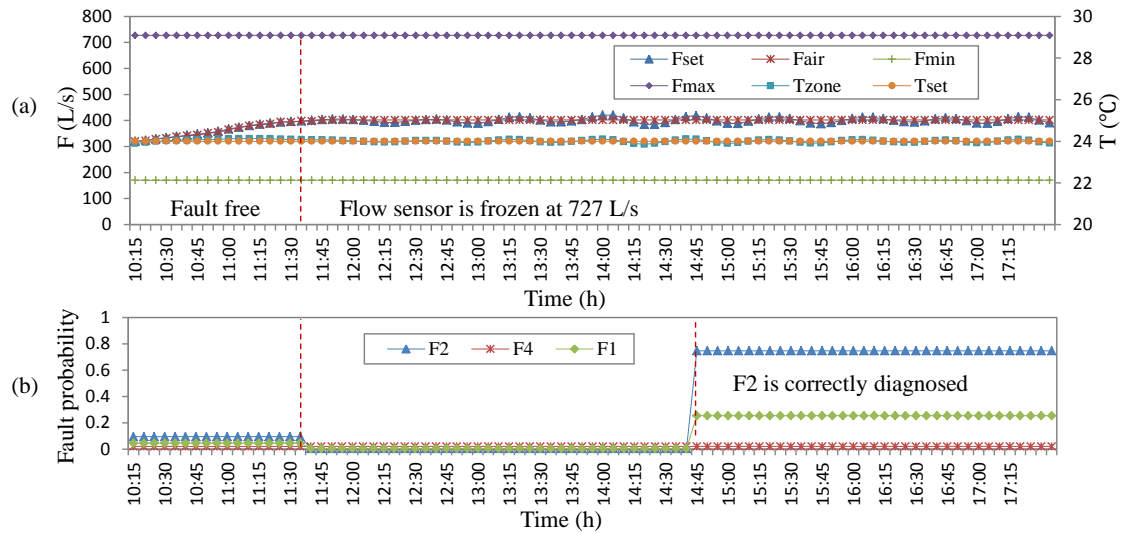
Figure 9.5 VAV flow sensor reading is frozen at 402 L/s at 11:35 in zone 6. (a) Behavior of the VAV terminal ; (b) FDD results.

F3: VAV damper stuck

This fault is introduced to the simulator by fixing the control signal of the VAV damper in Zone 6 at 40% from 11:35 to 20:00. The behavior of the VAV terminal is shown in Figure 9.6(a). The VAV terminal controller does not have the ability to actively control the air flow rate. The FDD results are shown in Figure 9.6(b). This fault is successfully diagnosed from 14:35 at belief of 1.00.
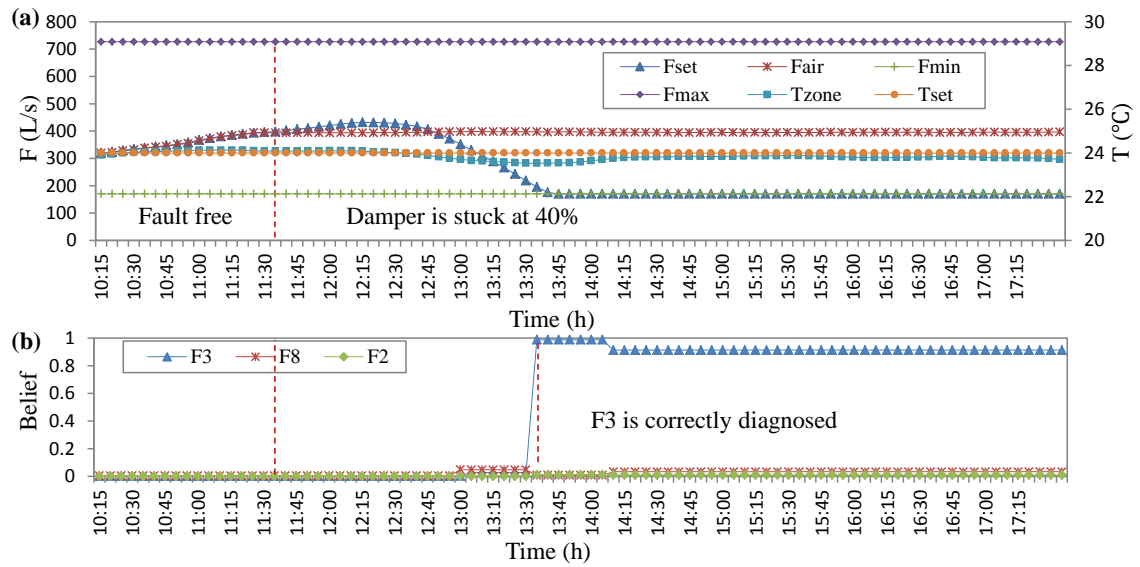
Figure 9.6 VAV damper is stuck at 40%

(a) Behaviour of the VAV terminal; (b) FDD results

F4: Flow sensor reading deviation to maximum/minimum
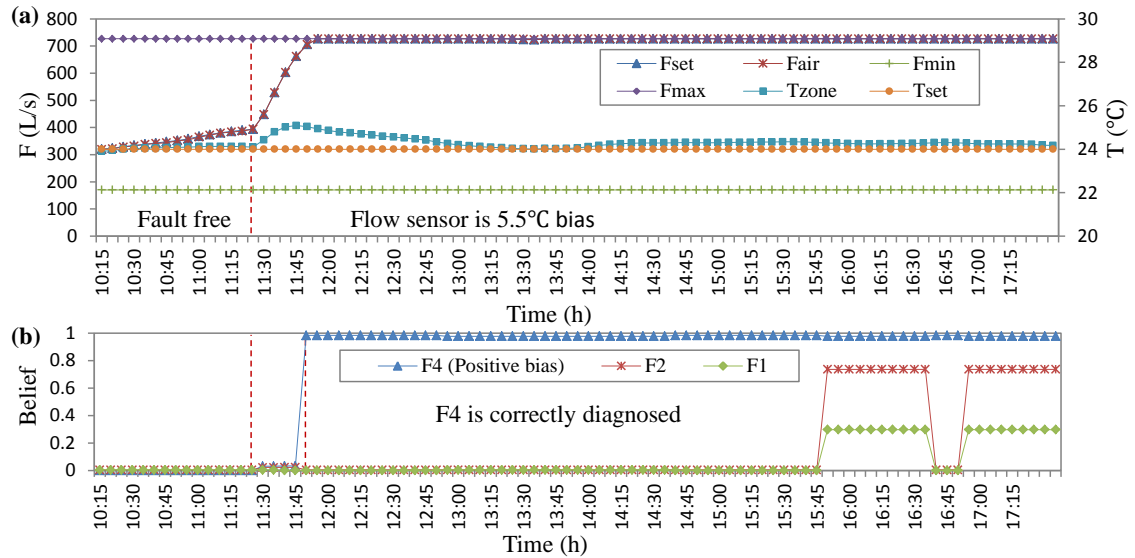
Figure 9.7 VAV flow sensor is 464 L/s bias

(a) Measured VAV terminal performance; (b) FDD results

This fault is introduced to the simulator adding 464 L/s (64% of F_{max}) bias at the flow sensor reading of VAV terminal in Zone 6 from 11:20. The behavior of the VAV terminal is shown in 10.7(a). The control process is ruined. It is correctly diagnosed from 11:45 when the air flow set-point is at maximum and zone temperature raised, as shown in Figure 9.7(b).

F5: Supply air temperature is too high/low, and F6: Supply air pressure is too high/low

Both F5 and F6 are diagnosed easily through comparing supply air temperature/pressure measurement from BMS with its set-point respectively. Both faults are removed at the beginning of FDD.

F7: VAV terminal under capacity, and F8: Extreme high cooling load

Both faults have same symptoms. They are introduced to the simulator by increasing cooling load to be 1.5 times higher from 11:30 to 20:00. The behavior of the VAV terminal is shown in Figure 9.8(a). Four scenarios (A, B, C and D as shown in Figure 9.8) are considered, and each scenario adopts different evidences from the BMS evidence nodes and additional information nodes. In period A, only evidences of all BMS evidence nodes are observed and inputted to DBN. The information is incomplete to isolate the faults. In additional to the observed BMS evidence nodes, extra evidences from additional information nodes are added in periods B, C and D respectively to demonstrate how additional information can help to distinguish the two faults.
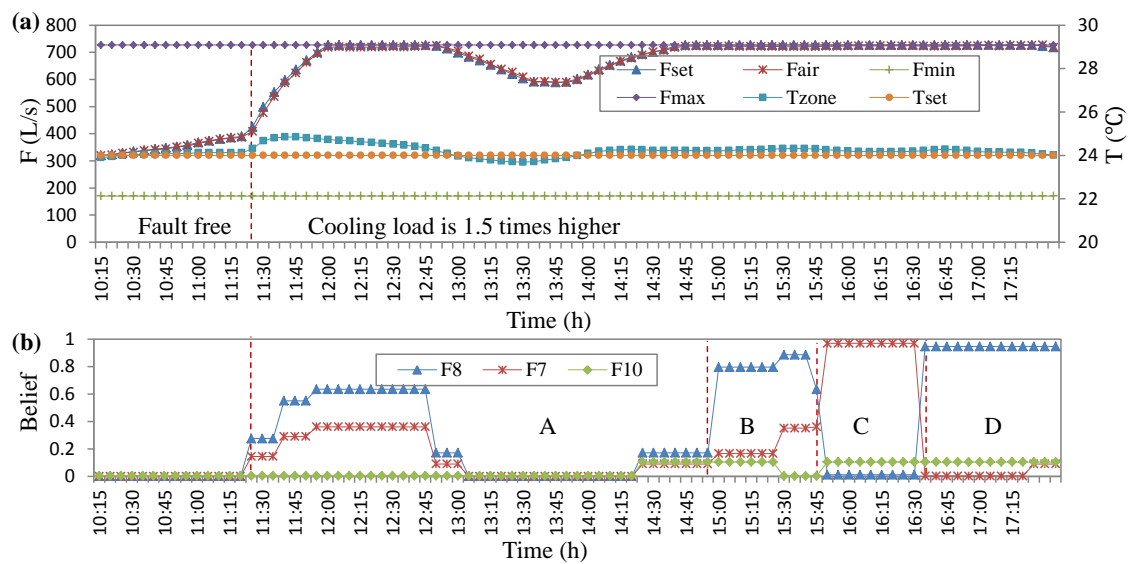
A: Only use evidence from BMS symptom nodes; B: M5 = *No*, M6= *Very hot*;
C: M5 = *Yes;* D: M5 = *No*, M7= *Too many*

Figure 9.8 Cooling load is 1.5 times higher.

(a) Measured VAV terminal performance; (b) FDD results.

In period A, both faults have low believes. In period B, two extra evidences are added, i.e. M5=*No* (the under capacity fault was not found in history) and M6= *Extremely hot* (the weather was very hot). The fault probability of F8 increases to 0.89,

and that of F7 reduces to 0.35. F8 is correctly diagnosed. In period C, one extra evidence is added while evidences from part B are removed, i.e., M5=*Yes* (the under capacity fault was found in history). The fault probability of F7 increases to 0.97, and that of F8 reduces to 0.02. In part D, two extra evidences are added while evidences from part B and C are removed, i.e. M5=*No* (the under capacity fault is not found in history) and M7=*Too many* (there are too many occupants in the zone). The fault probability of F8 increases to 0.95, and that of F7 reduces to 0.02. The evidences from additional information nodes are helpful to distinguish the two faults.

F9: Zone temperature sensor bias and F10: Zone temperature set-point is higher/lower

These two faults Zone temperature sensor bias (F9) would not affect the zone temperature control if it is compensated by resetting the zone temperature set-point (F10). Therefore, the root reason might be F9 if F10 is diagnosed. If zone temperature set-point is not reset, F9 might not be detected only using the system characteristics. However, occupants would complain (M8) since the actual zone temperature leads to discomfort.
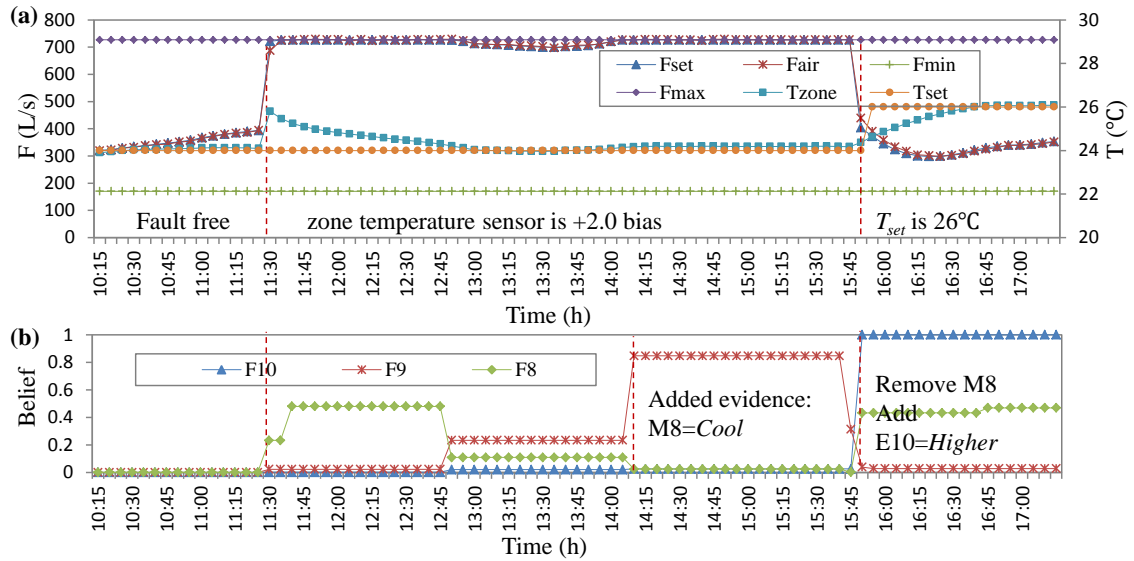
Figure 9.9 Zone temperature sensor is +2.0 ℃ bias.

(a) Measured VAV terminal performance; (b) FDD results.

F9 is conducted from 11:30 as shown in Figure 9.9(a) and 9.9(b). The VAV terminal adjusts F_{set} to maintain measured zone temperature T_{zone} to be T_{set}. There is no fault detected. M8=*Cool* is added to represent occupant complaint from 14:10 to 15:50. F9 is diagnosed at 85% probability. T_{set} is set to 26℃ from 15:50 to 20:00. M8 is removed, and E10= *Positive* is added. F10 is diagnosed at belief of 1.00. Fault probability of F9 reduces to 0.00.

In summary, all typical faults have been correctly diagnosed. The fault diagnosis is mainly based on BMS evidence nodes. Seven faults (F1-F6, and F10) can be diagnosed by only using BMS evidence nodes. The additional information nodes are helpful when faults cannot be isolated. The remainder three faults (F7, F8 and F9) can be diagnosed with the help of additional information nodes, i.e. VAV terminal under capacity, extreme high cooling load and zone temperature sensor bias. The evidences of these additional information nodes are easily to be obtained.

202

9.3.2.2 FDD results considering incomplete information

Two cases (F3 and F4 as presented in Section 4.1) are elaborated in detail to show how the DBN-based FDD strategy works when only incomplete information is available. In each case, a new piece of evidence is added at a step. The DBN infers the fault probabilities under current available evidences (ψ). The top three suspected faults in each step are listed as shown in the last column of Table 9.8 and Table 9.9. It can be found that the more evidences are inputted, the more accurate the FDD results would be.

Table 9.8 Fault diagnosis results considering incomplete information - Case-1

Step	Added evidence	Top three suspected faults
Step 1	E1=*Fairly positive*	P(F1=*Larger*|ψ) = 0.17, P(F2=*Present*|ψ) = 0.14, P(F4=*Max*|ψ) = 0.10
Step 2	E2=*Negative*	P(F5=*Low*|ψ) = 0.45, *P(F3=Lower*|ψ) = 0.37, P(F10=*Higher*|ψ) = 0.12
Step 3	E3=*Max value*	P(F5=*Low*|ψ) = 0.49, *P(F3=Lower*|ψ) =0.44, P(F10=*Higher*|ψ) = 0.14
Step 4	E8=*Within threshold*	P(F3=Lower|ψ) = 0.81, P(F10=*Higher*|ψ) = 0.17, P(F9=*Positive*|ψ) = 0.13

Case-1 aims to diagnose F3 (damper stuck), as shown in Table 10.8. In Step 1, Step 2 and Step 3, the evidences are insufficient to isolate this fault. F5 and F3 are the most suspected faults. In Step 4, E9=*Within threshold* does not support F5. The fault probability of F3 increases to 0.81. F3 is confirmed to be the root fault.

203

Table 9.9 Fault diagnosis results considering incomplete information - Case-2

Step	Added evidence	Top three suspected faults
Step 1	E1= *Fairly negative*	$P(F10=Higher|\psi) = 0.34$, $P(F9=Positive|\psi) = 0.29$, $P(F4=Min|\psi) = 0.14$
Step 2	E2=*Within threshold*	$P(F10=Higher|\psi) = 0.44$, $P(F9= Positive|\psi) = 0.39$, $P(F4=Min|\psi) = 0.19$
Step 3	E3=*Min value*	$P(F4=Min|\psi) = 0.38$, $P(F1=Lower|\psi) = 0.29$, $P(F6=Lower|\psi) = 0.19$
Step 4	E4=*Not frozen*	$P(F4=Min|\psi) = 0.38$, $P(F1=Lower|\psi) = 0.29$, $P(F6=Lower|\psi) = 0.19$
Step 5	M4=*No*	$P(F4=Min|\psi) = 0.69$, $P(F8=Too low|\psi) = 0.15$, $P(F6=Lower|\psi) = 0.07$

Case-2 aims to diagnose F4 (Flow sensor bias), as shown in Table 9.9. From Step 3 to Step 5, F4 is the most suspected fault. However, it could not be distinguished because its fault probability is not obviously higher than those of other faults. In Step 5, the belief of F4 increases to 0.69. F4 is confirmed to be root fault.

9.3.3 Sensitivity analysis

The prior probabilities of faults and conditional probabilities are very important to the fault diagnosis. However, the experts' estimations are subjective to some extent. For example, when FDD experts consider the probability of a fault at given symptom is low, they may assign 0.02, 0.05, 0.06 or others to the probability. Therefore, this section aims to analyze the sensitivity of the DBN-based FDD strategy to the pre-assigned probabilities.

9.3.3.1 Sensitivities analysis of prior probabilities

To analyze the sensitivities of the DBN-based strategy to prior probabilities of faults, different values are assigned to the prior probabilities to test the performance of the

DBN-based strategy. Case-3 is made in the same way as Case-1. In this case, the prior probabilities of all fault states of *F3* in the DBN are doubled, e.g. from 0.04 to 0.08; and the prior probabilities of *Fault-free* changes to 84% accordingly. The results are shown in Table 9.10. At each step, the list of top three suspected faults does not changed significantly. *F3* can still be diagnosed correctly. It is found that the fault diagnosis performance of the DBN-based strategy is more sensitive to the qualitative relationships among prior probabilities of faults than prior probabilities themself. The qualitative relationship is that the prior probability of one fault is larger/smaller than or equal to the prior probability of another fault. FDD experts usually have common views on this kind of large or small probabilities even though they may assign different values to them.

Table 9.10 Fault diagnosis results in Case-3

Step	Added evidence	Top three suspected faults
Step 1	E1=*Fairly positive*	$P(F2=Present|\psi) = 0.25$, $P(F1=Larger|\psi) = 0.19$, $P(F4=Max|\psi) = 0.12$
Step 2	E2=*Negative*	$P(F5=Low|\psi) = 0.48$, $P(F3=Lower|\psi) = 0.41$, $P(F2=Present|\psi) = 0.22$
Step 3	E3=*Max value*	$P(F5=Low|\psi) = 0.50$, $P(F3=Lower|\psi) = 0.45$, $P(F2=Present|\psi) = 0.22$
Step 4	E8=*Within threshold*	$P(F3=Lower|\psi) = 0.80$, $P(F2=Present|\psi) = 0.22$, $P(F10=Higher|\psi) = 0.21$

9.3.3.2 Sensitivities of conditional probabilities

Case-4 and Case-5 aim to evaluate the fault diagnosis performance when conditional probabilities among faults and symptoms are in the Boolean format. Case-4 is made in the same way as Case-1, and Case-5 is made in the same way as Case-2 in Section 4.2. The results are shown in Table 9.11 and Table 9.12 respectively. The results at each step

are not changed significantly compared with Table 9.8 of Case-1 and Table 9.9 of Case-2. Both faults are correctly diagnosed at higher believes than those in Case-1 and Case-2.

Table 9.11 Fault diagnosis results in Case-4

Step	Added evidence	Top three suspected faults
Step 1	E1=*Fairly positive*	P(F1=*Larger*|ψ) = 0.20, P(F4=*Max*|ψ) = 0.13, P(F6=*Higher*|ψ) = 0.13
Step 2	E2=*Negative*	P(F3=*Lower*|ψ) = 0.52, P(F5=*Low*|ψ) = 0.51, P(F2=*Present*|ψ) = 0.12
Step 3	E3=*Max value*	P(F3=*Lower*|ψ) = 0.52, P(F5=*Low*|ψ) = 0.51, P(F2=*Present*|ψ) = 0.12
Step 4	E8=*Within threshold*	P(F3=*Lower*|ψ) = 1.00, P(F2=*Present*|ψ) = 0.12, P(F10=*Higher*|ψ) = 0.11

Table 9.12 Fault diagnosis results in Case-5

Step	Added evidence	Top three suspected faults
Step 1	E1= *Fairly negative*	P(F9=*Positive*|ψ) = 0.43, P(F10=*Higher*|ψ) = 0.31, P(F4=*Min*|ψ) = 0.20
Step 2	E2=*Within threshold*	P(F57=*Positive*|ψ) = 0.43, P(F10=*Higher*|ψ) = 0.41, P(F4=*Min*|ψ) = 0.27
Step 3	E3=*Min value*	P(F4=*Min*|ψ) = 0.59, P(F6=Lower|ψ) = 0.29, P(F2=*Present*|ψ) = 0.12
Step 4	E4=*Not frozen*	P(F4=*Min*|ψ) = 0.59, P(F6=*Lower*|ψ) =0.29, P(F5=*Too high*|ψ) = 0.06
Step 5	M4=*No*	P(F4=*Min*|ψ) = 0.75, P(F8=*Too low*|ψ) = 0.15, P(F6=*Lower*|ψ) = 0.07

Table 9.13 Conditional probability table between F1 and E11 for Case-6

E11	F1: T_{zone} reading is frozen			
	Positive frozen	*Negative frozen*	*Frozen at set-point*	*Fault free*
Frozen	1	1	1	0
No frozen	0	0	0	1

Table 9.14 Conditional probability table between F1 and E12 for Case-6

| E12 | F1: T_{zone} reading is frozen | | | |
	Positive frozen	Negative frozen	Frozen at set-point	Fault free
Positive frozen	1	0	0	0
Negative frozen	0	1	0	0
Frozen at set-point	0	0	1	0
Not frozen	0	0	0	1

Case-6 aims to show the benefits of using probabilities. As shown in Figure 9.3, *F1* has casual relationships with *E11* and *E12*. Using parameters in Table 9.5 and Table 9.6, the belief of *F1* at *Fault-free* is 0.96 when *E11* is *frozen* and *E12* is *Not frozen*. T_{zone} reading is possible to be frozen for 0.5 hours in the power OFF period when this sensor is not frozen. If the conditional probabilities are Boolean type (0 and 1) as shown in Table 9.13 and Table 9.14, the belief of *F1* at *Fault-free* is 0.0 when *E12* is *Not frozen*. In such condition, it is impossible to set *frozen* in *E11* to be observed since the belief of *E12* at *Not frozen* is 0 (in the BBN, if the probability of state is 0, it means that such state never occurs. So, it will never be observed). The DBN can be robust if the uncertainties are considered in conditional probabilities. It also shows the information fusion capacity of the DBN using conflicting evidences.

Case-4 and Case-5 show that the conditional probabilities can be in the Boolean format if it is very difficult to estimate them. In such situation, the DBN-based FDD method works like the *if...then...* rule-based methods and fault tree-based methods. The major difference is that the DBN might still work well when information is incomplete; however, the rule-based methods and fault tree-based methods hardly work properly in such condition.

9.4. Summary

This chapter presents a robust DBN-based FDD strategy based on probability analysis and graph theory for VAV terminals. The strategy is evaluated using simulation tests where ten typical faults of VAV terminal are introduced. All faults are correctly diagnosed with high believes.

The prior probabilities and the conditional probabilities need to be assigned by the experts, which may be subjective to some extent. This study also analyzes the sensitivities of the DBN-based FDD strategy to the pre-assigned probabilities. The results show that small variations in the probabilities will not change the FDD results so long as the qualitative probability relationships between the states of one node (prior probabilities) or between the faults and symptoms (conditional probabilities) are correct, i.e. assign a large value to the high probability event and assign a small value to the low probability event.

The DBN-based strategy is tolerant with various uncertainties, such as measurement noises, considering that uncertainties are usually low probability events. The DBN is applicable to VAV terminals of the same type because it is developed based on the intrinsic relationships between faults and symptoms. The DBN-based strategy can be used for on-line and off-line FDD of VAV terminals.

CHAPTER 10 CONCLUSIONS AND

RECOMMENDATIONS

FDD tools are essential for reliable indoor environment control, saving maintenance efforts, and eliminating the associated energy waste. The aim of this PhD project is to develop enhanced and reliable FDD methods for HVAC systems in buildings. This chapter presents the main contributions of this thesis in *Section 10.1*, summary of performance of the proposed four methods in *Section 10.2*, and recommendations for further works in *Section 10.3*.

10.1 Main Contributions

The main contributions of this thesis are summarized as follows:

i. A simplified model-based FDD method with its customization tool is proposed to identify model parameters using limited training data, and then to generate benchmarks for fault detection using the calibrated models. It is preferable when there are limited fault-free data to train models.

ii. An enhanced statistical FDD method is proposed to improve the performance of conventional gray-box model-based FDD methods for the detection and diagnosis of incipient faults. Support vector regression (SVR) algorithm is adopted to improve accuracies of reference PI models. Exponentially-weighted moving average (EWMA) control charts are introduced to reduce the Type II error ratios. It is preferable when residuals are generated to detect and diagnose faults.

iii. A pattern recognition-based FDD method is proposed using support vector data description (SVDD) algorithm which transforms the FDD problem as a typical one-class classification problem. It shows some advantages to the available pattern recognition-based FDD methods in HVAC field. This method has some new potential applications. It is preferable when fault data are available.

iv. Diagnostic Bayesian networks (DBNs) are proposed for chiller FDD and VAV terminal FDD. The DBN-based FDD method benefits to simulate the diagnostic thinking and diagnosis process of HVAC experts mathematically. It is effective in diagnosing faults based on uncertain, incomplete and conflicting information.

10.2 Performance of The Proposed FDD Methods

10.2.1 The Simplified Mode-Based Method with Its Customization Tool

A customization tool was developed based on a simplified physical chiller model in order to identify the unknown chiller parameters. Evaluations are made on water-cooled centrifugal chiller as described in ASHRAE RP-1043. The customization model can be trained using limited measurements and has good performance in prediction. The ASHRAE RP-1043 data were used to validate the proposed method and made qualitative comparisons with the four typical FDD methods studied in the ASHRAE RP-1275. The test results show that the proposed method is capable of detecting and diagnosing the non-condensable gas (successfully ratios were 100% at each severity level) and refrigerant overcharge (22%, 37%, 93% and 100% for SL-1, SL-2, SL-3 and SL-4). Although the performances are not perfect for the refrigerant leakage (15%, 19%,

81% and 89% for SL-1 to SL-4) and condenser fouling (4%, 4%, 22% and 74% for SL-1 to SL-4), it is still better than most of the four referred typical FDD methods.

10.2.2 The Incipient Fault Detection and Diagnosis Method

An enhanced chiller FDD strategy is proposed as an improvement of conventional gray-box model-based chiller FDD method. Evaluations are made on the chiller as described in ASHRAE RP-1043. It is found that the proposed strategy improves the FDD performances significantly, especially at low severity levels. For example, in the case of condenser fouling, the proposed strategy achieves the ratios of correctly diagnosed points of 7.7%, 45.2%, 60.7% and 100.0% at four severity levels (SL-1 to SL-4) respectively at the confidence level of 99.73%. Using the conventional gray-box model-based strategy, this fault could not be correctly diagnosed at level SL-1, SL-2 and SL-3. Significant improvements can also be found in the cases of other two typical faults (refrigerant leakage and refrigerant overcharge). Other three faults (i.e. non-condensable gas, reduced evaporator water flow rate and reduced condenser water flow rate) can be easily diagnosed similarly as the conventional gray-box model-based.

A system-level incipient fault detection strategy is proposed. Evaluations are made on a simulated commercial building at four severity levels and two uncertainty levels. The proposed strategy improves the fault detection performance significantly especially when incipient faults are concerned. At SL-1 and UL-2, the fault detection ratios are 56% and 90% (cooling tower fault), 38% and 77% (chiller fault), 5% and 36% (heat exchanger fault) using the conventional gray-box model-based strategy and the proposed

strategy respectively. The SVR-EWMA-based strategy achieves much higher fault detection ratio compared with the conventional gray-box model-based methods.

10.2.3 The SVDD-Based Method

The SVDD-based method is validated using experimental data of seven typical chiller faults from RP-1043. The fault-free SVDD model correctly identifies 99.5% fault-free data. It has good fault detection performance. The fault SVDD models correctly identify more than 90% data of their own classes. They also correctly reject most data of other classes.

Compared with the existing FDD methods which use multi-class classification algorithms, the SVDD-based method is robust when the process data do not belong to any class involved in training. In such case, the SVM-based method could not report any correct FDD result. For instance, 94% data of excess oil is diagnosed to be refrigerant leakage when the fault data of excess oil are not involved in training. Using the SVDD-based method, this fault is detected correctly but not diagnosed. The false FDD report is avoided.

Compared with the PCA-based method, the SVDD-based method has no Gaussian assumption and is effective for nonlinear process modeling. That results in more powerful capacity in describing process data. The fault detection ratios are improved significantly. For instance, using the PCA-based method, fault detection ratios are 64%, 36%, 14% and 28% for refrigerant overcharge, refrigerant leakage, reduced evaporator water flow rate and reduced condenser water flow rate respectively at SL-1. Using the SVDD-based method, the ratios increase to 95%, 74%, 52% and 85% respectively.

212

Compared with model-based and rule-based FDD methods, SVDD-based method has much higher FDD ratios, particularly at low fault severity levels, where those FDD methods usually do not work well. For instance, using the MLR and t-statistic-based method, the ratios of correctly diagnosed points were 3.7%, 0%, 0% at SL-1 and 7.4%, 0%, 0% at SL-2 for refrigerant leakage, condenser fouling and excess respectively. Using SVDD-based method, such ratios are all increased to over 90% at both severity levels.

10.2.4 The DBN-Based FDD Method

The DBN-based FDD method is evaluated on a chiller, an AHU and VAV terminals respectively. It shows advantages compared with conventional FDD methods.

A DBN is developed to detect and diagnose component faults on a 90-ton water-cooled centrifugal chiller as described in ASHRAE RP-1043. Only using BMS measurements, the DBN has similar accuracy as rule-based chiller FDD methods when BMS measurements are complete. If BMS measurements are incomplete, the DBN still provides meaningful fault believes, while the rule-based chiller FDD methods fail to work. The diagnosis ratios increase if evidences of nodes in additional information layer are used. Refrigerant overcharge and non-considerable gas can be correctly diagnosed with the help of evidences of nodes in additional information layer.

Similarly, a group of DBNs are developed to detect and diagnose typical device faults and sensor faults in the air side of a typical single duct dual fan AHU of variable air volume as described in ASHRAE RP-1312 final report. Evaluations are made using experimental data in RP-1312 report. The DBNs enhance the fault diagnosis capacity

significantly. They provide plausible expect fault list with their believes when information is incomplete.

A DBN is developed to detect and diagnose faults of the pressure independent VAV terminals in an office building located in Hong Kong. It is evaluated through conducting the ten typical VAV terminal faults on a dynamic simulation platform of an office building. All faults are correctly diagnosed at high confidences.

10.3 Recommendations for Future Work

Major efforts of this PhD project are made on the development of enhanced and new FDD methods. It would be very desirable and valuable to make further efforts on the following aspects related to the research presented in this thesis:

i. DBN is an effective mathematical tool to erase gaps among methods of different natures. Therefore, it is possible to be a framework to merge the other three methods proposed in this thesis. For instance, the incipient fault detection method can enhance the sensitivities of some BMS evidence nodes (also see *Section 3.4.2.1*). New BMS evidence nodes can be added into DBNs to represent evidences which are found by the SVDD-based FDD method.

ii. On the basis of available evidences, DBN can provide a list of suspected faults in descending order of fault belief, as well as a list of additional information nodes for check in descending order of necessary. Therefore, it is possible to develop FDD assistants based on the proposed DBNs in this thesis to help users to find root faults of devices efficiently. For instance, a chiller FDD assistant can be developed using both DBN and the simplified model-based FDD method with its customization tool.

iii. The proposed methods mainly adopt diagnostic information of the components concerned. Actually, the measurements in the systems/subsystems might also be helpful for FDD. For instance, the health status of cooling water pumps is significant to the fault of reduced condenser water flow rate. It is suggested to develop bottom-to-up system-level FDD solutions based on component FDD methods.

REFERENCES

Andreassen, S., M. Woldbye, B. Falck and S. Andersen. 1987. MUNIN - A causal probabilistic network for interpretation of electromyographic findings. Proceedings of 10th International Joint Conference on Artificial Intelligence, Milan, Italy.

Bailey, M.B. 1998. The design and viability of a probabilistic fault detection and diagnosis method for vapor compression cycle equipment. PhD thesis, School of Civil Engineering, University of Colorado, Boulder.

Beinlich, I., H. Suermondt, R. Chavez and G. Cooper. 1989. The ALARM monitoring system: A case study with two probabilistic inference techniques for belief networks. Proceedings of the Second European Conference on Artificial Intelligence, Berlin. Springer-Verlag.

Bendapudi, S. 2004. Development and Evaluation of Modelling Approaches for Transients in Centrifugal Chillers, Ph.D. thesis, School of Mechanical Engineering, Purdue University, West Lafayette, IN.

Bourdouxhe, J.P., M. Grodent and J. Lebrun. 1999. HVAC1 Toolkit- A Toolkit for Primary HVAC System Energy Calculations, American Society of Heating, Refrigerating and Air-conditioning Engineers, Atlanta, GA.

Brambley, M.R., K.A. Cort, J.K Goddard, N. Fernandez, H. Cho, W. Wang and H. Ngo. 2011. Final Project Report: Self-Correcting Controls for VAV System Faults Filter/Fan/Coil and VAV Box Sections. Pacific Northwest National Laboratory.

Chang, C.C. and C.J. Lin. 2011. LIBSVM : a library for support vector machines. ACM Transactions on Intelligent Systems and Technology, 2:27:1--27:27. Software available at http://www.csie.ntu.edu.tw/~cjlin/libsvm

Chen, B. and J.E. Braun. 2001. Simple rule-based methods for fault detection and diagnostics applied to packaged air conditioners, ASHRAE Trans. 107 (1): 847–57.

Chen, Y.M. and L.L. Lan. 2009. A fault detection technique for air-source heat pump water chiller/heaters. Energy Build 41: 881-887.

Cho, H.W., M.K. Jeong and Y. Kwon. 2006. Support vector data description for calibration monitoring of remotely located microrobotic system. Journal of Manufacturing Systems 25:196–208.

Cibse, G.H., 2000. Buiding control systems, Butterworth-Heinemann, Oxford.

Claridge, D.E, C.H. Culp, M. Liu, S. Deng, W.D. Turner and J.S. Haberl. 2000. Campus Wide Continuous Commissioning SM of University Buildings. The 2000 ACEEE Summer Study. Washington, D.C.: American Council for an Energy Efficient Economy.

Comstock, M.C., and J.E. Braun. 1999a. Development of analysis tools for the evaluation of fault detection and diagnostics in chillers, ASHRAE Research Project 1043-RP. Report # HL 99-20. Purdue University, Ray W. Herrick Laboratories, West Lafayette, IN.

Comstock, M.C., and J.E. Braun. 1999b. Experimental data from fault detection and diagnostic studies on a centrifugal chiller, ASHRAE Research Project 1043-RP. Report # HL 99-18. Purdue University, Ray W. Herrick Laboratories.

Comstock, M. C., J. E. Braun and E. A. Groll. 2002. A survey of common faults for chillers. ASHRAE Transactions 108 (1):819-825.

Comstock, M.C. and J.E. Braun. 2002. Fault detection and diagnostic (FDD) requirements and evaluation tools for chillers, ASHRAE 1043-RP, Purdue University.

Cristianini, N. and J. Shawe-Taylor. 2000. An introduction to support vector machines and other kernel-based learning methods. Cambridge University Press, Cambridge, UK.

Cui, J.T. and S.W. Wang. 2005. A Model-Based Online Fault Detection and Diagnosis Strategy for Centrifugal Chiller Systems. International Journal of Thermal Sciences 44 (10): 986-999.

Dexter, A., and J. Pakanen. 2001. Fault detection and diagnosis methods in real buildings. International Energy Agency, Energy Conservation in Buildings and Community Systems, Annex 34: Computer-aided evaluation of HVAC system performance.

Druzdzel, M.J. 1999. SMILE: Structural Modeling, Inference, and Learning Engine and GeNIe: A development environment for graphical decision-theoretic models (Intelligent Systems Demonstration). In Proceedings of the Sixteenth National Conference on Artificial Intelligence (AAAI-99), pages 902-903, AAAI Press/The MIT Press, Menlo Park, CA, download at http://genie.sis.pitt.edu.

Du, Z.M. and X.Q. Jin. 2007. Detection and diagnosis for sensor fault in HVAC systems. Energy Conversion and Management 48(3): 693-702.

Du, Z.M. and X.Q. Jin 2008. Multiple faults diagnosis for sensors in air handling unit using Fisher discriminant analysis, Energy Conversion and Management 49(12): 3654-3665.

Du, Z.M., X.Q. Jin and L.Z. Wu. 2007a. Fault detection and diagnosis based on improved PCA with JAA method in VAV systems. Building Environment 42:3221–3232.

Du, Z.M., X.Q. Jin and X.B. Yang. 2009a. A fault diagnosis for temperature, flow rate and pressure sensors in VAV systems using wavelet neural network. Applied Energy 86:1624–1631.

Du, Z.M., X.Q. Jin and X.B. Yang. 2009b. A robot fault diagnostic tool for flow rate sensors in air dampers and VAV terminals. Energy and Buildings 41 (2009) 279–286.

Du, Z.M., X.Q. Jin and L. Wu. 2007b. Fault detection and diagnosis based on improved PCA with JAA method in VAV systems. Building and Environment 42: 3221–3232.

EMSD, Hong Kong energy end-use data. 2008. The Energy Efficiency Office, Electrical & Mechanical Services Department, Hong Kong.

Esen, H., M. Inalli, A. Sengur and M. Esen. 2008. Modeling a ground-coupled heat pump system by a support vector machine. Renewable Energy 33: 1814–1823.

Fan, B., Z.M. Du, X.Q. Jin, X. Yang and Y. Guo. 2010. A hybrid FDD strategy for local system of AHU based on artificial neural network and wavelet analysis. Building and Environment 45: 2698–2708.

Fisher Box, J. 1987. Guinness, Gosset, Fisher, and Small Samples. Statistical Science 2 (1): 45–52.

Garey, V.P. 1992. Liquid-vapour phase-change phenomena. New York: Hemisphere.

Ge, Z.Q., F.R. Gao and Z.H. Song. 2011. Batch process monitoring based on support vector data description method. Journal of Process Control 21:949–959.

Grace, I., D. Datta and S. Tassou. 2005. Sensitivity of refrigerate system performance to charge levels and parameters for on-line leak detection. Applied Thermal Engineering 25:557-566.

Grimmelius, H.T., J.K. Woud, and G. Been. 1995. On-line failure diagnosis for compression refrigeration plants. International Journal of Refrigeration 18(1):31–41.

Han, H., Z.K. Cao, B. Gu and N. Ren. 2012. PCA-SVM-based automated fault detection and diagnosis (AFDD) for vapor-compression refrigeration systems. HVAC&R Research 16:295-313.

House, J.M., H. Vaezi-Nejad and J.M. Whitcomb. 2001. An expert rule set for fault detection in air-handling units, ASHRAE Transactions 107 (1): 858-871.

House, J.M., W.Y. Lee and D.R. Shin. 1999. Classification techniques for fault detection and diagnosis of an air-handling unit. ASHRAE Transactions 105(1): 1987-1997.

Hsu, C.W., C.C. Chang and C.J. Lin. 2003. A practical guide to support vector classification. Technical report, Department of Computer Science, National Taiwan University.

Jaynes, E. T. 2003. Probability Theory: The Logic of Science. Cambridge University Press.

Jia, Y.Z., and T.A. Reddy. 2003. Characteristic physical parameter approach to modeling chillers suitable for fault detection, diagnosis, and evaluation. Journal of Solar Energy Engineering, Transactions of the ASME 125(3):258–65.

Kang, C.W. and M.W. Golay. 1999. A Bayesian belief network-based advisory system for operational availability focused diagnosis of complex nuclear power systems. Expert Systems with Applications 17(1): 21–32.

Katipamula, S. and M.R. Brambley. 2005a. Methods for fault detection, diagnostics and prognostics for building systems- A review, Part I. HVAC&R Research 11 (1):3-25.

Katipamula, S. and M.R. Brambley. 2005b. Methods for fault detection, diagnostics and prognostics for building systems- A review, Part II. HVAC&R Research 12(2):169-187.

Katipamula, S. and M.R. Brambley. 2008. Transforming the practices of building operation and maintenance professionals: A Washington State pilot program. 2008 ACEEE Summer Study on Energy Efficiency in Buildings Washington, DC: American Council for an Energy-Efficient

Khan, S.S. and M.G. Madden. 2010. A survey of recent trends in one class classification. Proceedings of the 20th Irish Conference on Artificial Intelligence and Cognitive Science, AICS'09. Springer-Verlag, Berlin, Heidelberg, 188–197.

Kim, M., S.H. Yoon, P.A. Domanski and W. Vance Payne. 2008. Design of a steady-state detector for fault detection and diagnosis of a residential air conditioner. International Journal of Refrigeration 31: 790-799.

Lam JC, Chan ALS. 1995. Building energy audits and site surveys. Building Research and Information 23(5):270–8.

Lee, W.-Y., J.M. House and N.-H. Kyong. 2004. Subsystem level fault diagnosis of a building's air-handling unit using general regression neural networks. Applied Energy 77, 153–170.

Li, H.R. and J.E. Braun. 2003. An improved method for fault detection and diagnosis applied to packaged air conditioners. ASHRAE Transactions 109 (2): 683–92.

Li, H.R. and J.E. Braun. 2007a. A methodology for diagnosing multiple simultaneous faults in vapor-compression air conditioners. HVAC&R Research 13: 369–395.

Li, H.R. and J.E. Braun. 2007b. Decoupling features and virtual sensors for diagnosis of faults in vapor compression air conditioners, Int. J. Refrigeration 30 (3): 546–564.

Li, H.R. and X.Z. Zhao. 2011. RP-1486 fault detection and diagnosis for centrifugal chillerss-phase III: online implementation. University of Nebraska-Lincoln.

Li, H.R. and X.Z. Zhao. 2011. RP-1486 fault detection and diagnostics for centrifugal chillers - Phase III: Online implementation. Sponsored by ASHRAE TC 7.5 Smart building. University of Nebraska-Lincoln.

Li, S. 2009. A Model-Based Fault Detection and Diagnostic Methodology for Secondary HVAC Systems. Drexel University.

Li, Y. 2011. Selecting training points for one-class support vector machines. Pattern Recognition Letters 32: 1517–1522.

Li, Z.W., C.J.J. Paredis, G. Augenbroe and G.S. Huang. 2012. A rule augmented statistical method for air-conditioning system fault detection and diagnostics. Energy and Buildings 54: 154–159.

Liu, M, D.E. Claridge, and W.D. Turner. 2003. Continuous commissioning SM of building energy systems." ASME Journal of Solar Energy Engineering, Transactions of the ASME, Special Issue on Emerging Trends in Building Design, Diagnosis and Operation 125(3):275-281.

Luo, H., Y.R. Wang and J. Cui. 2011. A SVDD approach of fuzzy classification for analog circuit fault diagnosis with FWT as preprocessor. Expert Systems with Applications 38:10554–10561.

Ma, Z.J., S.W. Wang and F. Xiao. 2009. Online performance evaluation of alternative control strategies for building cooling water systems prior to in situ implementation. Applied Energy 86:712–721.

Ma., Z.J. 2008. Online supervisory and optimal control of complex building central chilling system, PhD Thesis, The Hong Kong Polytechnic University, Hong Kong.

Mahadevan, S. and S.L. Shah. 2009. Fault detection and diagnosis in process data using one-class support vector machines. Journal of Process Control 19: 1627–1639.

Manly, B.J.F. 2005. Multivariate Statistical Methods: A Primer, 3rd Ed., Chapman & Hall/CRC, Boca Raton, FL.

McIntosh, I.B.D. 1999. A model-based fault detection and diagnosis methodology for HVAC subsystems. PhD thesis, University of Wisconsin, Madison.

McIntosh, I.B.D., J.W. Mitchell and W.A. Beckman. 2000. Fault detection and diagnosis in chillers - Part 1: Model development and application, ASHRAE Trans. 106 (2): 268–82.

Mehranbod, N., M. Soroush and C. Panjapornpon. 2005. A method of sensor fault detection and identification. Journal of Process Control 2005 15(3):321–39.

Mills, E. 2009. A golden opportunity for reducing energy costs and greenhouse gas emissions. Lawrence Berkeley National Laboratory.

Montgomery, D.C. 2005. Introduction to Statistical Quality Control, 5th edition. Hoboken, NJ: Wiley.

Najafi, M., D.M. Auslander, P.L. Bartlett, P. Haves and M.D. Sohn. 2012. Application of machine learning in the fault diagnostics of air handling units. Applied Energy 96: 347–358.

Nino-Murcia, G. and M. Shwe. 1991. An expert system for diagnosis of sleep disorders. Annual Meeting Abstracts p165, Toronto, CA. Association of Professional Sleep Societies.

Norford, L.K., J.A. Wright, R.A. Buswell and D. Luo. 2000. Demonstration of Fault Detection and Diagnosis Methods in a Real Building:Final Report. ASHRAE Research Project 1020-RP.

Norford, L.K., J.A. Wright, R.A. Buswell, D. Luo, C.J. Klaassen, and A. Suby. 2002. Demonstration of fault detection and diagnosis methods for air-handling units (ASHRAE 1020-RP). International Journal of Heating, Ventilating, Air Conditioning and Refrigerating Research 8(1):41-71.

Pan, Y.N., J. Chen and G.M. Dong. 2009. A hybrid model for bearing performance degradation assessment based on support vector data description and fuzzy c-means. Proceedings of the Institution of Mechanical Engineers, Part C: International Journal of Mechanical Sciences 223:2687 –2695.

Paniagua-Tineo, A., S. Salcedo-Sanz, C. Casanova-Mateo, E.G. Ortiz-García, M.A. Cony and E. Hernández-Martín. 2011. Prediction of daily maximum temperature using a support vector regression algorithm, Renewable Energy 36: 3054–3060.

Park, T.C., T.Y. Kim and Y.K. Yeo. 2010. Prediction of the melt flow index using partial least squares and support vector regression in high-density polyethylene (HDPE) process, Korean J. Chem. Eng. 27: 1662-1668.

Pearl, J. 1986. Fusion, propagation, and structuring in belief networks. Artificial Intelligence 29(3): 241–88.

Pearl, J. 1988. Probabilistic reasoning in intelligent systems: networks of plausible inference. San Mateo, CA.

Pearl, J. 1985. Bayesian networks: A model of self-activated memory for evidential reasoning. The 7th Conference of the Cognitive Science Society, University of California, Irvine.

Pérez-Lombard, L., J. Ortiz and C. Pout. 2008. A review on buildings energy consumption information. Energy and Buildings 40, 394–398.

Qin, J.Y. and S.W. Wang. 2005. A fault detection and diagnosis strategy of VAV air-conditioning systems for improved energy and control performances, Energ. Buildings 37(1): 035-1048.

Reddy, T. A., D. Niebur, J. Gordon, J. Seem. 2001. Development and comparison of on-line model training techniques for model-based FDD methods applied to vapor compression chillers: evaluation of mathematical models and training techniques, ASHRAE Research Project 1139.

Reddy, T.A. 2006. Evaluation and assessment of fault detection and diagnostic methods for centrifugal chillers - Phase II. Final project report of ASHRAE Research Project RP-1275, Atlanta, GA.

Reddy, T.A. 2007a. Application of a generic methodology to assess four different chiller FDD methods (RP-1275), HVAC&R Res. 13 (5): 711-729.

Reddy, T.A. 2007b. Formulation of a generic methodology for assessing FDD methods and its specific adoption to large chillers. ASHRAE Transactions 113(2):334-342.

Reddy, T.A., 2007c.Development and evaluation of a simple model-based automated fault detection and diagnosis (FDD) method suitable for process faults of large chillers. ASHRAE Transactions 113 (2): 27-39.

Reddy, T. A. 2008. Comparison of two model based automated fault detection and diagnosis methods for centrifugal chillers. ASME Conference Proceedings 2008, 43192: 577-588.

Roberts, S.W. 1959. Control chart tests based on exponentially weighted moving average. Technometrics (1): 239–250.

Rossi, T.M. 1995. Detection, diagnosis, and evaluation of fault in vapor compressor cycle equipment, Ph.D. Thesis, Purdue University.

Rossi, T.M., and J.E. Braun. 1997. A statistical, rule-based fault detection and diagnostic method for vapour compression air conditioners. HVAC&R Research 3(1): 19–37.

Sahin, F., M. Yavuz, Z. Arnavut and O. Uluyol. 2007. Fault diagnosis for airplane engines using Bayesian networks and distributed particle swarm optimization. Parallel Computing 33(2): 124–43.

Salsbury, T.I., and R.C. Diamond. 2001. Fault detection in HVAC systems using model-based feedforward control. Energy and Buildings 33:403-415.

Schein, J. 2006. Results from field testing of embedded air handling unit and variable air volume box fault detection tools. NISTIR 7365.

Schein, J. and J.M. House. 2003. Application of control charts for detecting faults in Variable-Air-Volume boxes. ASHRAE Transactions 109: 671-682.

Schein, J., S.T. Bushby, N.S. Castro and J.M. House. 2006. A rule-based fault detection method for air handling units. Energy and Buildings 38: 1485–1492.

Sch ölkopf, B., C.J.S. Burges and A.J. Smola. 1999. Advances in kernel methods: support vector learning, The MIT Press, Cambridge, MA.

Seem, J.E., J.M. House and R.H. Monroe. 1997. On-line monitoring and fault detection of control system performance, Proceedings of CLIMA 2000, Brussels.

Seem, J.E., J.M. House and R.H. Monroe. 1999. On-Line Monitoring and Fault Detection, ASHRAE Journal 41: 21-26.

Seem, J.E. and J.M. House. 2009. Integrated Control and Fault Detection of Air-Handling Units. HVAC&R Research 15: 25–55.

Shaw, S.R., L.K. Norford, D. Luo and S.B. Leeb. 2002. Detection and diagnosis of HVAC faults via electrical Lload monitoring. HVAC&R Research 8: 13–40.

Sch ölkopf, B., C.J.S. Burges and A.J. Smola. 1999. Advances in kernel methods: support vector learning. The MIT Press, Cambridge, MA.

Shewhart, W. A. 1926. Quality control charts. Bell System Technical Journal 593-603.

Shwe, M., B. Middleton, D. Heckerman, M. Henrion, E. Horvitz, H. Lehmann and G. Cooper. 1991. Probabilistic diagnosis using a reformulation of the INTERNIST-1/QMR knowledge base: I. The probabilistic model and inference algorithms. Methods of Information in Medicine 30(4): 241-255.

Stephan, K. and M. Abdelsalam. 1980. Heat-transfer correlations for natural convection boiling. International Journal of Heat and Mass Transfer 23:73-87.

Stylianou, M.P. 1997. Application of classification functions to chiller fault detection and diagnosis. ASHRAE Transactions 103(1): 645–56.

Sun, Y.J, S.W. Wang and G.S. Huang. 2010. Online sensor fault diagnosis for robust chiller sequencing control. International journal of thermal science 49:589-602.

Swider, D.J. 2003. A comparison of empirically based steady-state models for vapor-compression liquid chillers, Applied Thermal Engineering 23: 539–556.

Swider, D.J., M.W. Browne, P.K. Bansal and V. Kecman. 2001. Modelling of vapour-compression liquid chillers with neural networks, Applied Thermal Engineering 21: 311–329.

Tassou, S.A. and I.N. Grace. 2005. Fault Diagnosis and Refrigerant Leak Detection in Vapour Compression Refrigeration Systems. Int. J. Refrigeration 28 (5): 680–688.

Tax, D.M.J. 2012. DDtools, the Data Description Toolbox for Matlab. http://prlab.tudelft.nl//david-tax/dd_tools.html

Tax, D.M.J. and R.P.W. Duin. 1999. Support vector domain description. Pattern Recognition Letters 20:1191-1199.

Tax, D.M.J. and R.P.W. Duin. 2004. Support vector domain description. Machine Learning 54: 45–66.

Tax, D.M.J., A. Ypma and R.P.W. Duin. 1999. Pump failure detection using support vector data descriptions. Lecture Notes in Computer Science 1642:415-425.

Thomson, M., P.M. Twigg, B.A. Majeed and N. Ruck. 2000. Statistical process control based fault detection of CHP units, Control Engineering Practice 8: 13–20.

Tian, J., H. Gu, C. Gao and J. Lian. 2011. Local density one-class support vector machines for anomaly detection. Nonlinear Dynamics 64: 127–130.

Wall, J., Y. Guo, J.M. Li and S. West. 2011. A dynamic machine learning-based technique for automated fault detection in HVAC systems. ASHRAE Transactions 117: 449–456.

Wang, H.T., Y.M. Chen, C.W.H. Chan and J.Y. Qin. 2011. A robust fault detection and diagnosis strategy for pressure-independent VAV terminals of real office buildings, Energ. Buildings 43: 1774–1783.

Wang, S.W. and F. Xiao. 2004. AHU sensor fault diagnosis using principal component analysis method. Energy and Buildings 36, 147–160.

Wang, S.W. 1999. Dynamic simulation of building VAV air-conditioning system and evaluation of EMCS on-line control strategies. Building and Environment 34: 681–705.

Wang, S.W. and F. Xiao. 2006. Sensor fault detection and diagnosis using condition-based adaptive statistical analysis. HVAC&R Research 12(1): 127-150.

Wang, S.W. and J.T. Cui. 2005. Sensor-fault detection, diagnosis and estimation for centrifugal chiller systems using principal-component analysis method. Applied Energy 82:197–213.

Wang, S.W. and J.Y. Qin. 2005. Sensor fault detection and validation of VAV terminals in air conditioning systems, Energy Conversion and Management 46: 2482-2500.

Wang, S.W. and J.B. Wang. 2000. A mechanistic model of a centrifugal chiller to study HVAC dynamics. Building Services Engineering Research and Technology 21(2):73-83.

Wang, S.W. and J.T. Cui. 2006. A robust fault detection and diagnosis strategy for centrifugal chillers. HVAC&R Research 12:407–428.

Wang, S.W., Q. Zhou and F. Xiao. 2010. A System-level Fault Detection and Diagnosis Method for HVAC Systems Involving Sensor Faults. Energy and Buildings 42(4):477-490.

Wang, Y., D.L. Wu, C.X. Guo, Q.H. Wu, W.Z. Qian and J. Yang. 2010. Short-term wind speed prediction using support vector regression, 2010 IEEE Power and Energy Society General Meeting, 1–6.

Wen, J. and S. Li. 2011. ASHRAE 1312-RP: Tools for Evaluating Fault Detection and Diagnostic Methods for Air-Handling Units - Final report. Drexel University.

Xiao, F. 2004. Sensor fault detection and diagnosis for air handling units. The Hong Kong Polytechnic Univeristy.

Xiao, F., S.W. Wang and J. Zhang. 2006. A diagnostic tool for online sensor health monitoring in air-conditioning systems. Automation in Construction 15: 489–503.

Xiao, F., S.W. Wang, X.H. Xu and G.M. Ge. 2009. An isolation enhanced PCA method with expert-based multivariate decoupling for sensor FDD in air-conditioning systems, Applied Thermal Engineering 29: 712–722.

Xiao, F., C. Zheng and S. Wang. 2011. A fault detection and diagnosis strategy with enhanced sensitivity for centrifugal chillers, Applied Thermal Engineering 31: 3963–3970.

Xu, Z.Y. 2008. Development of an intelligent building integration platform based on web services middleware technologies. The Hong Kong Polytechnic University.

Xu, B.G. 2012. Intelligent fault inference for rotating flexible rotors using Bayesian belief network. Expert Systems with Applications 39: 816–822.

Xu, P., P. Haves and M. Kim. 2005. Model-Based Automated Functional Testing--Methodology and Application to Air-Handling Units. ASHRAE Transactions 111: 979–989.

Xu, X.H., F. Xiao, S.W. Wang. 2008. Enhanced chiller sensor fault detection, diagnosis and estimation using wavelet analysis and principal component analysis methods. Applied Thermal Engineering 28: 226–237.

Yang, H., S. Cho, C.-S. Tae and M. Zaheeruddin. 2008. Sequential rule based algorithms for temperature sensor fault detection in air handling units. Energy Conversion and Management 49, 2291–2306.

Yang, L. and J. Lee. 2012. Bayesian belief network-based approach for diagnostics and prognostics of semiconductor manufacturing systems. Robotics and Computer-Integrated Manufacturing 28 (1): 66–74.

Yang, X.B., X.Q. Jin, Z.M. Du, Y.H. Zhu and Y.B Guo. 2013. A hybrid model-based fault detection strategy for air handling unit sensors. Energy and Buildings 57: 132–143.

Yoshida, H. and S. Kumar. 1999. ARX and AFMM model-based on-line real time data base diagnosis of sudden fault in AHU of VAV system, Energy Conversion and Management 40: 1191-1206.

Yoshida, H., S. Kumar and Y. Morita. 2001. Online fault detection and diagnosis in VAV air handling unit by RARX modeling. Energy and Buildings 33: 391–401.

Yoshida, H., T. Iwami, H. Yuzawa and M. Suzuki. 1996. Typical faults of air-conditioning systems and fault detection by ARX model and extended Kalman Filter, ASHRAE Transactions 102: 557-564.

Zagorecki, A. and M. J. Druzdzel. 2006. Knowledge engineering for Bayesian networks: How common are Noisy-MAX distributions in practice? Proceedings of the Seventeenth European Conference on Artificial Intelligence (ECAI-06) 482–489.

Zhao, X., M. Yang and H. Li. 2011. Decoupling features for fault detection and diagnosis on centrifugal chillers (1486-RP). HVAC&R Research 17(1): 86-106.

Zhou, Q., S.W. Wang and Z.J. Ma. 2009a. A Model-based Fault Detection and Diagnosis Method for HVAC Systems. International Journal of Energy Research 33:903-918.

Zhou, Q., S.W. Wang, and F. Xiao. 2009b. A novel strategy of fault detection and diagnosis for centrifugal chiller systems, HVAC&R Research 15(1): 57-76.